Master Thesis

Civil Engineering

Non-symmetrical column splice

Ajay Katta

TU Delft

Non-symmetrical column splice

By

Ajay Katta

in partial fulfilment of the requirements for the degree of

Master of Science
In Civil Engineering

at the Delft University of Technology,
to be defended publicly on Wednesday January 30th, 2019 at 10:00 AM.

Student number:	4619722	
Committee:	Prof. Dr. M. Veljkovic	TU Delft, Supervisor & Chairman
	Dr. M.A.N. Hendriks	TU Delft
	Ir. P.A. de Vries	TU Delft
	Ir. R. Yan	TU Delft

TU Delft

Acknowledgement

This thesis is written in partial fulfillment of the requirements for the degree of Master of Science in Civil engineering at the Delft University of Technology. I would like to thank the committee members, Prof. Dr. M. Veljkovic, Ir. P.A. de Vries, Ir. R. Yan and Dr. M.A.N. Hendriks for their expert guidance and critical reviews of my work. Special thanks to my daily supervisor, Rui, who was always happy to help with and discuss any pertaining issues. This thesis is dedicated to my family, who have made this possible and have been a constant inspiration. Finally, I thank my friends for their constant support and encouragement throughout this whole journey.

Ajay Katta
Delft, January 2019

Abstract:

Standardized column splices consist of bolted end-plate connection or bolted/welded cover plate splice connection. In this thesis a non-symmetrical column splice connection that uses a combination of bolted end-plate splice and cover plate splice is studied. End-plate column splice may interfere with installation of cladding elements and may interfere with architectural requirements. Proposed column splice provides a solution to the underlying issue with space optimization. Splice connections are modeled on Abaqus using solid elements. Based on the location in the building non-symmetrical column splice connections are classified as non-symmetrical corner splice connection and non-symmetrical intermediate splice connection.

Aim of this thesis is to study the structural behavior of non-symmetrical column splice connections with the aid of moment-rotation curves, individual component behavior and force distribution obtained from finite element analysis. A quasi-static analysis is conducted on software package Abaqus using dynamic explicit solver. In addition, an attempt is made to characterize the non-symmetrical column splice connection based on component method. Stiffness coefficients of end-plate in bending produced too high stiffness when used for hollow-section end-plate connection. A modified stiffness model for end-plate in bending and bolts in tension are considered for the component characterization of current connections. Effects of end-plate thickness, cover plate thickness and bolt edge distances on overall moment-rotation behavior and initial stiffness was studied.

Non-symmetrical column splice connections are studied under bending and tensile behavior. Due to uneven force distribution in the connection, torsion is noticed in bending cases of non-symmetrical corner splice and intermediate splice. Eurocode stiffness model for end-plate in bending and bolts in tension produced high stiffness compared to the results obtained from Abaqus. Stiffness was overestimated by at least 2 times. Whereas, acceptable values of initial rotational stiffness were obtained using modified stiffness model for end-plate in bending and bolts in tension. Increase in thickness of end-plate and cover plate had a positive effect on the resistance of non-symmetrical column splice connection. However, local failure in column cross-section was noticed when the thickness of end-plate and cover plate was 10 mm. Bolt distance from the column face and edge distance was varied. Overall resistance and initial rotational stiffness increased when the bolts were moved closer to the column face and the opposite was noticed when bolts were moved away from the column face. Similar behavior was also noticed in case bolts in end-plate were moved close to each other.

CONTENTS

LIST OF FIGURES

LIST OF TABLES

Chapter 1 – Introduction

1.1 Background

Joints and connections in steel structures contribute significantly towards the total cost of structure. Efficient and reliable design methods combined with meticulous care for connection details can lead to considerable savings in construction costs. In this research, a new type of column splice connection known as “non-symmetrical column splice connection” is studied. Traditional column splice connections either consists of end-plate splice or cover plate splice. In this case, hollow section columns are connected with a combination of both kinds of splice, leading to an efficient system in terms of architecture and strength. This kind of splice connection can be used in modular construction and allows significant space optimization. A sustainable solution for façade can’t be achieved with the traditional solution. Proposed solution can be used in case the façade is attached to column on the side with cover plate. A case of non-symmetrical column splice connection located in the corner of the building and intermediate is further evaluated under bending and tensile behavior as shown in figures 1-1 and 1-2. Generally, bending behavior of connections varies depending on the direction mainly due to the properties of sections connected. In the proposed connection, bending behavior is not varied by the connected sections, but due to the connection components themselves.

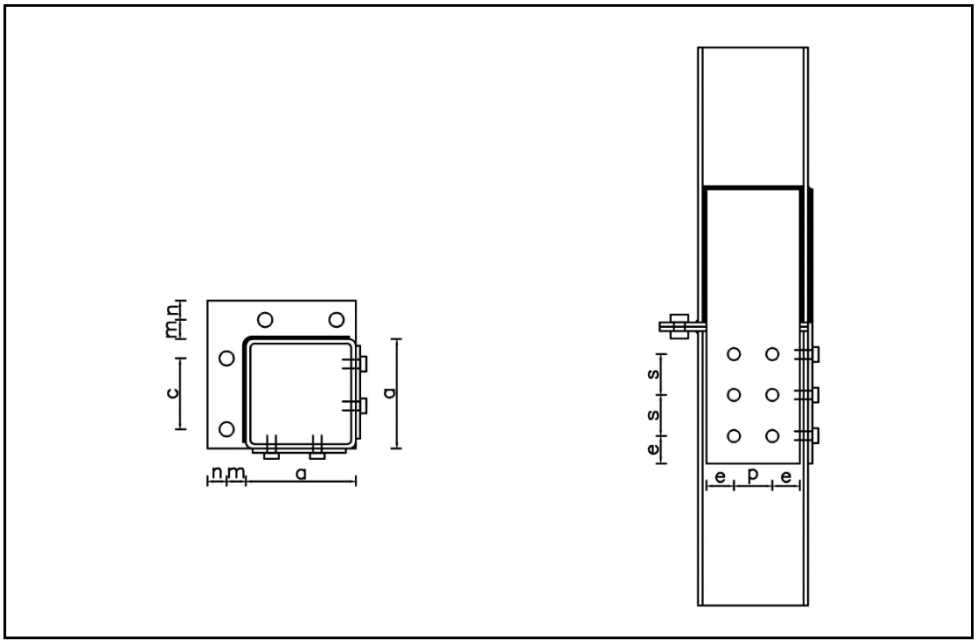

Figure 1-1: Plan and elevation of non-symmetrical corner splice connection

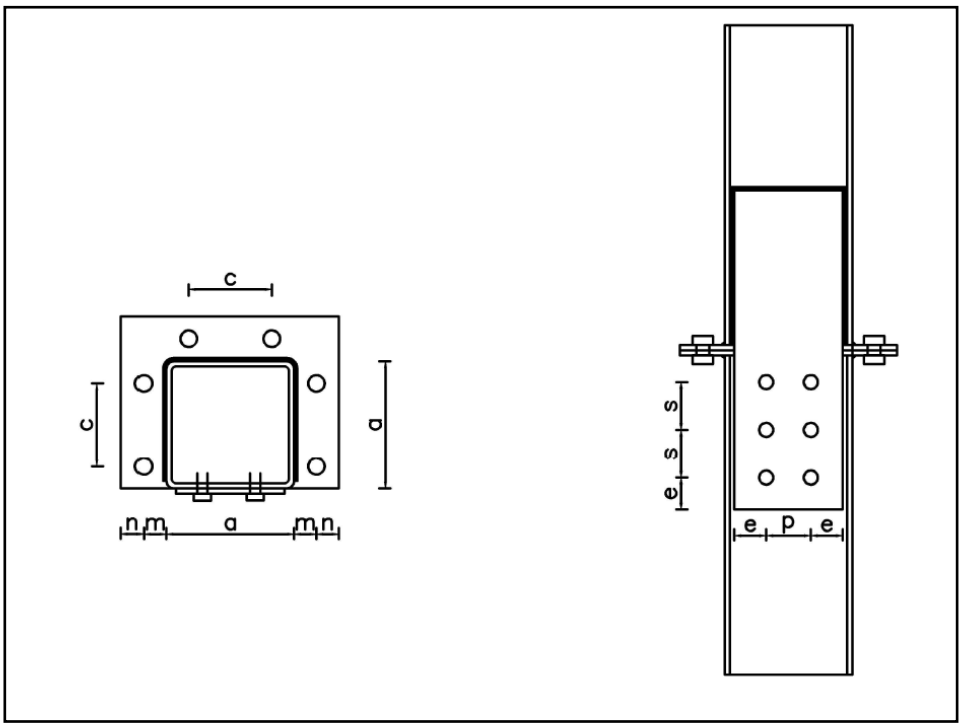

Figure 1-2: Plan and elevation of non-symmetrical intermediate splice connection

Evaluation and characterization of steel connections can be done by three parameters, namely, resistance, stiffness and ductility. Characterization based on stiffness and inclusion of appropriate parameters in global analysis is of significance for semi-rigid connections. Complete behavior of connections is always desired and can be established by their corresponding moment-rotation curves. While characterization of joints can be done by various procedures, "component method" has been widely accepted by the research community and accurate at considering various interactions that might occur amongst the connection components. In component method, stiffness of individual joint components is computed and then assembled together to produce the total initial rotational stiffness of the joint. Component method is also described in Eurocode-1993-1-8. However, faces the disadvantage of being applicable only to a few types of joint configurations. In this thesis, it is aimed to characterize the proposed connection type based on component method and compute initial joint stiffness. Based on literature studies, a modified Eurocode approach for component method was applied to the connection.

Finite element program Abaqus was used to perform numerical simulations of the proposed connection type. Complete moment-rotation curves and individual component behavior are studied with aid of finite element results. Parametric studies were conducted by varying the connection component thickness and bolt position in end-plate. These simulations were conducted to the aid experimental work which is not included in this thesis.

1.2. Objective and research questions

Primary objective of this thesis is to investigate the structural performance of non-symmetrical column splice connection. Connection layout of non-symmetrical splice column splice connection depends on the location of the column in building. Thus, specimens studied in this thesis can be classified as non-symmetrical corner splice and non-symmetrical intermediate splice. Non-symmetrical column splice is investigated under tensile and bending behavior. In addition, initial joint stiffness of the connection is predicted based on modified stiffness coefficients described in chapter 7. The current Eurocode procedure for component method is not suitable to be applied to some of the components in the connection under study. Hence, this would require modification of current procedures and application of new stiffness coefficients.

Research questions can be summarized into following points:

1. **How does non-symmetrical column splice connection perform compared to conventional end plate connection?**
   The proposed column splice performs well in terms of architectural aesthetics. This also being one of the primary functions of non-symmetrical column splice. However, structural performance of the proposed connection type needs to be known for use in industry. Resistance to tensile and bending loads and initial rotational stiffness of the connection are some of the key parameters that affect the structural behavior of a connection present in a building. A moment-rotation curve of the connection needs to be developed to obtain the earlier mentioned parameters. Finite element analysis of the proposed column splice is done to obtain the moment-rotation curves.

2. **Which of the connection components contribute to initial joint stiffness? How does the force distribute among connection components?**
   A conventional end-plate connection welded to column ends is bolted together on two sides, four sides or corners of the hollow section. Distribution of applied load among connection components is well known in this case. This is not yet known in the proposed column splice type. Knowledge of connection components contributing to initial rotational stiffness is essential to apply analytical methods like component method. Force distribution in connection is to be analyzed at different stages of the moment-rotation curve to identify the behavior of components.

3. **Which of the existing components provided in EC 1993-1-8 can be applied to the proposed connection? Which new components would require further study?**
   Eurocode currently provides 22 stiffness coefficients that can be applied to joints made of I and H sections. Initial stiffness of an end-plate connection made of I section varies hugely to one designed between tubular sections. New stiffness coefficients may need to be applied to predict $s_{j,ini}$. However, some of the stiffness coefficients maybe directly applied depending on the connection component.

Chapter 2 – Literature review

2.1 Types of column splices

2.1.1 Standardized column splices

Structural steel available in market is usually of lengths between 12-15 meters. Available lengths in market are limited due to fabrication, transportation and erection problems. Hence, a splice connection needs to be provided to obtain desired lengths of structural members such as beam and column. Column splices are usually provided at floor level. Column splice is designed to hold the connected members in line and transfer the internal forces. Column splices can be classified into two categories:

1) End plate splices:
   This type of splice connection includes welding two end plates to the faces of column that need to be connected as shown in figure 2-1. These end plates are then bolted together to complete the connection. Bolts may be provided on two sides or on four sides of the column section. Sometimes, bolts in the end plate maybe preloaded. This is the most economical and widely used column splice.

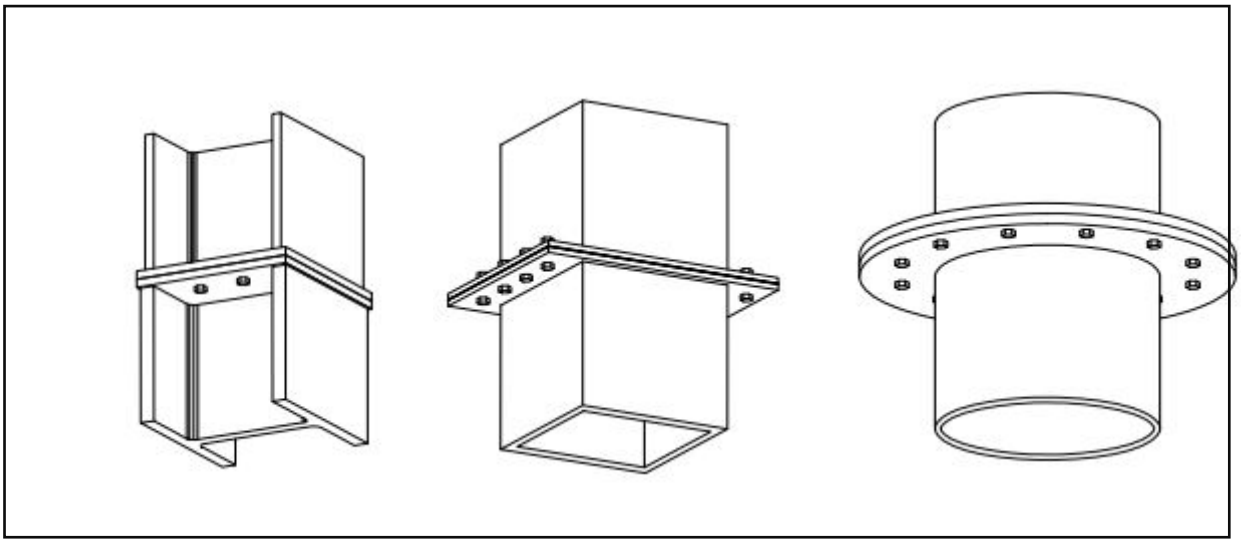

Figure 2-1: End plate splice between open and tubular section [7]

2) Cover plate splices:
Cover plate splices are usually provided on all four sides of the column section. Cover plate may be bolted to the upper and lower column or bolted to the lower column and welded to the upper column as seen in figure 2-2. In case of hollow sections with cover plate splices, blind bolts are preferred over regular bolts due to fabrication issues. An access hole needs to be provided for hollow section to tighten the bolts on both ends in case regular bolts are used. There are two types of column cover plate splices depending on load transfer mechanism:

2.1) Bearing type splice
In this case, column ends that need to be connected are in direct contact with each other. Surface preparation is required and limits for unevenness are provided in EN 1090-2. Cover plates are connected to the upper and lower columns using bolts as shown in figure 2-2. In case of full contact in bearing, the splice material should be designed to resist transmit 25% of the compressive force, provide continuity of stiffness and resist any tension developed in case of moments. Splice plates are mainly intended to hold the upper and lower column in place.

2.2) Non- bearing type splice
In this case, the cover plates are designed to transmit 100% of the forces. Moments and axial loads are assumed to be transferred entirely by the splice material. Bearing between the columns is ignored in design process. Sometimes, a physical gap may be provided between upper and lower columns.

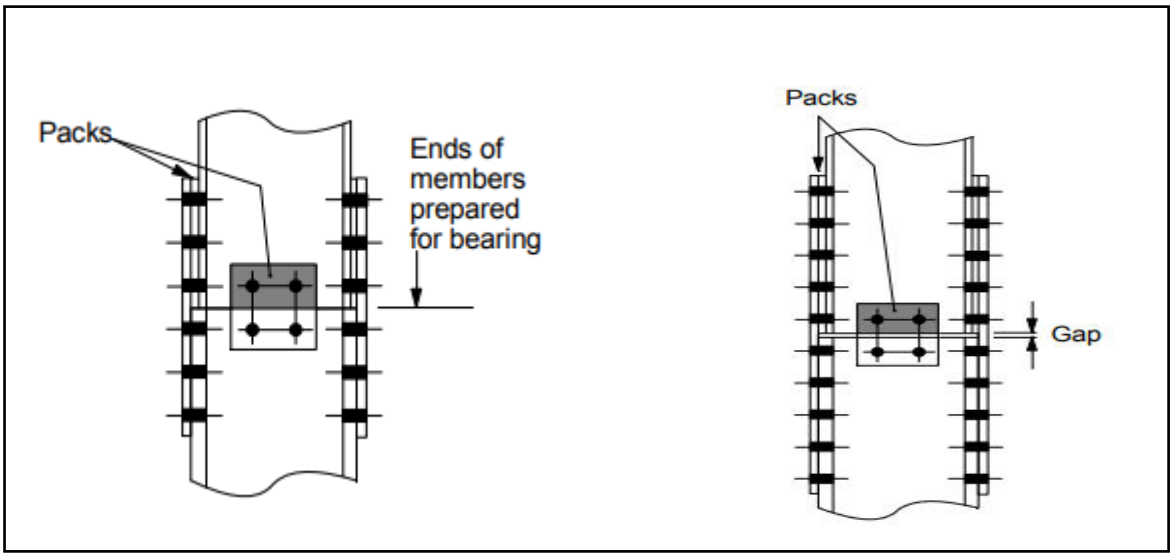

Figure 2-2: Bearing and non-bearing cover plate splice connection [7]

2.1.2 Blind bolting system

Bolts that can be tightened from one-side are called blind bolts. These bolts can be used for steel connections involving hollow sections. Using a regular bolt in hollow section is a time consuming and labor-intensive process. It requires creating an access hole in the section, so that the regular bolts can be tightened on both sides. Blind bolts can be used to avoid these issues with hollow sections. Lindapter hollo-bolt and ajax one side bolt are the most widely used blind bolting system. Lindapter hollo-bolt differs hugely in geometry from a regular hexagonal bolt as seen in figure 2-3. Nut is shaped in the form of a cone with sleeves and is made of different material. Therefore, the clamping areas are different. Sleeves of a lindapter hollo bolt expand and exert clamping force after tightening. Finite element modelling of lindapter hollo bolt requires modifications to that of a regular bolt since the clamping areas are different.

On the other hand, an ajax one side bolt has head and nut shaped similar to a regular bolt as seen in figure 2-4. So, the clamping areas of the bolt are similar to a regular hexagonal bolt. A one side bolt can be modelled as a regular bolt due to similar shape and contact areas. A one side blind bolt requires special equipment and oversized holes for installation. For instance, a M16 ajax one side bolt requires a hole of diameter 24mm. Shear sleeves can also be used to reduce the gap in bolt holes to required tolerance. Shear sleeve is also made of the same material as bolt and its thickness can be chosen according to strength requirements and tolerance [23]. Ajax one side bolt has been extensively modeled similar to a regular bolt producing acceptable results with experiments [8,21]. Ajax one side bolt without sleeve exhibits slightly lower stiffness than with sleeve. However, the effect of ajax one side bolt with shear sleeve provided with 2mm clearance and ajax one side bolt without sleeve on moment-rotation curve was negligible. The effects of type of blind bolt (Lindapter hollo-bolt and ajax one side bolt) on overall moment rotation behavior of a steel composite joint were found to be negligible [22].

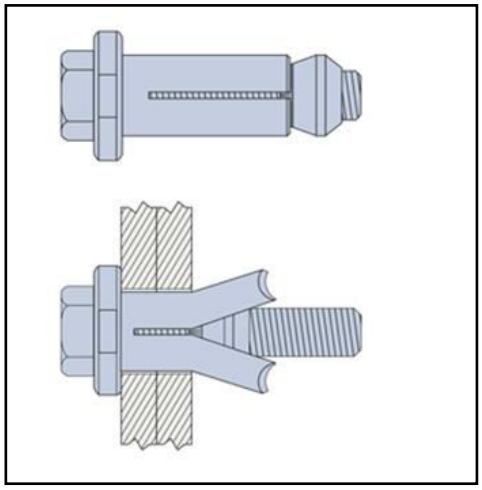

Figure 2-3: Lindapter hollo bolt

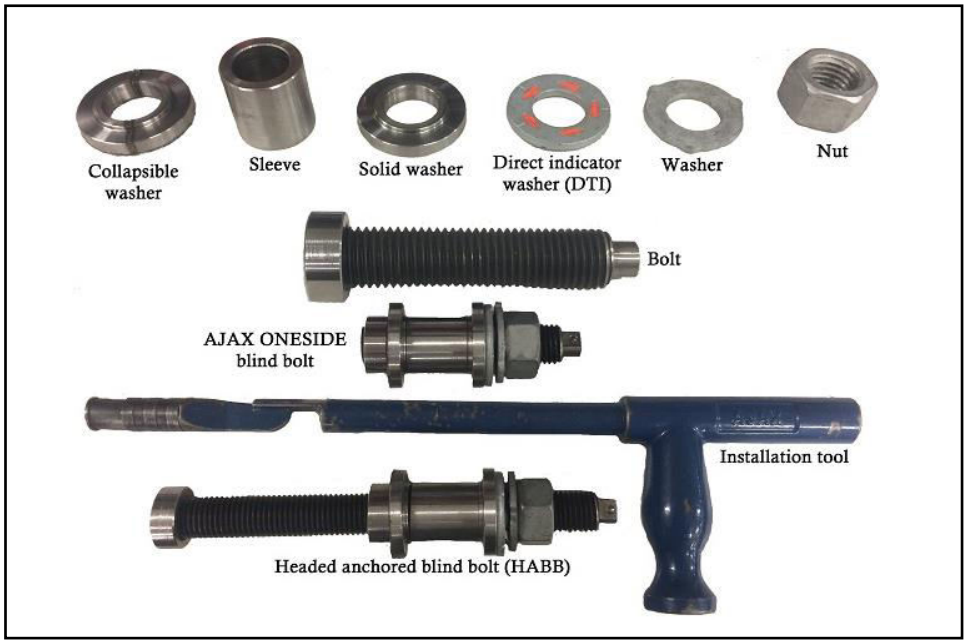

Figure 2-4: Ajax one side bolt

Installation of ajax one side bolt requires a special installation tool as seen in figure 2-14. The bolt and collapsible washer are placed in the installation tool. Bolt and collapsible washer are passed through the bolt holes with the aid of installation tool. Collapsible washer is then unfolded by pulling the installation tool back. Bolt is then tightened on the outside with a solid washer and nut. Shear sleeve may also be used in case of strength requirements. Shear sleeves are placed onto the bolt before placing it on the installation tool.

2.2 Research on bolted end-plate connection for hollow section

Higher strength to weight ratio and superior torsional resistance has led to increased use of hollo sections. Hollow sections are also preferred for architectural aesthetics in exposed structures. Welding is usually preferred to connect hollow sections to connection components, since using bolts is a complex process. In case of splices between hollow section, bolted end-plate connection is most widely used. This connection involves welding of end-plates onto column ends and then bolting them. Concept of bolting only on two faces of a rectangular hollow section was initially introduced by Birkemoe and Olynyk (1980). Kato and Mukai (1985), dismissed this type of connection, concluding that bolting only on two faces of rectangular hollow section leads to reduced ultimate strength and stiffness in comparison to a four-side bolted joint [16].

Kato and Hirose (1985) conducted experimental tests on end plate flanges joining circular hollow sections with 53 specimens. In these the diameter and thickness of the tubular section, bolt pitch diameter, end plate diameter and its thickness were varied. It was observed that, decreasing the flange thickness with a constant size of fillet weld led to a relatively larger rigid zone around the circular section. Also, by using a larger preload for the bolts for a certain range of flange thickness, joint strength can be increased and that critical flange thickness is nearly equal to bolt diameter. Meaning, bolt failure occurs before yielding of the flange if a thickness higher than critical thickness is used [16].

Packer et al (1989) conducted an analysis of bolted RHS flange plate joints with bolts only on two sides of the hollow section under tensile force as shown in figure 2-5. 16 bolted connections were tested and bolt forces were measured using “load cell washers” to calculate the separation load. In this type of joint, phenomenon of prying forces was found to be complex and the joint was thus assumed to be statically indeterminate. Bolt response was recorded and was seen to be bilinear with joint separation load occurring at the point of deviation. Also, it was concluded that increase in bolt size increased the joint strength, initial joint stiffness, separation load and prying ratio [17].

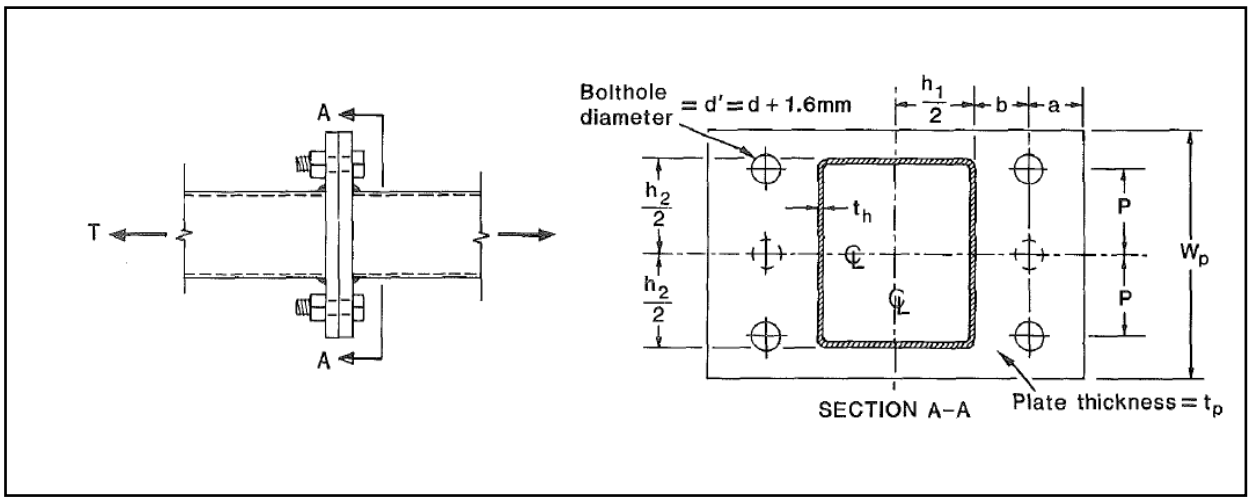

Figure 2-5: Bolted flange plate joint studied by Packer et al [17]

Wheeler et al (1998) conducted experimental study on bolted moment end plate connections joining rectangular hollow sections with bolts only near the four corners of the end plate as shown in figure 2-6. Connections were subjected to four-point bending tests with parameters varied included plate size, plate thickness, section shape and position of bolts. Stiffness and strength of the connection increased as the bolts were moved closer to the flange of the section. A generalized connection model for predicting the ultimate capacity of the connection involving the integration of both the yield line and T-stub analysis was derived. It was noticed that the position of yield lines was affected by the size of fillet weld. As the bolts were moved farther away from the flange of the section, yield moment of the connection was found to decrease. End plate was assumed to behave in the same manner as a wide beam and a recommendation that ideal failure mode should involve bolt capacity combined with intermediate plate behavior was made [15].

Wheeler et al (2000) conducted finite element analysis of tubular moment end-plate connections for bolt layout as shown in figure 2-7. FE software ABAQUS was used to perform the analysis. An attempt was made to consider the effect of cold-forming on the corners of hollow sections. Tested material properties were obtained with little variation; hence, average material properties were used for corner and flat sides of the hollow section. 8 node linear hybrid elements were used to model end plates to avoid possible effect of volume strain locking. Weld was modelled as an individual component with material properties exceeding those of end plate and tubular sections. Welding of end plate to the tubular sections induces significant residual stresses and bowing deformations in the end plate. This heat induced distortion was believed to have a considerable effect on the stiffness of the connection as shown in the figure 2-7. Heat induced distortions were modelled by applying a displacement to the end plate, varying linearly from zero at the flanges to maximum value at the plate edges [18].

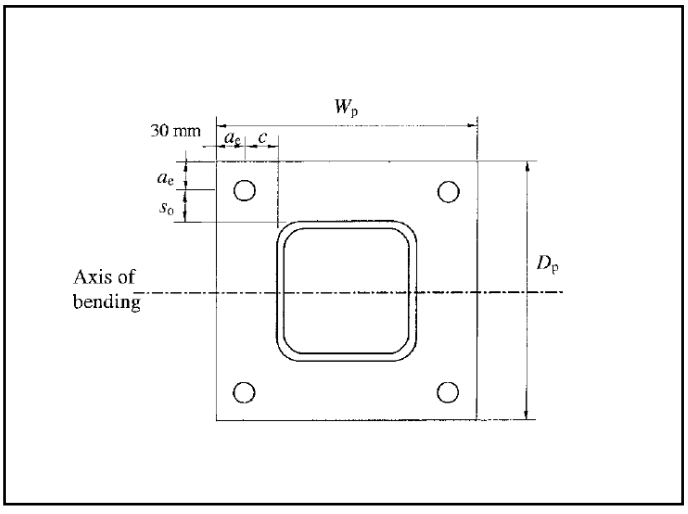

Figure 2-6: End plate connection studied by Wheeler et al (2000) [18]

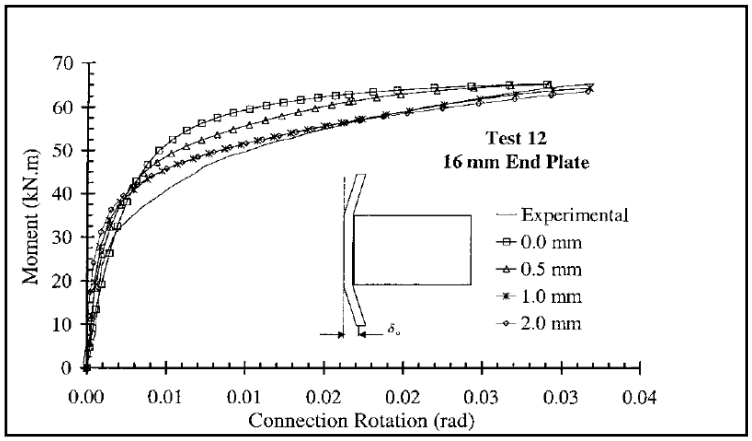

Figure 2-7: Effect of end-plate welding on moment resistance [18]

Preload effect was found to have a negligible effect on the overall moment-rotation response. Stiffness of the connection was found to be a function of the end plate thickness and positioning of bolts with respect to the section perimeter. As the thickness of end plate was increased, agreements between ABAQUS and experiments became poorer.

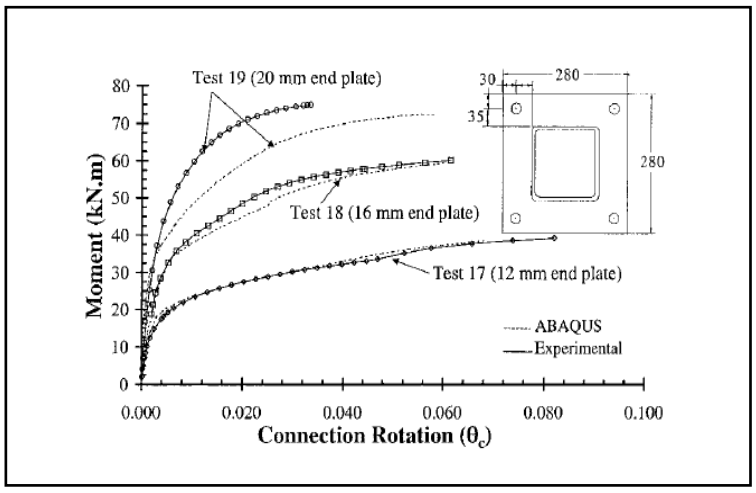

Figure 2-8: Effect of end plate thickness on connection resistance [18]

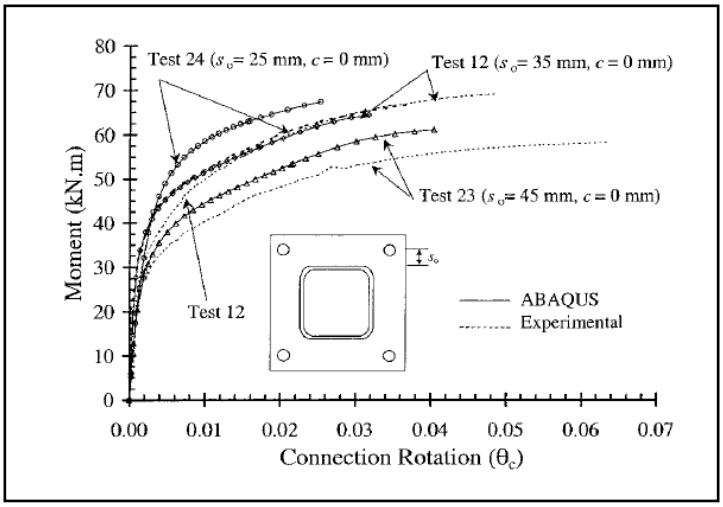

Figure 2-9: Effect of bolt position on connection resistance [18]

Willibald et al (2002), performed experimental studies on bolted hollow section flange-plate connections in axial tension. A total of 16 specimen containing three types of bolt layout as shown in figure 2-10 were tested. Deformation was more pronounced in case of thinner end plates. Bolt layout B was noticed to cause uneven stress distribution, due to inner bolts being highly stressed compared to outer bolts. For all layouts, prying ratio was lowered as the bolts were moved closer to the flanges of hollow section as shown in figure 2-11. Fillet welds reduced the distance of bolts from flange of hollow section and were found to act as stiffeners for the end plates [19].

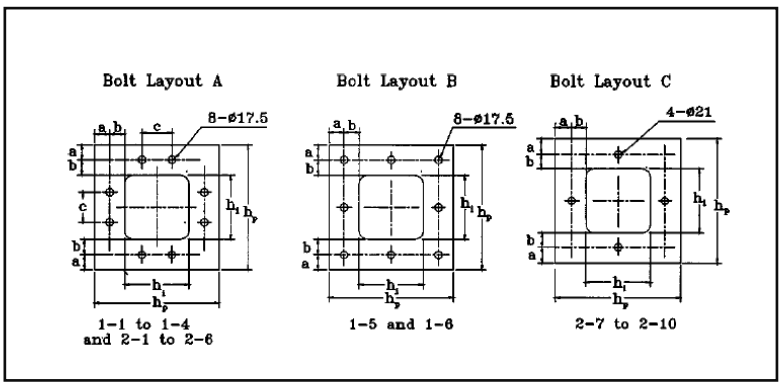

Figure 2-10: Bolt layouts studied by Willibald et al (2002) [19]

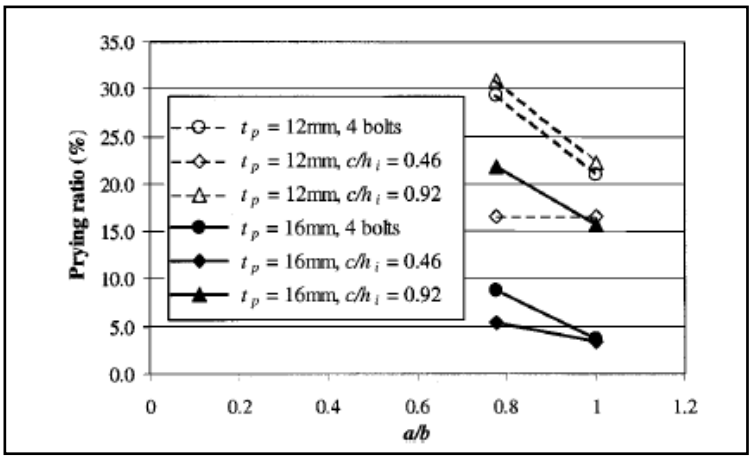

Figure 2-11: Effect of bolt position on prying ratio [19]

Wang et al (2012), conducted experimental and numerical studies on bolted flange plate connections for tubular sections. Square and circular hollow sections with and without stiffeners were studied. Stiffeners significantly increased the stiffness and ultimate strength of the connection for circular hollow sections as shown in figure 2-12. While, use of stiffeners for square hollow sections didn't seem to have a considerable effect either on stiffness or ultimate strength as shown in figure 2-13. Prying action was noticed be lower for stiffened connections, due to stiffener and related fillet welds sharing the loads. [20].

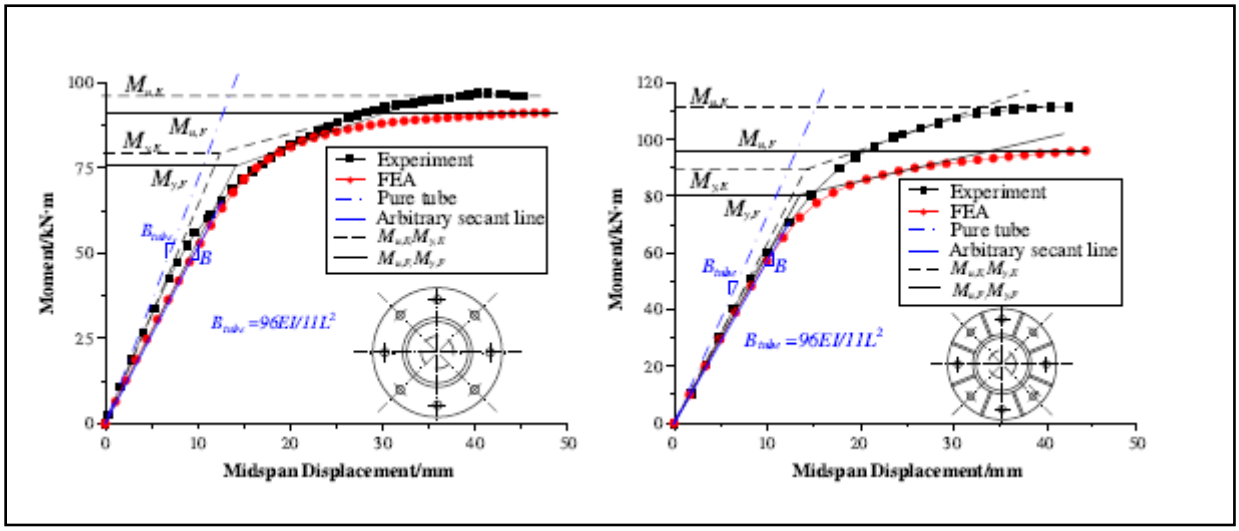

Figure 2-12: Tensile behavior of unstiffened and stiffened circular end-plate connections [20]

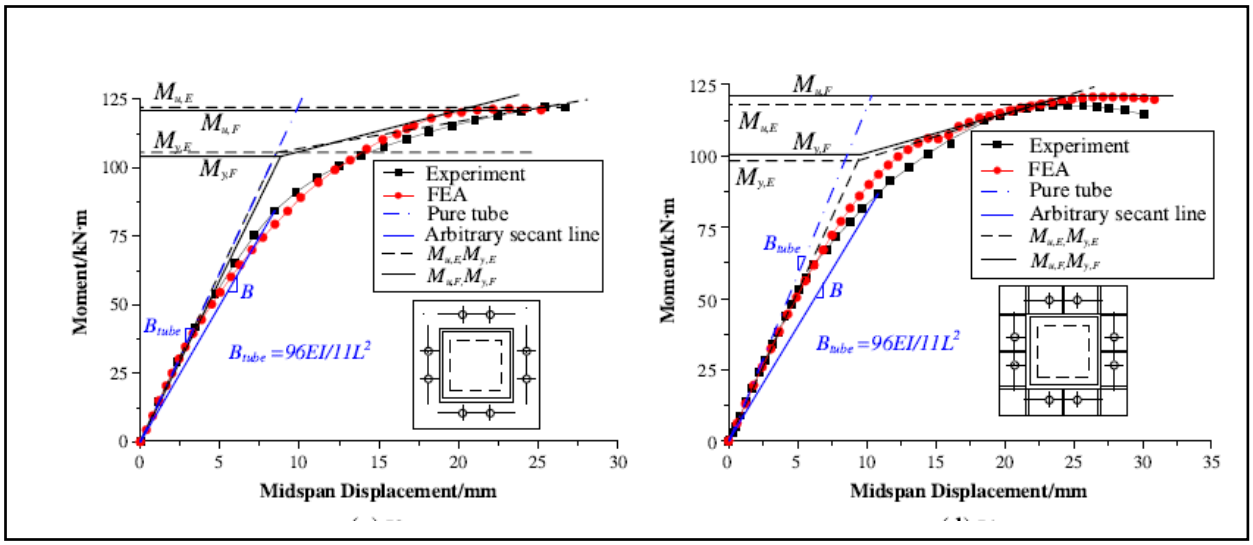

Figure 2-13: Tensile behavior of unstiffened and stiffened square end-plate connections [20]

2.3 Joint characterization

2.3.1 Introduction

Characterization of joints is important to classify them based on stiffness, strength and ductility. To learn the complete behavior of a joint in bending, establishment of appropriate moment rotation curves is required. Also, the moment-rotation curves can be simplified to be used in elastic or plastic global analysis. A design moment-rotation curve should define design moment resistance, rotational stiffness and rotation capacity. Moment rotation curves of a connection can be obtained in three ways:

A. Analytical methods

Analytical procedures make use of functions expressed in terms of geometrical parameters of the joint components. Moment-rotation curves were initially developed using experimental tests. With the help of extensive test results, various mathematical models have been proposed over time. Power law developed by Richard and Abbott (1975) is one of the well-known procedures for establishing the moment-rotation curve. Power model provides a realistic moment-rotation behavior and can be easily implemented in 2nd order frame analysis. Ramberg and Osgood (1943), developed a three-parameter function to model stress-strain data, which was also used to obtain moment-rotation curves. Component method is the most widely used analytical method by researchers. Component method can be applied to any type of steel joint, given that the behavior of joint components is known.

B. Experimental method

This procedure involves testing of a real scale specimen in the laboratory. Experiments are time consuming and involves additional material and transportation costs. But then, initially most of the analytical models were developed based on extensive test results over many years. Experimental tests are the source of the confirmation for finite element results. Confirming the validity of finite element models will allow one to study the effects of geometrical parameters, as well as avoid unnecessary future experimental tests.

C. Finite element method

Recent advancements in technology has provided engineers and researchers with a wide range of finite element software packages like Abaqus, Nastran, Ansys, Diana FEA etc. This method is the most popular method in recent times. Conducting static, dynamics and transient analysis is easier with a software tool compared to experiments. Accurate modelling of connection parameters and material properties is of importance here. Even a minor discrepancy in modelling might lead to variations between finite element results and actual behavior. One can input their own material properties, conduct parametric studies and address non-linear behavior of materials

quite effectively using this method. FE software packages have proved to be an effective substitute for experiments. However, validation of results obtained though software is done by conducting experimental tests for certain cases.

2.3.2 Classification based on stiffness

Stiffness of a joint is necessary when performing an elastic global frame analysis. Engineers usually designed structures by considering joints to be pinned (zero stiffness) or rigid (infinite stiffness). Eurocode provides the possibility to account for joint behavior which is intermediate between that of pinned and rigid. Stiffness of steel joint depends on the connected sections and components used. Stiffness is given in terms of moment resistance per unit rotation. Moment-rotation curves need to be developed for joints to obtain stiffness, if individual component behavior is unknown. According to Eurocode 1993-1-8, joints are classified based on stiffness by comparing the initial rotational stiffness $S_{j,ini}$ of the joint to the stiffness of the connected member [1]. Referring to figure 2-14, joints are classified based on stiffness as follows,

1) Pinned connection: A pinned connection is designed is to only transmit shear, no bending moments and is assumed to have zero rotational stiffness. A beam with pinned end connection behaves similar to a simply supported beam. A typical example of pinned connection is a beam connected to column using fin plates. A pinned connection exhibits the properties of a perfect hinge between the connected member.

2) Rigid connection: Rigid connection is provided to transfer all the forces and moments without significant rotations. All the joint components are sufficiently stiff, while there is limited or no rotation between the ends of connected members. Rather, a single global rigid body rotation is noticed. This type of connection might increase the cost due to larger sizes of component to be used. A typical example of rigid connection is a beam connected to column using an extended end plate

3) Semi-rigid connection: Behavior of a semi-rigid connection is in between that of pinned and rigid connection. They possess some degree of rotational deformability. They allow for design optimization of connected members. An optimal distribution of bending moments in beam can be achieved by tuning the rotational stiffness of the connection [2]. A typical example of semi-rigid connection is a beam connected to column using bolted angle members. There is considerable rotation between the ends of connected members due to transmitted moment.

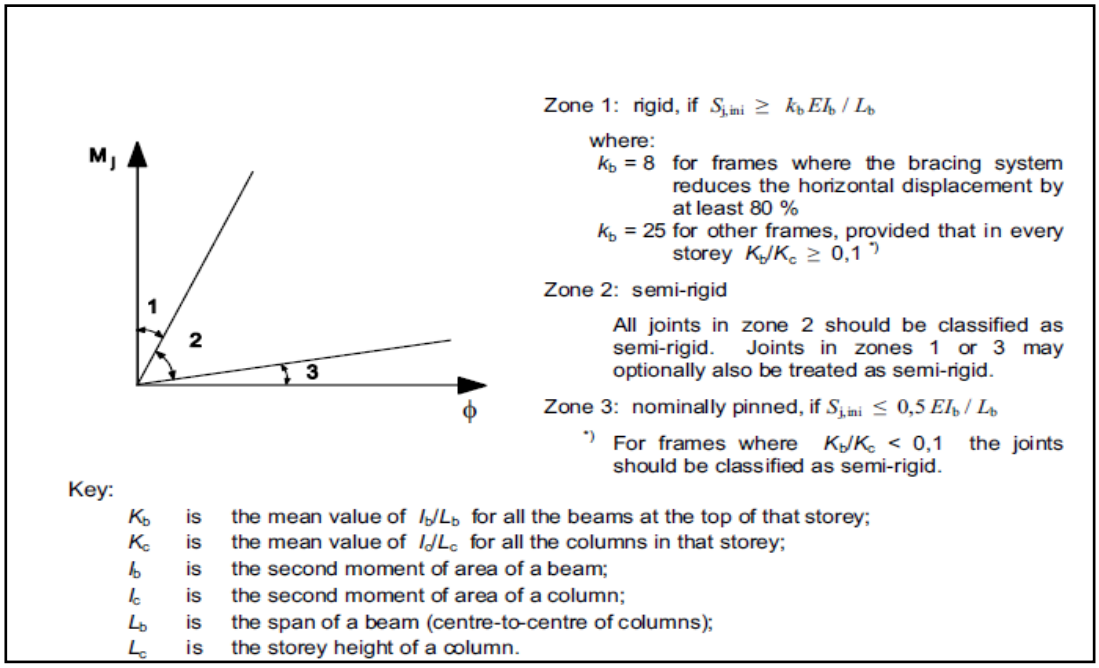

Figure 2-14: Classification of joints based on stiffness [1]

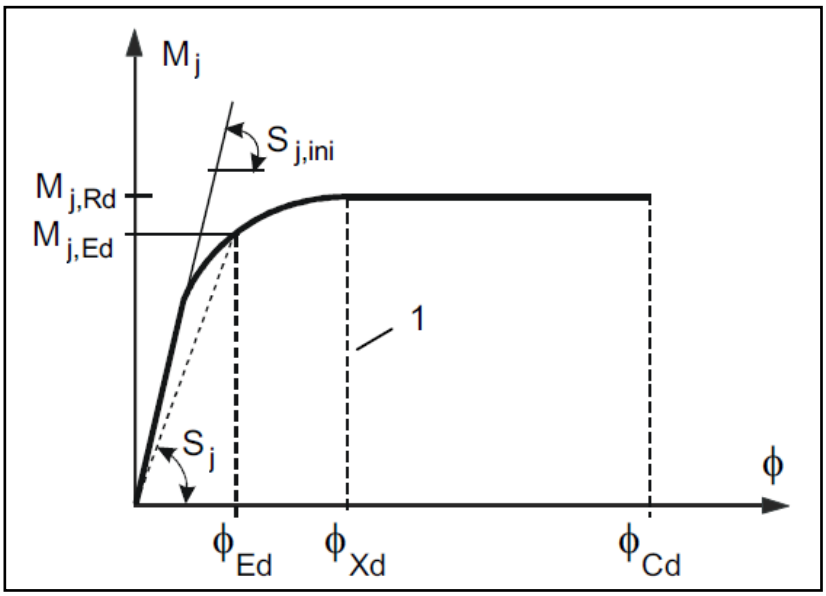

Figure 2-15: Typical moment-rotation curve indicating the initial joint stiffness [1]

2.3.3 Classification by strength

Design moment resistance $M_{j,Rd}$ is considered as the strength of joint. Resistance of joints are necessary when conducting a rigid-plastic analysis. Joints are classified based on strength by comparing its design moment resistance with that of the weakest connected member.

1) Nominally pinned joints: A joint designed to carry not more than 25% of the design resistance of a rigid connection is classified as nominally pinned joint. Shear forces are transmitted without developing significant moments.

2) Full-strength joints: Design moment resistance of a full-strength joint is greater than that of the weakest connected member. They provide full continuity of moments. A full-strength connection is recommended for welded connections, where in brittle failure needs to be avoided.

3) Partial-strength joints: These joints are designed for a resistance somewhere between that of a pinned and full-strength joint. These joints allow partial continuity of moments. A partial strength joint is designed to transfer the internal forces and to not resist the full capacity of connected members.

2.3.4 Classification based on ductility

Classification of joints based on ductility classes was introduced to access the rotational capacity of a joint. Most structural steel joints exhibit a bilinear moment rotation behavior. The curve follows a linear path until yield resistance or elastic capacity is reached. Moment rotation curve thereafter exhibits yielding behavior with reduced slope. This corresponds to onset of strain hardening and possible membrane effects. Resistance of a joint doesn't usually plummet after peak moment resistance. However, collapse of joint immediately after peak moment can be expected in case of weld failure for instance. Performing plastic global analysis requires development of plastic hinges. Plastic hinges occur if there is a sufficiently long yield plateau to allow redistribution of internal forces. Overall, the current classification measures the ability of a joint to resist premature local instability and brittle failure.

2.4 Introduction to component method

Experimental, numerical and analytical approaches can be followed to study the characteristics of a joint. Component method is an analytical tool that can be used to calculate the initial rotational stiffness of a joint $S_{j,ini}$. Component method takes into account the connection behavior at individual component level. Component method is widely recognized by the research community, is a convenient procedure to evaluate the mechanical properties of joints subjected to various loading situations like static, dynamic, fire and earthquake.

Component method doesn't consider joint as a whole, rather it evaluates joint as a set of individual connection components. This is done by evaluating stiffness of individual connection components. Stiffness of any one component depends on its loading situation. Eurocode 1993-1-8 provides a list of 22 formulas that can be used to calculate the individual component stiffness. These stiffness coefficients can be used to compute the rotational stiffness of a beam-column, beam-splice and column base connections made of I and H-sections.

1) Identification of active components:

   Firstly, the whole joint is idealized into individual components such as end plate, beam web, column flange etc. While several of these components exist in a joint, identification of those that contribute towards the initial stiffness of the joint is of importance. Identification of active components also depends on loading conditions, since some of the components active in bending around major axis might not be active in bending around minor axis. In figure 2-16 an example of beam-column connection, where beam is subjected to bending is shown. In this case, beam is connected to column using bolted end plate that is welded to beam ends. Welds are considered to not affect the initial rotational stiffness [1]. Only top bolt row in end plate is activated in tension and contributed to initial rotation stiffness. In the column there are two equal and opposite forces at top bolt row level and at point of compression level. This causes shear stresses in the column web panel. Due to the tensile forces in top bolt row, flange and web of the column are subjected to tension. Compression at the point of rotation causes compressive stresses in column web, while interaction with shear is also considered. Individual components are numbered based on table 6.11 of Eurocode shown in figure A-1.

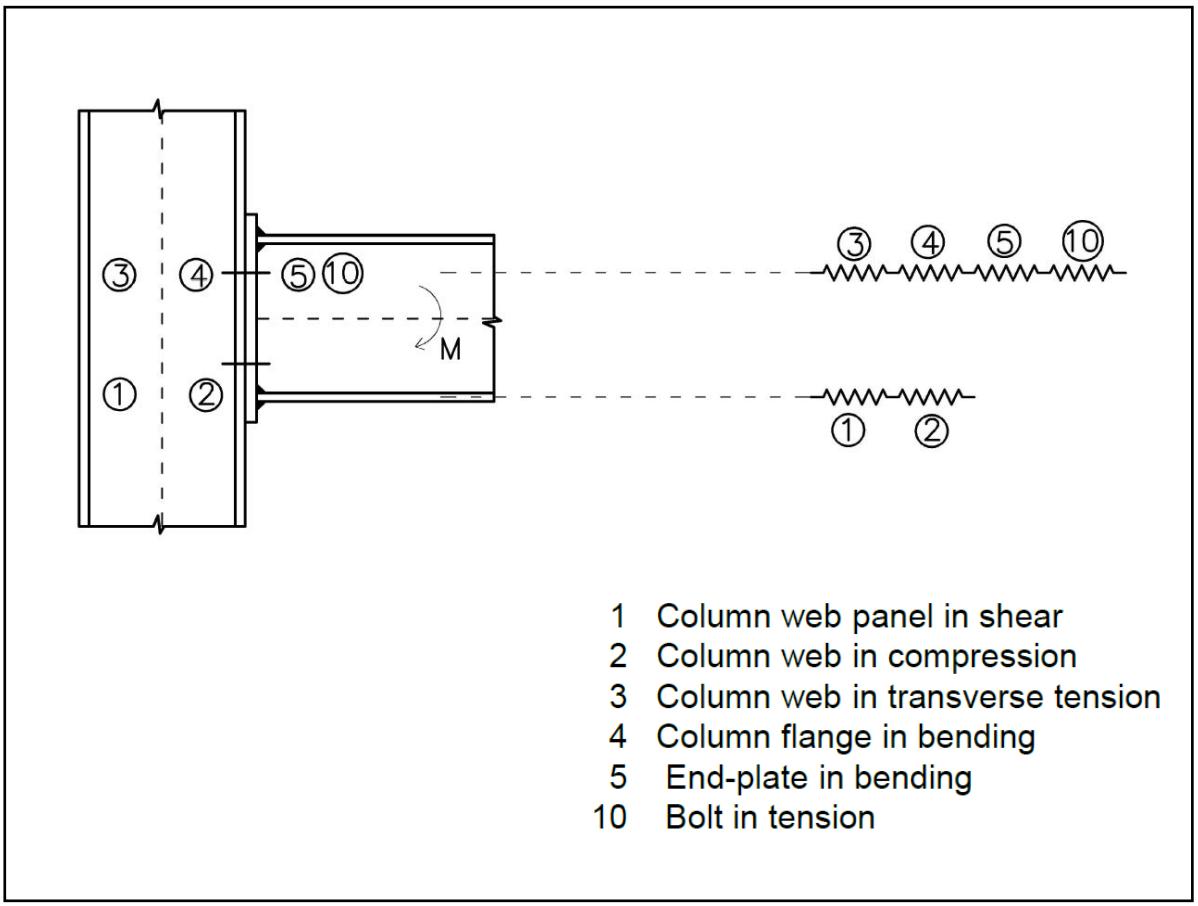

Figure 2-16: Identification of active components in a connection

2) Evaluation of the stiffness and/or resistance characteristic of each individual basic component:

   Based on experimental and analytical data, individual analytical formulas and procedures for certain individual joint components have been established [3,4]. To perform this step of component method, knowledge of forces acting on individual components is required. This was done in the previous step where active components were identified. Table 6.11 in Eurocode 1993-1-8 gives a list of basic components for the application of component method to the example described in figure A-1. Stiffness co-efficient of column web in tension, column flange in bending and end plate in bending were derived using T-stub theory. This requires calculation of effective lengths at the bolt row of interest.

3) Assembly of all constituent components and evaluation of the stiffness and/or resistance characteristics of the whole joint:

   Main idea of component method is to idealize individual components as flexible springs that possess certain stiffness. Stiffness of these springs can be computed as described in the previous step. These idealized springs are then arranged in series and parallel depending on the joint layout as shown in figure A-2. Initially, the effective stiffness of components in series at top bolt row level and at point of compression is calculated. Then, the equivalent stiffness of two effective stiffnesses arranged parallelly is computed. Distance between the top bolt row and point of compression is taken as the lever arm. If more than one bolt row is active in tension, then equivalent lever arms need to be calculated.

2.5 T-stub idealization

T-stub model was initially developed by Zoetemeijer in 1974. In Eurocode 1993-1-8, some of the components are idealized as a T-stub in order to calculate their design resistance and stiffness. Basic components in a beam-column and column base joint that idealize T-stub are column flange in bending, end plate in bending, flange cleat in bending and base plate in bending under tension. These are the basic component that allows transfer of tensile forces in bolted connections. These joint components are further idealized as T-stub using their effective lengths. An example of T-stub idealization for end plate in bending present in a beam-column connection is shown in figure 2-17.

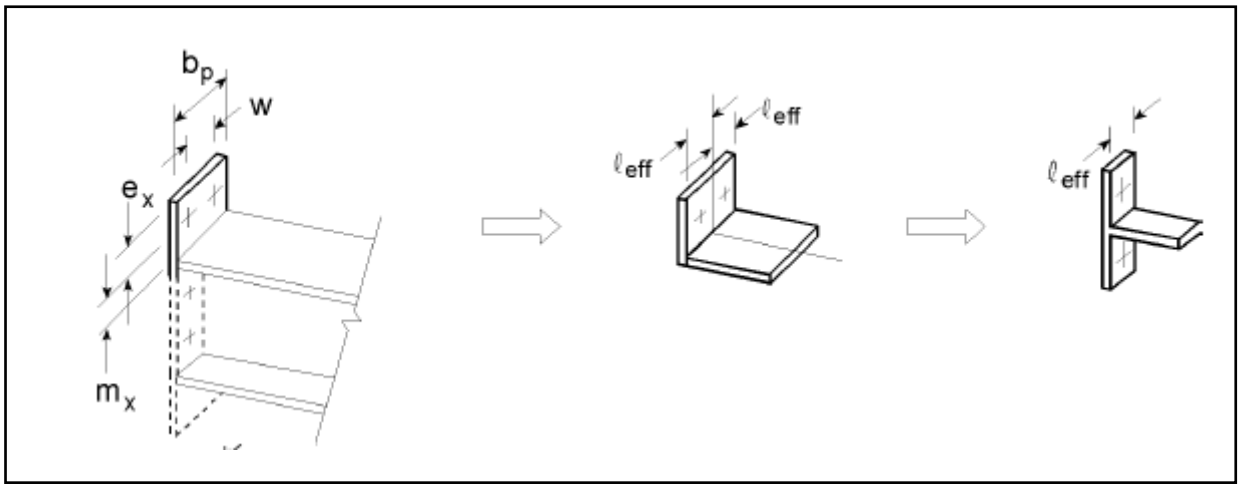

Figure 2-17 – T- stub idealization of end plate in bending [1]

A T-stub consists of two parts, web in tension and flange in bending. The flange of a T-stub is assumed to be bolted to a rigid foundation. The individual effective length depends on the yield pattern and bolt row position, which in turn depends on the layout of the connection. In case of T-stub, effective lengths are classified are circular and non-circular patterns. These individual effective lengths also differ when a bolt row in considered individually and as part of a group of bolt rows. Lowest magnitude of effective length that gives the least design resistance will be governing for design purposes [5]. A T-stub connection may fail in three ways:

Mode 1: Yielding of flange
This mode is associated with bolts being considerably stronger than the flange. Plastic hinges are formed in the flange while it bends as shown in figure B-1a. Four plastic hinges are formed at bolt locations and adjacent to the web on both sides. This failure mode is usually observed in case of a thin flange.

Mode 2: Failure of bolts with partial yielding of the flange
Yield lines are formed in the flange adjacent to web on both sides as shown in figure B-1b. Full plastic mechanism is still not reached in the flange. Bolts are critical in this failure mode, as they fail before the flange. Bolts fail due tensile strength being reached. This mode can be noticed in case of a moderately thick flange. There is an

increase in bolt forces due to prying action and leads to failure of bolts before flange yields.

Mode 3: Failure of the bolts
Deformation of the flange is considerably smaller leading to no prying force as shown in figure B-1c. Failure of bolts in tension is the primary failure mechanism in this case. This mode can be observed in case of thick flange where flange is much stiffer than the bolts.

Design resistance of T-stub depends on the three failure modes mentioned earlier and hence calculated for all these modes. Failure mode that gives least resistance is considered to be the governing failure mechanism and design resistance. Eurocode 3 part 1-8 provides appropriate formulas to calculate design resistance of T-stub as shown below,

Mode 1: Yielding of flange

$$F_{T,Rd,1} = \frac{4\, l_{eff,1}\, m_{pl,1,Rd}}{m} \quad (2.1)$$

Mode 2: Failure of bolts with partial yielding of flange

$$F_{T,Rd,2} = \frac{2\, l_{eff,2}\, m_{pl,1,Rd} + n\Sigma F_{t,Rd}}{m+n} \quad (2.2)$$

Mode 3: Failure of bolts

$$F_{T,Rd,3} = \Sigma F_{t,Rd} \quad (2.3)$$

$m_{pl,Rd} = plastic\ bending\ resistance\ of\ the\ T-stub\ flange\ per\ unit\ length$

$l_{eff,1}\,, l_{eff,2} = minumum\ effective\ lengths\ of\ the\ yield\ lines\ for\ mode\ 1\ and\ 2\ respecively$

$m\ and\ n = Bolt\ distance\ from\ column\ face\ and\ plate\ edge$

2.6 Modified stiffness model of hollow section end-plate connection

As mentioned earlier, Eurocode 1993-1-8 provides stiffness coefficient for end plate in bending. These can be applied to column-flange in bending, base plate in bending etc. It is to be noted that these stiffness co-efficients are applicable if only I and H-sections are used for connection. However, use of stiffness coefficients of Eurocode for RHS end-plate connection produced too high stiffness [9]. In some cases, initial stiffness was overestimated by more than 50%. Karlsen and Aalberg developed a modified stiffness model for RHS end-plate connections bolted on two sides. This modified stiffness model was based on beam theory. Similar failure mechanisms as described by Eurocode were noticed in experiments and finite element results.

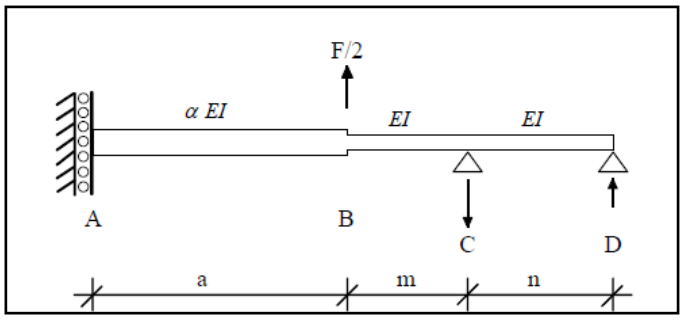

Figure 2-18: Structural model proposed by Karlsen and Aalberg [9]

The above model was developed from a RHS end plate joint connected with bolts on two sides. It is a one-dimensional model, representing a beam strip of the end-plate. Due to symmetry, only half of the joint was considered, which spans from point A to D as shown in figure 2-18. Point A is the center of RHS, B is the outer edge of RHS, C is the bolt position and D is the free edge of the end-plate. Applying beam theory, initial elastic stiffness of this joint was derived. Modified stiffness co-efficient for end plate in bending (k_p) and bolts in tension (k_b) is shown below. These stiffness coefficients are further used to evaluate the joint stiffness of non-symmetrical column splice connection. Part of the end plate inside the hollow section is given an increased rigidity due to the profile of hollow section. This is introduced using factor α, where in $\alpha = 1$ refers to stiffness being the same throughout the plate.

$$k_b = \frac{4n\,(3a+3m\alpha+n\alpha)\,A_s}{(6am+6an+3m^2\alpha+2n^2\alpha+6nm\alpha)\,L_b} \tag{2.4}$$

$$k_p = \frac{2\,(3a+3m\alpha+n\alpha)\,l_{eff,ini}\,t_p^3}{m^2(3m^2\alpha+4nm\alpha+12am+12an)} \tag{2.5}$$

Chapter 3 – Finite element modelling of non-symmetrical column splice connection

3.1 Introduction

Numerical simulation is an effective tool to study new types of geometries, connections and effects of geometrical parameters on the characteristics of a steel joint. Initial attempts at numerical analyses of bolted end-plate connections were performed using two-dimensional models by Krishnamurthy et al in (1979) and Chen (1984) [10]. Over time, computational capacity of computers was increased and new finite element packages employing three-dimensional models were developed. Finite element package Abaqus was initially released in 1978. Bursi and Jaspart (1997) used Abaqus software package to model end plate bolted connections using brick elements [24]. A realistic simulation can be obtained if the underlying assumptions of modeling are accurate enough. Interactions between various connection components, finite element type and geometric and material non-linearities are some of the complications that need to be taken into account.

Numerical simulations are conducted using FE software package Abaqus. Using Abaqus a three-dimensional model of the non-symmetrical column splice connection was built. Firstly, the specimens were pre-designed according to Eurocode 3, conforming to bolt hole clearance, bolt edge distance etc.

3.2 Geometry

Three-dimensional models were initially built on AutoCAD and then imported into Abaqus. Bolt head, nut and shank were modeled as one single part. This is done to avoid defining numerous interactions in the pre-processing stage. Regular hexagonal bolts used for end plates were idealized as circular parts and created in AutoCAD. A solid bolt model is the most accurate at predicting the physical behavior of a connection [11]. Hollow section columns were modeled considering appropriate corner radii for filleted corners. End plate and cover plate were modelled as it is, in accordance with standard tolerances for bolt holes. All these three-dimensional models were imported into Abaqus as solid 3-D elements and then assembled appropriately.

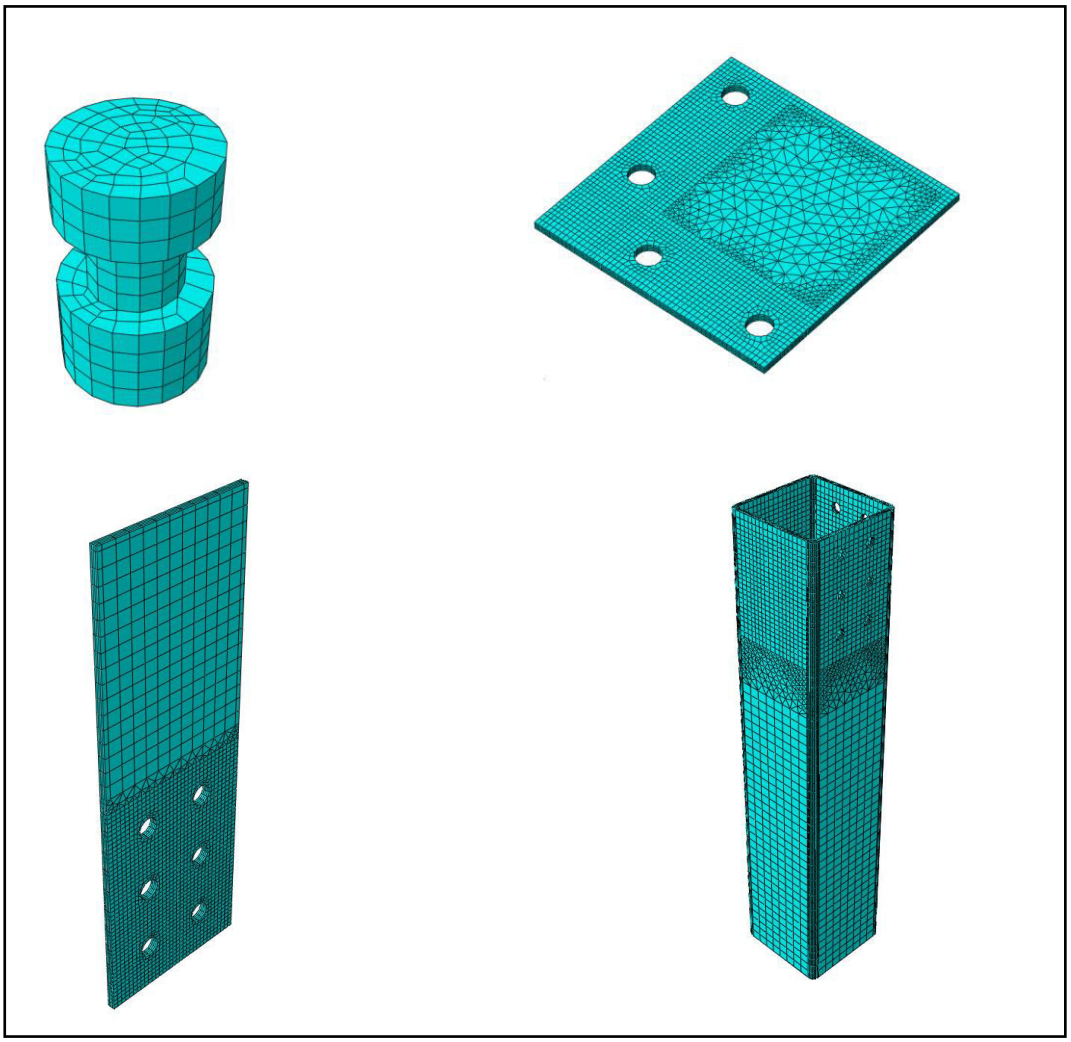

Figure 3-1: Finite element model of connection components built on Abaqus

3.3 Material properties

Steel grade S355 with a density of 7850Kg/m3 was assumed for hollow section profile, end plate and cover plate. Bolts were assumed to be of grade 10.9 with a density of 7850 Kg/m3. Abaqus requires true stress-strain properties for incorporating material non-linearity appropriately [12]. True stress by definition is the load applied to the actual cross-section i.e. changing area of the specimen with respect to time. True stress-strain data offers a much accurate simulation that is close to physical behavior than the engineering stress-strain data. Data obtained through coupon tests in experiments is engineering data. This can be converted to true stress-strain curve using the following formula provided in Annex-C of Eurocode 1993-1-5.

$$\sigma_{true} = \sigma\,(1 + \epsilon) \quad (3.1)$$

$$\epsilon_{true} = l\mathrm{n}(1 + \epsilon) \quad (3.2)$$

Engineering stress (MPa)	Engineering strain	True stress (MPa)	True strain
0	0	0	0
355	0.001690476	355.600119	0.001689049
360	0.0125	364.5	0.01242252
470	0.05	493.5	0.048790164
520	0.1	572	0.09531018
520	0.175	611	0.161268148
504	0.23	619.92	0.207014169
360	0.26	453.6	0.231111721

Table 3-1: Stress-strain data for steel grade S355

A homogenous solid section where in material properties are uniformly distributed through the section was applied to the modelled connection. In Abaqus, these solid elements can be used for linear analysis and for complex non-linear analyses involving complex interactions, plasticity and large deformations.

3.4 Analyses method

A quasi-static analysis was performed using Abaqus dynamic explicit solver to account for material and geometric non-linearity. Implicit solver has convergence issues and this can be avoided by using the explicit solver [13]. Abaqus creates a special initial step that can't be edited in the analysis procedure. Boundary conditions, predefined fields and interactions that are applicable at the very beginning of the analysis are allowed to be defined in this initial step. Non-linear geometric effects can be considered by using the option "NLGEOM".

Natural time scale is generally not important in quasi-static analysis. However, the time required for analysis needs to be decreased in order to obtain an economical solution. Speed of simulations in Abaqus depends on maximum stable time increment, which affects the time period of each loading step. Stable time increment in an explicit analysis is affected by wave propagation speed, size of finite element and density of the material. While maximum stable time increment directly relates to the lowest possible magnitude of stable time increment and this affects the whole analysis. Higher the value of stable time increment, higher will be the time required for calculation [12].

These issues related to computational speed can be solved by implementing techniques such as mass-scaling. Mass-scaling is a technique where in non-physical mass is added to the model to increase the value of maximum stable time increment and increased computational efficiency. Mass-scaling can be done only for a portion of the model or entire model. If only a portion of the model is scaled, then the elements that are not scaled might have a higher maximum stable time increment than the value assigned. With this technique, a minimum stable time increment value can be set and Abaqus scales the elements in a model to match individual stable time increments to the target set by user. In addition, the stable time increment determined through element-by-element estimator will be lower than the global estimator. Hence, mass-scaling is applied to the whole model. Non-uniform mass scaling where in masses of elements are scaled according to their element sizes was used in the present analyses.

One should also note that, increasing the mass of elements using mass-scaling technique might lead to huge inertial forces. Due to this, finite element model may not behave as expected or might output unacceptable results. Therefore, the minimum stable time increment value chosen should be such that a balance is obtained between economy and acceptable results. Smooth step amplitude option available in Abaqus is used to avoid inertial effects to a considerable extent [13]. An example of smooth step amplitude is shown in the figure 3-2. In figure 3-3, a comparison between different values of user-defined stable time increment is shown. A stable time increment of 0.001s was used for the present numerical analysis.

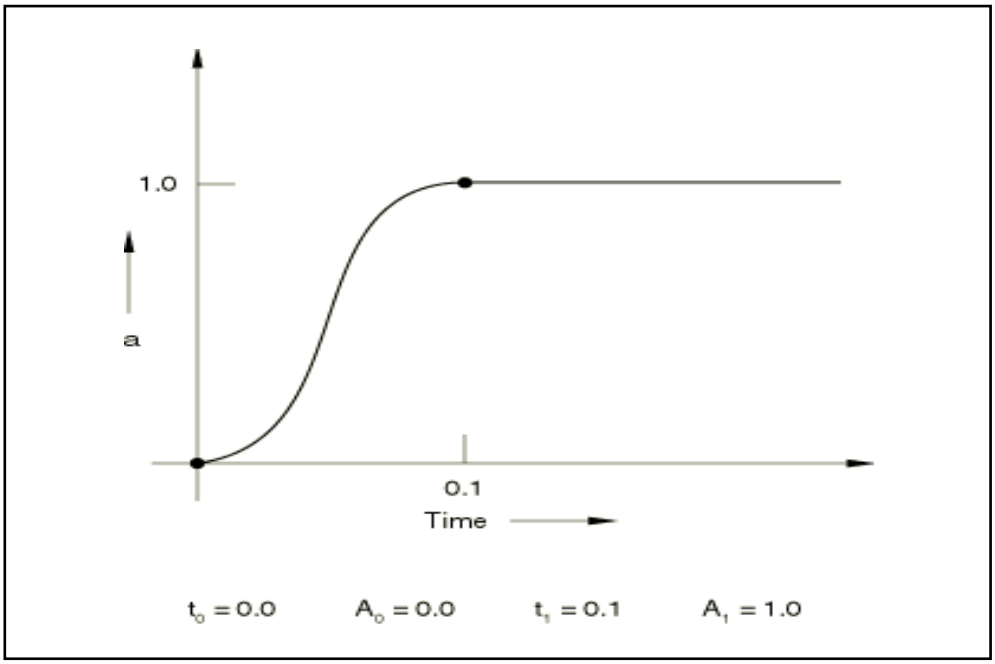

Figure 3-2: An example of smooth step amplitude [12]

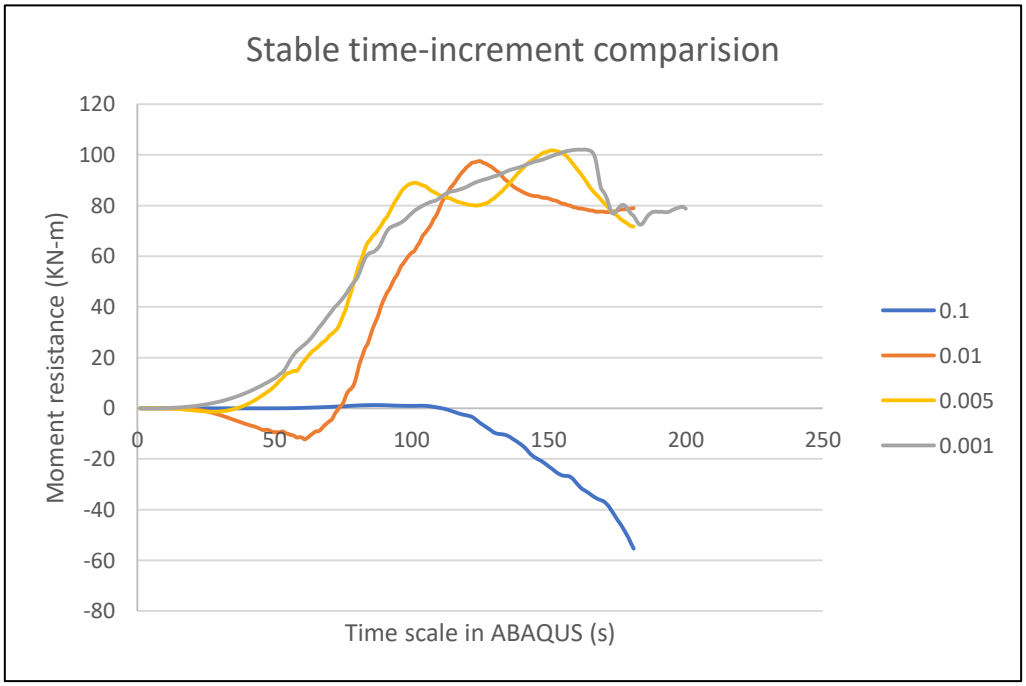

Figure 3-3: Comparison for choosing appropriate time increment value

3.5 Interactions and boundary conditions

Modelling the contact behavior between basic components in the model is of high importance, since it affects the results significantly. Contact interaction property in Abaqus can be defined as tangential behavior (friction and elastic slip) and normal behavior (hard, soft or damped contact and separation). Contact interaction for friction surfaces were defined using tangential behavior. A friction co-efficient of 0.4 was used. Rest of the contacts in the model were defined using normal behavior and all surfaces were allowed to separate. Interaction between the two end plates was defined as a friction surface. Bolt head and nut surface interaction with end plate and cover plate surface were also defined as friction surfaces. Interaction of bolt surface with bolt holes was defined as a hard contact.

Another important step is to define weld in the numerical models. Column ends are welded to the end plate and cover plate is welded to the top column on three edges. Welds were not modelled as individual components in this study. Instead, welds were defined using "tie-constraint" option at required locations in the model. Tie-constraint ties the surfaces to be connected using nodes along the edges of the connected surfaces. The sides of column end that are not welded also interacts with the end plate. This interaction is defined as hard contact.

Tensile load was applied using displacement control method at the top of the specimen. Bottom of the specimen was modelled with pinned boundary conditions and top of the specimen was free with displacement applied in vertical direction. Reaction force was taken at the bottom pinned point of the specimen, while vertical displacement was taken at the top of the specimen. Bending behavior of the specimens were obtained by adopting a four-point bending test. Rotation was taken as the rotation between top and bottom end-plates.

3.6 Meshing

Choice of finite element model and meshing is the final step of pre-processing stage. Fine mesh was used at locations where high stresses are expected and course mesh was used on other locations. Most appropriate type of finite element for explicit analysis as advised in Abaqus guide is an 8-node continuum hexahedral element with reduced integration (C3D8R). Reduced integration elements were developed to increase computation efficiency without loss of accuracy. Description of 8-node hexahedral element with full-integration and reduced integration is shown in the figure 3-4 and 3-5.

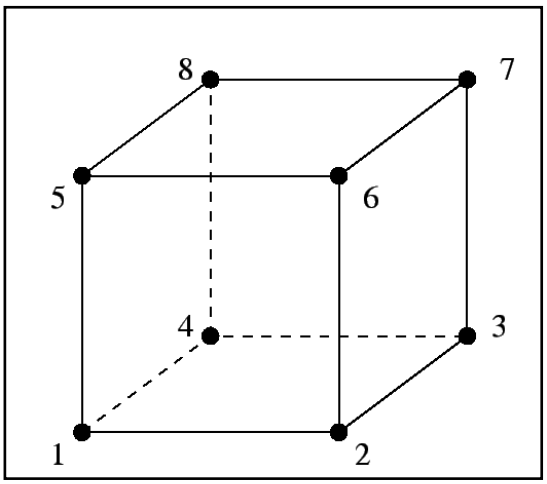

Figure 3-4: 8 node fully integrated hexahedral finite element (C3D8), [14]

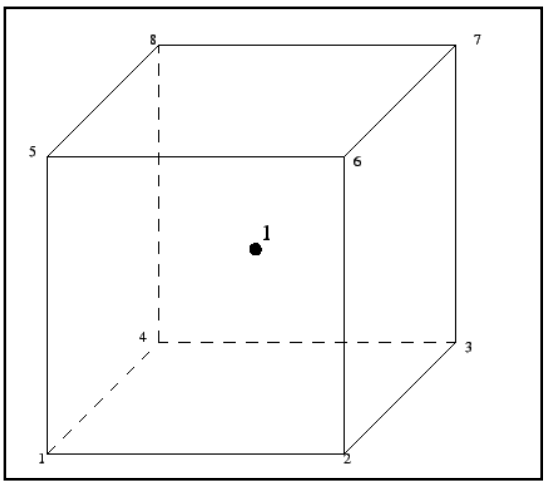

Figure 3-5: 8 node hexahedral elements with reduced integration (C3D8R), [14]

Reduced integration uses a lower-order of integration to form the element stiffness matrix. For a three-dimensional model, reduced integration reduces the running time of simulation. For example, a C3D8 has 8 integration points, while C3D8R has one integration point. C3D8

is observed to be too stiff in bending, while C3D8R tends to be not stiff enough in bending. Integration point for C3D8R is located in the middle of the element and that's where stresses and strains are highly accurate. Thus, small elements are required at the boundaries to capture stress concentrations. C3D8R elements sometimes to lead to hour glassing. Hour glassing is a phenomenon where in large displacements are noticed without significant increase in strains. This can be avoided by using at least four elements in thickness direction. In addition, use of reduced integration elements over fully integrated elements eliminates the possibility of shear and volumetric locking [25]

3.7 Specimen matrix

Non-symmetrical column splice connections are studied under bending and tensile behavior. A total of six specimen models were created for non-symmetrical corner splice connection and six specimens for non-symmetrical intermediate splice connection. Experimental tests are planned to be conducted for specimen CC-1 and IC-1 as part of future work. Hence, these specimens are discussed extensively in chapter 4 and 5. Thickness of end-plate and cover plate was varied to study the effects on connection resistance and initial rotational stiffness. In addition, bolt arrangement in end-plate is studied by varying parameters m and c. All bolts were made of grade 10.9 provided nominal bolt hole clearance.

Specimen	**Column cross-section**	**End-plate details**					**Cover plate details**			
		Bolts	**t (mm)**	**m (mm)**	**n (mm)**	**c (mm)**	**Bolts**	**e (mm)**	**s (mm)**	**p (mm)**
CC-1	SHS 200X8	M24	8	35	35	130	M20	50	75	70
CC-2	SHS 200x8	M24	6	35	35	130	M20	50	75	70
CC-3	SHS 200X8	M24	10	35	35	130	M20	50	75	70
CC-4	SHS 200X8	M24	8	45	35	130	M20	50	75	70
CC-5	SHS 200X8	M24	8	55	35	130	M20	50	75	70
CC-6	SHS 200X8	M24	8	45	35	80	M20	50	75	70

Table 3-2: List of specimens for non-symmetrical corner splice connection

Specimen	Column cross-section	End-plate details					Cover plate details			
		Bolts	t (mm)	m (mm)	n (mm)	c (mm)	Bolts	e (mm)	s (mm)	p (mm)
IC-1	SHS 200X8	M24	8	35	35	130	M20	50	75	70
IC-2	SHS 200x8	M24	6	35	35	130	M20	50	75	70
IC-3	SHS 200X8	M24	10	35	35	130	M20	50	75	70
IC-4	SHS 200X8	M24	8	45	35	130	M20	50	75	70
IC-5	SHS 200X8	M24	8	55	35	130	M20	50	75	70
IC-6	SHS 200X8	M24	8	45	35	80	M20	50	75	70

Table 3-3: List of specimens for non-symmetrical intermediate splice connection

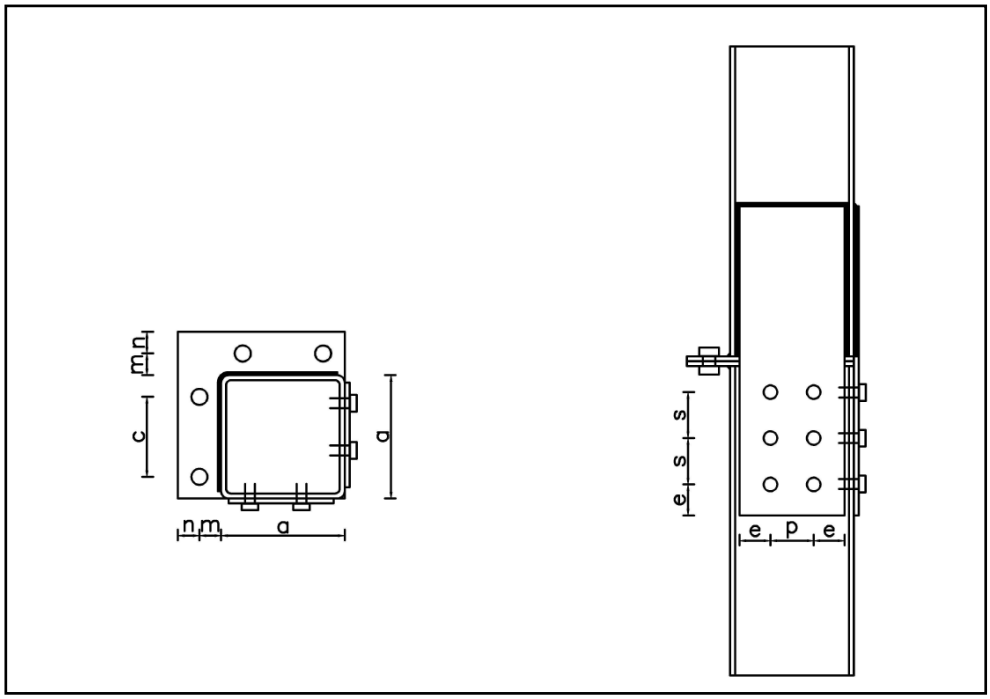

Figure 3-6: Plan and elevation of non-symmetrical corner splice connection

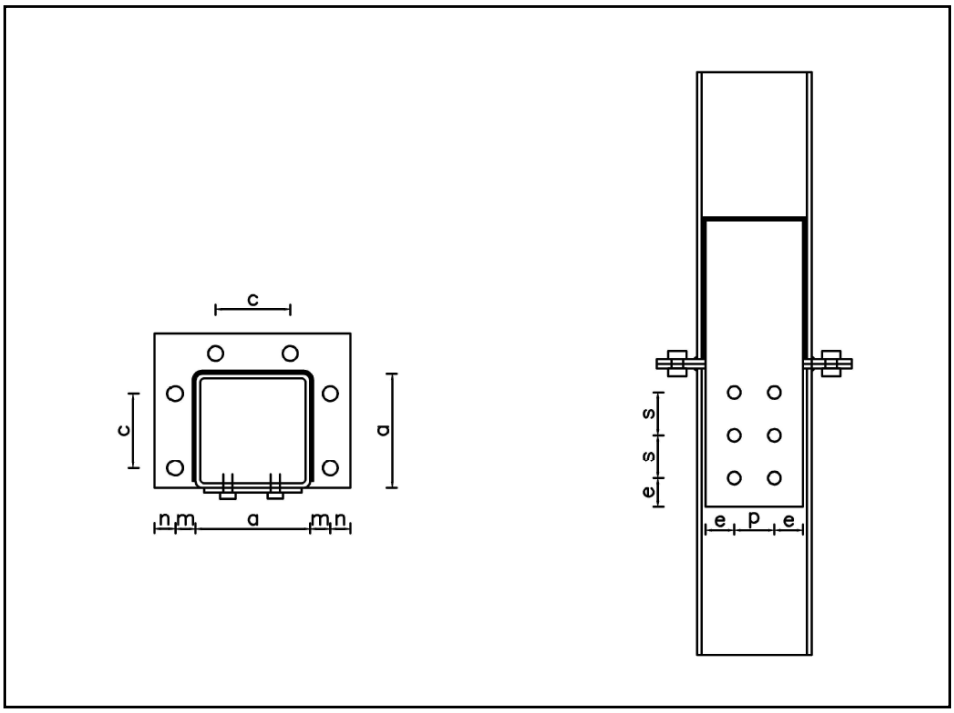

Figure 3-7: Plan and elevation of non-symmetrical intermediate splice connection

Chapter 4– Finite element results of non-symmetrical corner splice connection

4.1 Introduction

In this chapter finite element results obtained for non-symmetrical corner splice connection specimen CC-1 are discussed. Non-symmetrical column splice connection for corner column can be evaluated under tensile case and two bending cases. Whole specimen is subjected to an axial load to evaluate the connection components under tensile force. In bending it can be seen that the connection behaves differently for bending around X and Z-axes of the column cross-section. Since, square hollow sections are used, bending resistance is varied by the connection in itself and not due to column cross-section. First bending case is around X-axis away from Z-axis causes main cover plate to act in compression. Second bending case is around Z-axis away from X-axis that causes side cover plate to be loaded in tension as seen in figure 4-2.

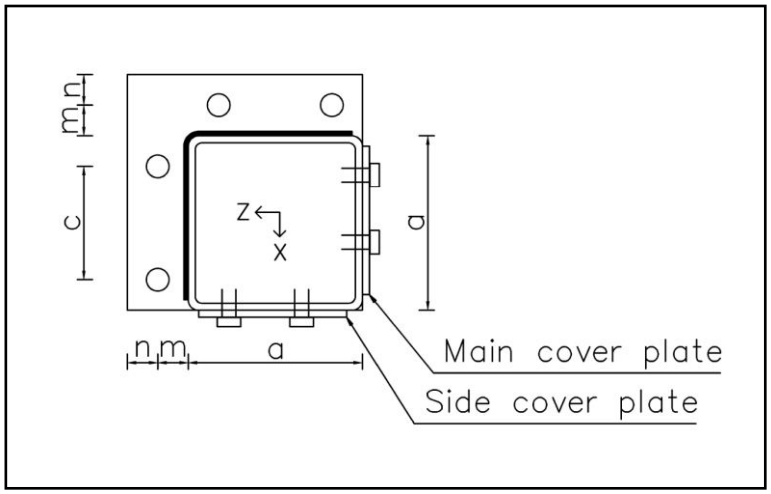

Figure 4-1: Bolt layout of non-symmetrical corner splice connection

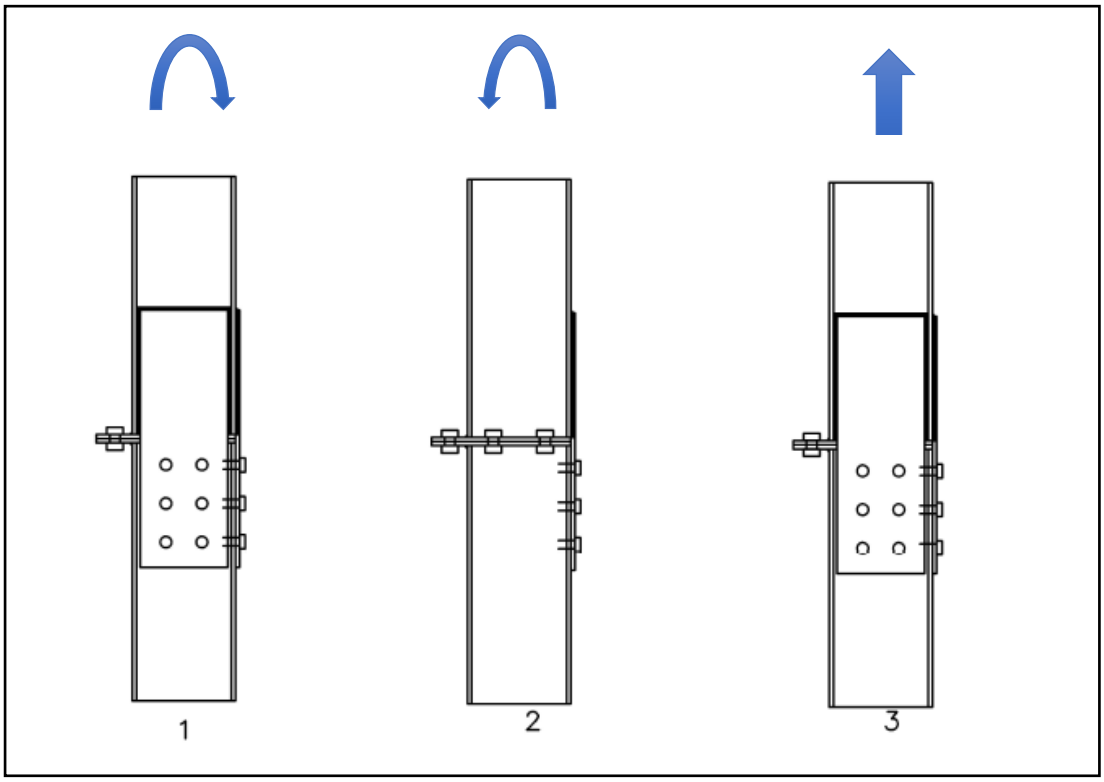

Figure 4-2: Load cases for non-symmetrical corner splice connection

List of load cases for non-symmetrical corner splice connection:
Load case 1 – Cover plate in compression (bending)
Load case 2 – Cover plate in tension (bending)
Load case 3 – Specimen in tension

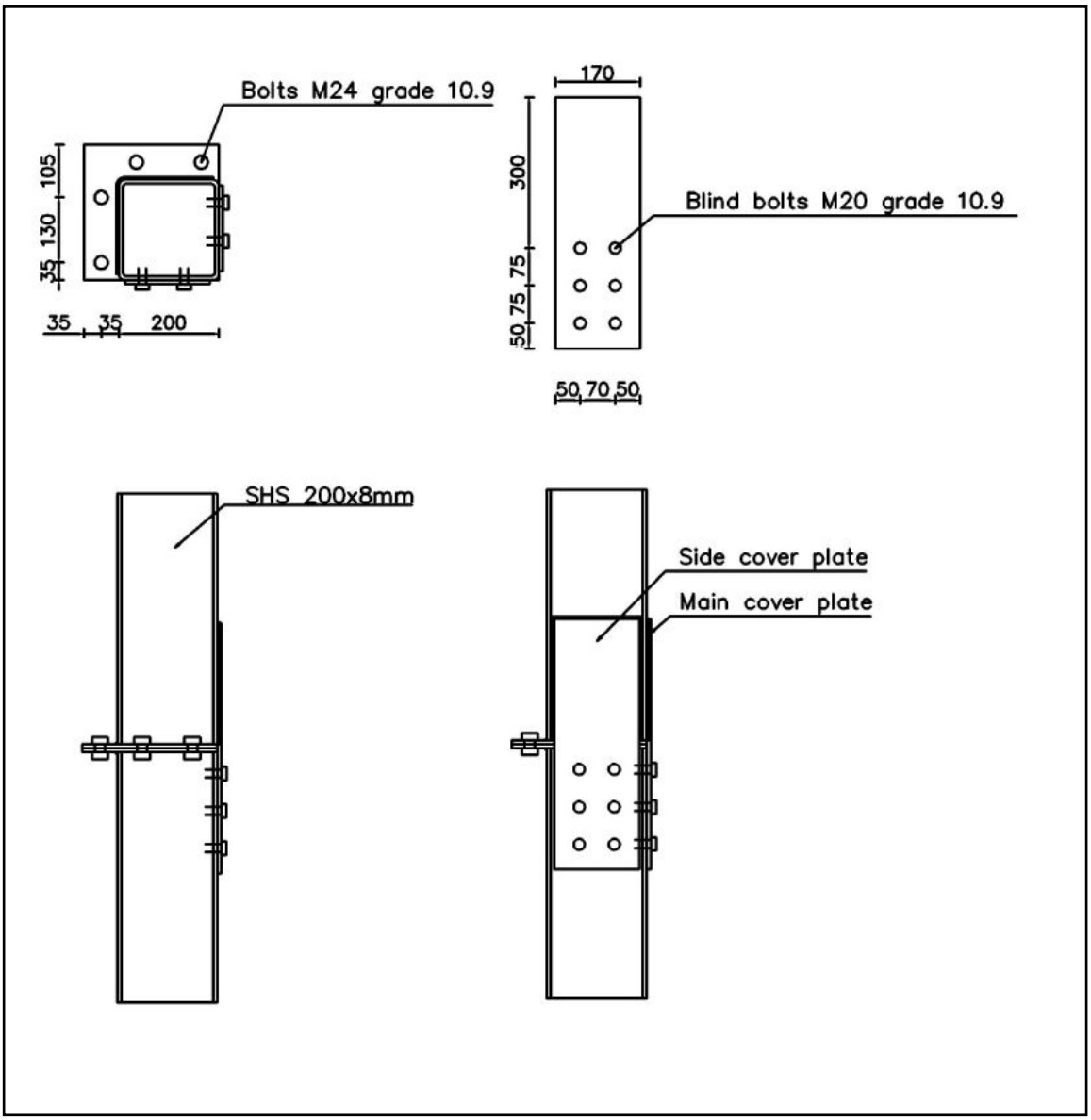

Figure 4-3: Plan and elevation of specimen CC-1

4.2 Non-symmetrical corner splice – cover plate in compression

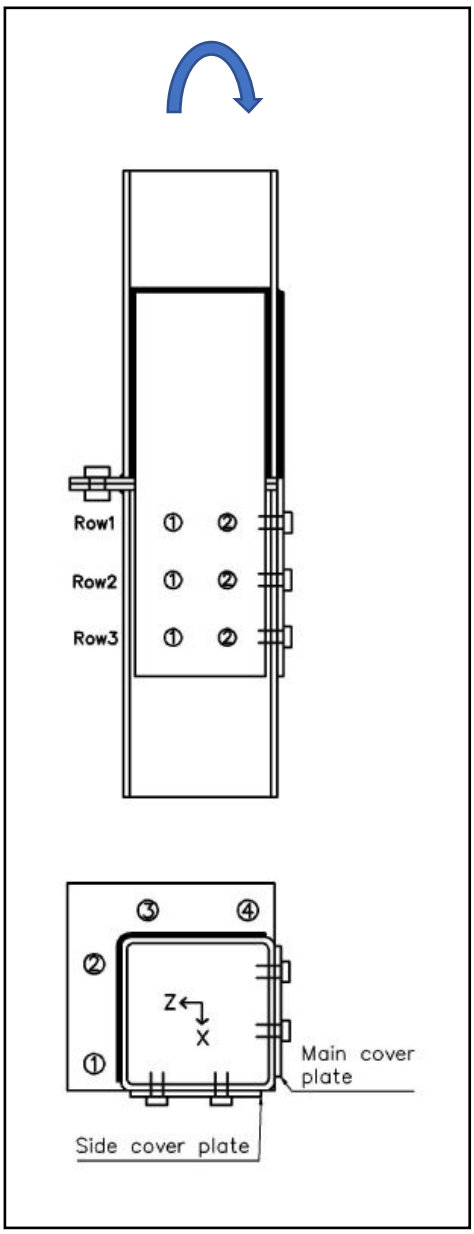

Figure 4-4: Plan and elevation of specimen CC-1 (Case 1)

Top column bends around X-axis towards the main cover plate due to applied load. Rotation of the connection is taken as the rotation between end-plates. End-plate rotation is calculated between top and bottom end plate as shown in figure 4-5. Non-symmetrical layout of the connection leads to uneven force distribution. This causes rotation of end plate to vary based on the section of end plate that is considered. This causes torsion in the connected columns. This is not the case for a conventional end-plate connection. End-plate rotation can be calculated at section 1 and section 2 of end plate as shown in figure 4-6.

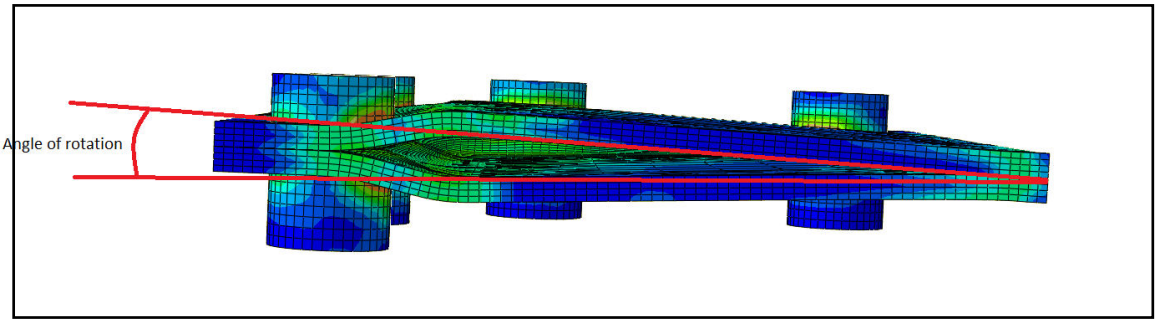

Figure 4-5: Angle of rotation between end-plates (CC-1/case 1)

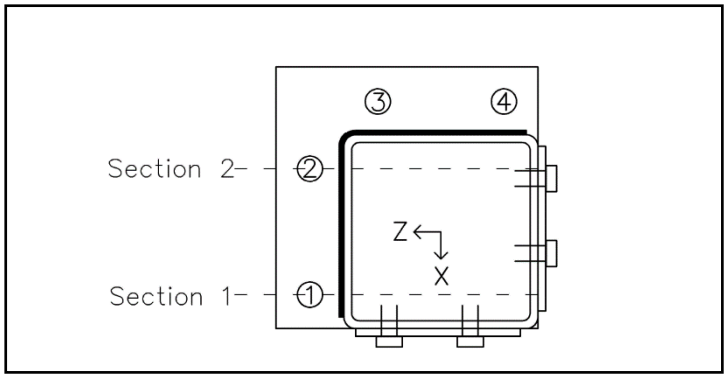

Figure 4-6: Locations in end-plate to calculate rotation (CC-1/case 1)

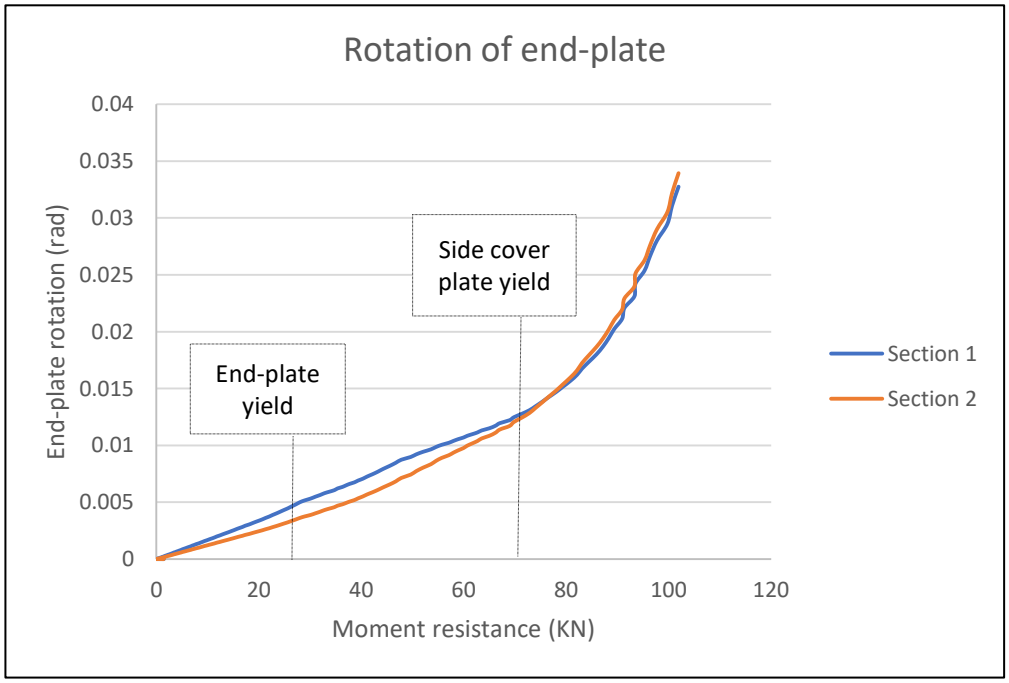

Figure 4-7: Moment resistance vs end-plate rotation (CC-1/case 1)

Rotation calculated along section 1 is higher than section 2 until yield resistance of the connection is reached as seen in figure 4-7. Stiffness at section 2 is higher than section 1 and marginally lower after side cover plate yield. However, secant stiffness is approximately the same for both sections. Since emphasis is placed on initial rotational stiffness, section 1 is considered to study the moment rotation behavior of non-symmetrical corner splice for the present bending case.

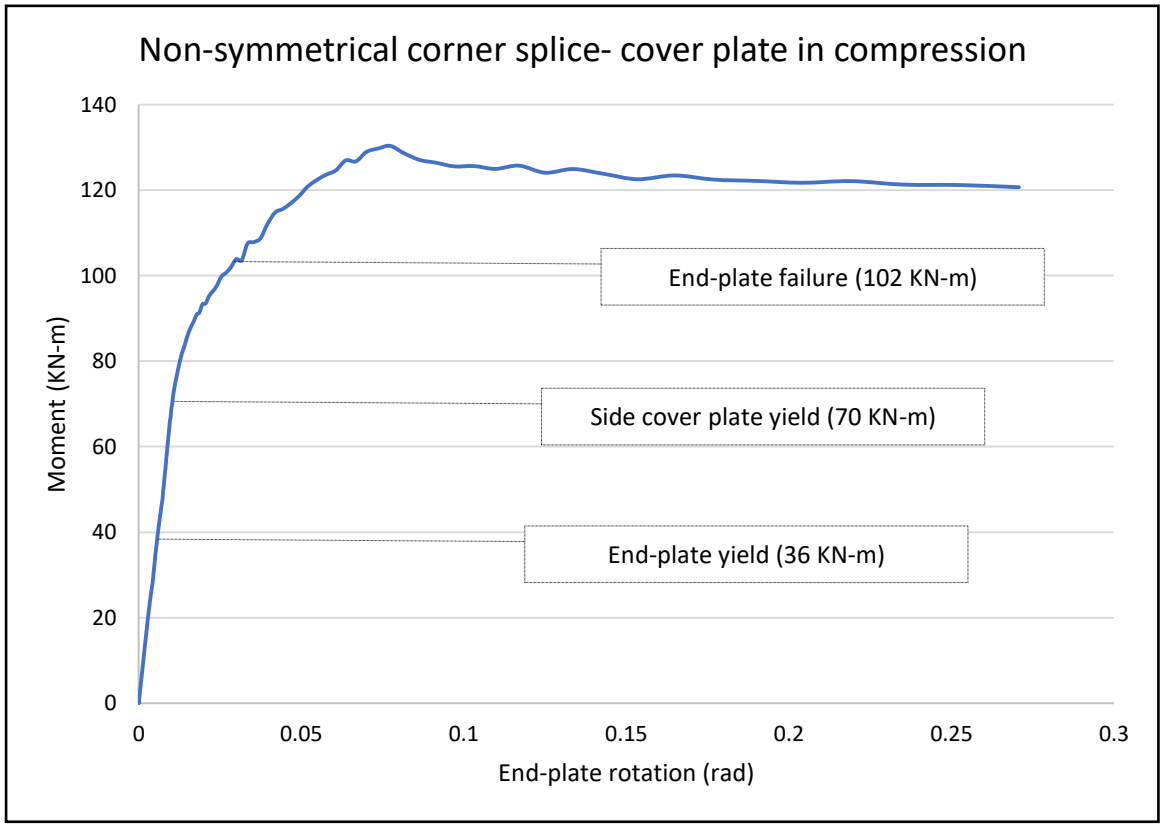

Figure 4-8: Moment-rotation curve of specimen CC-1 (case 1)

In the initial stages of loading, bolts 1,2 and 3 in end-plate carry most of the applied load. Varying tensile force in bolt 1 and 2 was noticed as seen in figure 4-10. This is caused due to uneven force distribution in the connection. Tensile and shear forces carried by bolts in side and main cover plate are lower than 10 KN until the moment resistance is close to 36 KN-m. This is due to the nominal bolt hole clearances provided in cover plates and bottom column. At a moment resistance of 36 KN-m, yield stresses are attained in end-plate. End-plate yields in the region near bolt 1 and 2 as shown in figure 4-9. Side cover plate contributes towards resistance fully after a moment resistance of 36 KN-m is reached. Hence, a typical non-linear behavior of the moment-rotation curve is not seen after 36 KN-m. End-plate doesn't deform freely after yield point, since its deformation is limited by the presence of side cover plate.

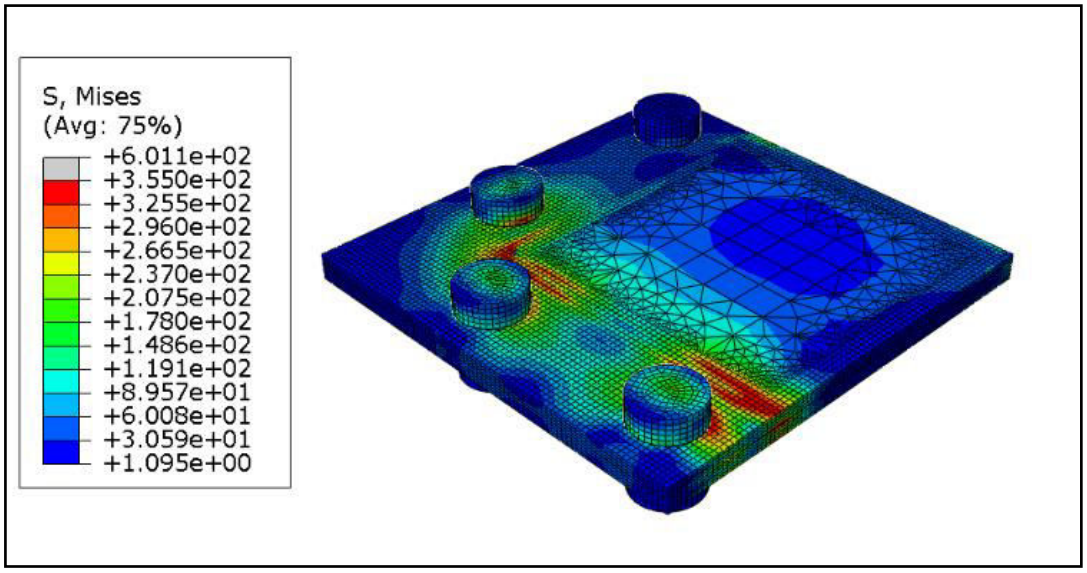

Figure 4-9: Von mises stress distribution in end-plate at 36 KN-m (CC-1/case 1)

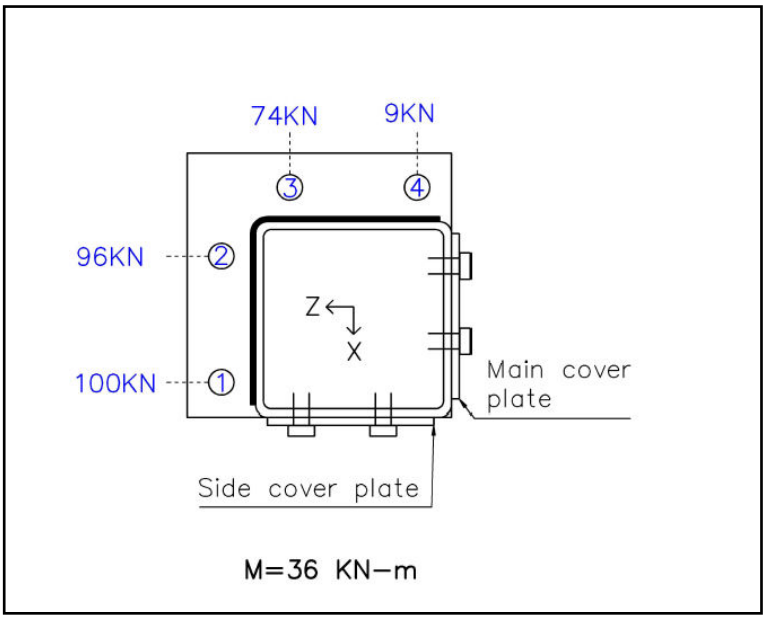

Figure 4-10: Tensile forces of bolts in end-plate at 36 KN-m (CC-1/case 1)

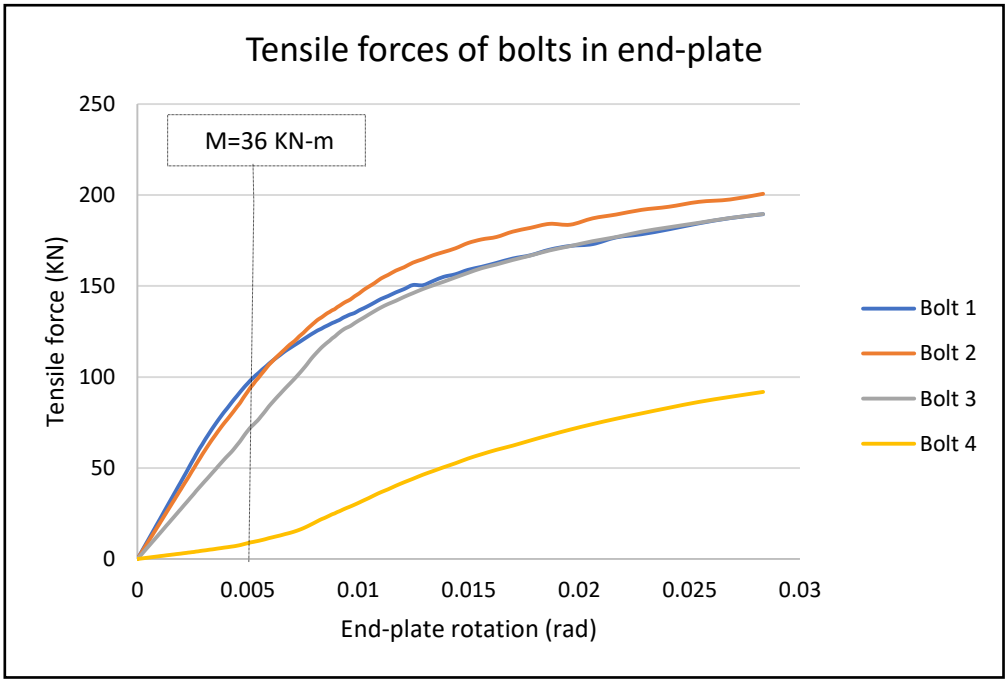

Figure 4-11: Tensile force carried by bolts in end-plate (CC-1/case 1)

Bolt 1 and 2 are highly stressed in end-plate due to a large lever arm length. Bolt 3 carries approximately 75% of the load carried by bolt 1 or 2 at yield point. Side cover plate contributes fully towards resistance after end-plate yield. Hence, tensile force in bolt 2 is larger than bolt 1 after resistance reaches 36 KN-m in figure 4-11.

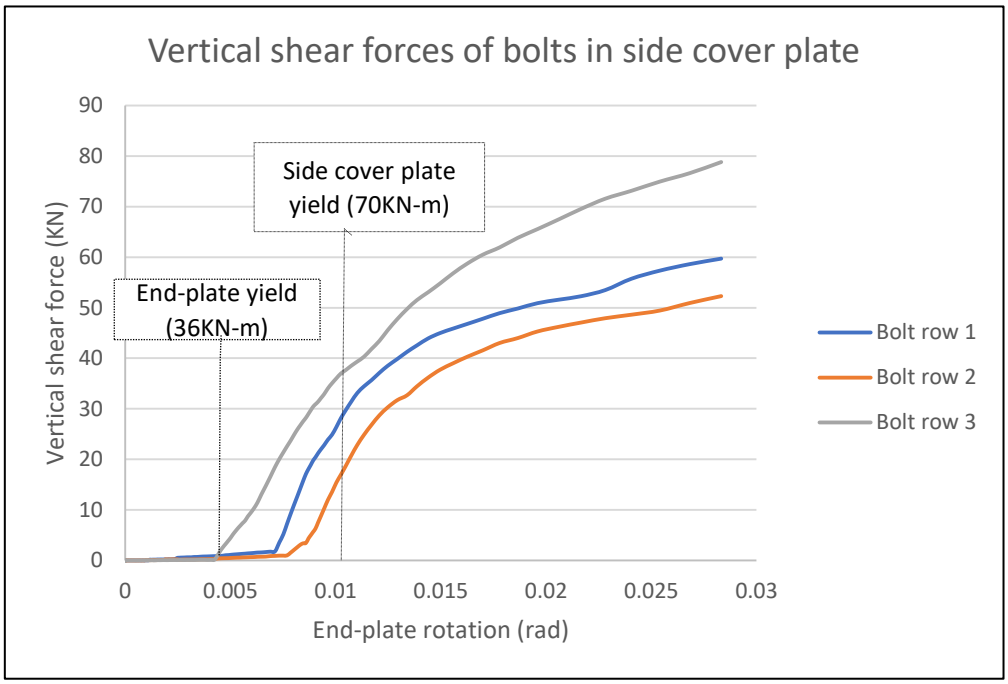

Figure 4-12: Vertical shear force carried by bolts in side cover plate (CC-1/case 1)

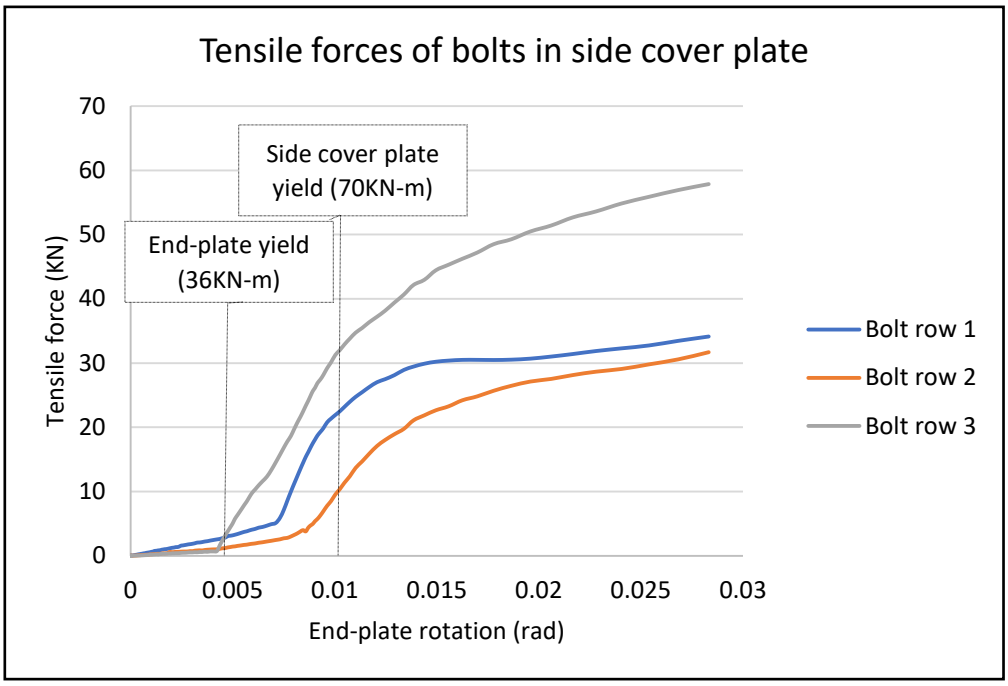

Figure 4-13: Tensile force carried by bolts in side cover plate (CC-1/case 1)

As seen in figures 4-12 and 4-13, bolt forces in side cover plate do not exhibit a sharp increase until a moment resistance of 36 KN-m is reached. One can expect side cover plate in the present case to behave similar to web cover plate in a regular splice connection. Shear forces are usually dominant in bolts used for web cover plate. In the present case, tensile forces are considerable for bolts in side cover plate due to torsion developed in the connection.

Side cover plate attains yield stresses near top bolt row at a moment resistance of 70 KN-m as seen in figure 4-14. Tensile and shear forces carried by bolts in side cover plate exhibit a linear increase with end-plate rotation until a resistance of 70 KN-m is reached. Yielding behavior is noticed in the load-rotation curves of bolts in side cover plate as shown in figures 4-12 and 4-13, which also confirms the yielding of side cover plate as noticed in contour plot.

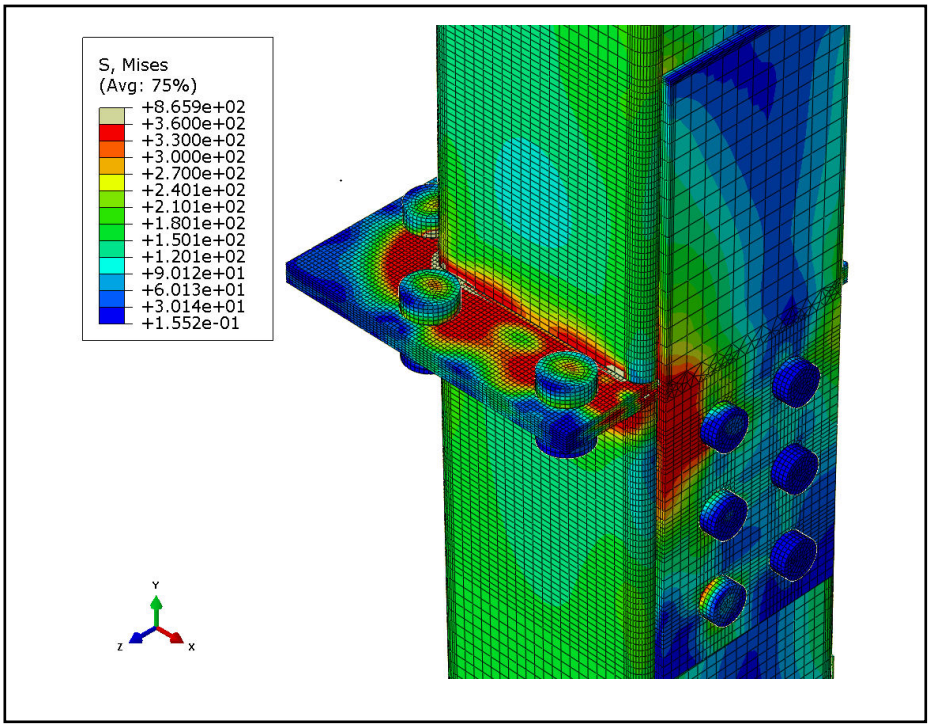

Figure 4-14: Von-mises stress distribution in specimen at 70KN-m (CC-1/case 1)

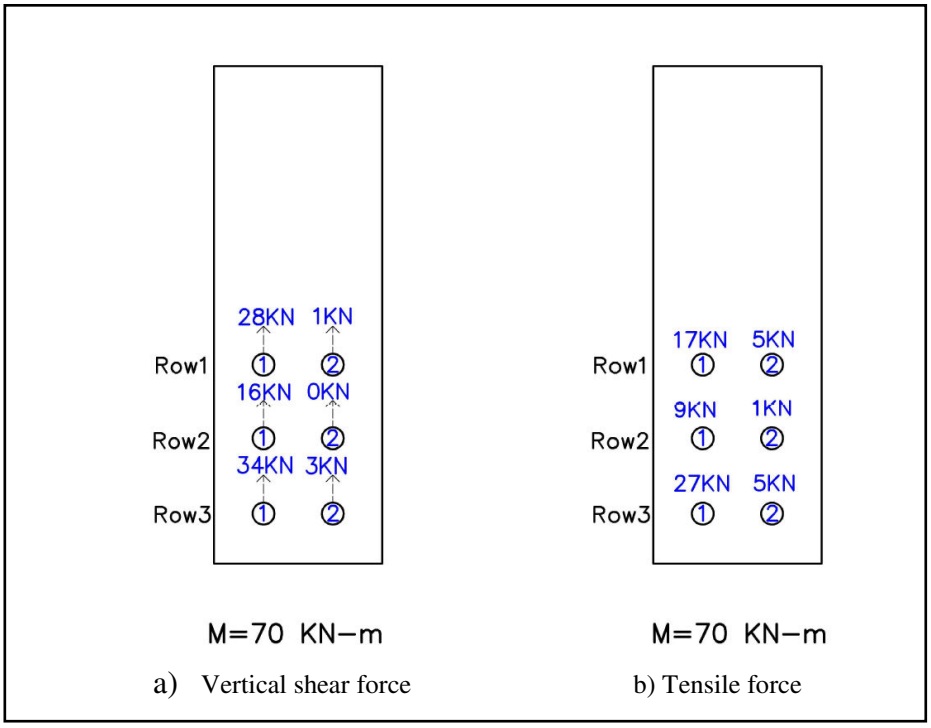

a) Vertical shear force

b) Tensile force

Figure 4-15: Load carried by bolts in side cover plate at 70 KN-m (CC-1/case 1)

Due to rotational motion of side cover plate, left hand side carries 95% of vertical shear in the plate at yield point. Bolt 1 in bottom bolt row carries 42% of the vertical shear force in side cover plate. Main cover plate undergoes considerable elastic deformation after end-plate has yielded at 36 KN-m. Vertical shear force carried by bolts in main cover plate are negligible until ultimate resistance of the connection is reached. However, tensile forces are generated in main cover plate bolts due to elastic deformation. Top bolt row in main cover plate carry 64% of total tensile force in the plate. In addition, varying tensile forces between the two bolts in row 1 can be noticed in figure 4-16-b. As discussed before, this is due to varying end-plate rotations at section 1 and section 2 caused by uneven force distribution.

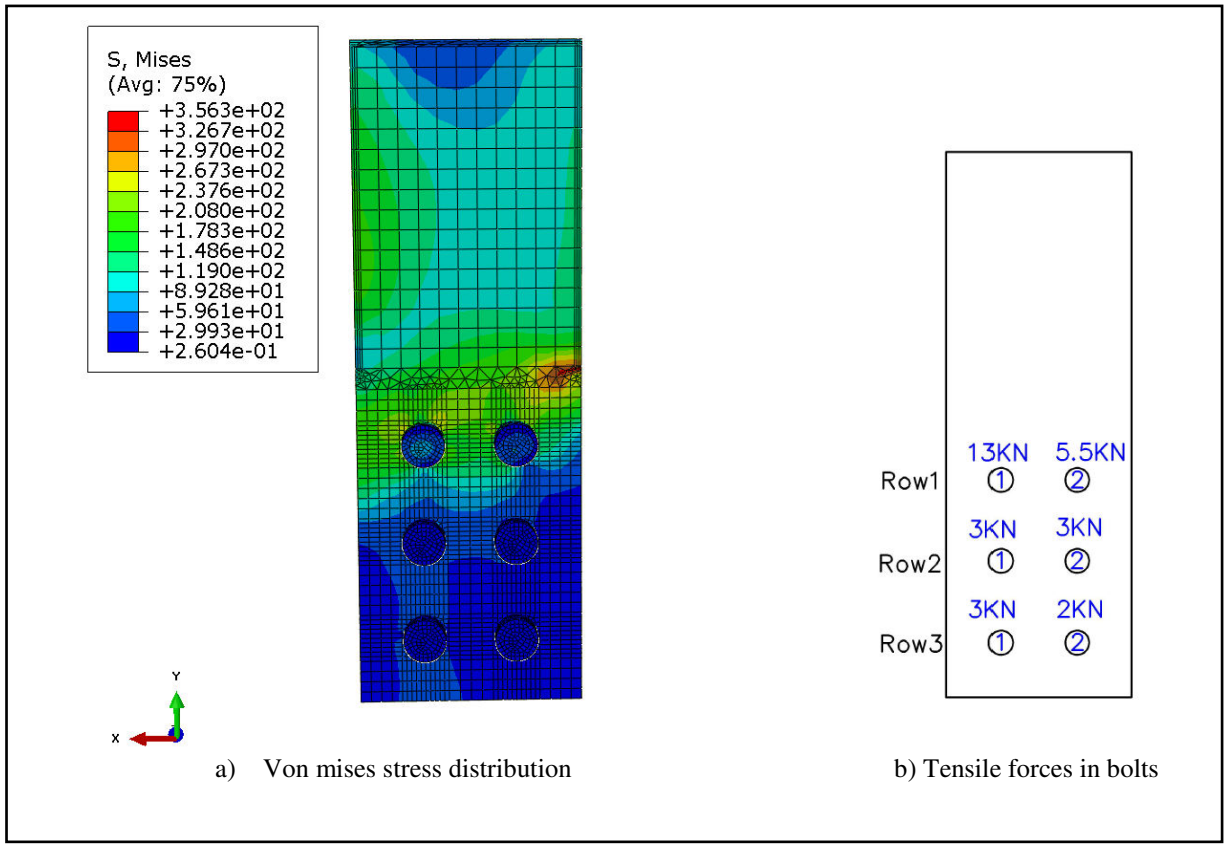

a) Von mises stress distribution

b) Tensile forces in bolts

Figure 4-16: Main cover plate at 70 KN-m (CC-1/case 1)

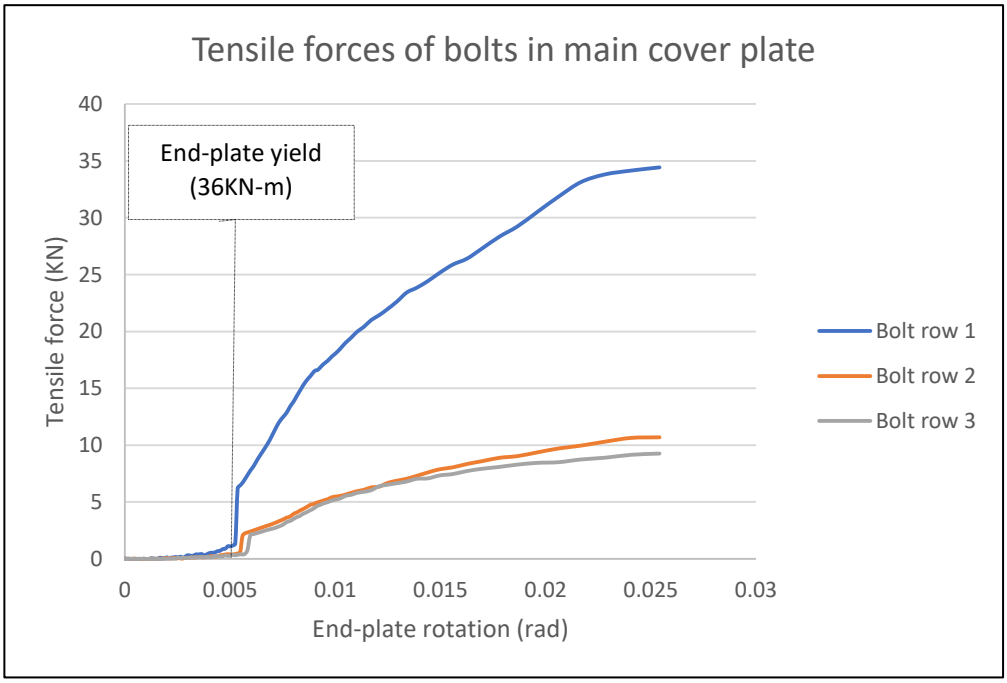

Figure 4-17: Tensile force carried by bolts in main cover plate (CC-1/case 1)

Ultimate bending resistance of corner column connection is reached at 102 KN-m. 5% plastic strains are reached in the end plate and side cover plate as seen in figure 4-18. Main cover plate is still in elastic stage at ultimate resistance of the connection and vertical shear loads carried by bolts in main cover plate are negligible at this stage. Significant plastification of end-plate leads to deformation of main cover plate as the applied load is increased. In addition, main cover plate would have to deform significantly before bolts in it carry considerable vertical shear.

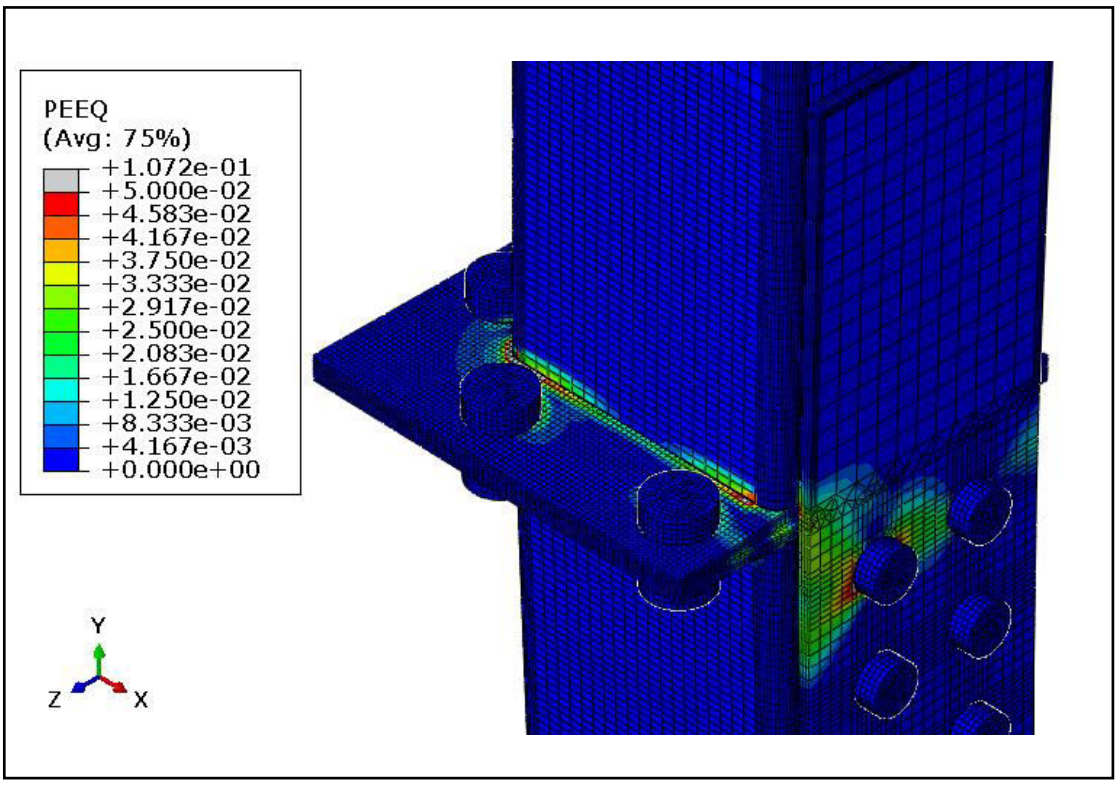

Figure 4-18: Plastic strain distribution 102 KN-m (CC-1/case 1)

4.3 Non-symmetrical corner splice – cover plate in tension

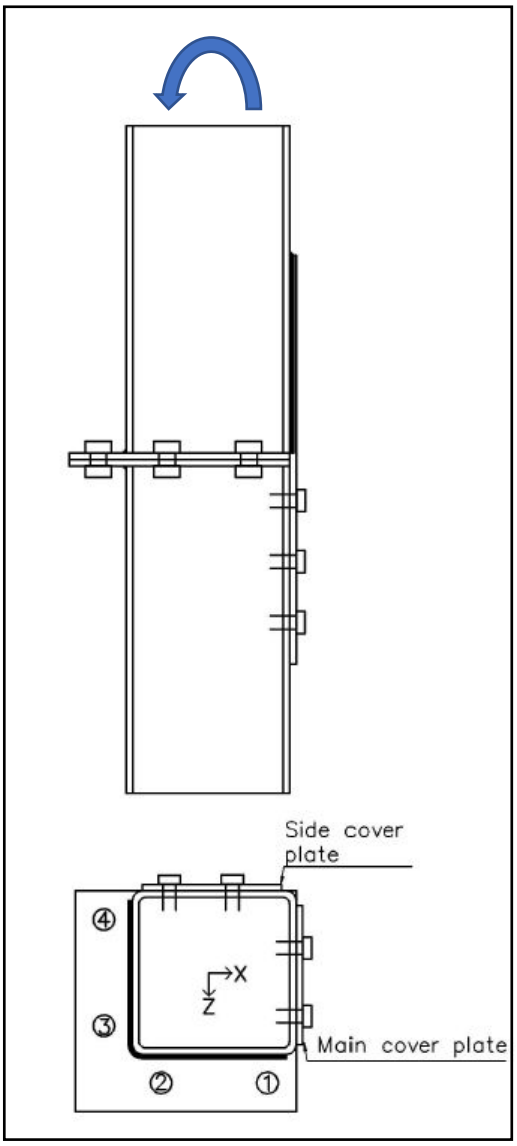

Figure 4-19: Plan and elevation of specimen CC-1 (case 2)

Second case of bending for non-symmetrical corner splice connection is discussed in this section. Top column is bending around Z-axis away from the main cover plate due to applied load as seen in figure 4-19. End-plate rotation between top and bottom end plate for this case is calculated as shown in figure 4-20. Similar to the previous case, rotation of end-plate depends on the section of end-plate where rotation is calculated. This occurs due to uneven force distribution in the connection. Non-symmetrical bolt force distribution is noticed in both cases of bending around X and Z-axis.

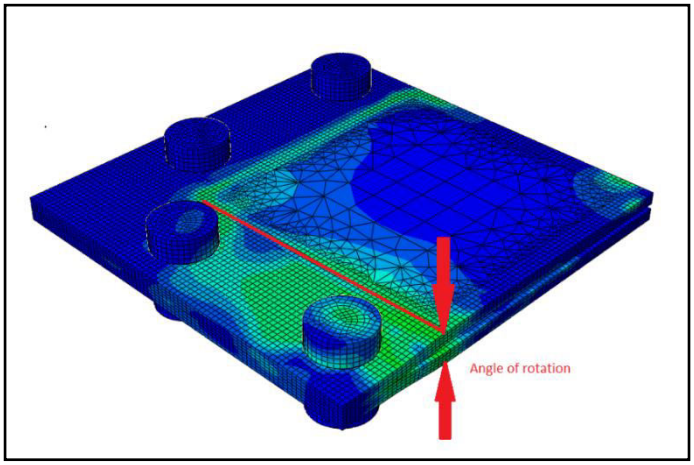

Figure 4-20: Angle of rotation between end-plates (CC-1/case 2)

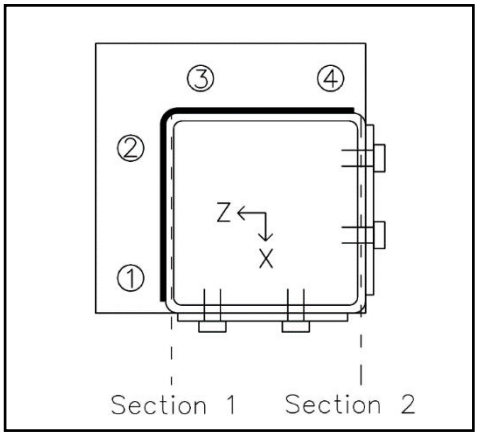

Figure 4-21: Locations in end-plate to calculate rotation (CC-1/case 2)

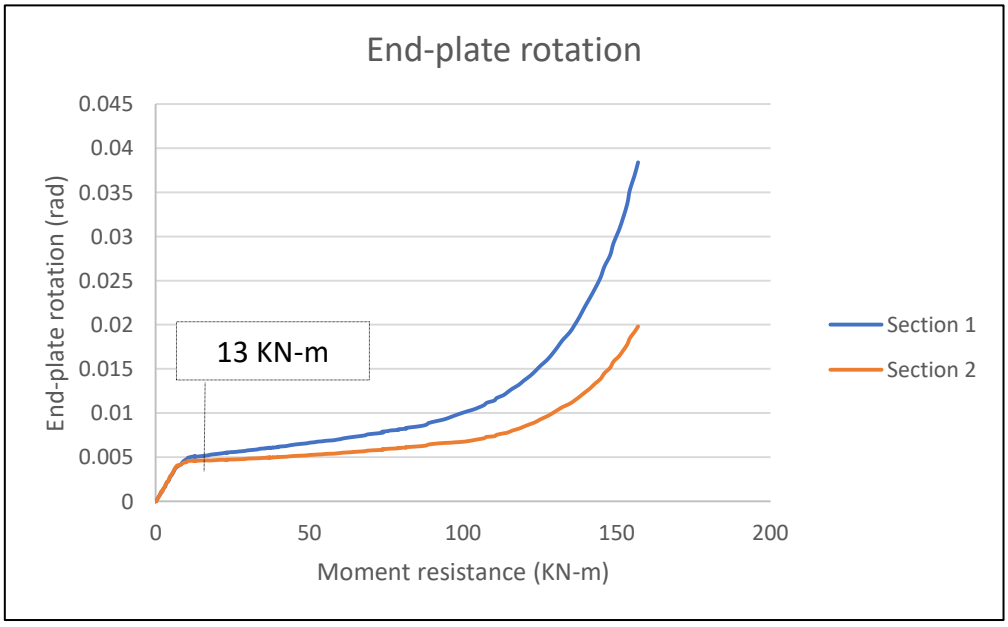

Figure 4-22: Moment resistance vs end-plate rotation of specimen CC-1 (CC-1/case 2)

End-plate rotation can be calculated at two sections as shown in figure 4-21. Section 1 involves column end welded to end-plate. While, there is no connection between column and end-plate along section 2. This evidently produces higher rotation along section 1 than section 2 and also causes uneven force distribution.

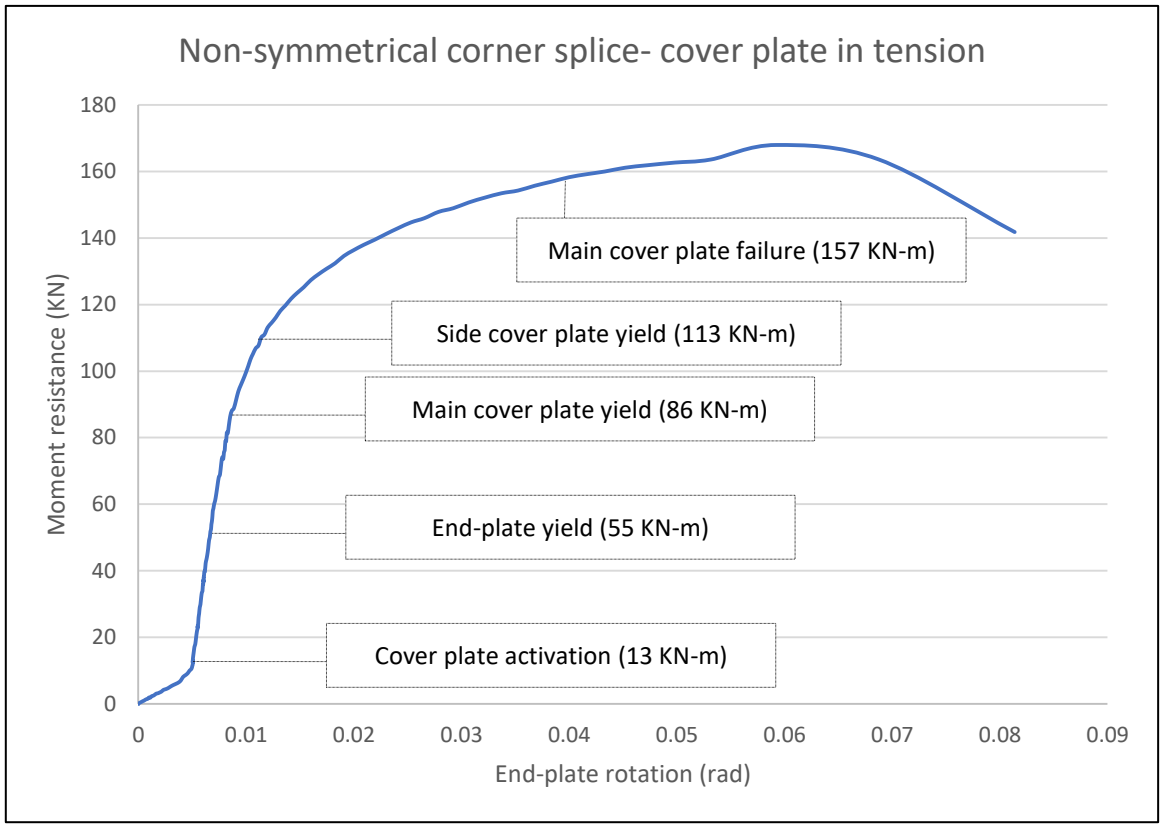

Figure 4-23: Moment rotation curve of specimen CC-1 (case 2)

Two different elastic parts can be noticed in the moment-rotation curve shown above. This is due to the bolt hole clearance provided in cover plates. Bolts in cover plates were placed at the center of bolt holes in finite element models. Main cover plate and side cover plate do not fully contribute towards resistance in the initial stages of loading. In the initial stage, most of the applied load is carried by bolt 1 and 2 in end plate as seen in figure 4-25. Load carried by bolts in main cover plate and side cover plate attain a sharp increase at 13 KN-m. Yield stresses are initially attained in end-plate and later in both the cover plates before failure occurs. In curve shown in figure 4-23, flattening of the curve after end-plate yield is not clearly expressed. This is due to the presence of cover plates which restricts free rotation of end-plate.

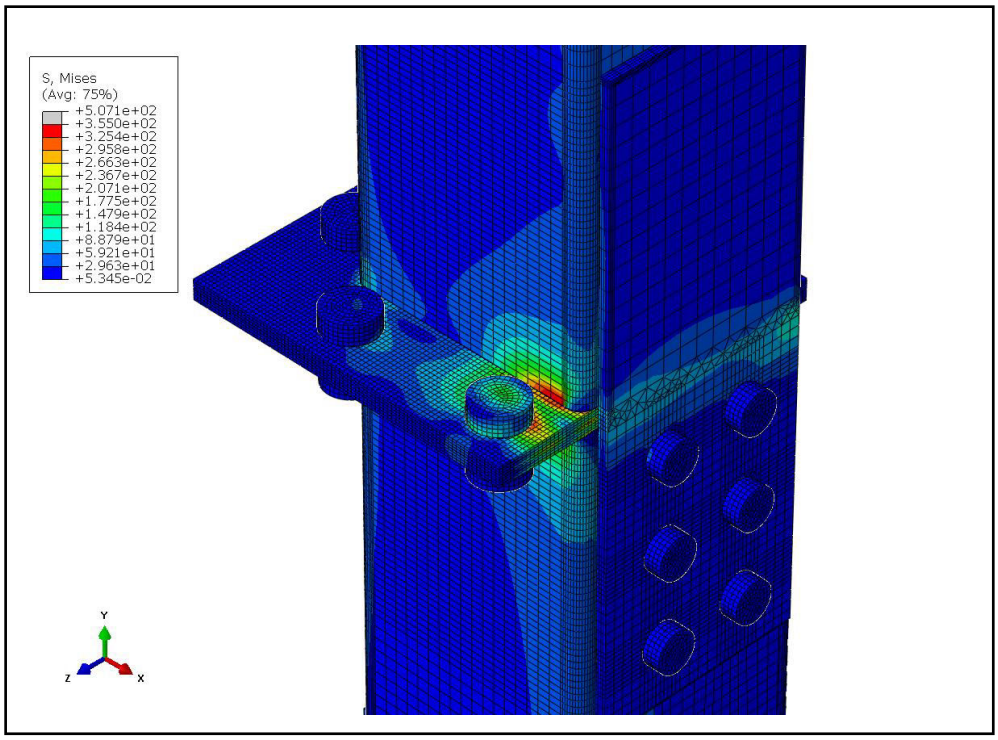

Figure 4-24: Von mises stress distribution at 13 KN-m (CC-1/case 2)

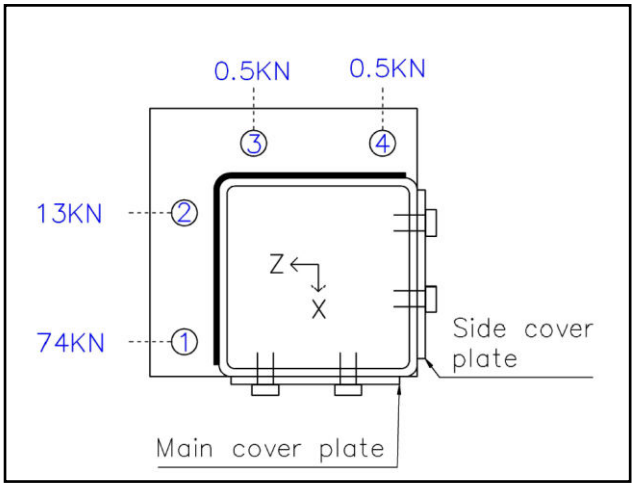

Figure 4-25: Tensile forces of bolt in end-plate at 13 KN-m (CC-1/case 2)

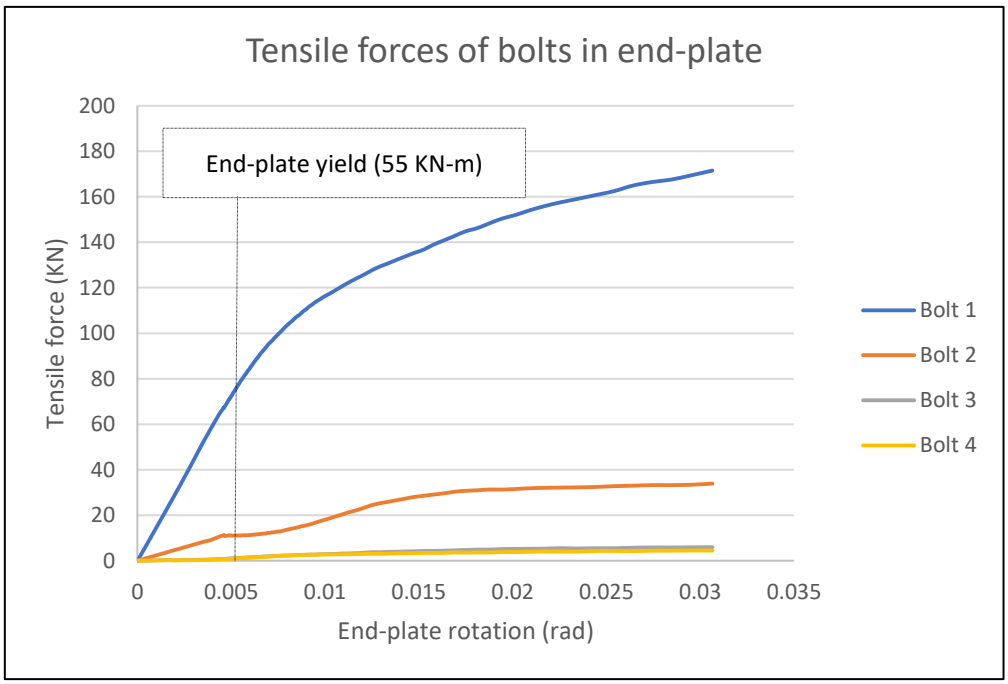

Figure 4-26: Tensile force carried by bolts in end-plate (CC-1/case 2)

At a moment resistance of 55 KN-m, yield stresses are attained in end plate. End plate yields in the region near bolt 1 as seen in figure 4-27. Tensile force in bolt 1 exhibits a linear behavior with end plate rotation until a moment resistance of 55 KN-m and later the curve flattens. This also confirms the yielding of end plate as noticed in contour plot. Bolt 1 carries approximately 85% of the tensile load in end-plate, while contribution of bolt 2 is negligible at a resistance of 55 KN-m.

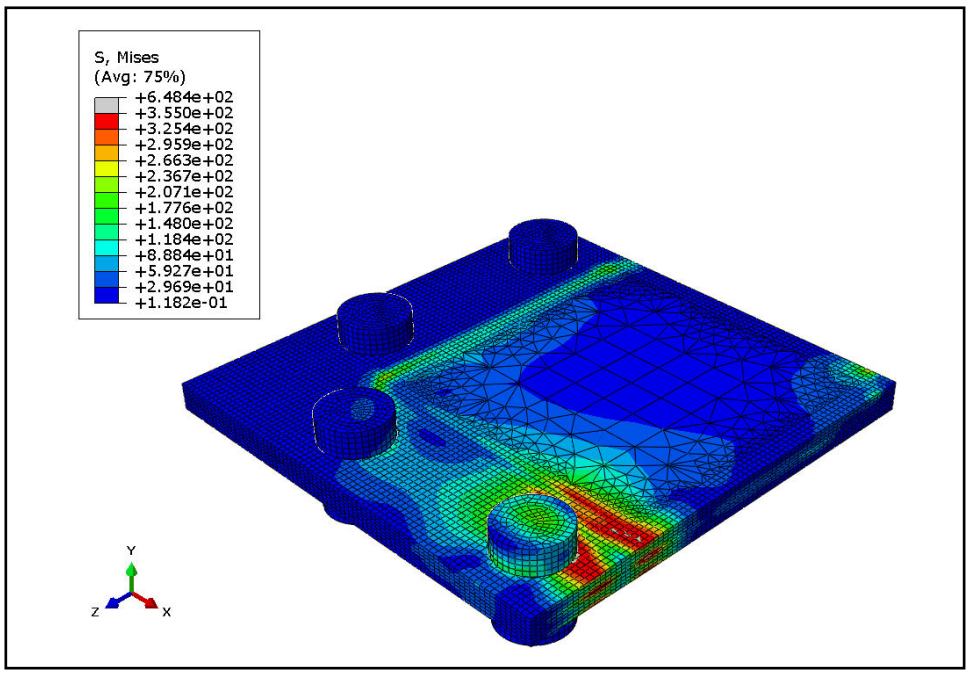

Figure 4-27: Von mises stress distribution in end-plate at 55 KN-m (CC-1/case 2)

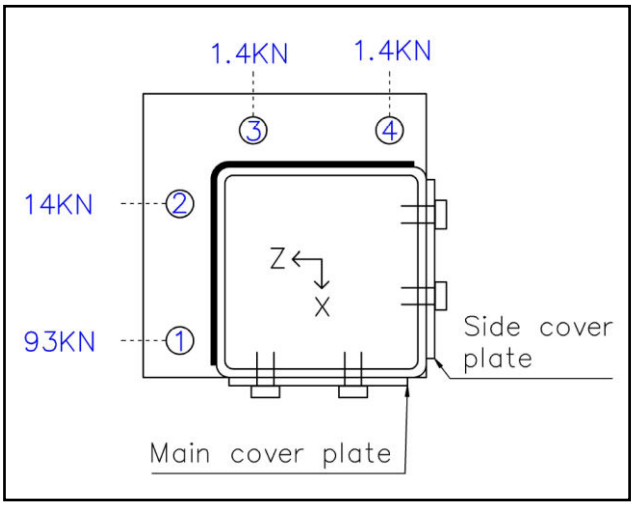

Figure 4-28: Tensile forces of bolts in end-plate at 55 KN-m (CC-1/case 2)

At a moment resistance of 86 KN-m, main cover plate yields in a region near the top bolt row as seen in figure 4-29. Main cover plate while in tension is also subjected to bending at its mid-height. This causes the bolts in main cover plate to carry vertical shear and tensile forces. Vertical shear forces are equally distributed among the top two bolt rows due to yielding. However, before yielding it is seen that top and bottom bolt rows carry relatively high shear forces than bolt row 2 as seen in figure 4-31. Tensile forces are relatively high at the last bolt row compared to top two bolt rows due to bending of main cover plate towards column face.

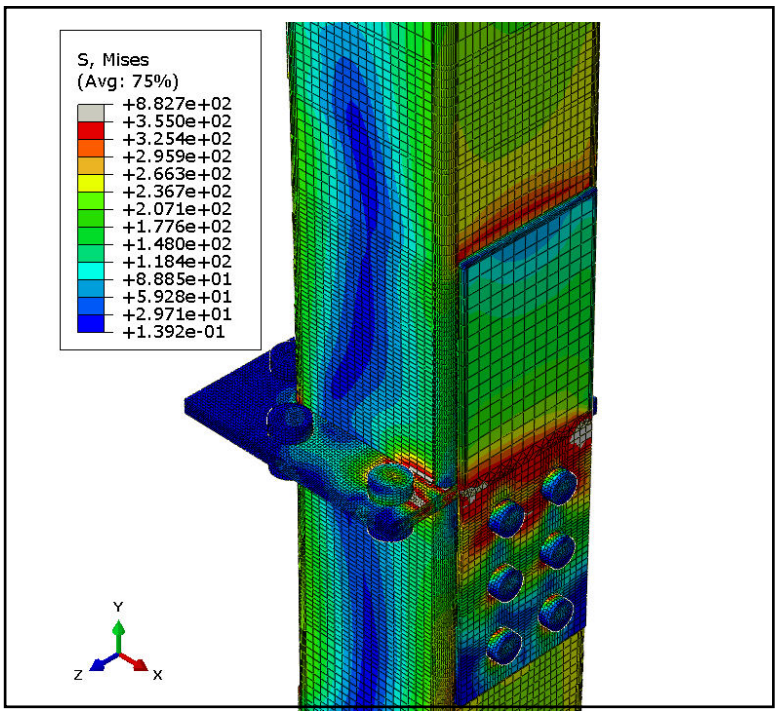

Figure 4-29: Von mises stress distribution at 86 KN-m (CC-1/case 2)

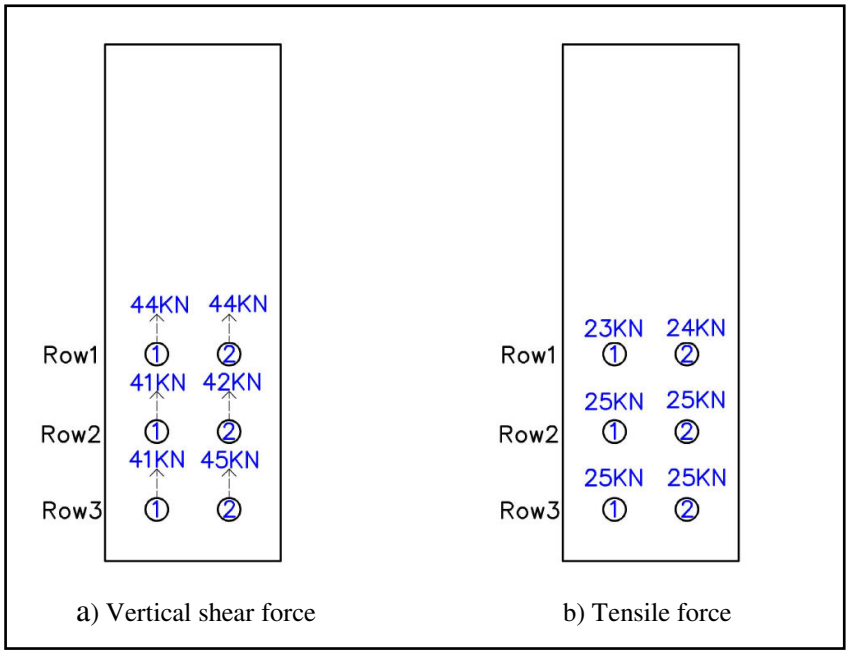

Figure 4-30: Bolt forces in main cover plate at 86 KN-m (CC-1/case 2)

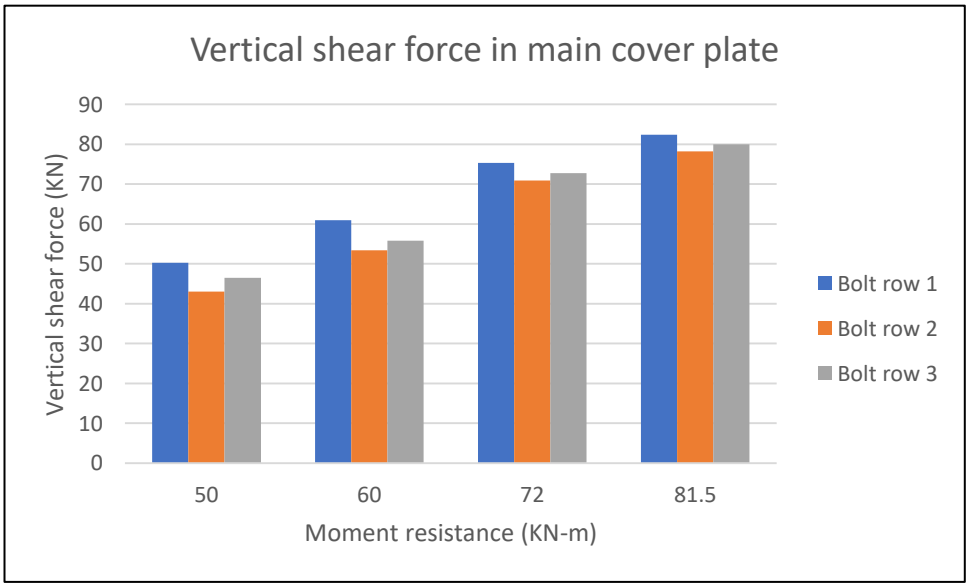

Figure 4-31: Vertical shear force carried by bolt rows in main cover plate (CC-1/case 2)

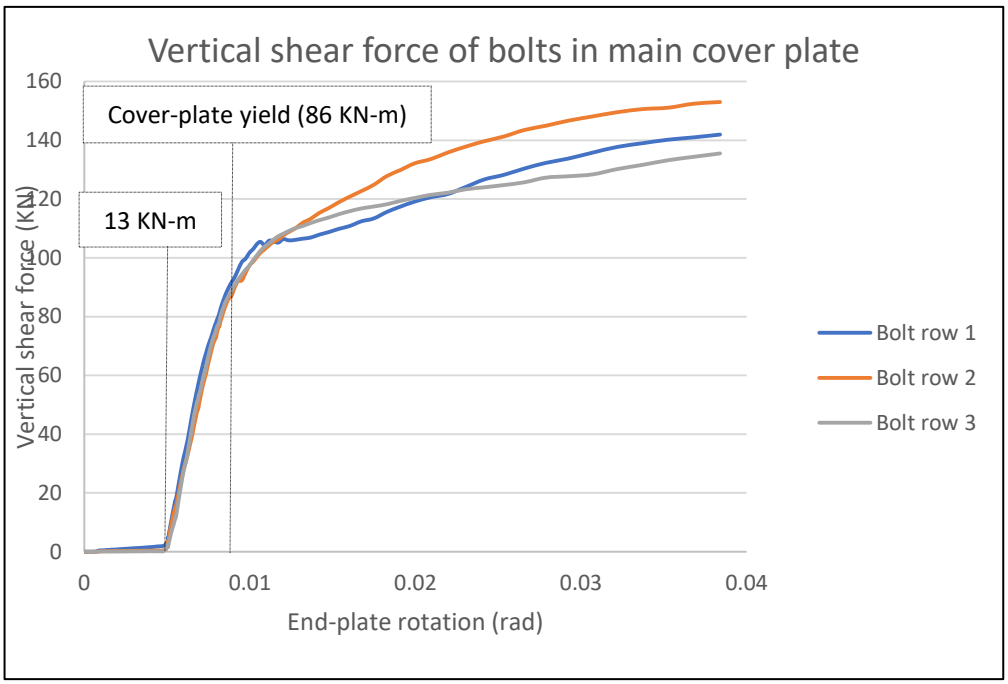

Figure 4-32: Vertical shear force carried by bolts in main cover plate (CC-1/case 2)

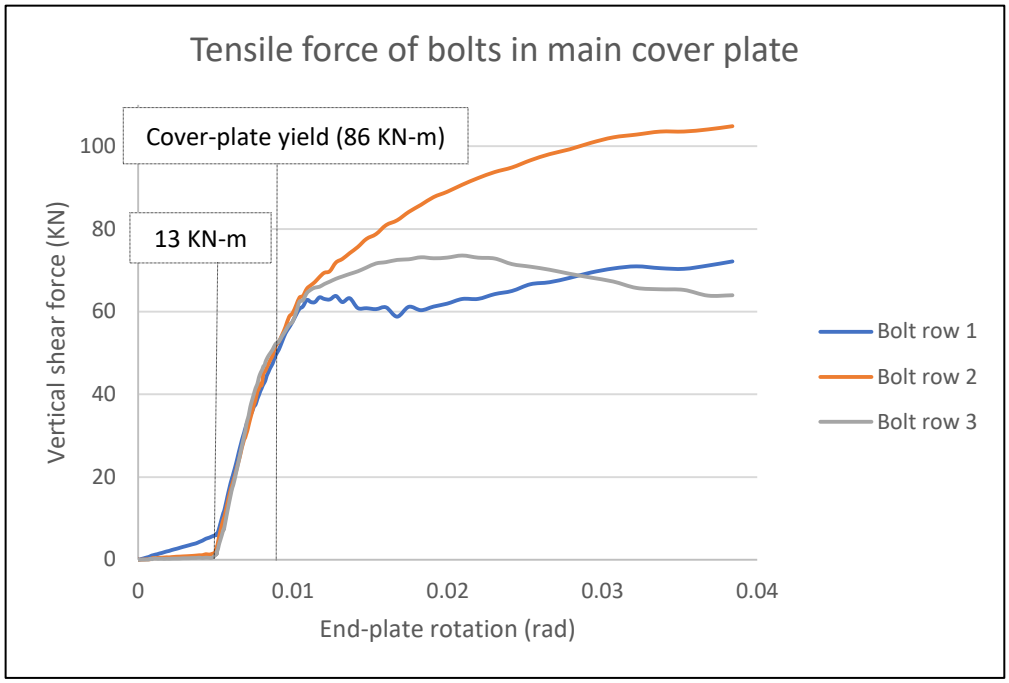

Figure 4-33: Tensile force carried by bolts in main cover plate (CC-1/case 2)

As seen in figures 4-32 and 4-33, vertical shear force and tensile force carried by bolts in main cover plate are very low until a moment resistance of 13 KN-m is reached. Load carried by bolts in main cover plate exhibits yielding behavior after a moment resistance of 86 KN-m is reached. This also confirms the yielding of main cover plate as seen in the contour plots.

Side cover plate is in rotational motion due to applied load. Load carried by bolts in side cover plate exhibit a sharp linear increase just before the moment resistance reaches 13 KN-m. Yield stresses are attained in side cover plate at a moment of 113 KN-m. As noticed in the

previous case, bolt 1 in bottom bolt row carries the highest vertical shear load in the plate. Approximately, 48% of the vertical shear load in plate is transferred at bolt 1 in bottom bolt row. In addition, left hand side carries approximately 97% of the vertical shear load in side cover plate at yield point.

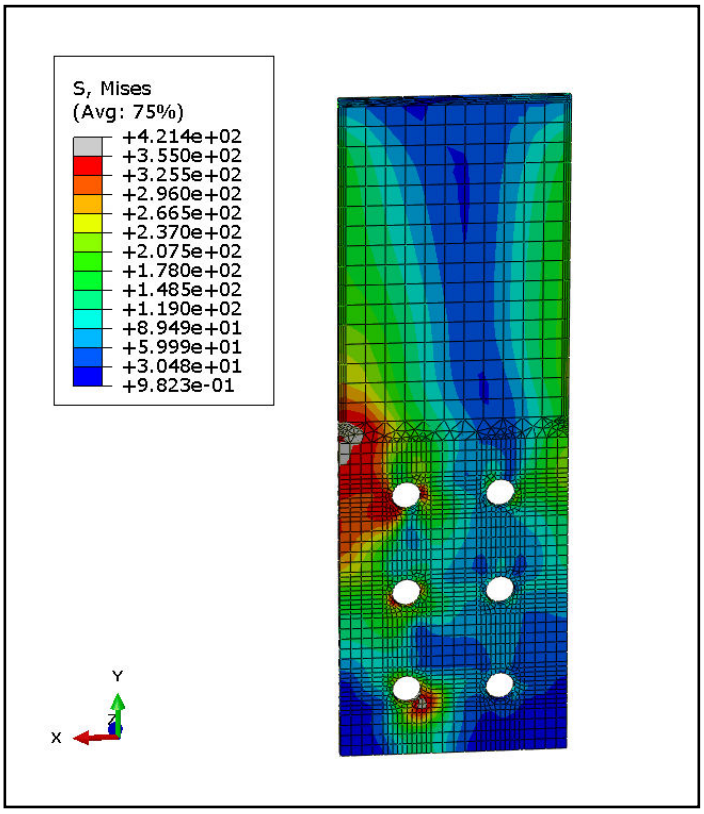

Figure 4-34: Von-mises stress distribution in side cover plate at 113KN-m (CC-1/case 2)

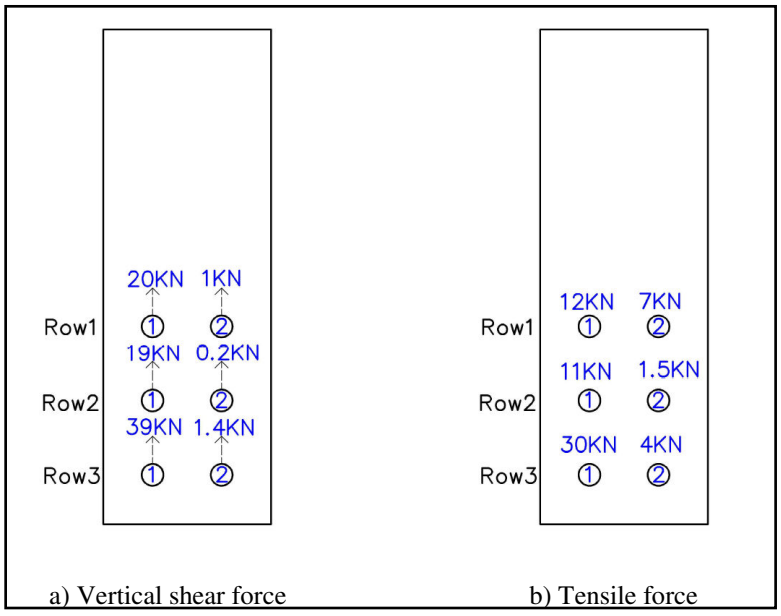

Figure 4-35: Bolt forces in side cover plate at 113 KN-m (CC-1/case 2)

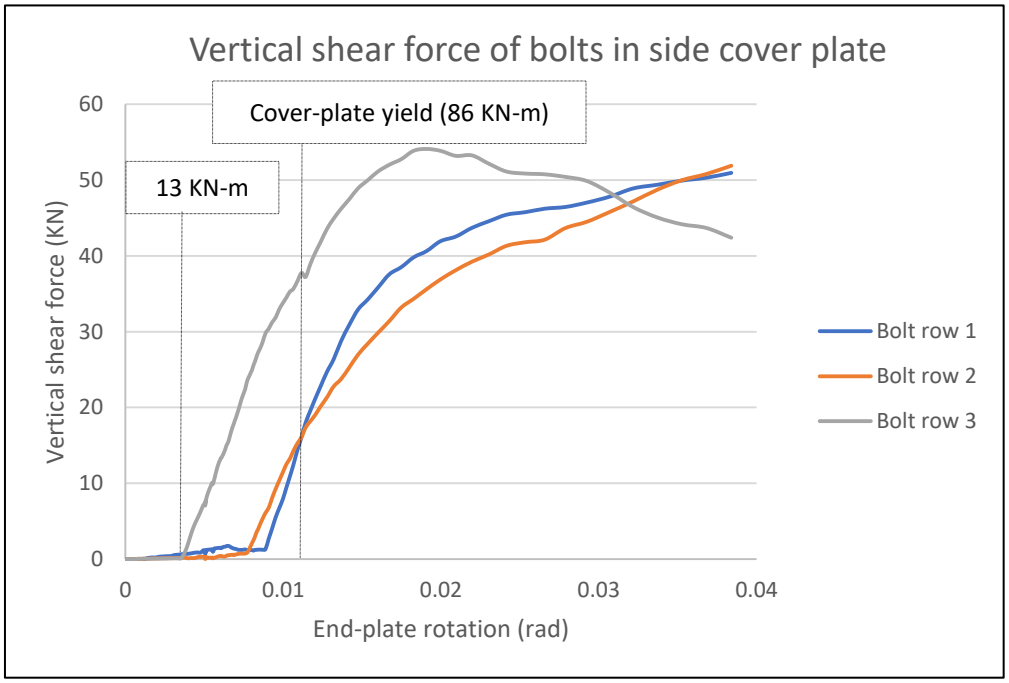

Figure 4-36: Vertical shear force carried by bolts in side cover plate (CC-1/case 2)

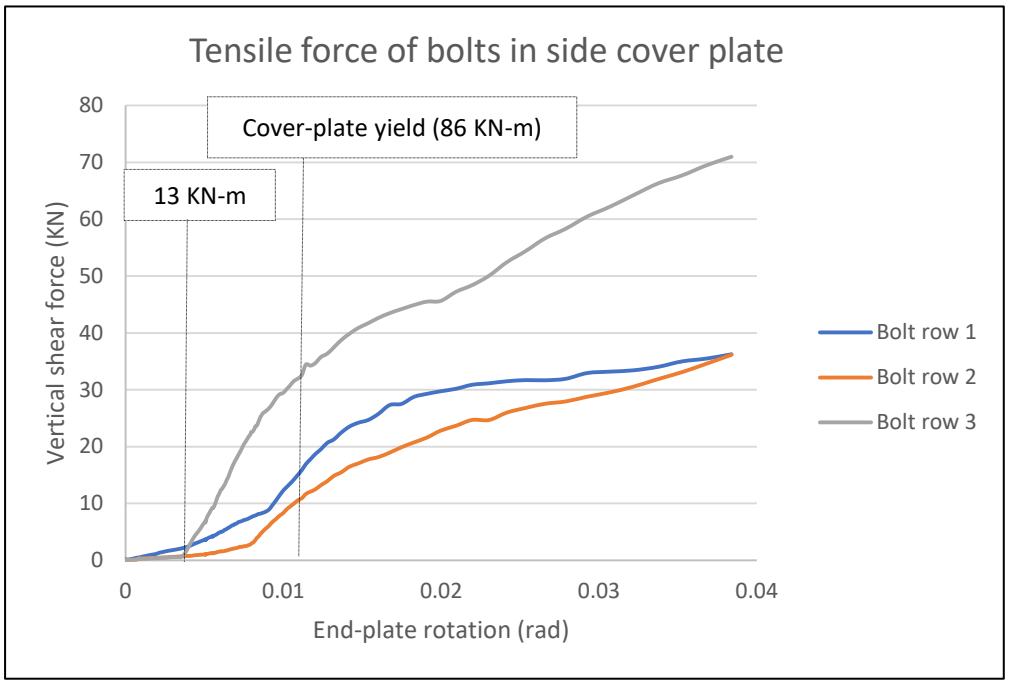

Figure 4-37: Tensile force carried by bolts in side cover plate (CC-1/case 2)

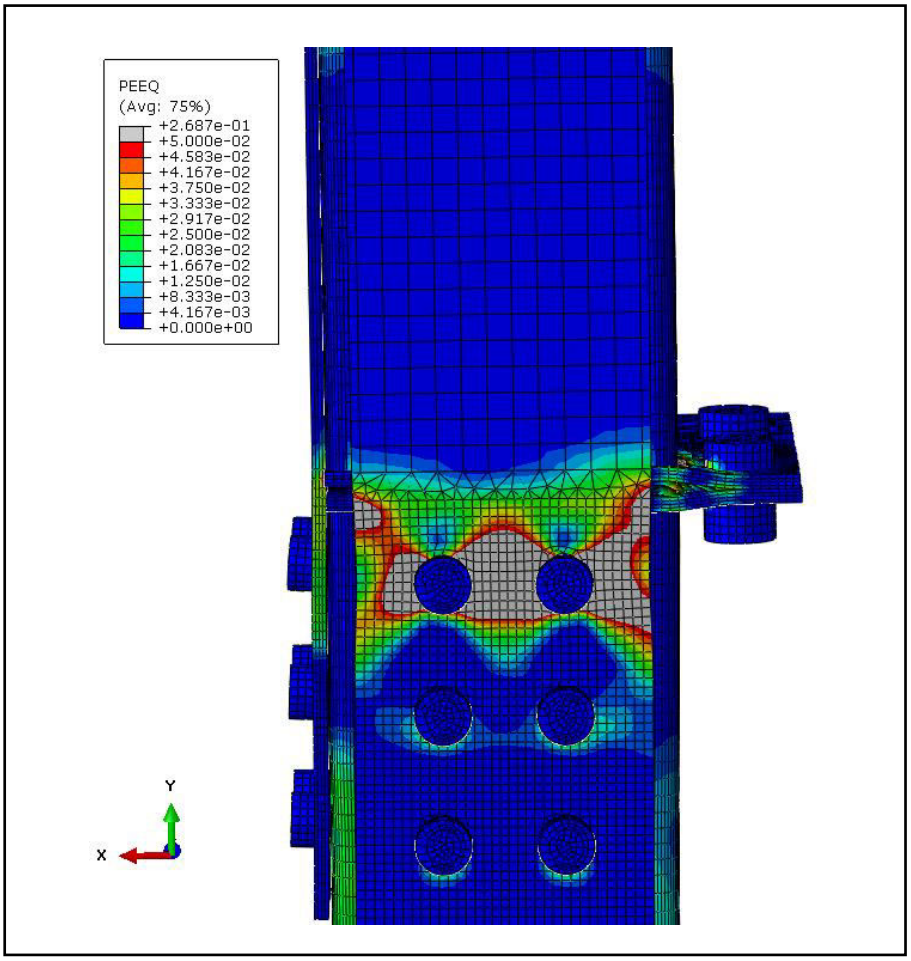

Figure 4-38: Plastic strain distribution at 157 KN-m (CC-1/case 2)

Ultimate resistance of this connection is reached at 157 KN-m. 5% plastic strain is reached in main cover plate near top bolt row as shown in figure 4-38. This causes failure of cover plate along its net-section.

4.4 Non-symmetrical corner splice – tensile load

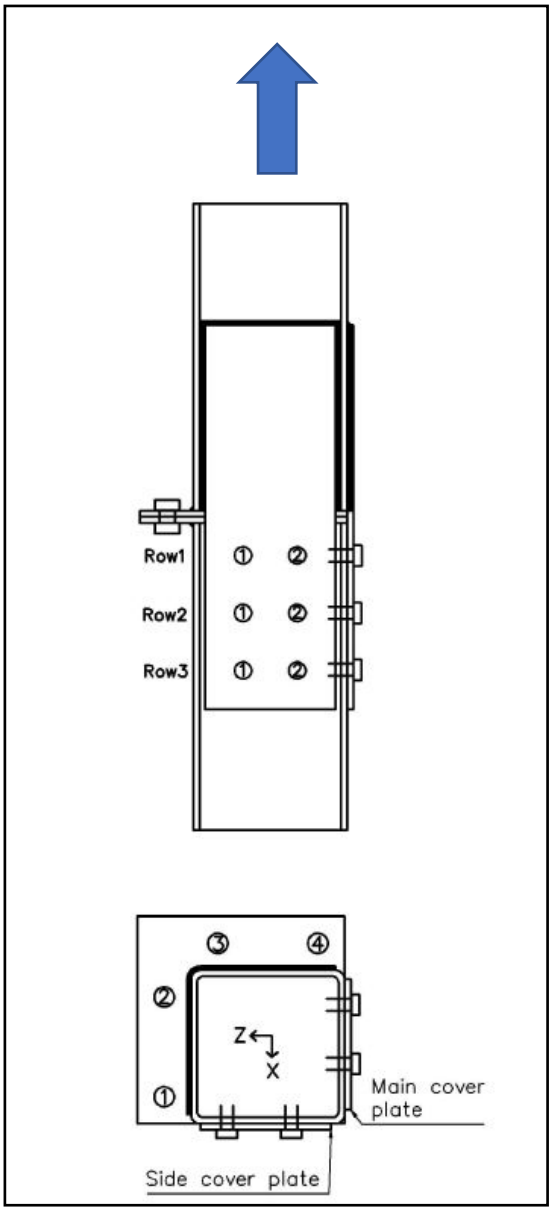

Figure 4-39: Plan and elevation of specimen CC-1 (case 3)

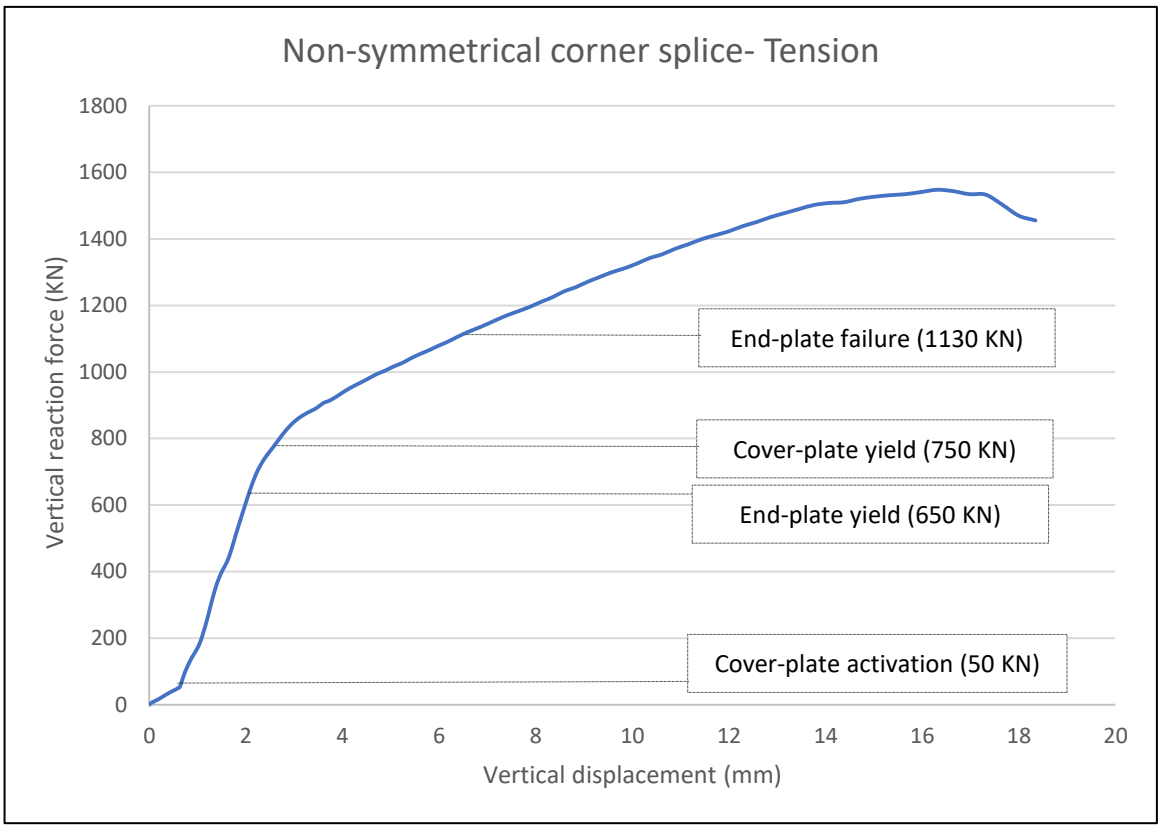

Figure 4-40: Load displacement curve of specimen CC-1 (case 3)

In this section behavior of non-symmetrical corner splice connection under a tensile force is discussed. In the initial stages of loading cover plates do not fully contribute towards resistance. This as explained in earlier situations is caused to due to bolt hole clearances provided in cover plate and bottom column. This leads to two elastic parts in the force-displacement curve shown in figure 4-40. Most of the applied load is carried by four bolts in end-plate during the initial stages of loading. A sharp increase in loads carried by bolts in cover plate is noticed when the tensile resistance reaches 50 KN.

End-plate attains yield stresses at a reaction force of 650 KN. End plate yields near all four bolts as observed in figure 4-41. As expected, force amongst the bolts in end-plate in unevenly distributed. Also, group behavior is noticed between bolts 2 and 3 in end-plate. Yield stresses are higher between bolt 2 and 3, compared to the regions around bolt 1 and 4. This causes uneven vertical displacement at two diagonally opposite corners of top column.

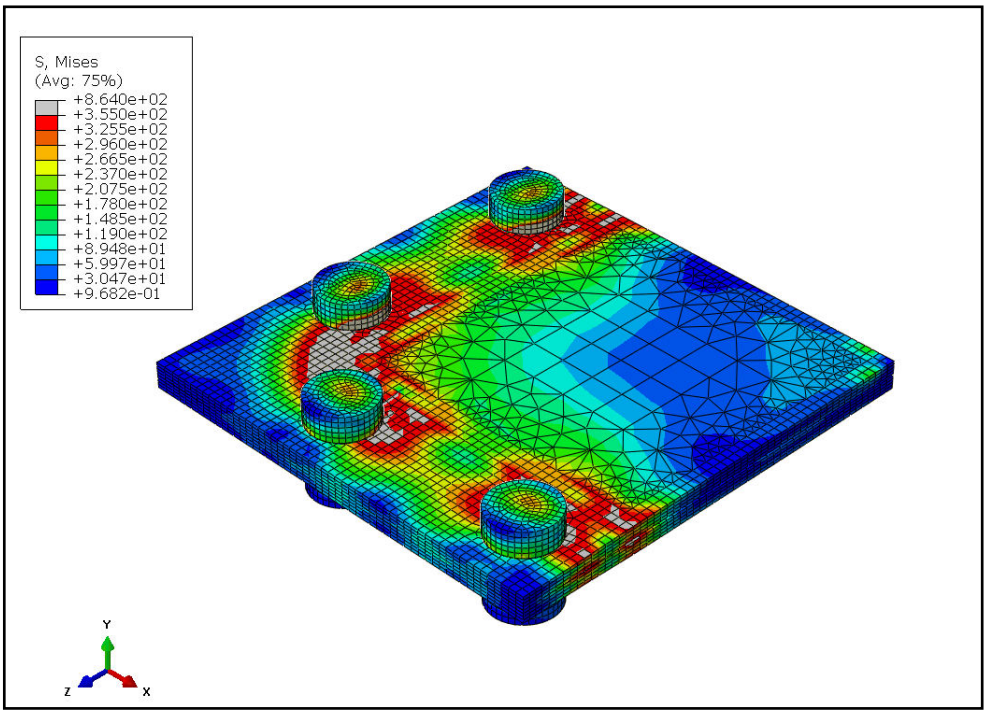

Figure 4-41: Von mises stress distribution in end-plate at 650 KN (CC-1/case 3)

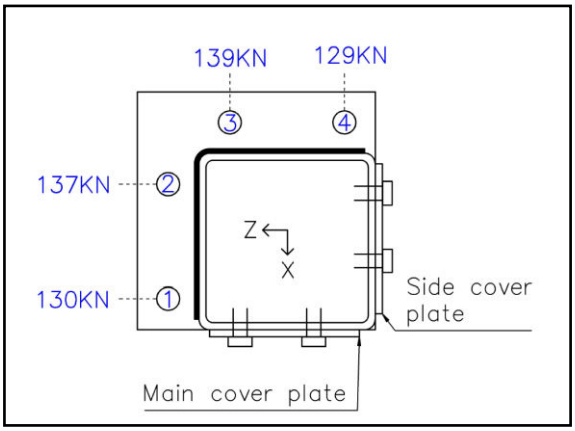

Figure 4-42: Tensile force of bolts in end plate at 650 KN (CC-1/case 3)

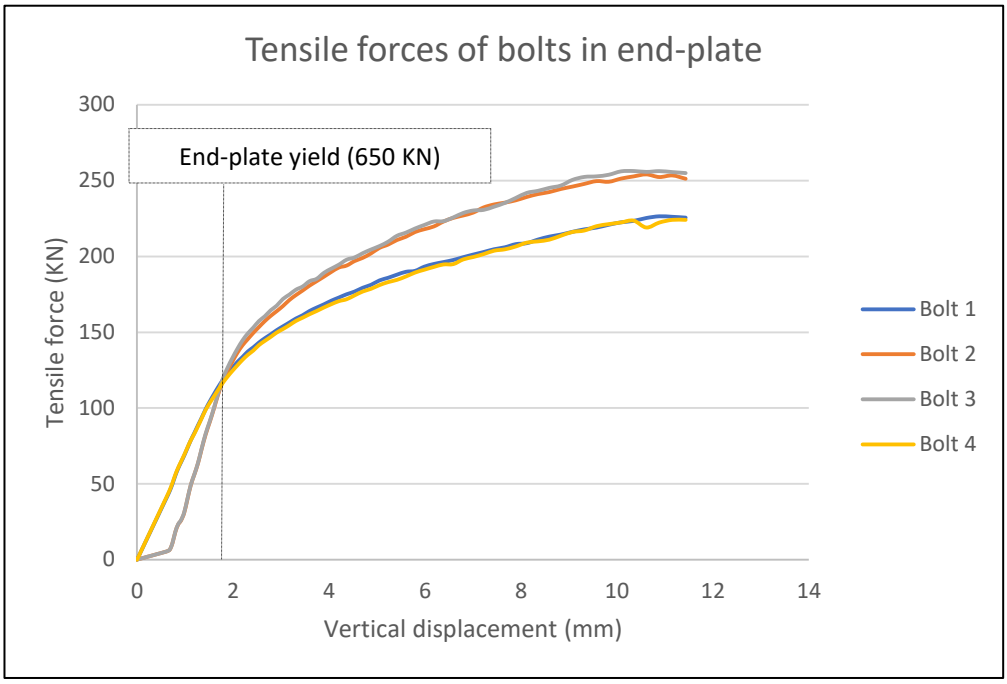

Figure 4-43: Tensile force carried by bolts in end-plate (CC-1/case 3)

Two bolts 1 and 4, that are close to the cover plates carry similar amount of tensile force. While, two bolts 2 and 3, that are away from the cover plates similar amount of tensile force. Initially, bolts close to cover plates carry relatively high forces compared to bolts away from the cover plates. After yielding of end-plate, bolts away from cover plates carry higher forces than bolts close to the cover plate. A linear increase in bolt forces can be seen until end-plate yield as seen in figure 4-43. Bolt forces exhibit a yielding behavior after this point, which confirms yielding of end-plate as seen in figure 4-41.

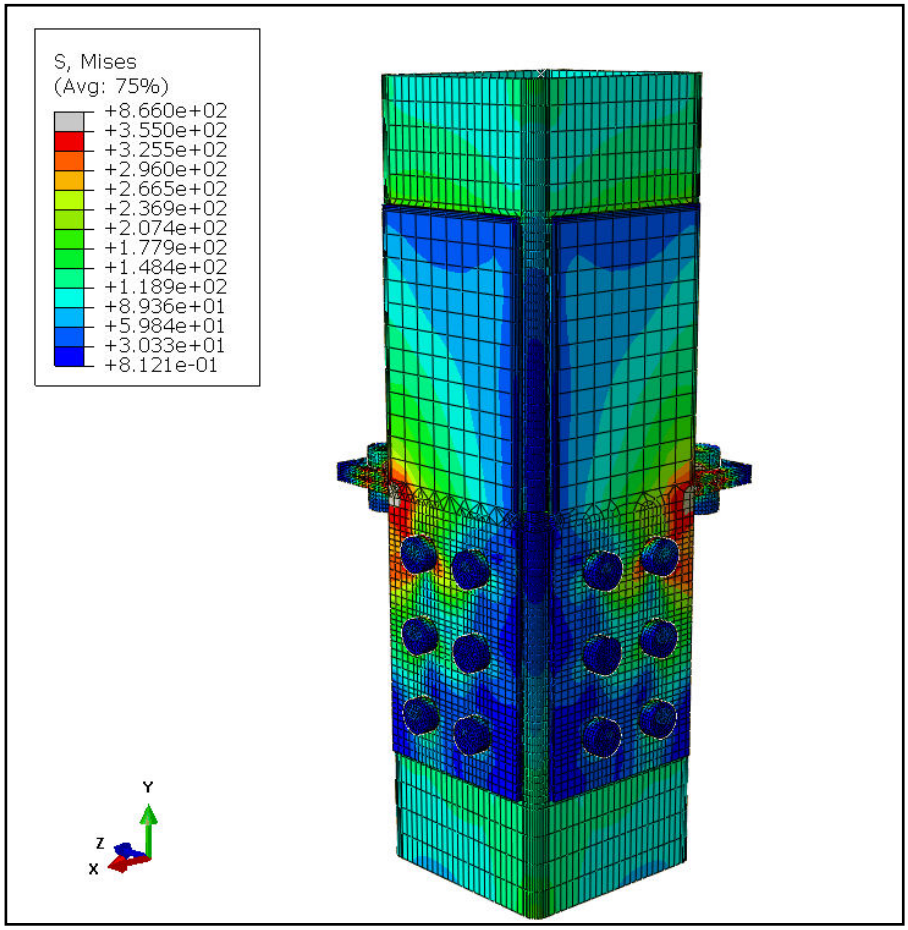

Figure 4-44: Von mises stress distribution at 750 KN (CC-1/case 3)

Higher magnitude of yielding between bolts 2 and 3 in end-plate lead to uneven force distribution in cover plates. Cover plates yield at a tensile resistance of 750 KN. However, yield stresses are noticed only along half the width of cover plates as seen in figure 4-44. Hence, the load carried by bolts in the same bolt row are different. Bolt row 1,2 and 3 in cover plates carry 37%, 30% and 32% of the vertical shear force in plate at yield point.

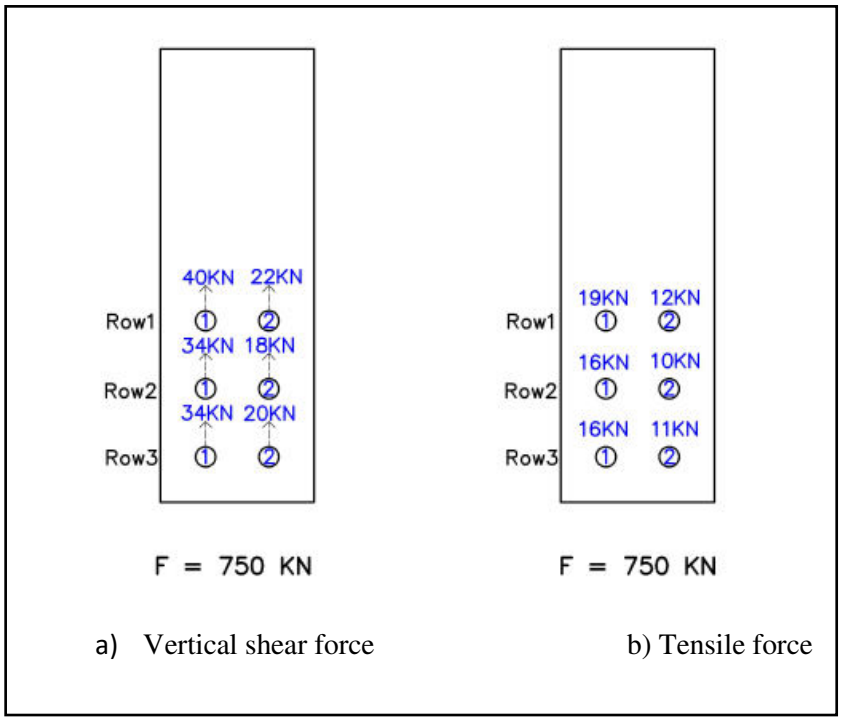

Figure 4-45: Bolt forces in side cover plate at 750 KN (CC-1/case 3)

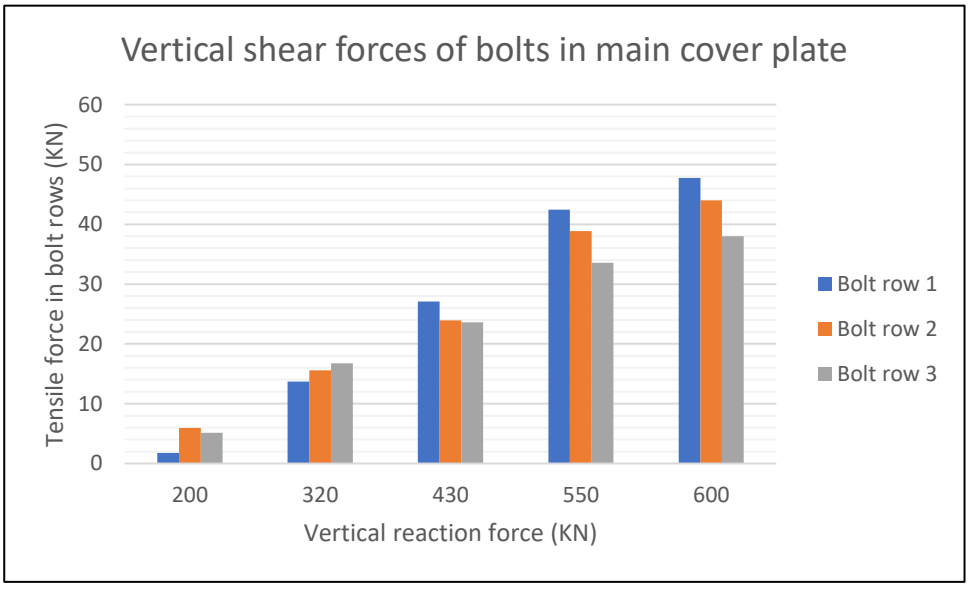

Figure 4-46: Vertical reaction force vs Tensile force in bolt rows of main cover plate (CC-1/case 3)

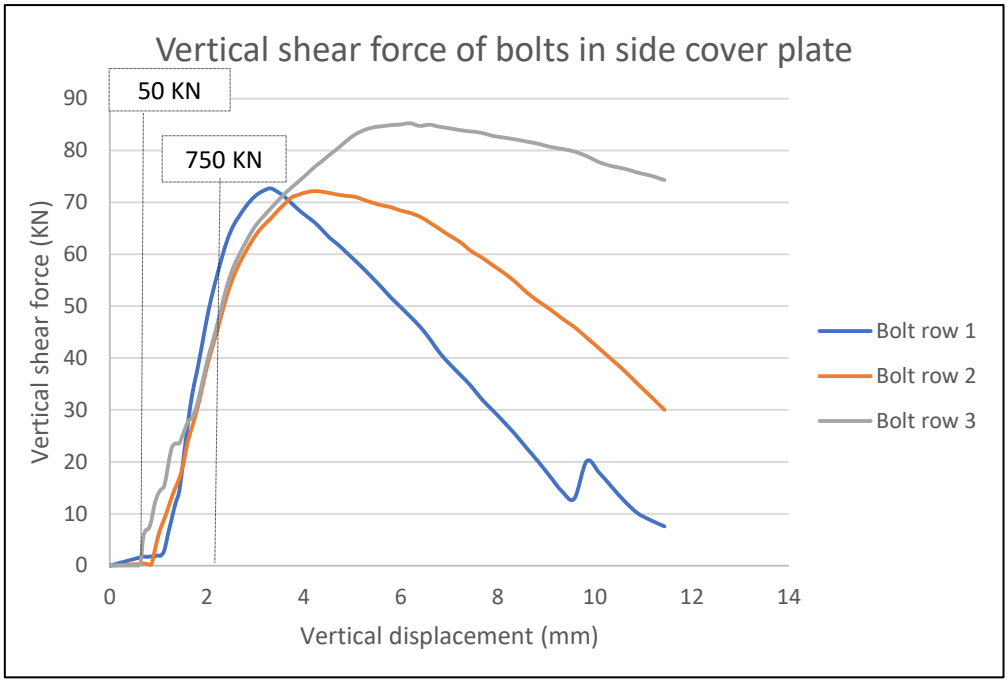

Figure 4-47: Vertical shear force carried by bolts in side cover plate (CC-1/case 3)

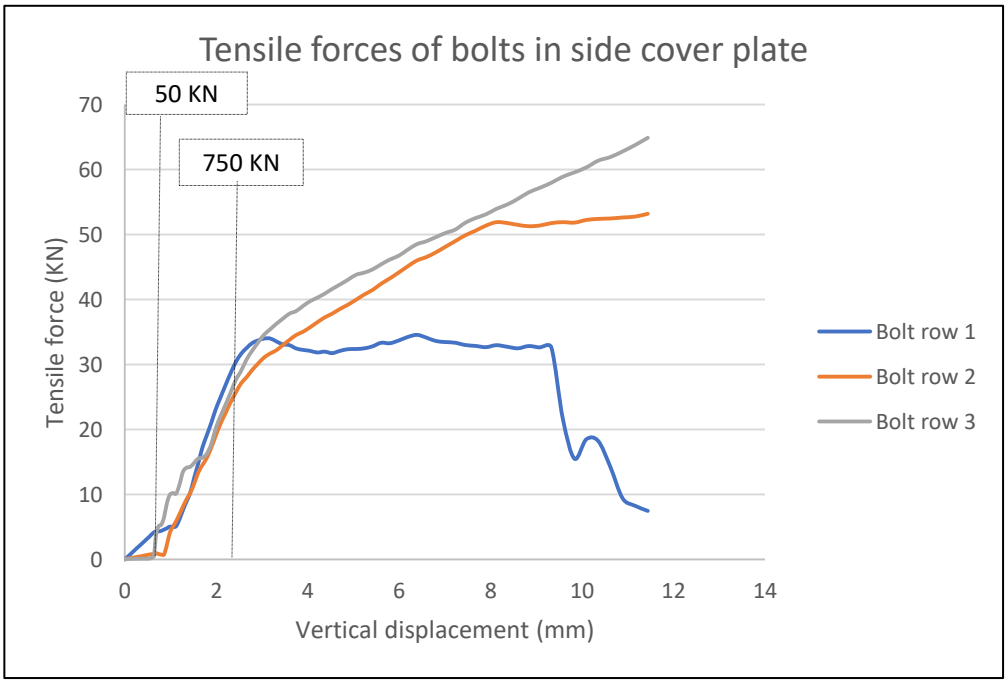

Figure 4-48: Tensile force carried by bolts in side cover plate (CC-1/case 3)

Bolt forces in both cover plates are similar up to ultimate resistance. Hence, bolt forces of only one cover plate is shown in this section. Vertical shear forces of bolts in cover plate see a sharp increase at a reaction force of 50 KN as seen in figures 4-47 and 4-48. Also, yielding behavior can be noticed in the shear force carried by bolt row 1 at a reaction force of 750KN. Similar behavior is also noticed with tensile forces in cover plates.

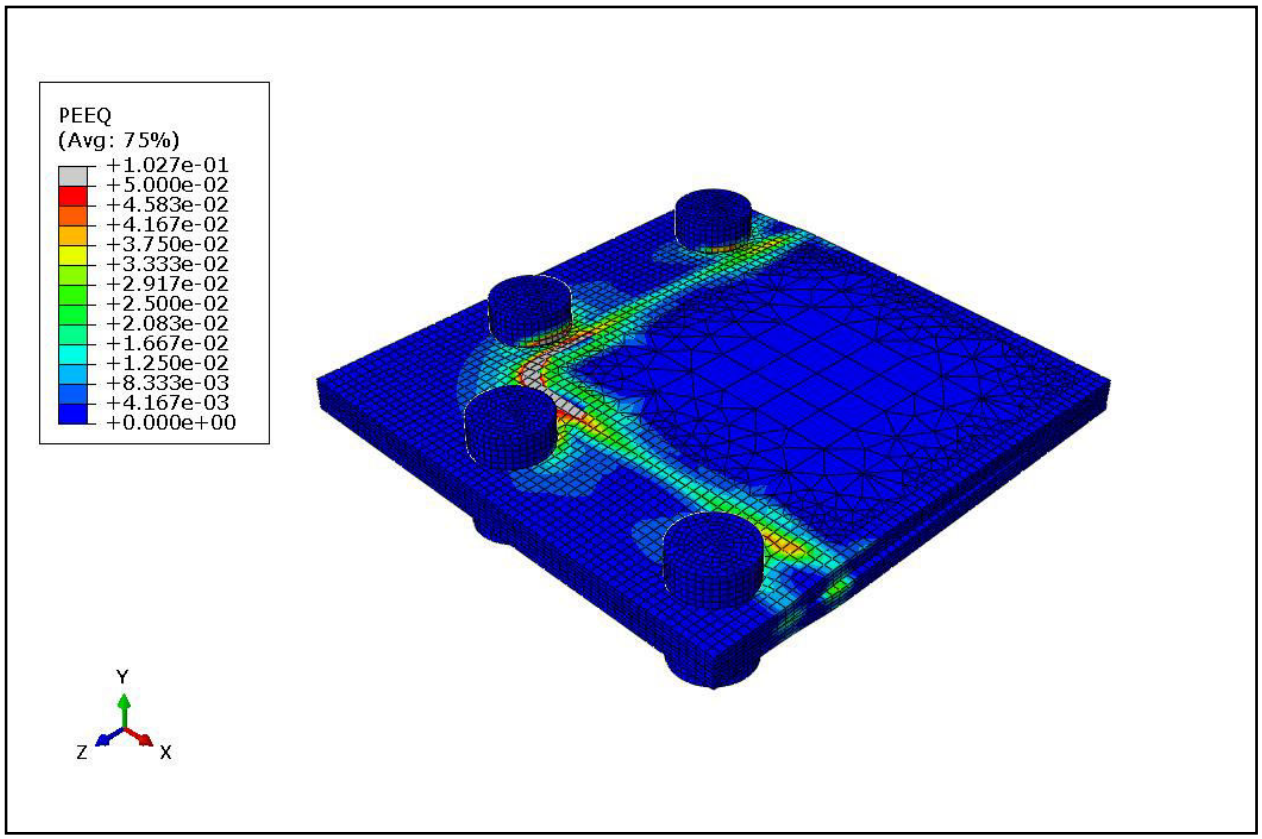

Figure 4-49: Plastic strain distribution in end-plate at 1130 KN (CC-1/case 3)

Ultimate tensile resistance of corner column is reached at 1130 KN. 5% plastic strains are attained in end-plate as shown in figure 4-49. Cover plate have significantly yielded by this point. However, cover plates haven't yet attained ultimate strain at 1130KN.

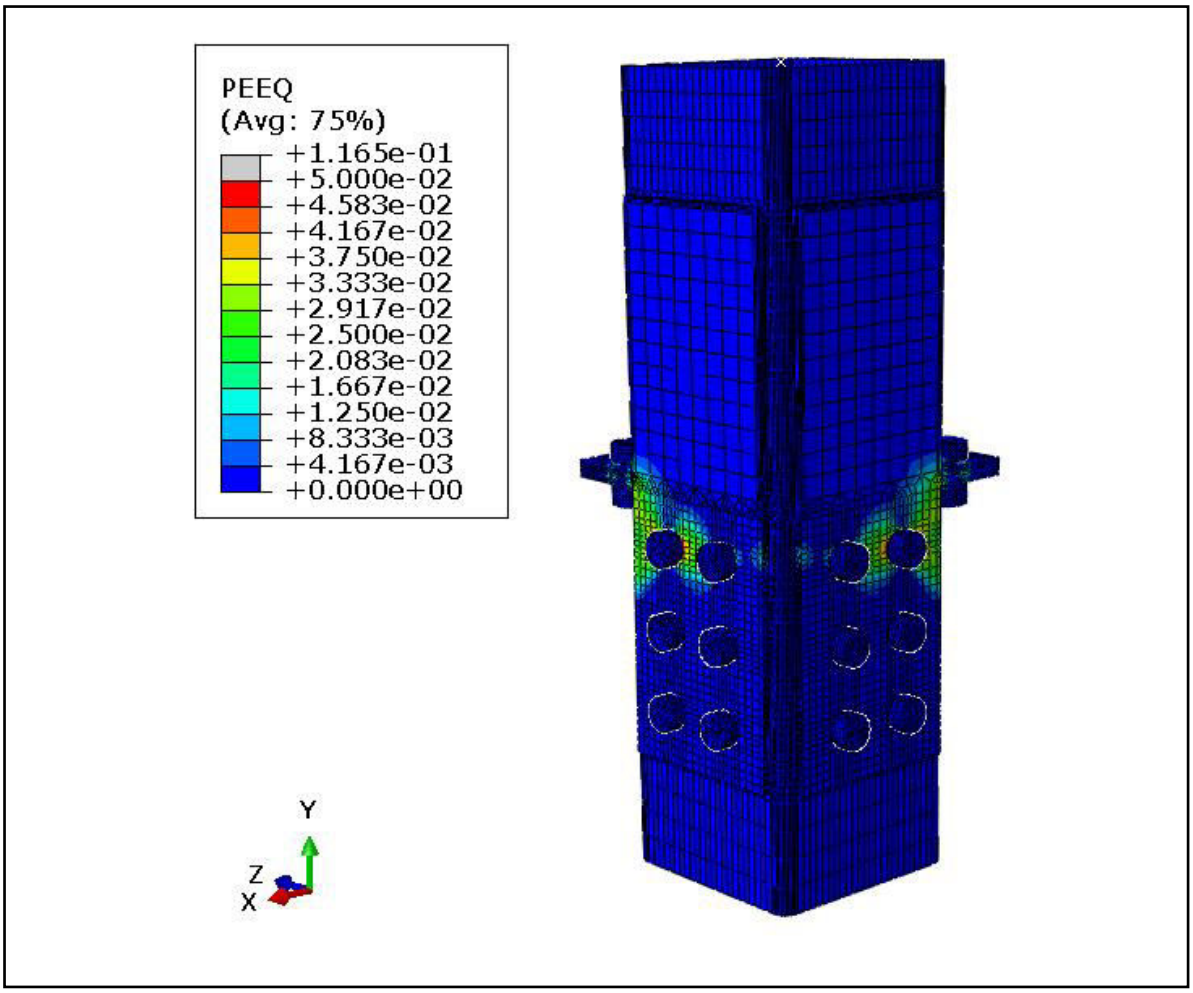

Figure 4-50: Plastic strain distribution in specimen at 1130KN (CC-1/case 3)

Chapter 5 – Finite element results of non-symmetrical intermediate splice connection

5.1 Introduction

In this chapter finite element results obtained for non-symmetrical intermediate splice specimen IC-1 are discussed. Non-symmetrical column splice connection for intermediate column can be evaluated under tensile case and three bending cases. Whole specimen is subjected to an axial load to evaluate the connection components under tensile force. In bending it can be seen that the connection behaves differently for bending around X and Z-axes of the column cross-section. First bending case is around Z-axis away towards X-axis, causing the cover plate to act in compression as seen in figure. Second bending case is around Z-axis away from X-axis that causes side cover plate to be loaded in tension. Third bending case is around X-axis that causes cover plate to act in rotation as seen in figure 5-2.

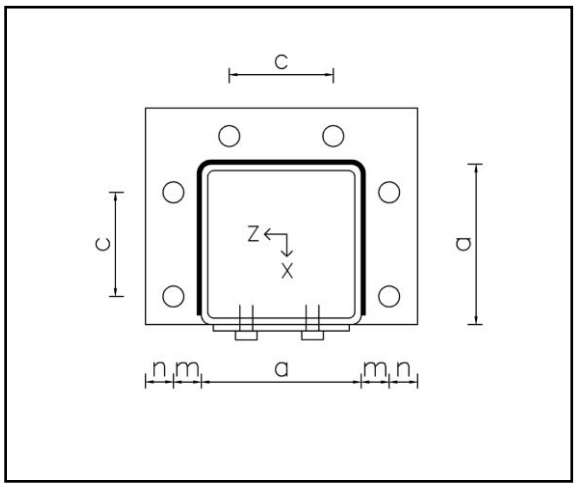

Figure 5-1: Bolt layout of non-symmetrical intermediate splice connection

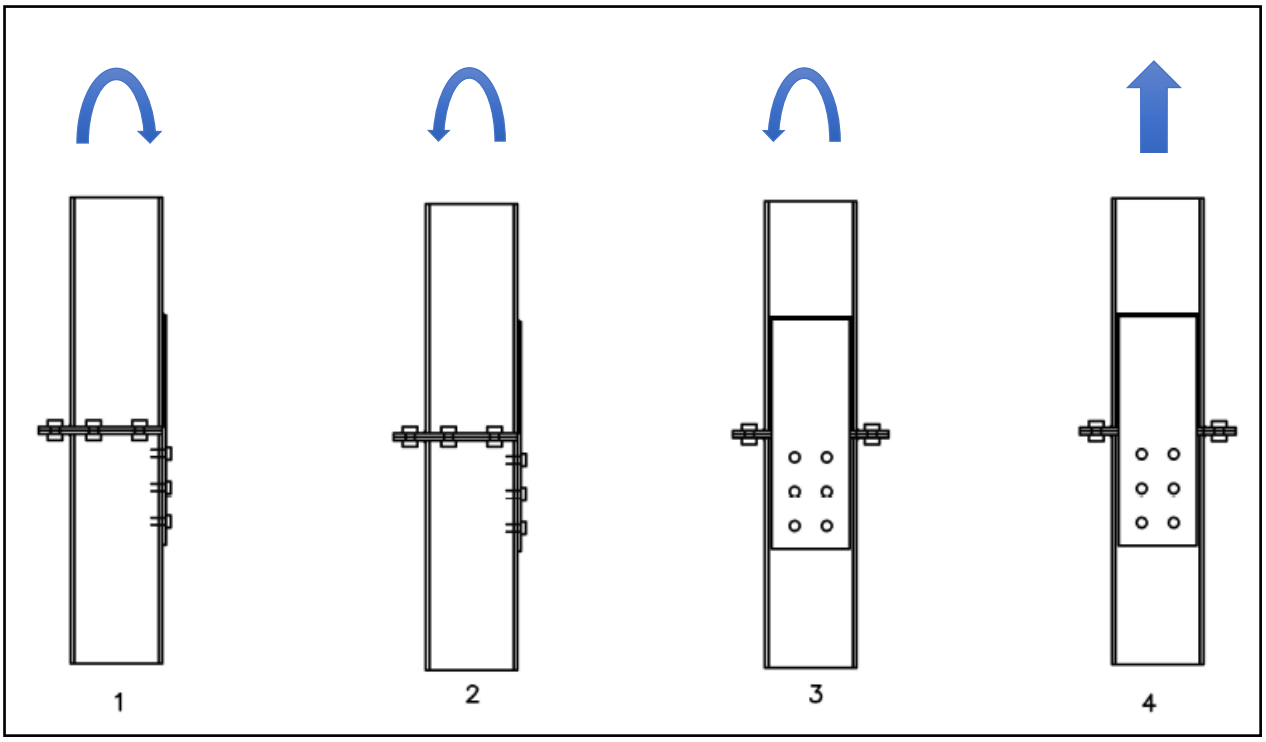

Figure 5-2: Load cases for non-symmetrical intermediate splice connection

List of load cases for non-symmetrical intermediate splice connection:
Case 1 – Cover plate in compression (bending)
Case 2 – Cover plate in tension (bending)
Case 3 – Cover plate in rotation (bending)
Case 4 – Specimen in tension

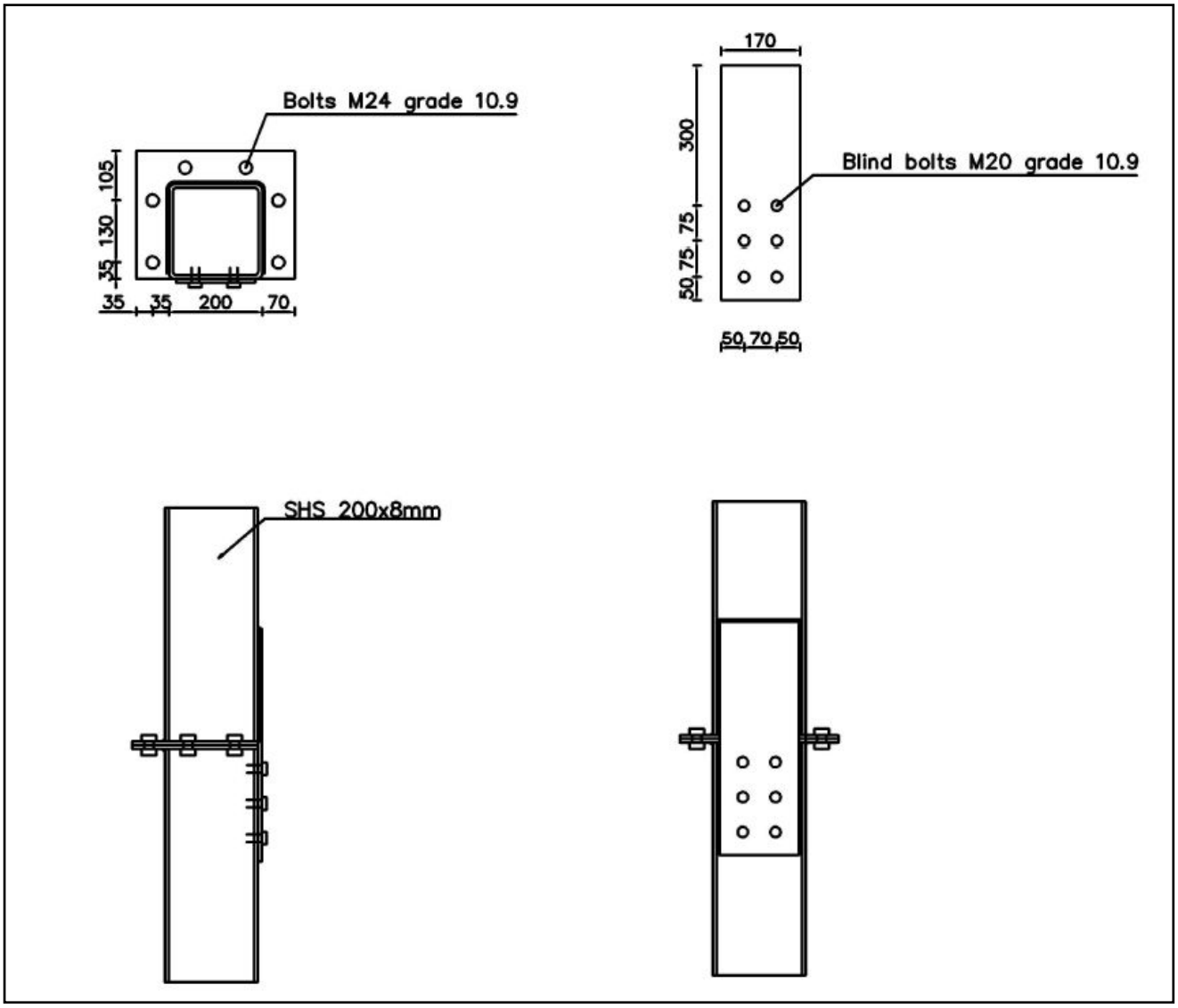

Figure 5-3: Plan and elevation of specimen IC-1

5.2 Non-symmetrical intermediate splice – cover plate in compression

First bending case of non-symmetrical intermediate splice connection is discussed in this section. Top column bends around X-axis towards the cover plate due to applied load as seen in figure 5-4. Rotation of connection is taken as the rotation between top and bottom end plates as shown in figure 5-5. In both the bending cases of corner column connection, end-plate rotation varied based on the section where rotation was calculated. For the present case, end-plate rotation can be calculated at two sections of end plate as shown in figure 5-6. But the rotation remains identical at both sections due to symmetrical layout of connection for bending around X-axis. While it would be otherwise if bending was around Z-axis.

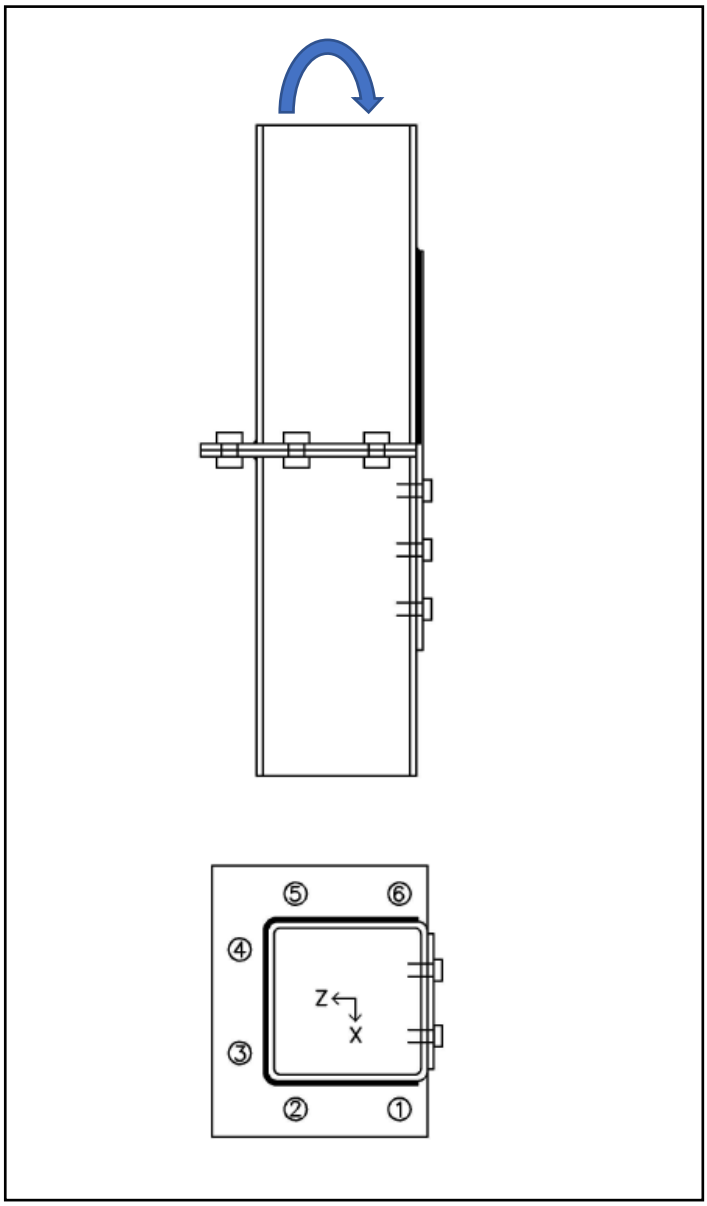

Figure 5-4: Plan and elevation of specimen IC-1 (case 1)

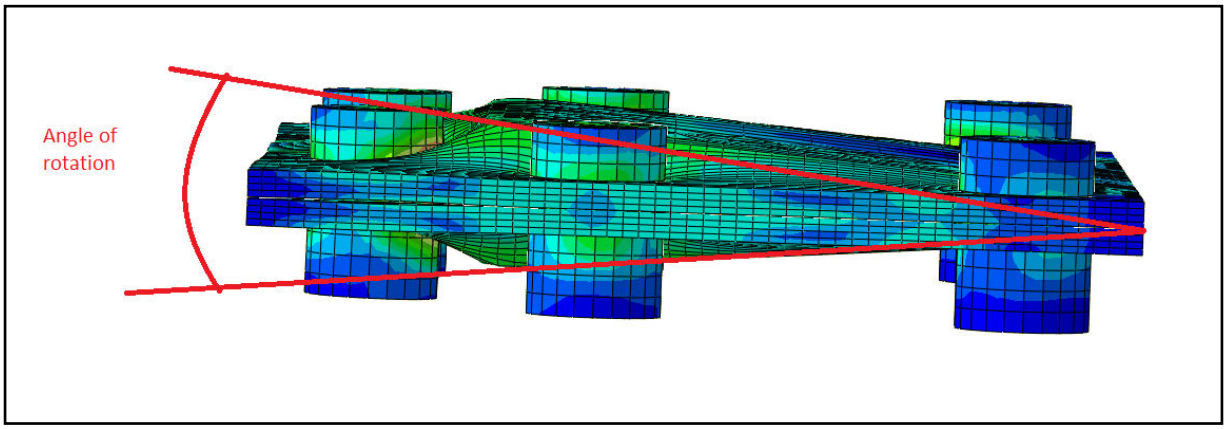

Figure 5-5: Calculation of rotation between end-plates (IC-1/case 1)

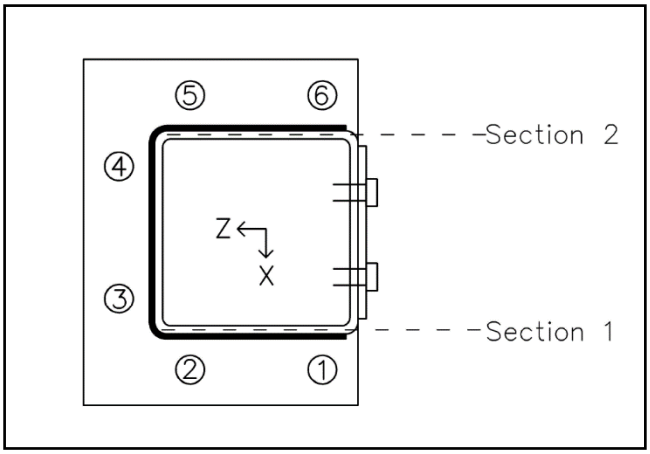

Figure 5-6: Locations in end-plate to calculate rotation (IC-1/case 1)

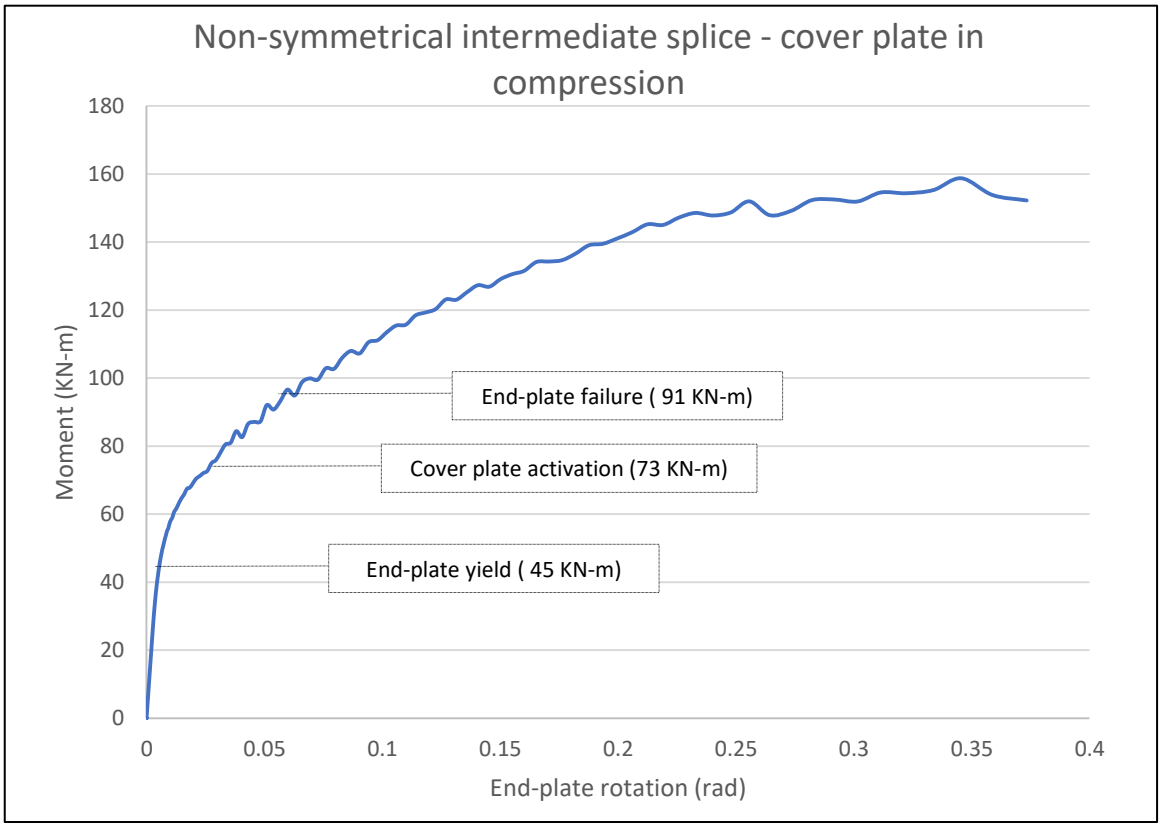

Figure 5-7: Moment rotation curve of specimen IC-1 (case 1)

In the initial stage of loading, bolts 2,3,4 and 5 in end-plate carry most of the applied. Load carried by bolts in cover plate are negligible until a moment resistance of 73 KN-m is reached. Since, significant deformation of end-plate is required for bolts in cover plate to be active during loading. Bending yield resistance of intermediate column connection for present bending case is reached at 45 KN-m. Yield stresses are attained in end-plate near bolts 3 and 4 as seen in figure 5-8.

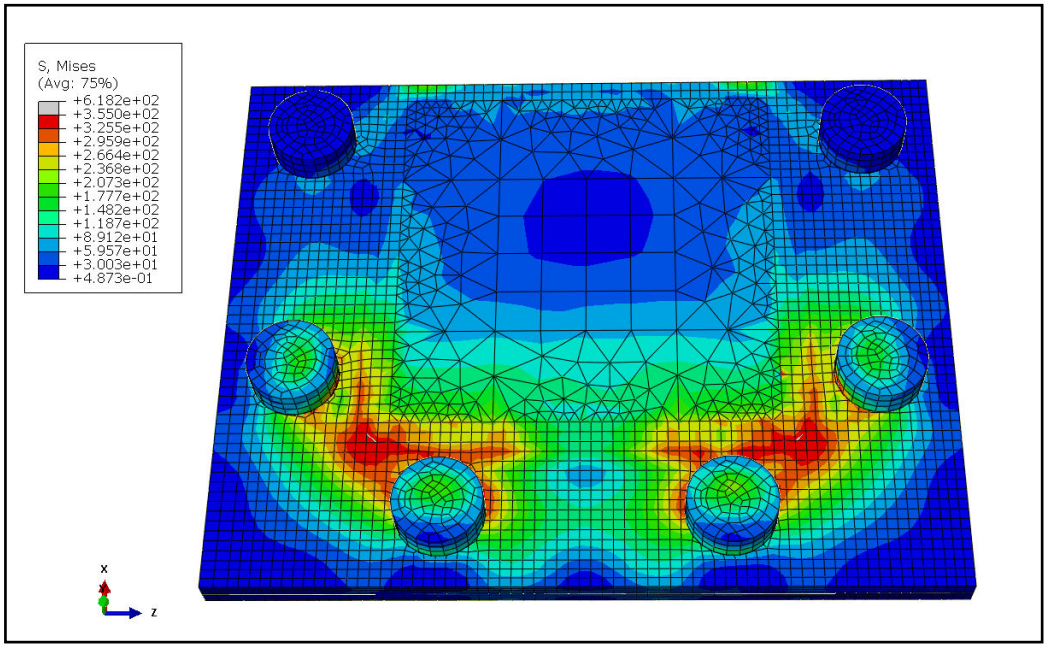

Figure 5-8: Von mises stress distribution in end-plate at 45 KN-m (IC-1/case 1)

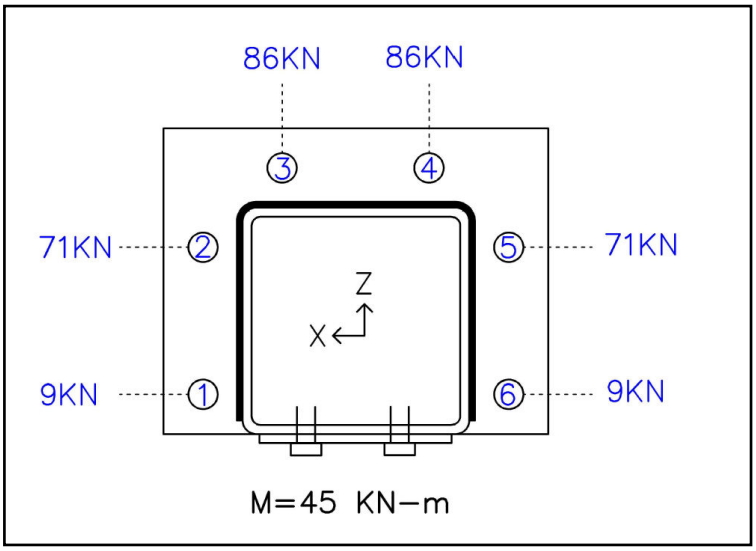

Figure 5-9: Tensile forces of bolts in end plate at 45 KN-m (IC-1/case 1)

At 45 KN-m, top, middle and bottom bolt groups carry 50%, 42% and 7% of the load transferred by end-plate. Tensile forces of end-plate bolts 2,3,4 and 5 exhibit a linear behavior in the initial stages. This linear behavior ends at a moment resistance of 45 KN-m as seen in figure 5-10. This also confirms the yielding of end-plate as noticed in the contour plots.

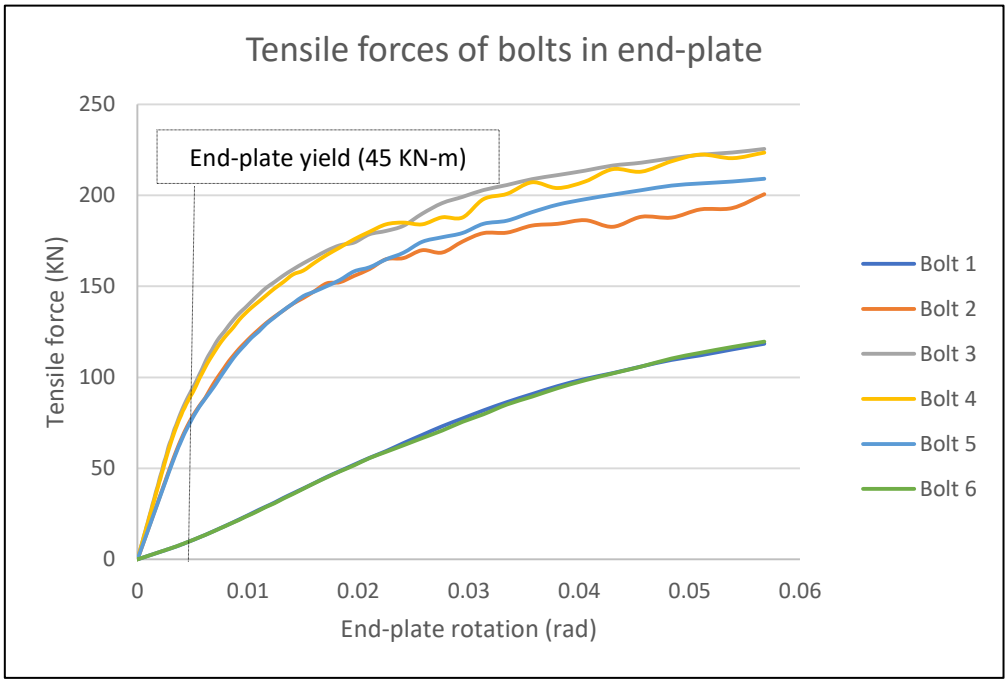

Figure 5-10: Tensile force carried by bolts in end-plate (IC-1/case 1)

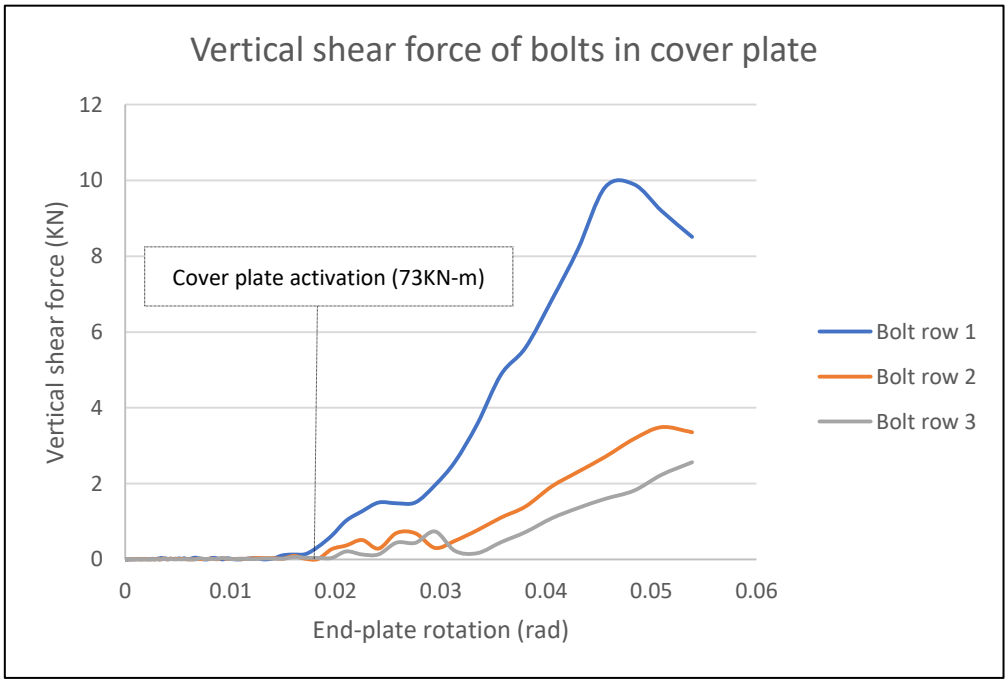

Figure 5-11: Vertical shear force carried by bolts in cover plate (IC-1/case 1)

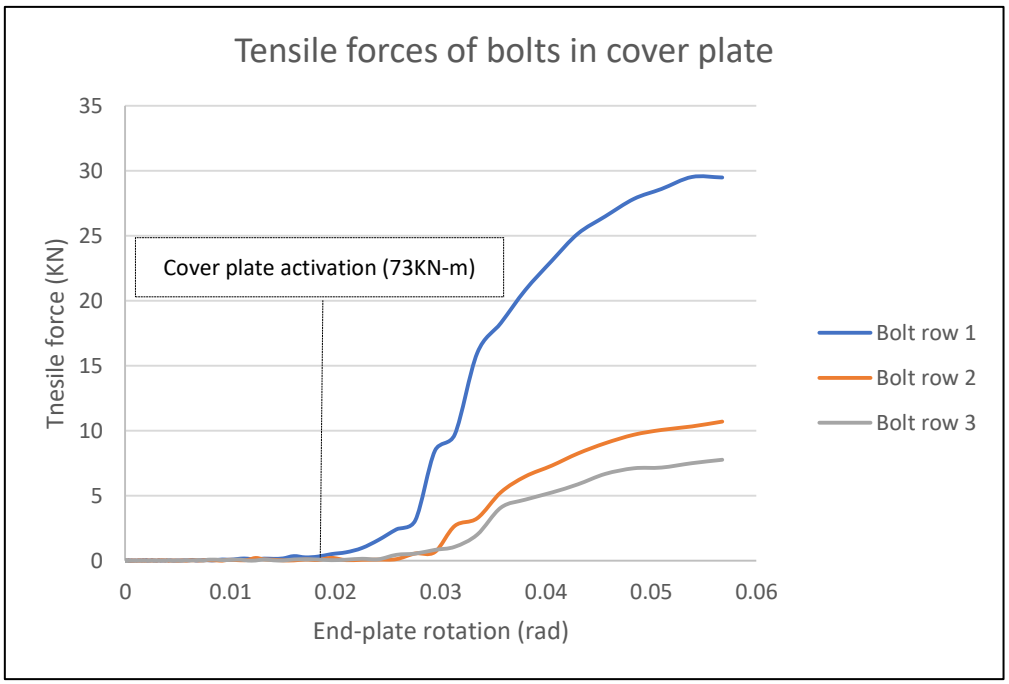

Figure 5-12: Tensile force carried by bolts in main cover plate (IC-1/case 1)

At a moment resistance of 73 KN-m, bolts in cover plate attain a sharp increase in tensile load carried by them. Significant yielding of end plate has led to elastic deformation of cover plate, which causes considerable tensile forces at top bolt row. It should be noted that cover plate is still in elastic stage at this point. Vertical shear load carried by bolts in cover plate also experience a sharp increase at this stage, but the magnitude remains low.

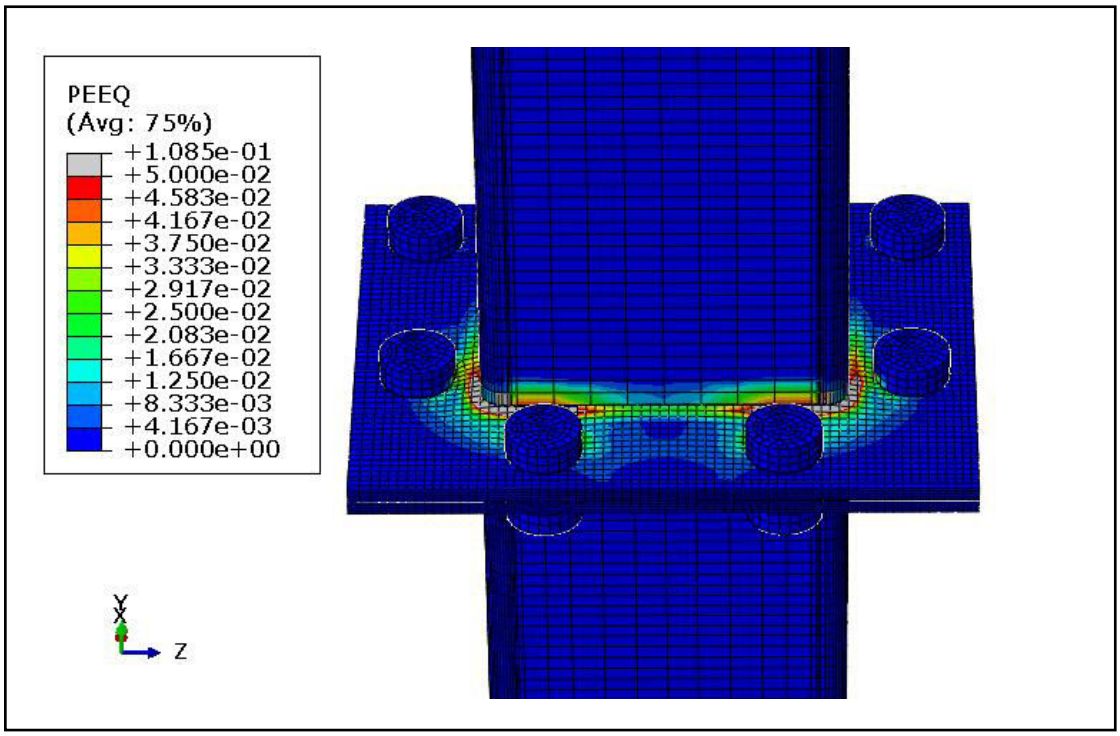

Figure 5-13: Plastic strain distribution at 91 KN-m (IC-1/case 1)

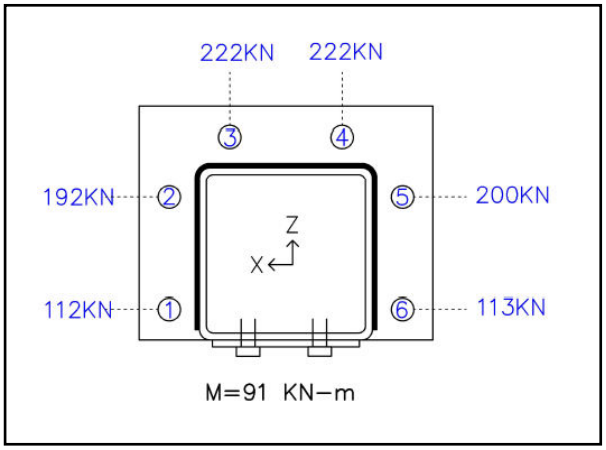

Figure 5-14: Tensile forces in end-plate at 91 KN-m (IC-1/case 1)

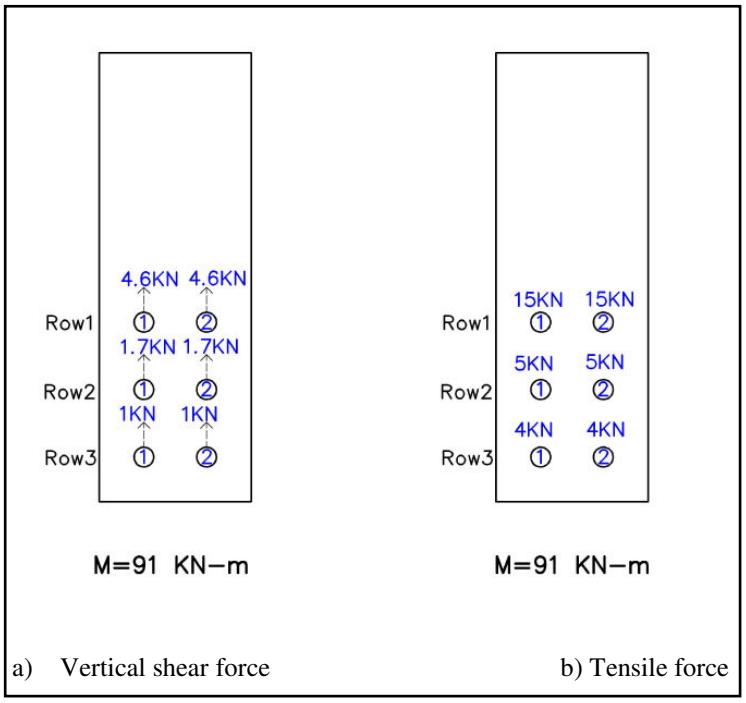

Figure 5-15: Bolt forces in cover plate at 91 KN-m (IC-1/case 1)

At a moment resistance of 91 KN-m, the ultimate resistance of intermediate column for the present bending case is reached. This occurs due to failure of end plate as shown in figure 5-13. High plastic strains are attained in end-plate near bolt 2,3,4 and 5. Significant deformation in end-plate leads to bending of cover plate outwards. Cover plate attains yield stresses as the resistance of the connection approaches ultimate limit as seen in figure 5-16. At ultimate resistance, bolt row 1 carries 63% of the vertical shear, while bolt rows 2 and 3 carry 22% and 13% respectively.

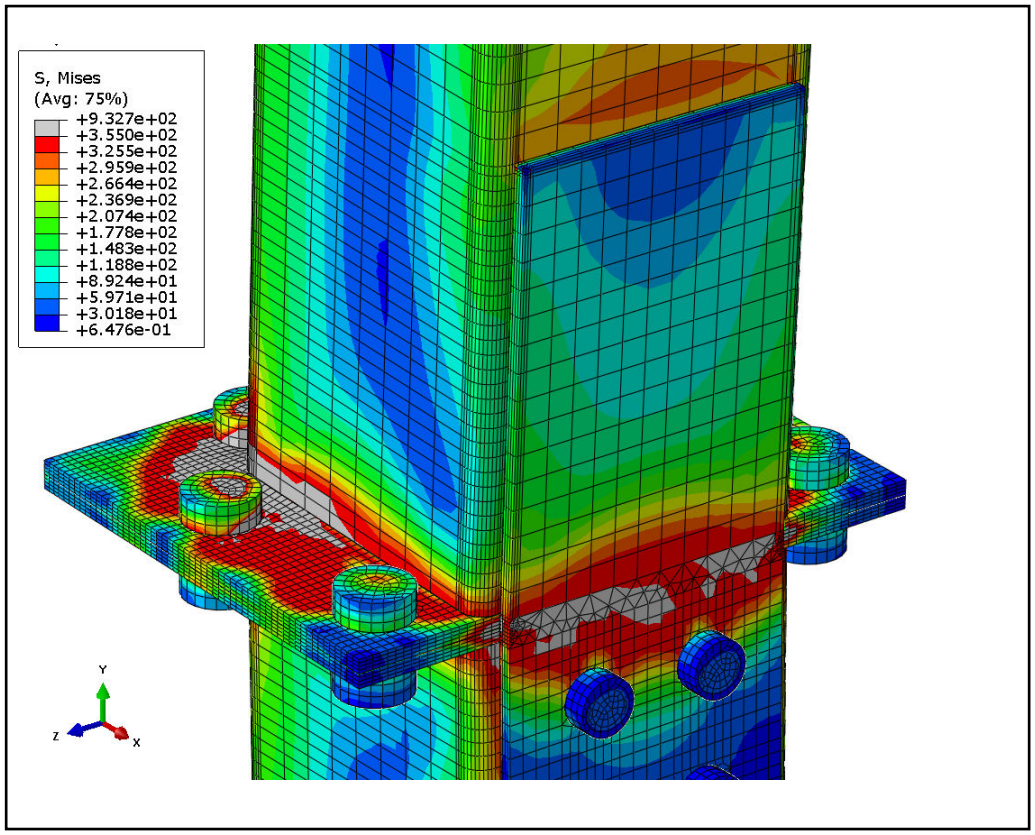

Figure 5-16: Von mises stress distribution at 91 KN-m (IC-1/case 1)

5.3 Non-symmetrical intermediate splice – cover plate in tension

In this section second bending case of non-symmetrical intermediate column splice, where in cover plate is in tension is discussed. Due to applied load, top column bends around X-axis away from the cover plate as shown in figure 5-17. Rotation of the connection is taken as the rotation between top and bottom end plates are shown in figure 5-18. Similar to the previous case, end-plate rotation remains the same along section 1 and section 2. Which is due to symmetrical layout of connection for bending around Z-axis.

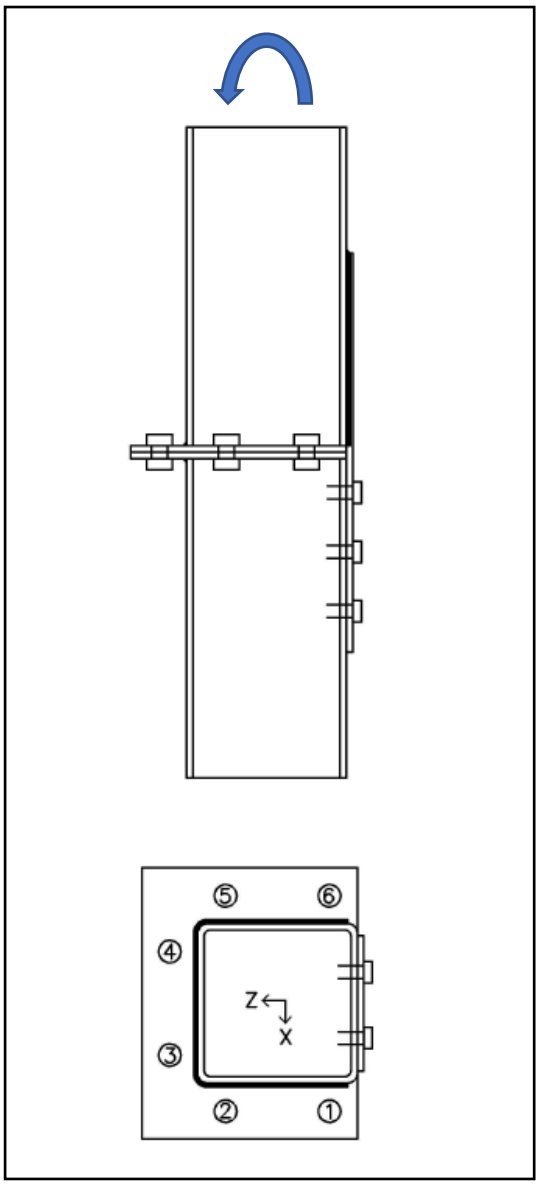

Figure 5-17: Plan and elevation of specimen IC-1 (case 2)

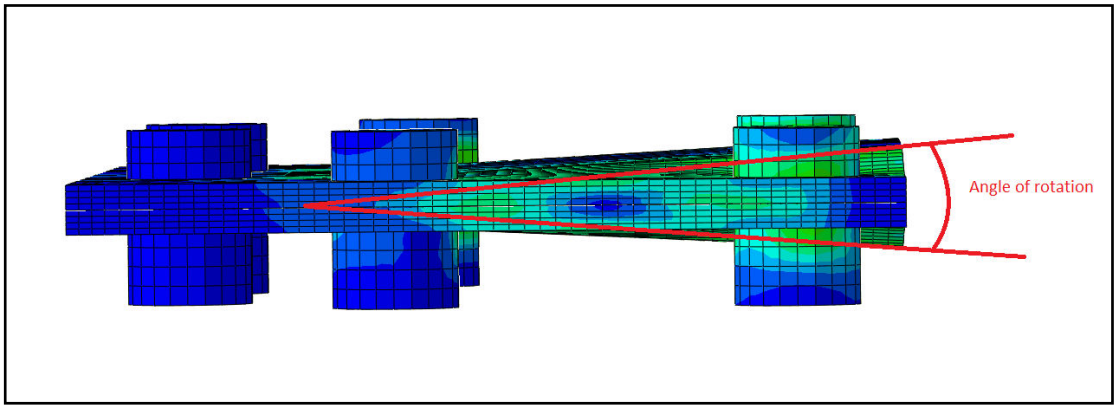

Figure 5-18: Calculation of rotation between end-plates (IC-1/case 2)

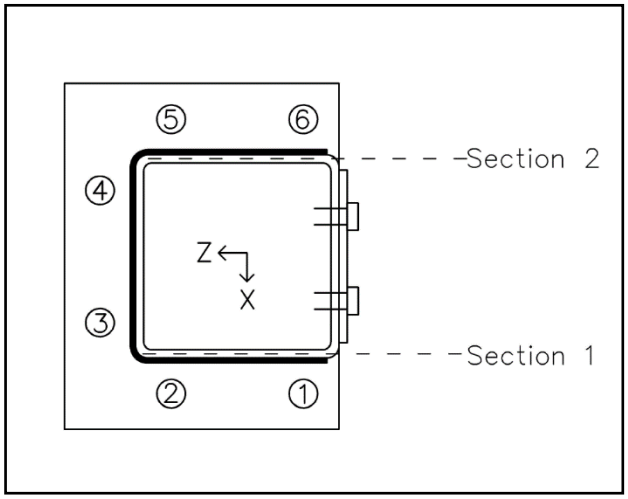

Figure 5-19: Location in end-plate to calculate rotation (IC-1/case 2)

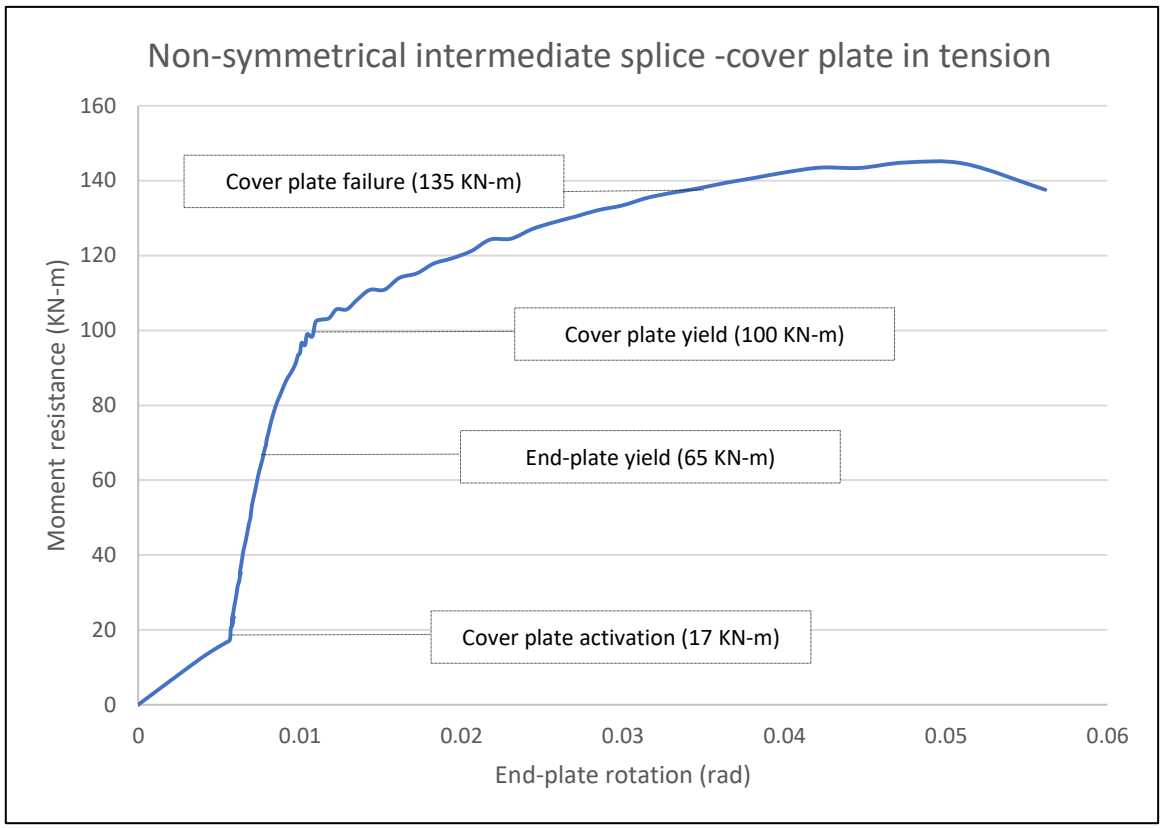

Figure 5-20: Moment rotation curve of specimen IC-1 (case 2)

In the initial part of the moment-rotation curve shown in figure 5-20, two elastic parts can be noticed. This is due to bolt hole clearance provided in cover plate and bottom column. In the initial stages, bolt 1 and 6 in end-plate carry most of the applied load. Main cover plate doesn't fully contribute towards resistance in initial stages of loading. Bolts in cover plate attain a sharp increase in load carried when a moment resistance of 17 KN-m is reached. End-plate yield at a moment resistance of 65 KN-m. The moment-rotation curve doesn't exhibit significant flattening at 65 KN-m due to the presence of cover plate. This restricts the rotation of end-plate.

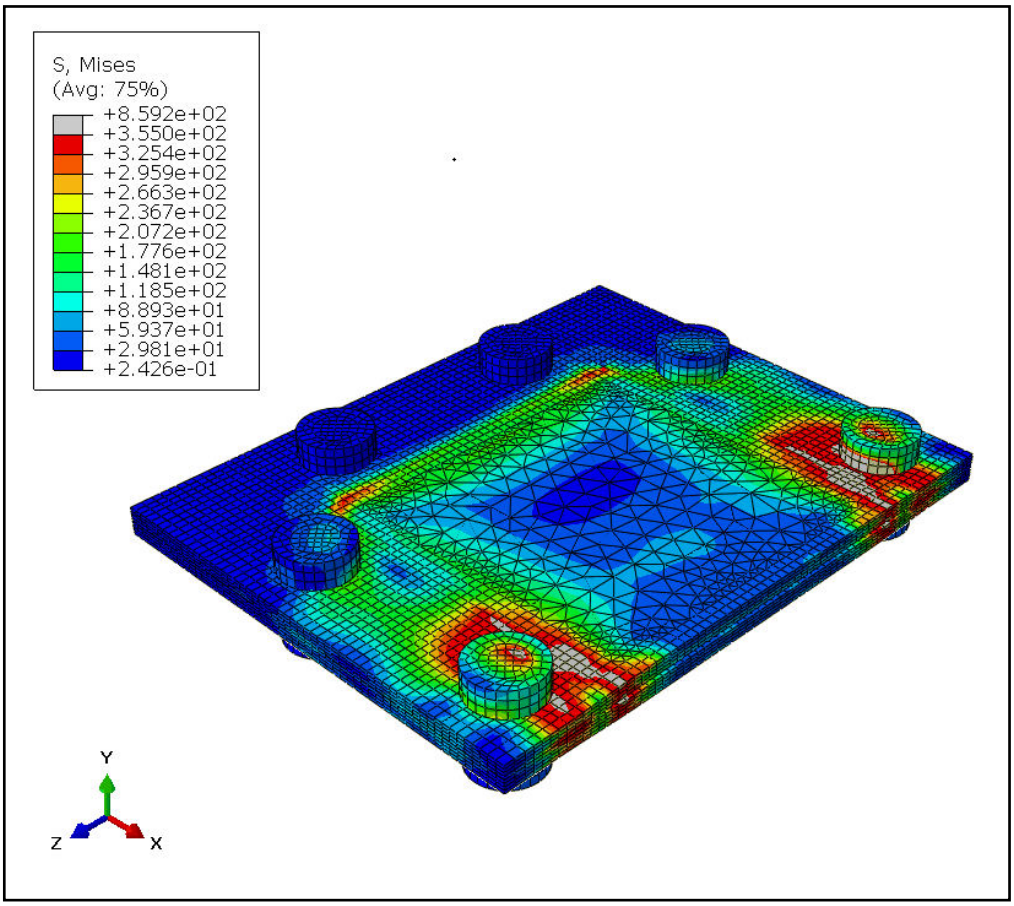

Figure 5-21: Von mises stress distribution in end-plate at 65 KN-m (IC-1/case 2)

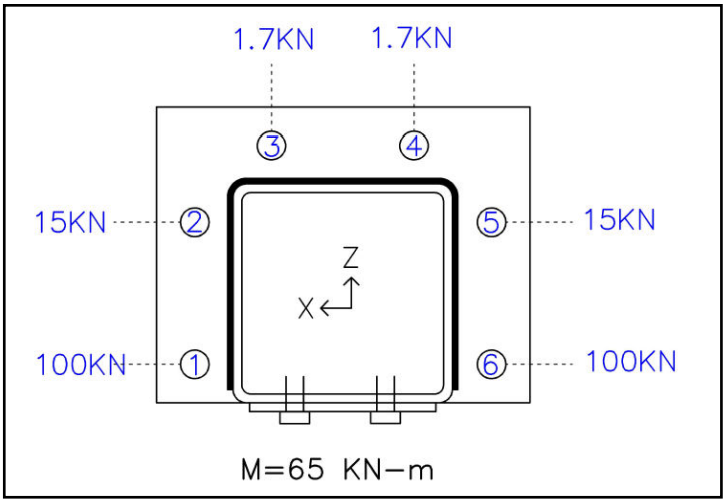

Figure 5-22: Tensile forces of bolts in end-plate at 65 KN-m (IC-1/case 2)

End-plate yields at a moment resistance of 65 KN-m. Yield stresses are attained in end-plate near bolts 1 and 6 as seen in figure 5-21. Bolts 1 and 6 carry the highest amount of tensile force in end-plate. Bolts 2 and 5 carry approximately 15% of the load carried by bolts 1 and 6 at yield resistance. Up to a moment resistance of 65 KN-m, linear increase in tensile forces of

bolts 1 and 6 can be noticed as seen in figure 5-23. The slope of the curve changes after this point, confirming the yielding of end-plate as mentioned in the global moment-rotation curve.

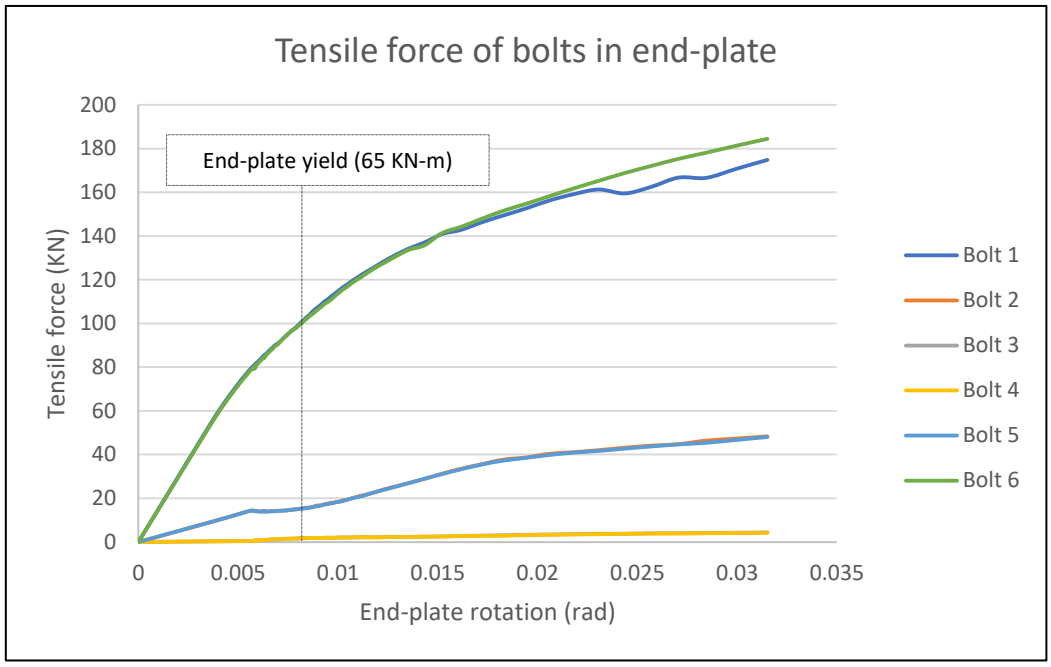

Figure 5-23: Tensile force carried by bolts in end-plate (IC-1/case 2)

Main cover plate, while in tension is also subjected to bending at its mid-height. This causes the bolts in main cover plate to carry vertical shear and tensile forces. It is noticed that, relatively high loads were transferred at top and bottom bolt row compared to middle bolt row as seen in figure 5-28. At a moment resistance of 100KN-m, yield stresses are attained in cover plate as shown in figure 5-24. Cover plate yields near the top bolt row. Vertical shear force and tensile force are almost equally distributed among top two bolt rows due to yielding.

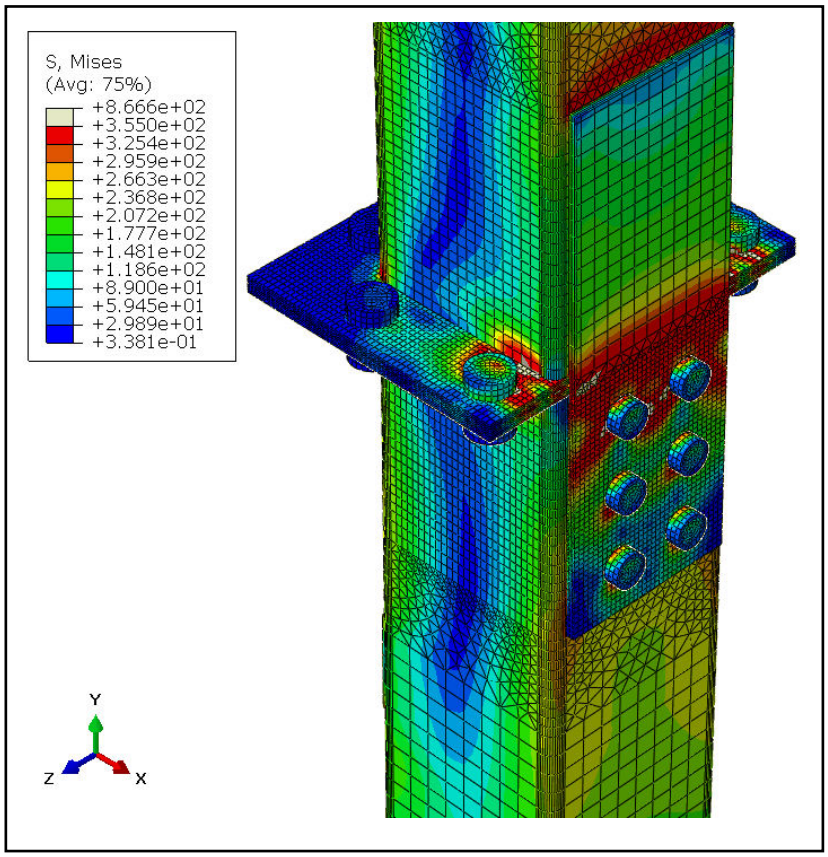

Figure 5-24: Von mises stress distribution at 100 KN-m (IC-1/case 2)

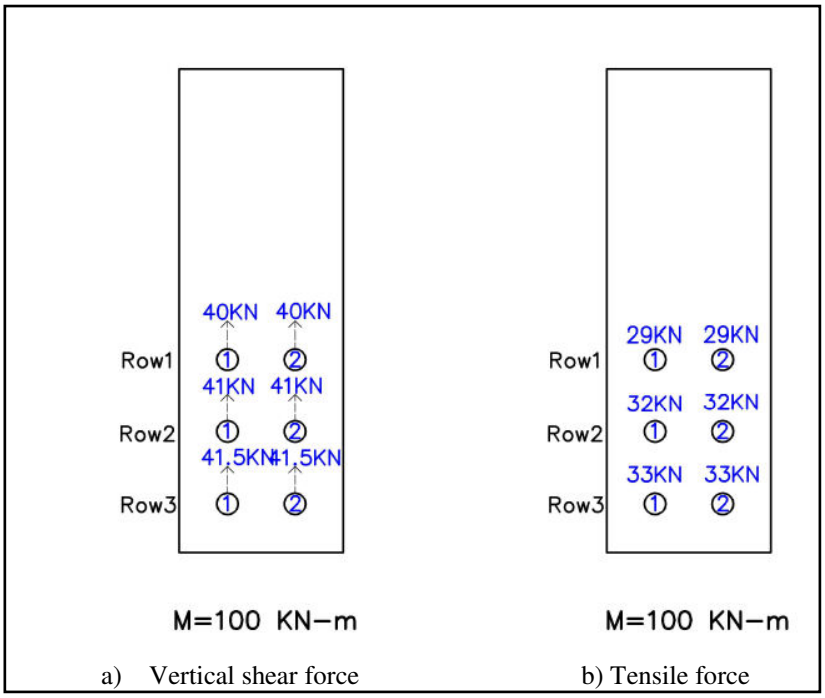

a) Vertical shear force b) Tensile force

Figure 5-25: Bolt forces in cover plate at 100 KN-m (IC-1/case 2)

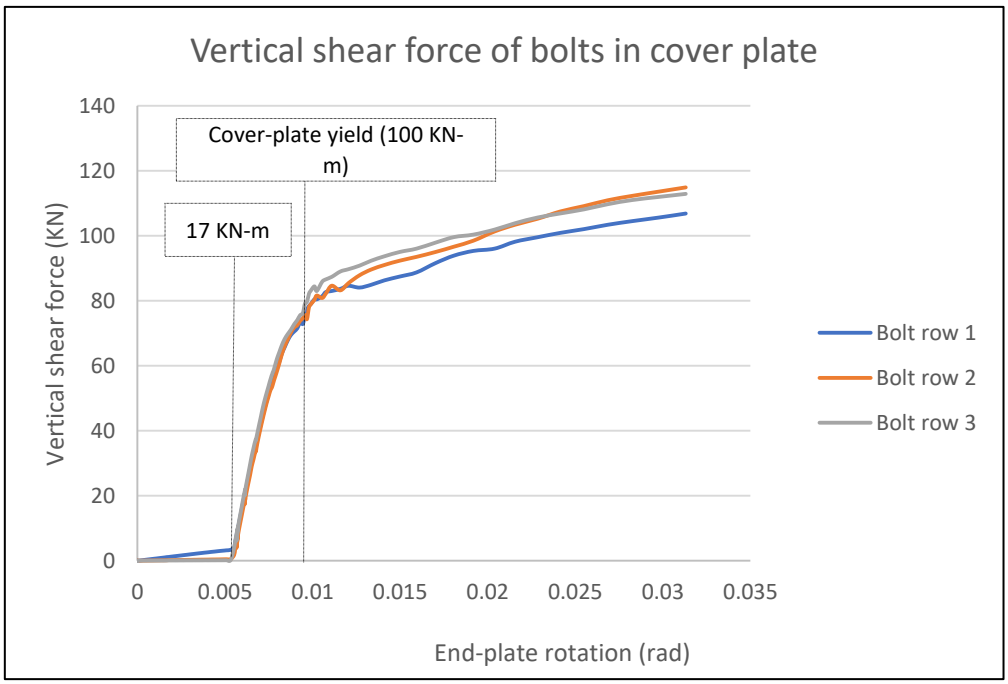

Figure 5-26: Vertical shear force carried by bolts in cover plate (IC-1/case 2)

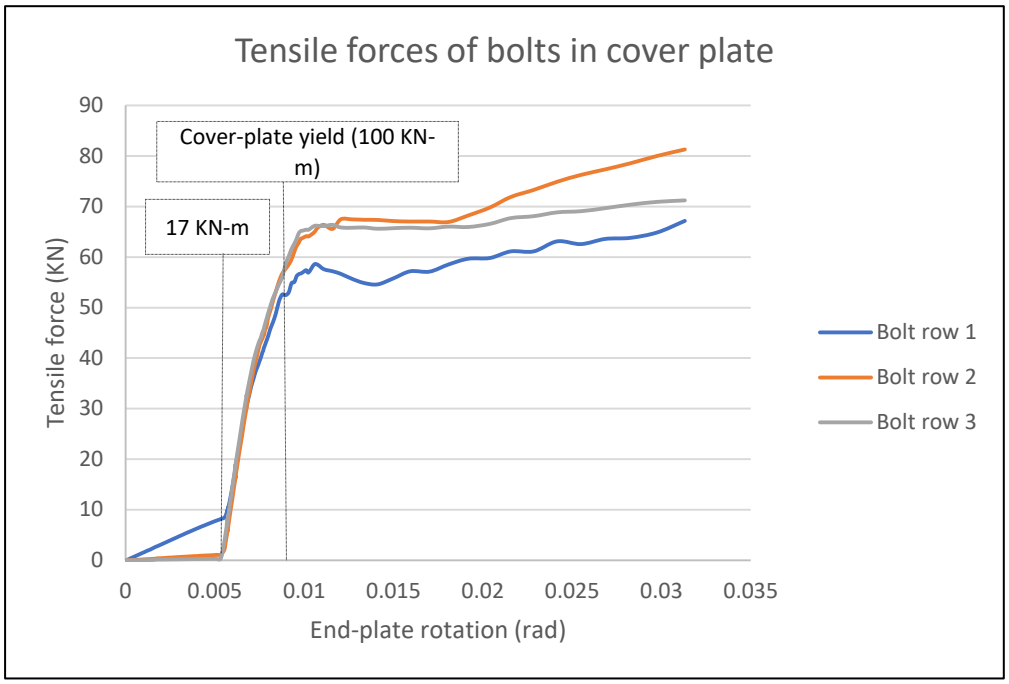

Figure 5-27: Tensile force carried by bolts in cover plate (IC-1/case 2)

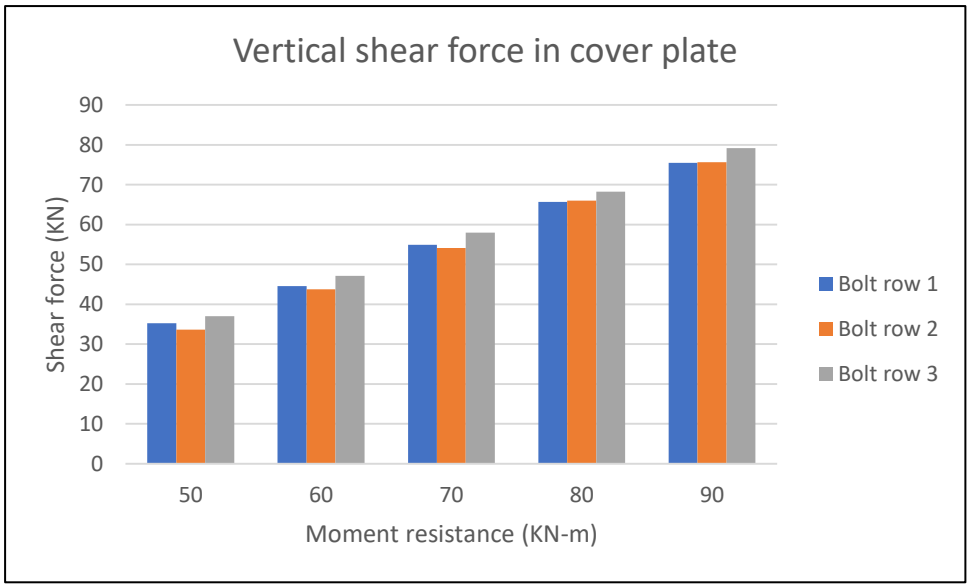

Figure 5-28: Vertical shear force carried by bolt rows in cover plate (IC-1/case 2)

As seen in figure 5-26, vertical shear forces of bolts in cover plate are very low until a moment of 17KN-m is reached. Also, the curve shows a linear increase until a moment of 90 KN-m and curve flattens. Similar characteristics can be found with tensile forces of bolts in cover plate shown in figure 5-27. Bottom bolt row of cover plate carries a higher tensile force than other two bolt rows in the initial stages due to bending of the cover plate towards column face.

.

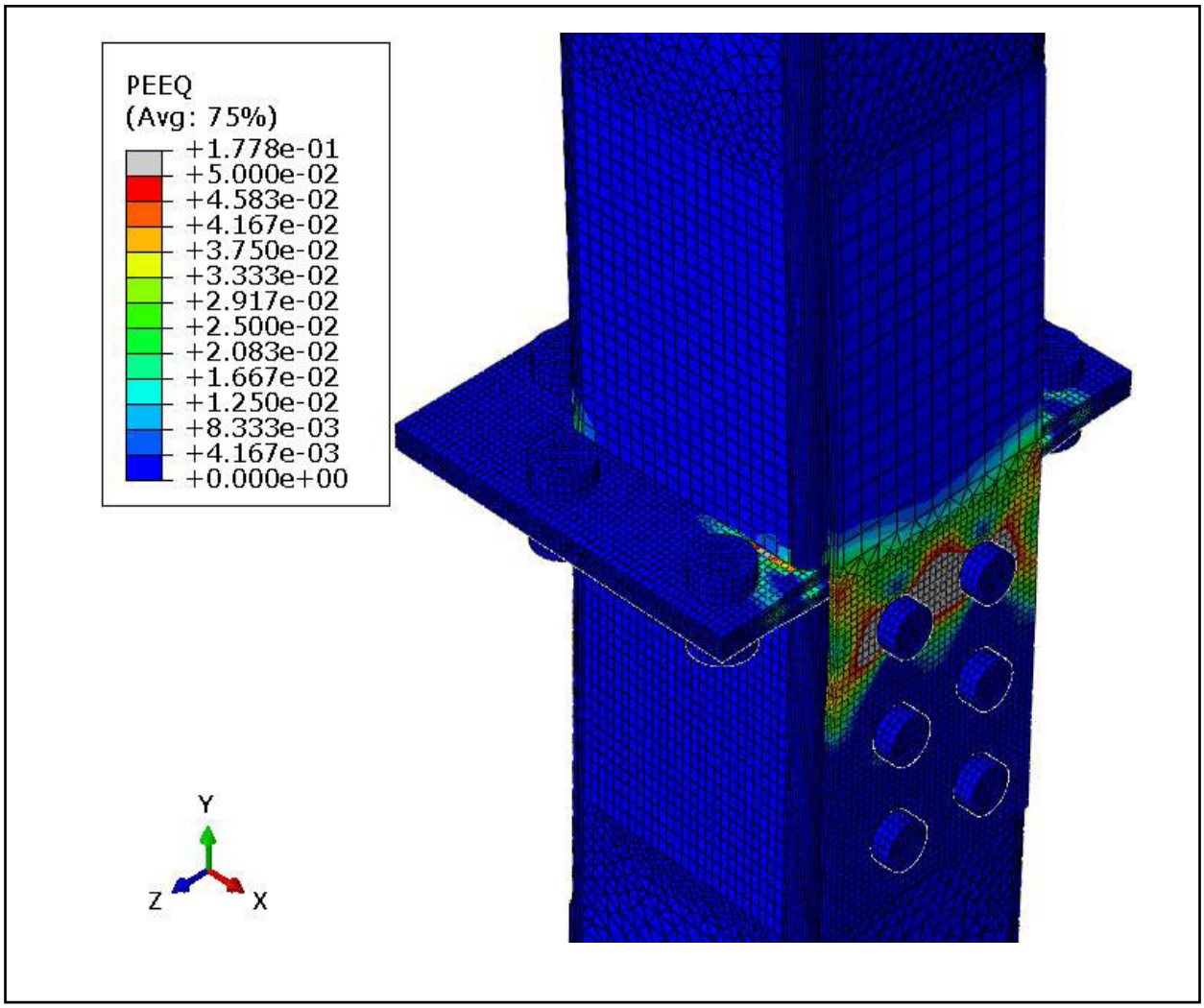

Figure 5-29: Plastic strain distribution at 135 KN-m (IC-1/case 2)

Ultimate resistance of intermediate column connection for cover plate in tension bending case is reached at a moment resistance of 135 KN-m. 5% plastic strains are reached in the cover plate near top bolt row as shown in figure 5-29. This causes failure of cover plate along net section.

5.4 Non-symmetrical intermediate splice – cover plate in rotation

In this section third bending case of non-symmetrical intermediate splice connection, where in cover plate is in rotation is discussed. Top column rotates around X-axis due to applied load as shown in figure 5-30. Rotation of the connection is taken as the rotation between top and bottom end plates as shown in figure 5-31. Layout of the connection is non-symmetrical for bending around X-axis. End-plate rotation is calculated at section 1 and section 2 as shown in figure 5-32.

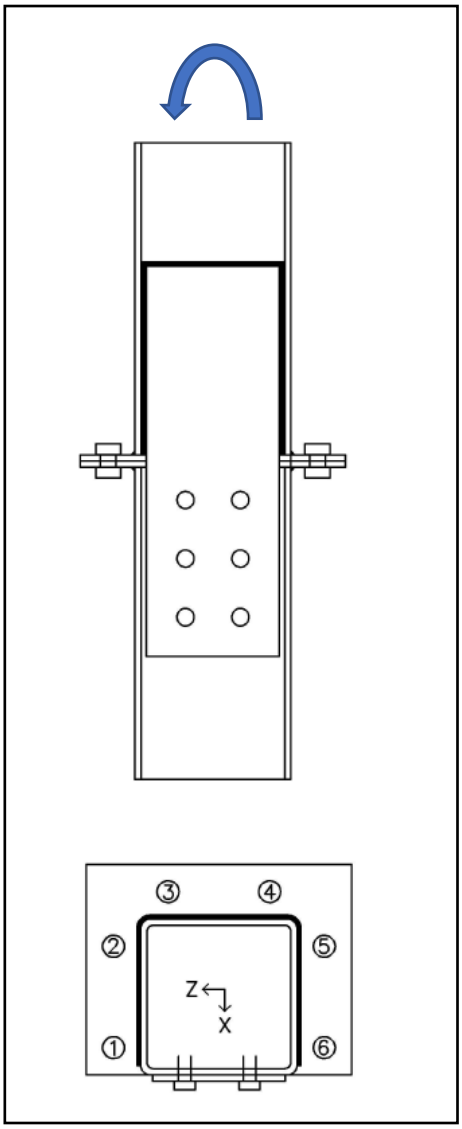

Figure 5-30: Plan and elevation specimen IC-1 (case 3)

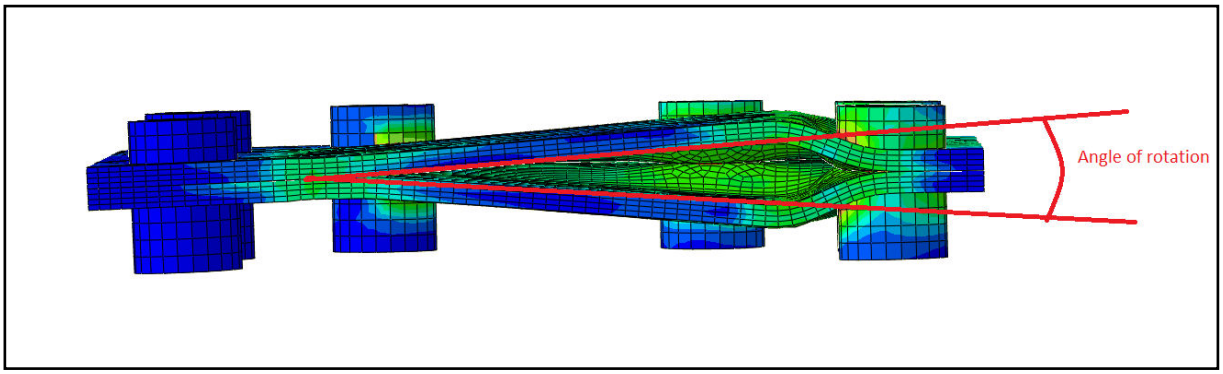

Figure 5-31: Calculation of rotation between end-plates (IC-1/case 3)

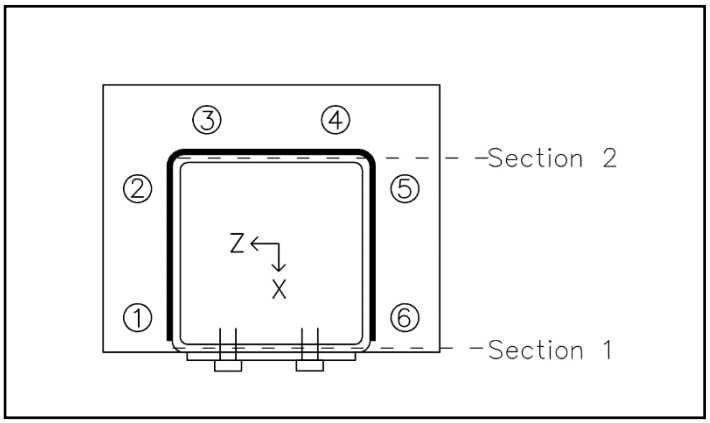

Figure 5-32: Location in end-plate to calculate rotation (IC-1/case 3)

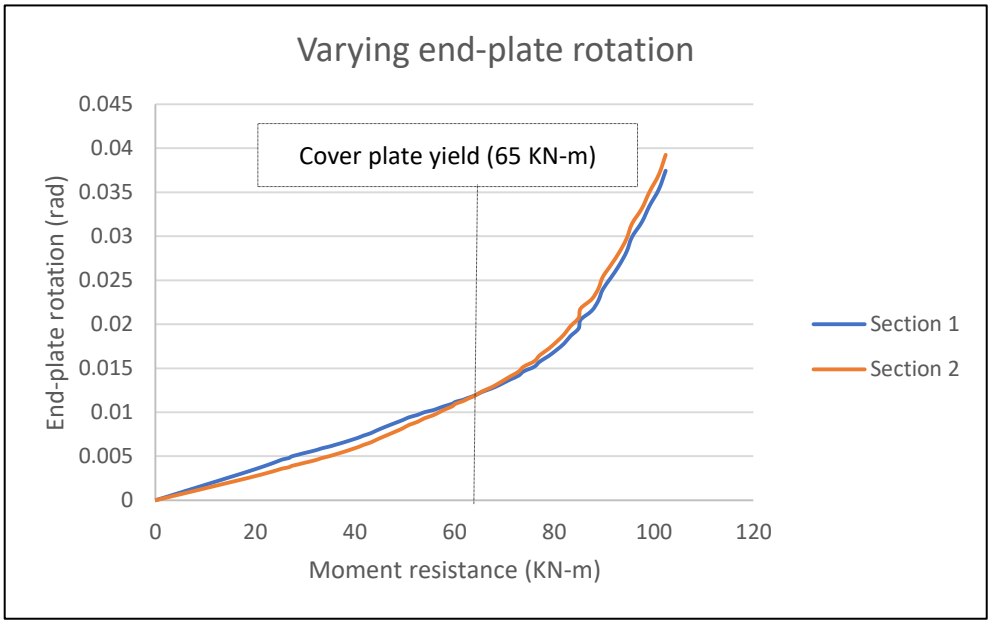

Figure 5-33: Moment resistance vs end-plate rotation (IC-1/case 3)

Varying rotation of end-plate can be noticed at section 1 and 2 as seen in figure 5-33. This occurs due to layout of the connection being non-symmetrical for the present bending case. Rotation along section 1 is higher than section 2 until the yield resistance of the connection is reached. However, secant stiffness is similar for both sections at yield resistance. Since, emphasis is placed on initial joint stiffness, rotation at section 1 is considered to study the overall moment-rotation behavior of the connection.

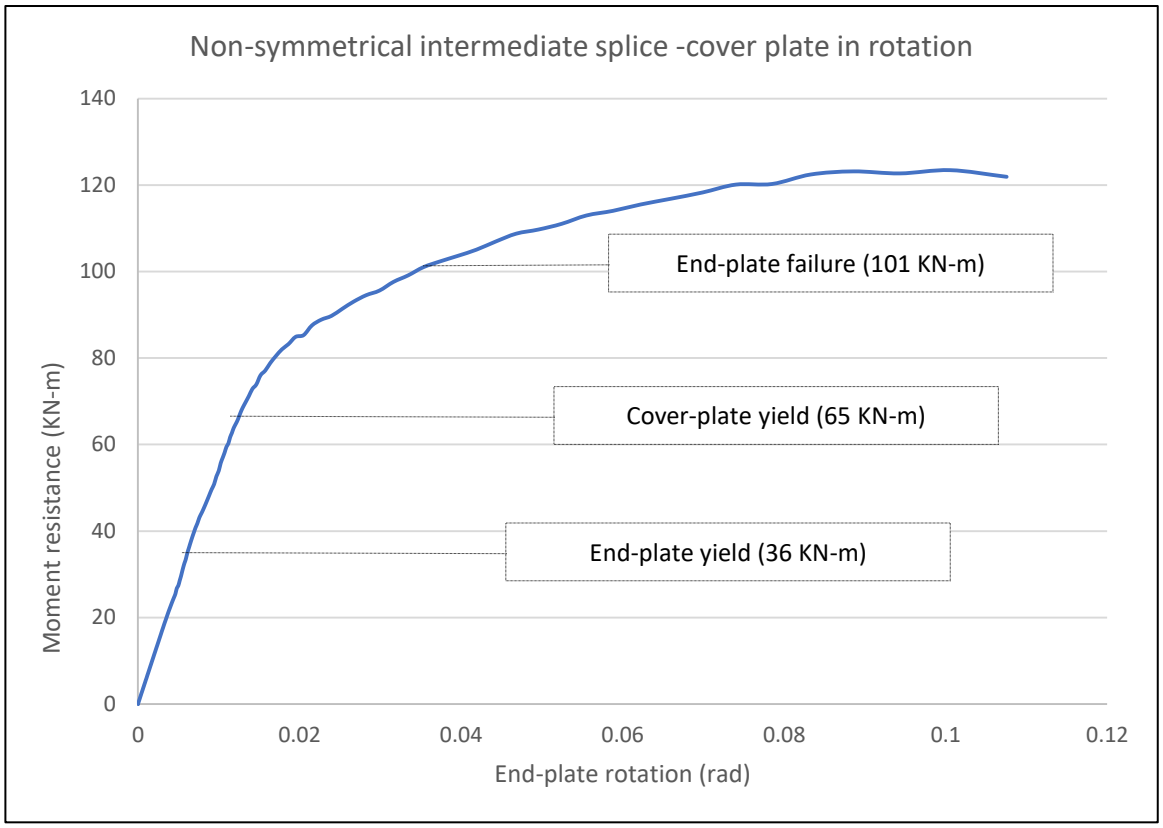

Figure 5-34: Moment rotation curve of specimen IC-1 (case 3)

In the initial stages of loading, bolts 1,2, and 3 in the end-plate carry most of the applied load. Contribution of cover plate towards resistance in the initial stages is negligible. Bolt forces in cover plate see a sharp increase at a moment resistance of 25 KN-m. Bolt 1 and 2 carry varying amount of tensile force due to non-symmetrical nature of the connection. Bolt 3 carries approximately 80% of the force carried by bolt 1 or 2. Yield stresses are attained in end-plate at a moment resistance of 36 KN-m. End-plate yields in the region close by to bolts 1 and 2 as seen in figure 5-35. However, the overall moment-rotation curve doesn't exhibit clear yielding or flattening of the curve at this point. This is due to the presence of cover plate which is still in elastic stage and doesn't allow end-plate to deform freely.

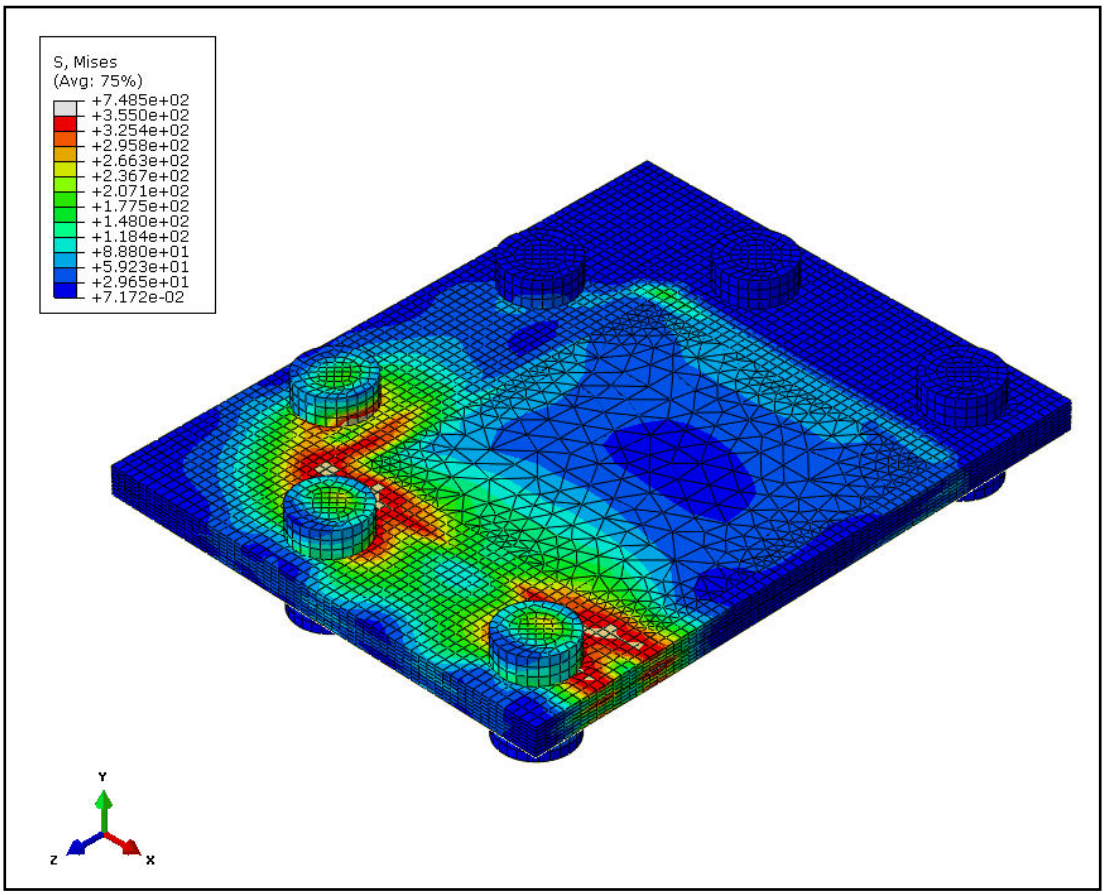

Figure 5-35: Von mises stress distribution in end-plate at 36 KN-m (IC-1/case 3)

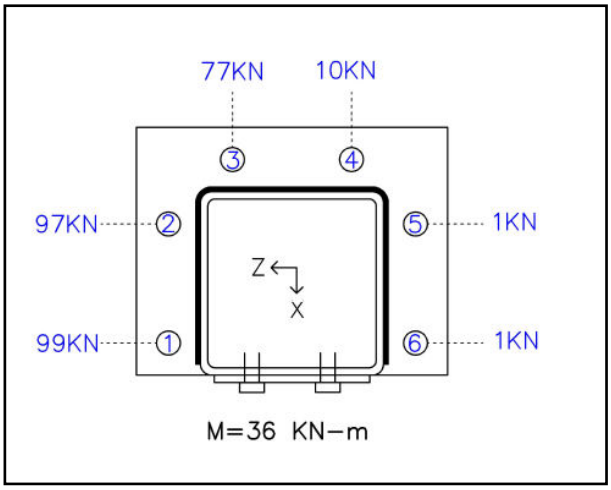

Figure 5-36: Tensile forces of bolts in end-plate at 36 KN-m (IC-1/case 3)

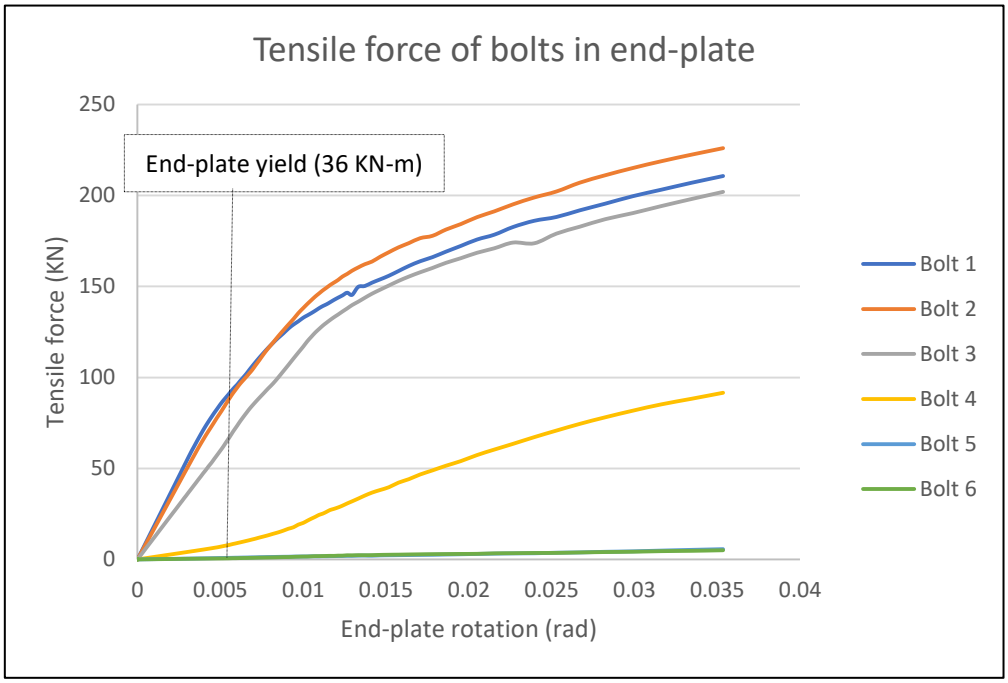

Figure 5-37: Tensile force carried by bolts in end-plate (IC-1/case 3)

Distribution of tensile force among bolts in end-plate is shown in figure 5-37. Bolt 1 carries higher load than bolt 2 until yield resistance of the connection is reached. Also, load carried by bolt 2 is higher than bolt 1 after yield resistance. This also explains varying end-plate rotation at section 1 and 2 as seen in figure 5-33.

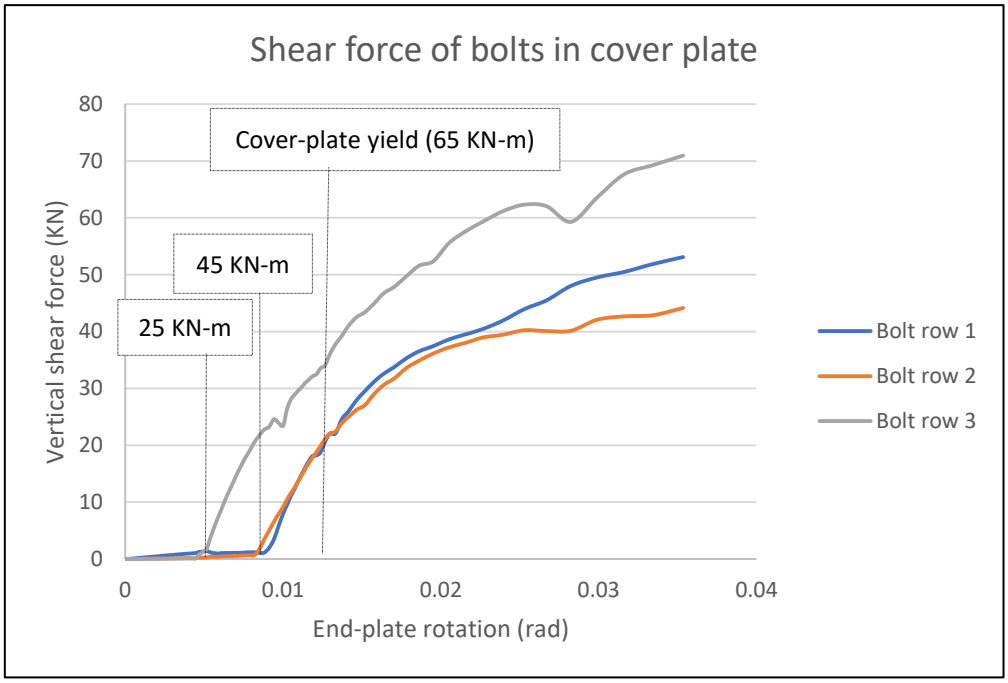

Figure 5-38: Vertical shear force carried by bolts in cover plate (IC-1/case 3)

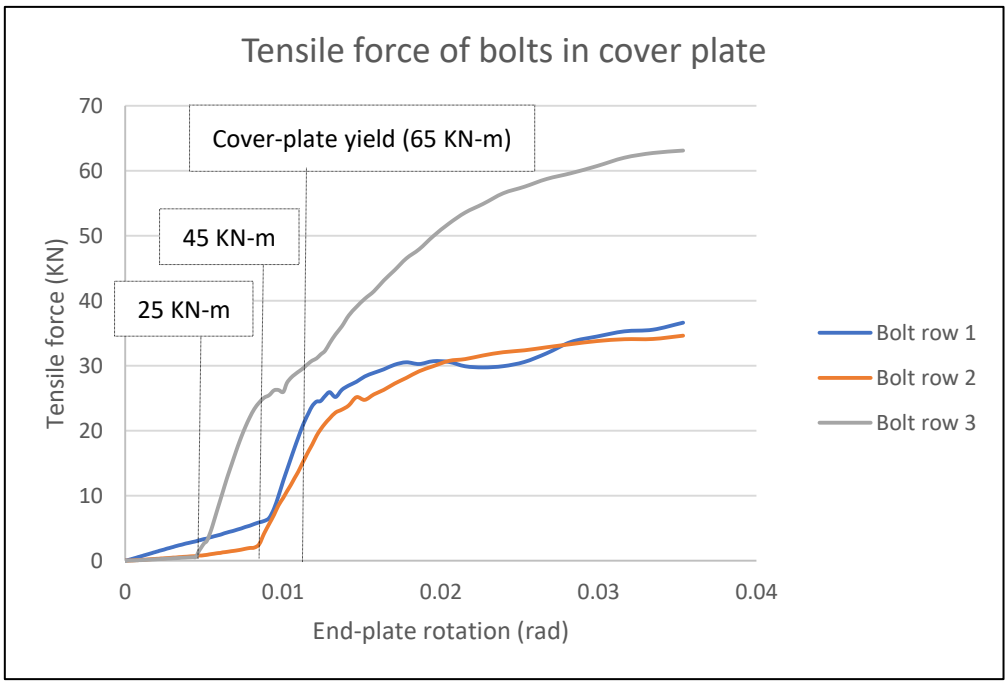

Figure 5-39: Tensile force carried by bolts in cover plate (IC-1/case 3)

As mentioned earlier, bolts in cover plate exhibit a sharp increase in load carried at a moment resistance of 25 KN-m. However, due to rotational motion of the cover plate, bolt rows 2 and 3 are activated at a moment resistance of 45 KN-m. Cover plate yields at a moment resistance of 65 KN-m. Yield stresses are attained in cover plate near bolt row 1 as seen in figure 5-40. Tensile and vertical shear force carried by bolt row 1 exhibits a linear behavior until a moment of 65 KN-m is reached as seen in figures 5-38 and 5-39. Rotational motion of the cover plate causes bolt 1 in row 3 to carry the highest vertical shear in cover plate. Left hand side of the cover plate carries 94% of the vertical shear in plate. Bolt row 1,2 and 3 carry 25%, 28% and 46% of the vertical shear in plate. While, bolt row 1,2 and 3 carry 32%, 25% and 43% of the tensile force in plate.

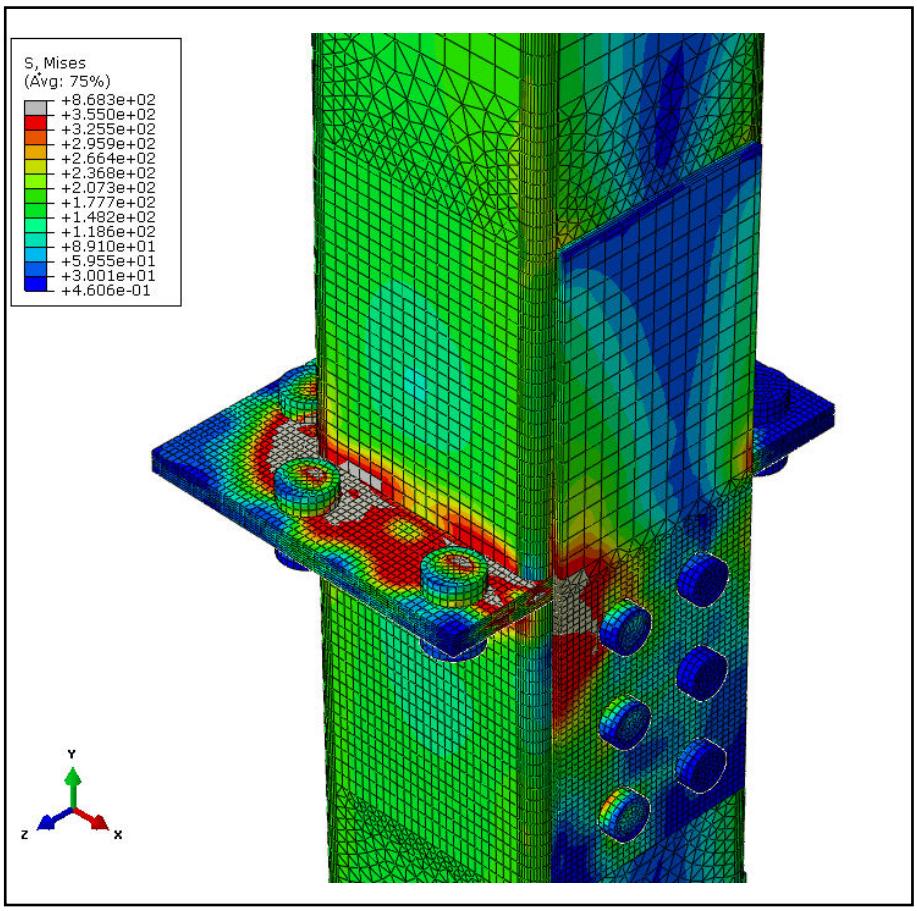

Figure 5-40: Von mises stress distribution at 65 KN-m (IC-1/case 3)

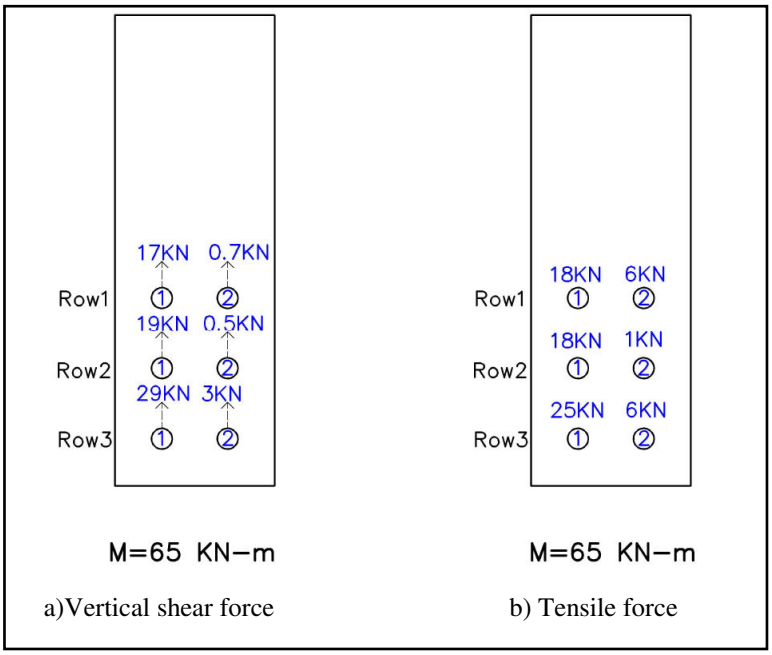

Figure 5-41: Bolt forces in cover plate at 65 KN-m (IC-1/case 3)

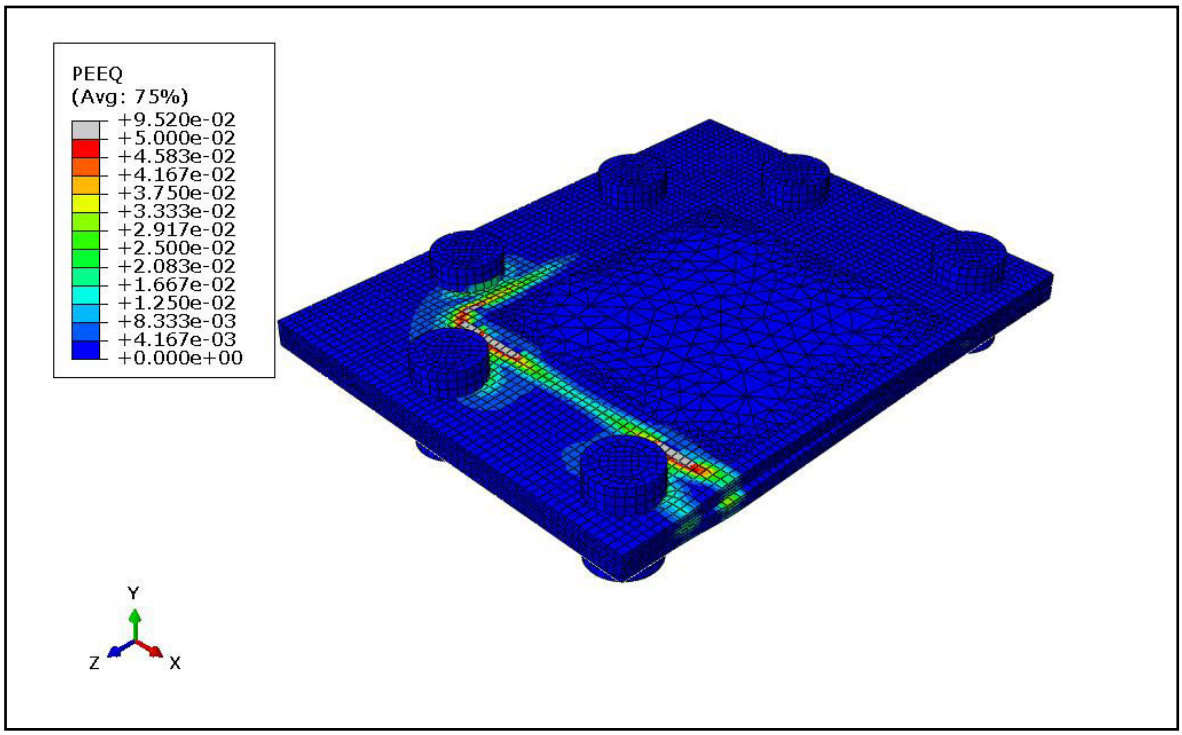

Figure 5-42: Plastic strain distribution in end-plate at 101 KN-m (IC-1/case 3)

Ultimate bending resistance of intermediate column connection with case cover plate in rotation is reached at a moment resistance of 101 KN-m. This occurs due to failure of end-plate. 5% plastic strains are attained in the end-plate near bolt 1 and 2 as shown in figure 5-42.

5.5 Non-symmetrical intermediate splice – tension

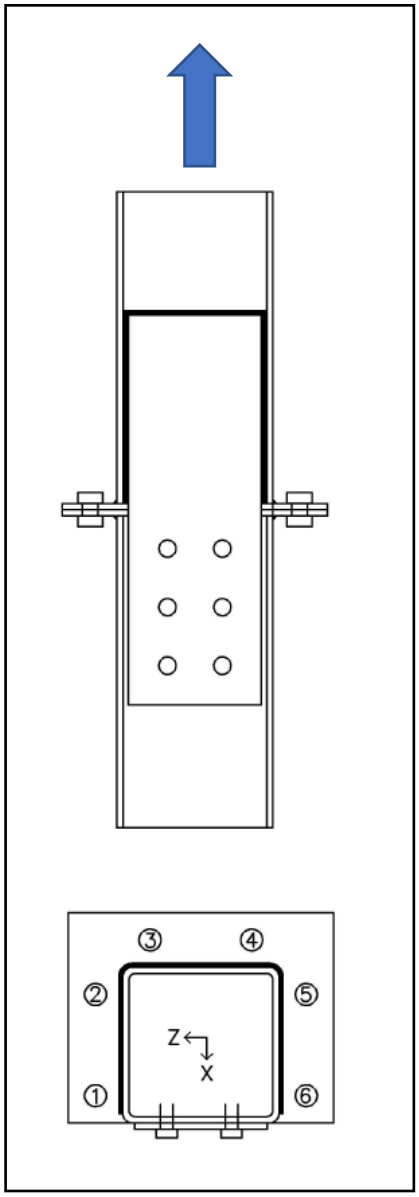

Figure 5-43: Plan and elevation of specimen IC-1 (case 4)

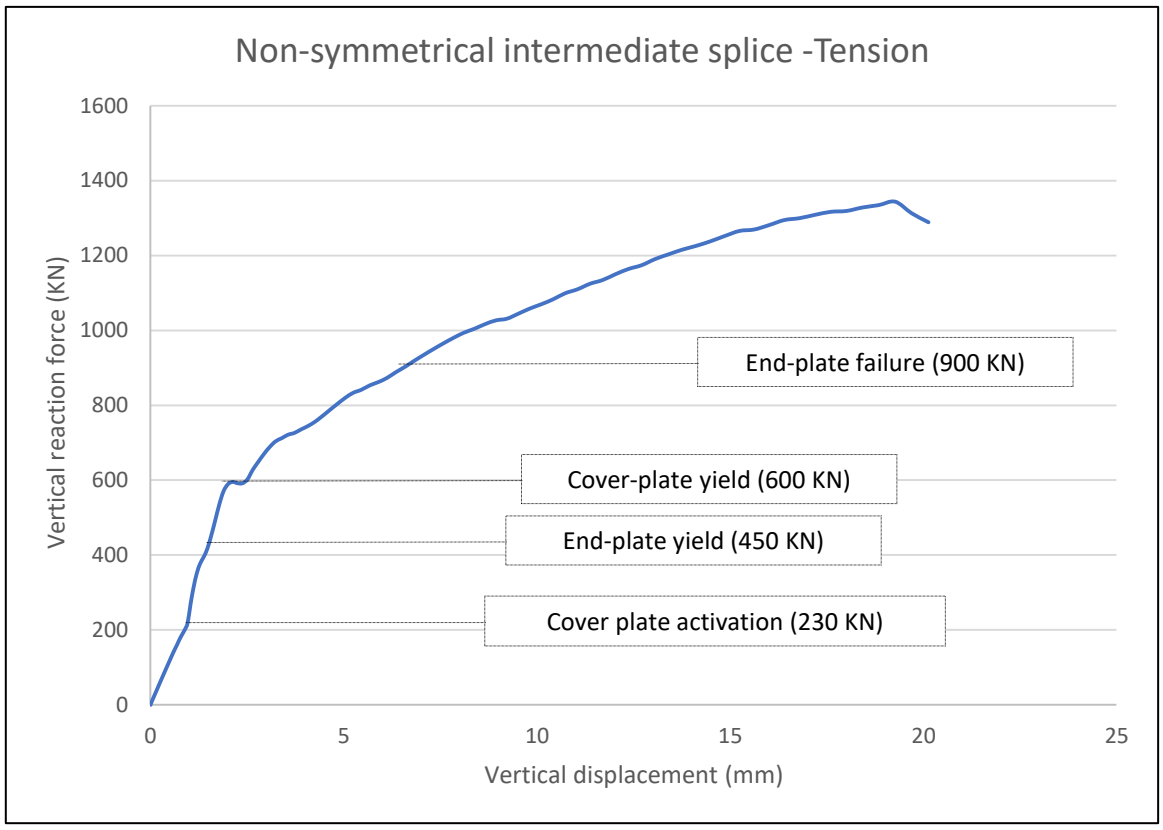

Figure 5-44: Load displacement curve of specimen IC-1 (case 4)

In this section behavior of non-symmetrical intermediate splice connection under a tensile force is discussed. In the initial stages of loading cover plate doesn't fully contribute towards resistance. This as explained in earlier situations is caused to due to bolt hole clearances provided in cover plate and bottom column. This leads to two elastic parts in the force-displacement curve shown in figure 5-44. Most of the applied load is carried by six bolts in end-plate during the initial stages of loading. A sharp increase in loads carried by bolts in cover plate is noticed when the tensile resistance reaches 230 KN. Yield stresses are attained in end-plate at 450 KN as seen in figure 5-45. This causes, change of slope of the curve at this point. However, clear flattening of load-displacement curve is not noticed at 450 KN, due to presence of cover plate. Free deformation of end-plate region close to cover plates is restricted.

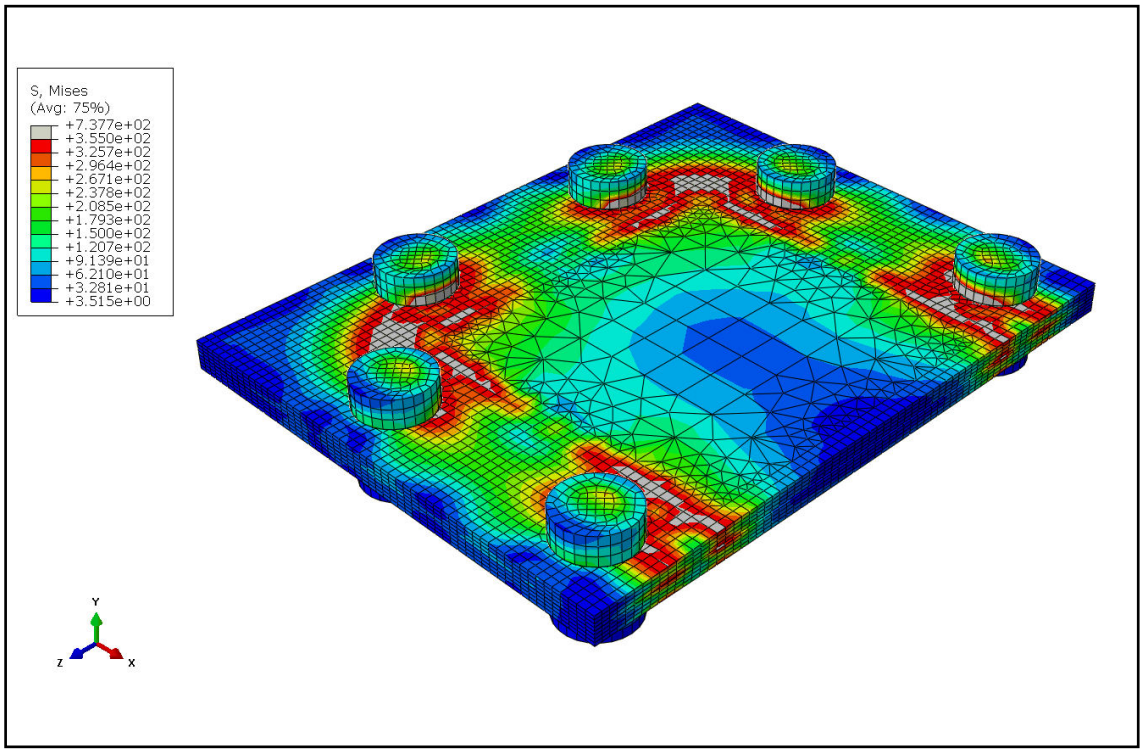

Figure 5-45: Von mises stress distribution in end-plate at 450KN (IC-1/case 4)

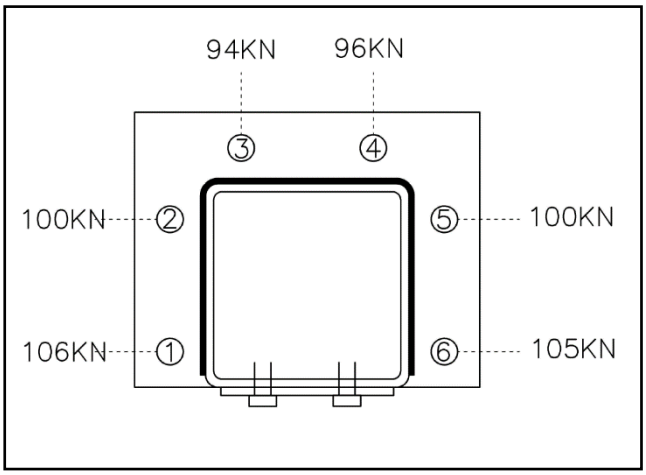

Figure 5-46: Tensile forces of bolts in end-plate at 450 KN (IC-1/case 4)

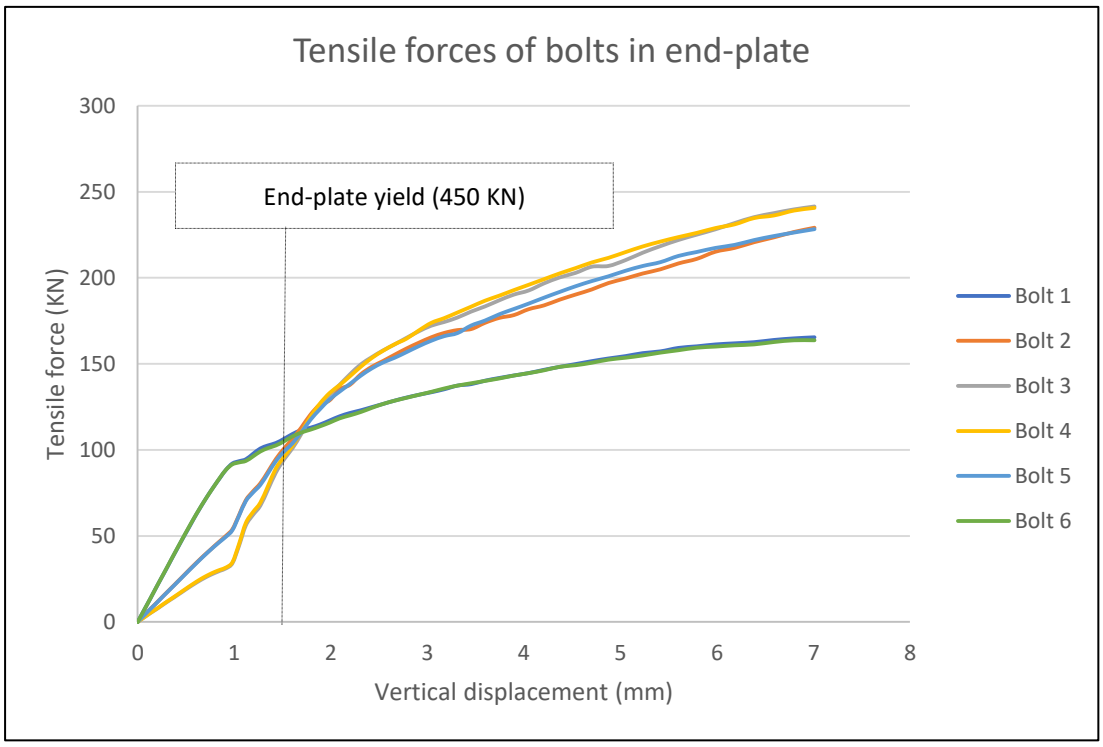

Figure 5-47: Tensile force carried by bolts in end-plate (IC-1/case 4)

Tensile force of bolts 5 and 6 show a linear characteristic until end-plate yield as shown in figure 5-47. Until end-plate yield, bolt 5 and 6 carry relatively higher tensile force than other four bolts. Individual load carried by bolts 1,2,3 and 4 gets higher than bolts 5 and 6 after end-plate yield. Connection region is much stiffer on the cover plate side than near bolts 2,3,4 and 5 in end-plate. This causes a slightly higher vertical displacement near bolts 3 and 4 compared to the column side connected with cover plate. This causes the main cover plate to bend away from column face while also loaded in tension.

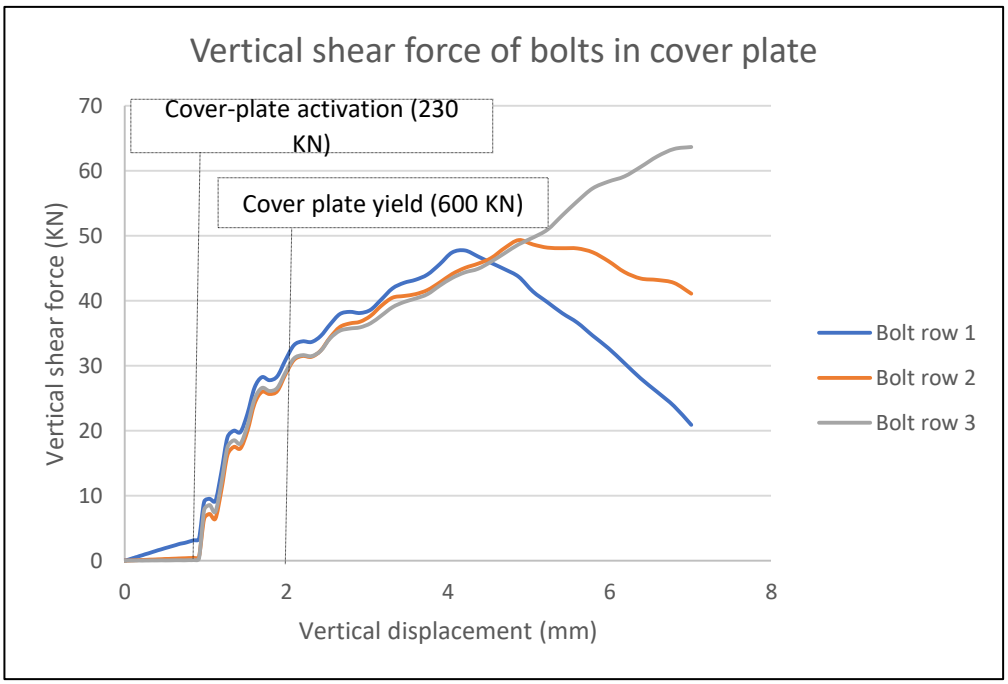

Figure 5-48: Vertical shear force carried by bolts in cover plate (IC-1/case 4)

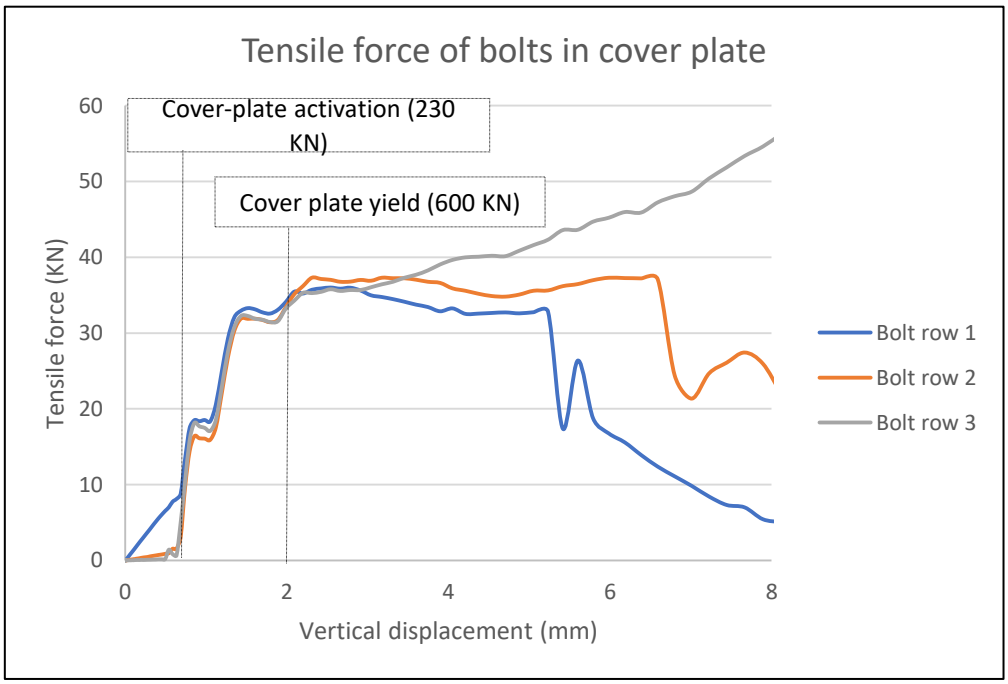

Figure 5-49: Tensile force carried by bolts in cover plate (IC-1/case 4)

A sharp increase in load carried by bolts in cover plate at 230 KN can be seen in figure 5-48 and 5-49. The cover plate is bent at its mid-height and is also in tension. At approximately 600 KN, yield stresses are attained in cover plate at the top bolt row as shown in figure 5-50.

Also bolt forces in cover plate exhibit yielding behavior at a reaction force of 600 KN. This also confirms the yielding of cover plate at this point. At yield point, load is almost equally distributed in all three bolt rows. However, in figures 5-48 and 5-49 it can be noticed that bolt row 1 and 2 carry higher load than bolts row 2 in elastic stage of the cover plate.

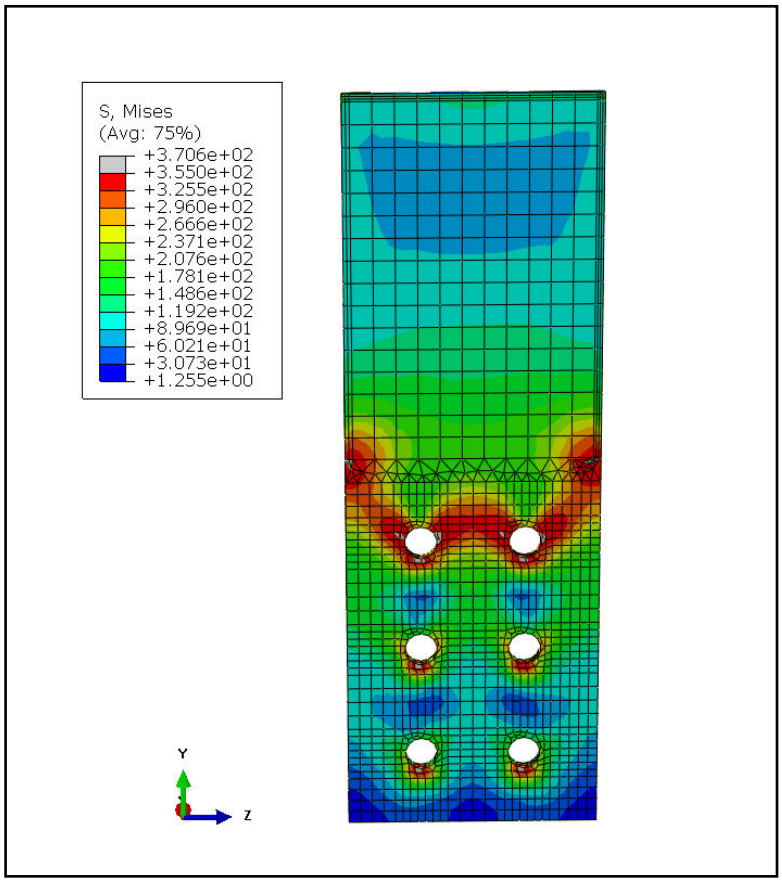

Figure 5-50: Von mises stress distribution in cover plate at 600 KN (IC-1/case 4)

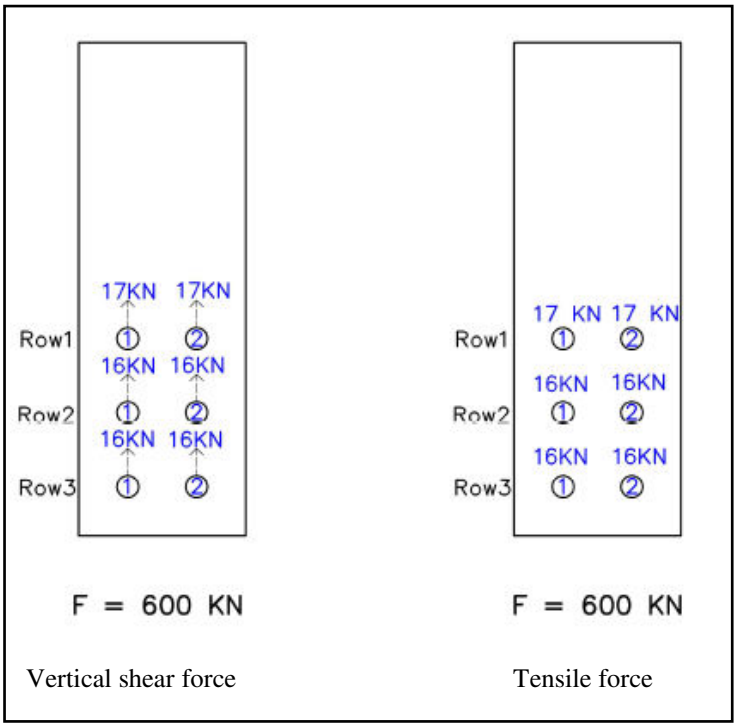

Figure 5-51: Bolt forces in cover plate at 600 KN (IC-1/case 4)

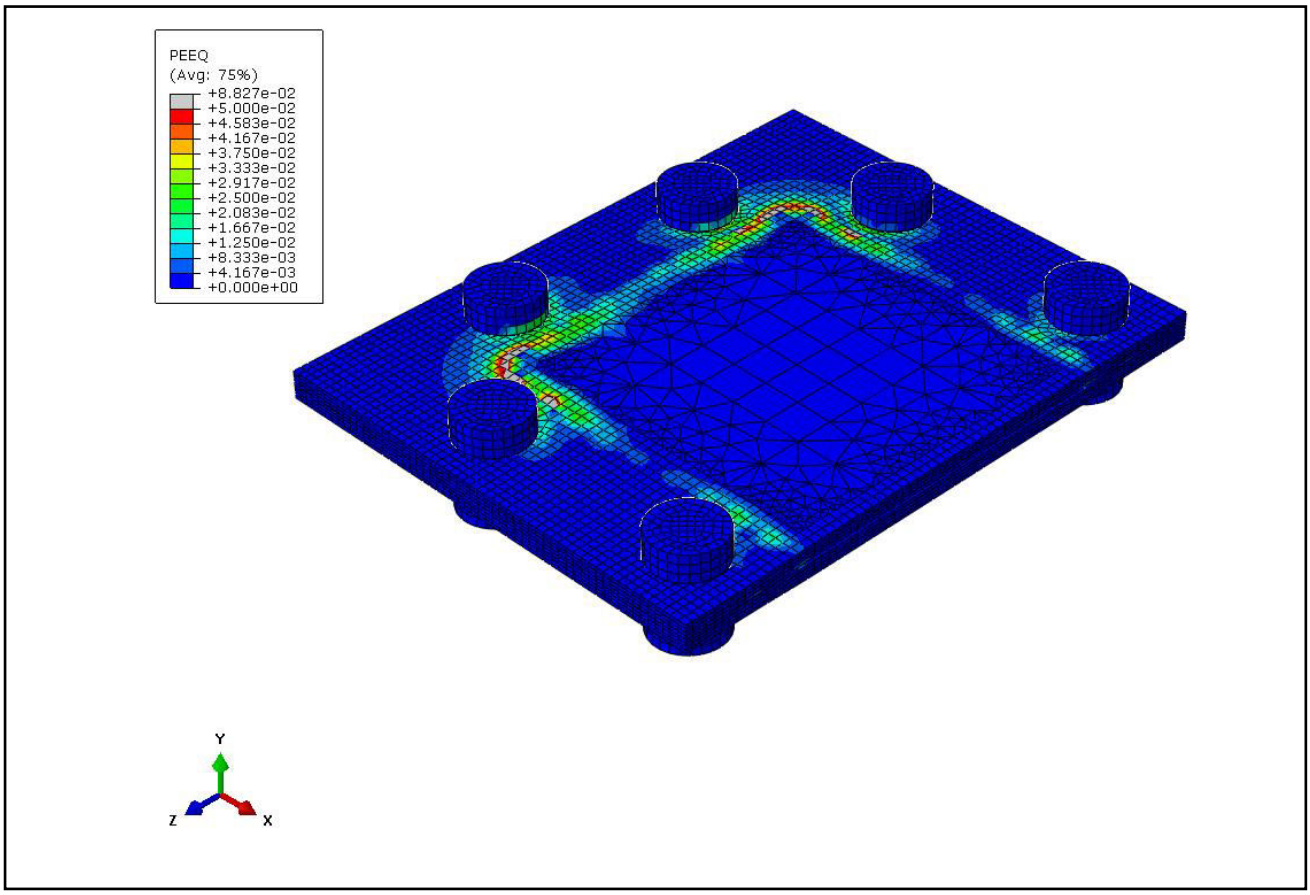

Figure 5-52: Plastic strain distribution in end plate at 900KN (IC-1/case 4)

Ultimate tensile resistance of intermediate column is reached at a reaction force of 900 KN. High plastic strains are formed in the end-plate near bolts 2,3,4 and 5 as shown in figure 5-53. While, cover plate is still in post yield stage at 900 KN.

Chapter 6 – Parametric analysis

6.1 Comparison of non-symmetrical column splice with traditional end-plate splice

As discussed, earlier end-plate splice is an economical and widely adopted solution. In this section, non-symmetrical column splice connection for corner and intermediate column is compared with end-plate. Specimens CC-1 and IC-1 are used for comparison in this case. Layout of end-plate connection is as shown in the figure 6-1. End-plate of thickness 8mm is adopted, which is similar to the connection component thickness of specimen CC-1 and IC-1.

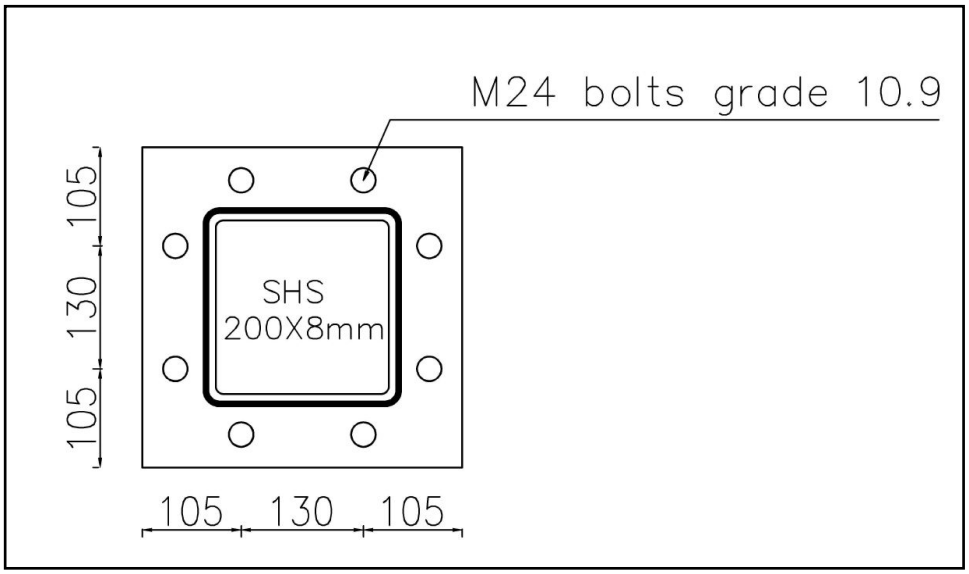

Figure 6-1: Layout of end-plate splice connecting columns

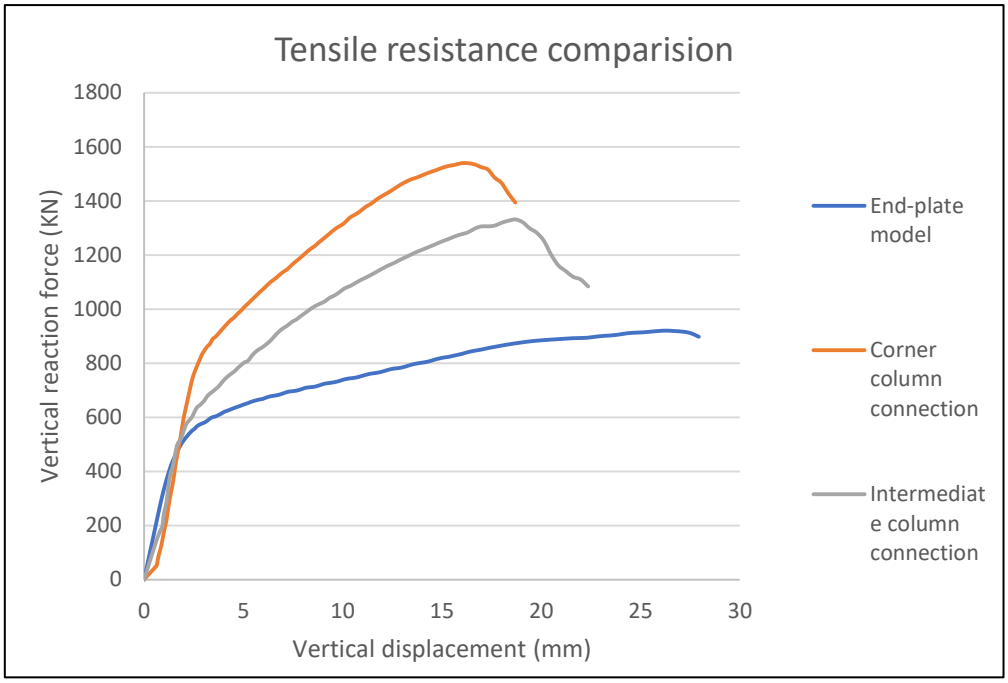

Figure 6-2: Comparision of end-plate model with non-symmetrical column splice (tension)

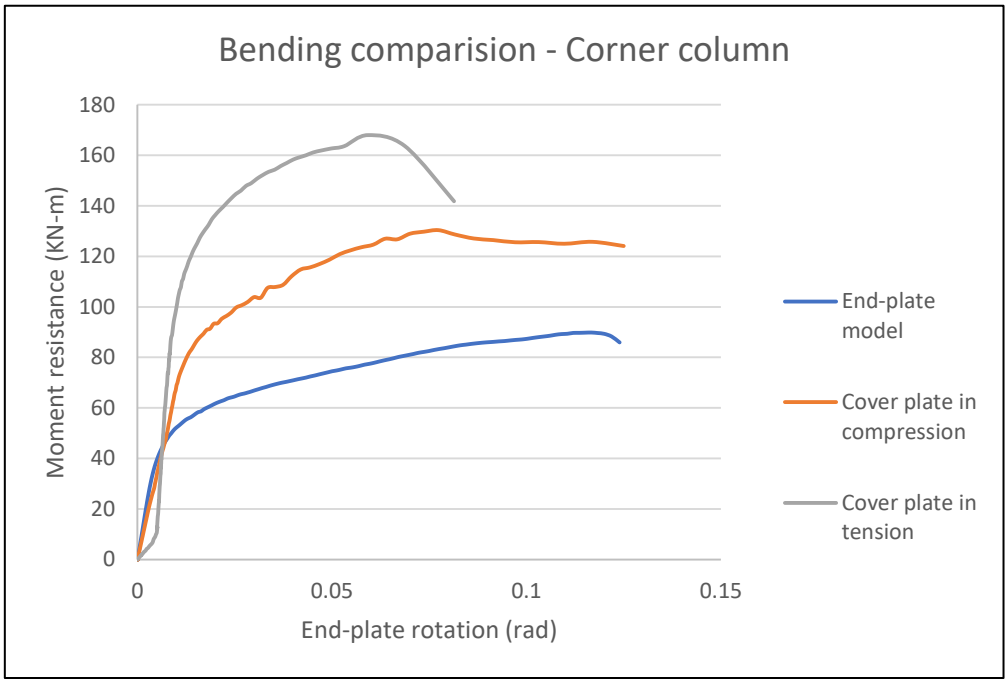

Figure 6-3: Comparison of end-plate model with non-symmetrical corner splice (bending)

LOAD CASE	CORNER COLUMN	END-PLATE MODEL	VARIATION
Cover plate in compression (moment)	102 KN-m	80 KN-m	27.5%
Cover plate in tension (moment)	157 KN-m	80 KN-m	94%
Specimen in tension	1130 KN	800 KN	41%

Table 6-1: Comparison of non-symmetrical corner splice with end-plate connection

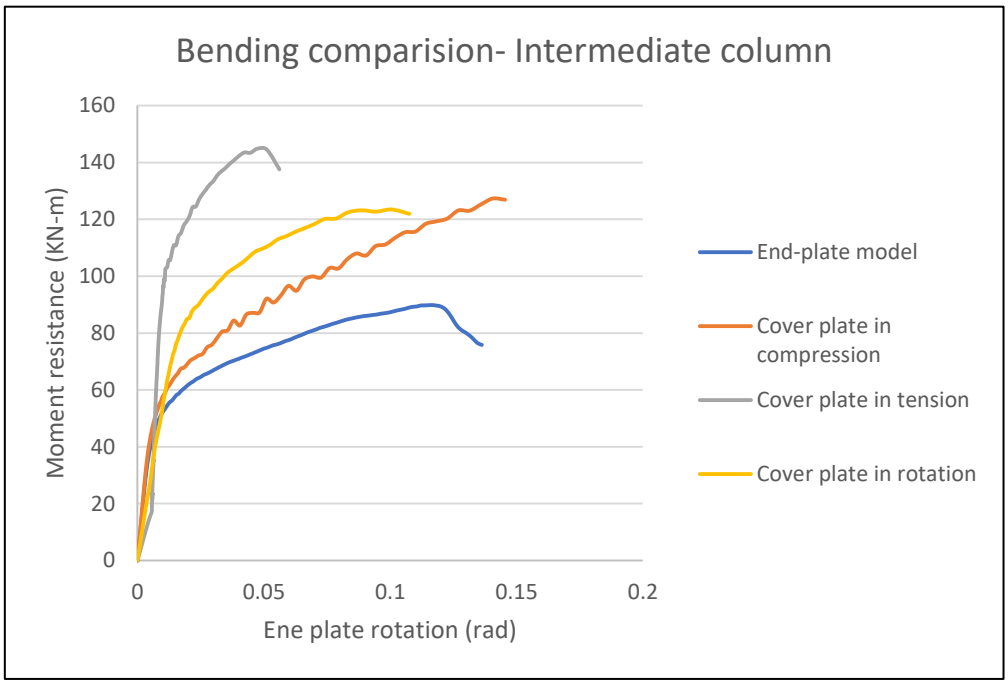

Figure 6-4: Comparison of end-plate model with non-symmetrical intermediate splice (bending)

SPECIMEN	INTERMEDIATE COLUMN	END-PLATE MODEL	VARIATION
Cover plate in compression (moment)	91 KN-m	80 KN-m	13%
Cover plate in tension (moment)	135 KN-m	80 KN-m	68%
Cover plate in rotation (moment)	101 KN-m	80 KN-m	27%
Specimen in tension	900 KN	800 KN	12.5%

Table 6-2: Comparison of non-symmetrical intermediate splice with end-plate connection

6.2 Effect of bolt position in end-plate of non-symmetrical column splice

In this section effect of bolt position on overall moment-rotation behavior of non-symmetrical column splice is given. Effect of bolt position with respect to column face is obtained by varying parameter “m” shown in figure 6-5. Effect of distance between two bolts in the same row is obtained by varying parameter “a”.

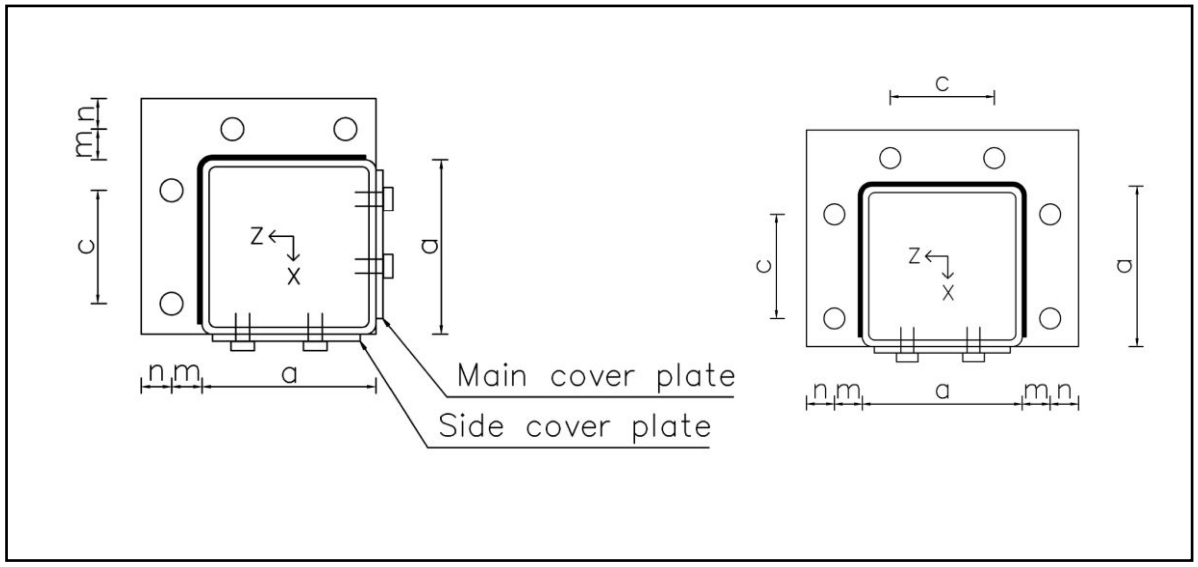

Figure 6-5: Bolt layout for non-symmetrical column splice

6.2.1 Effect of parameter “m”:

Increasing parameter “m” had a negative effect on the overall load-displacement curve and moment rotation curve. A lower initial stiffness and yield resistance was obtained as parameter “m” was increased. Effect of parameter “m” was much more pronounced in case of connection under cover plate in compression and rotation case. This is due to end-plate transferring most of the applied load. However, this was not the same in case of connection under cover plate in tension case. Since, most of the load was transferred by cover plates in this case. Variation in initial stiffness was higher in case of cover plate in compression and rotation case, compared to cover plate in tension case.

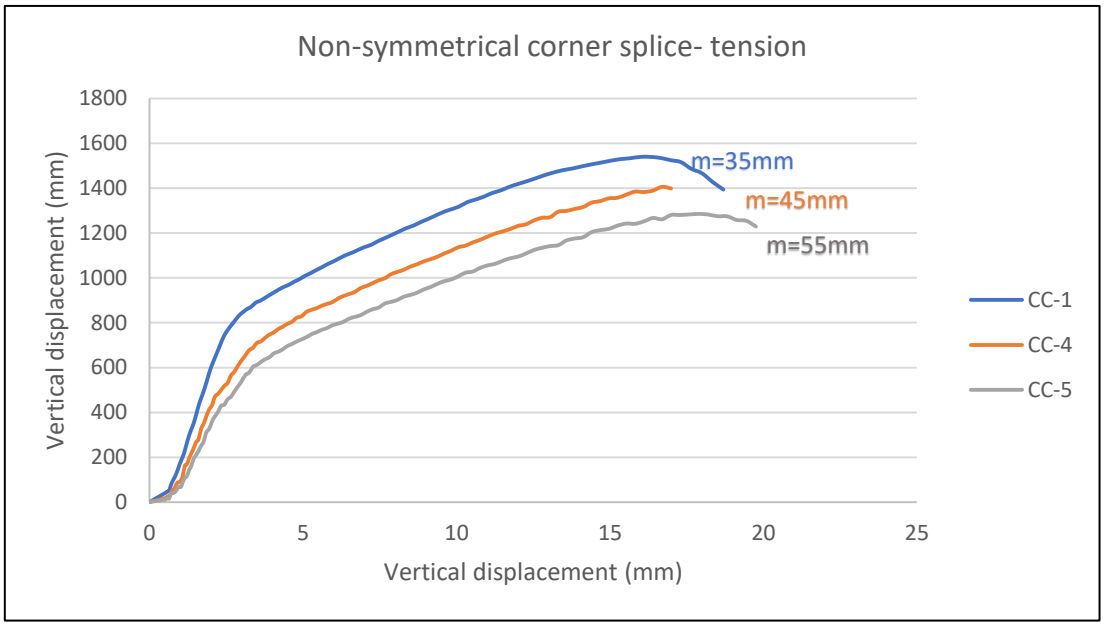

Figure 6-6: Effect of “m” on tensile resistance of non-symmetrical corner splice

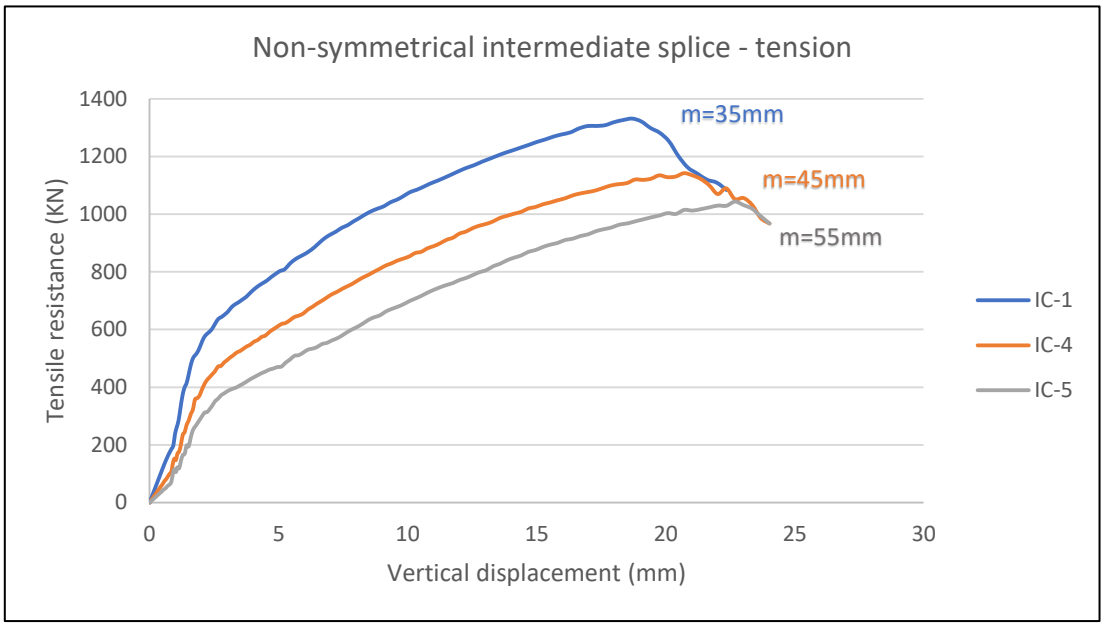

Figure 6-7: Effect of "m" on tensile resistance of non-symmetrical intermediate splice

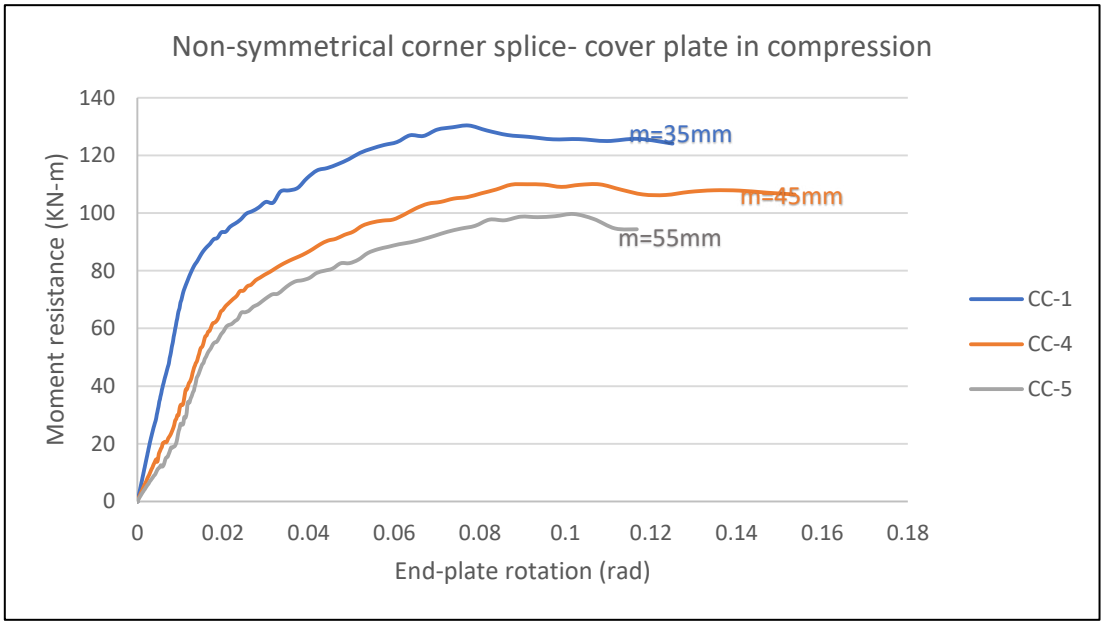

Figure 6-8: Effect of "m" on non-symmetrical corner splice (case 1)

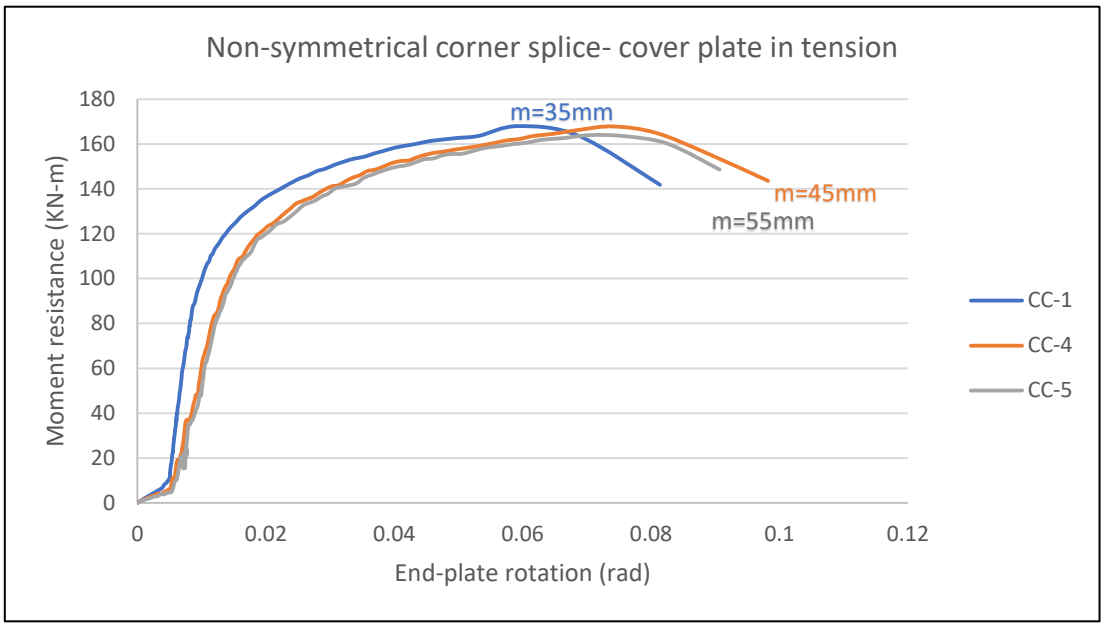

Figure 6-9: Effect of "m" on non-symmetrical corner splice (case 2)

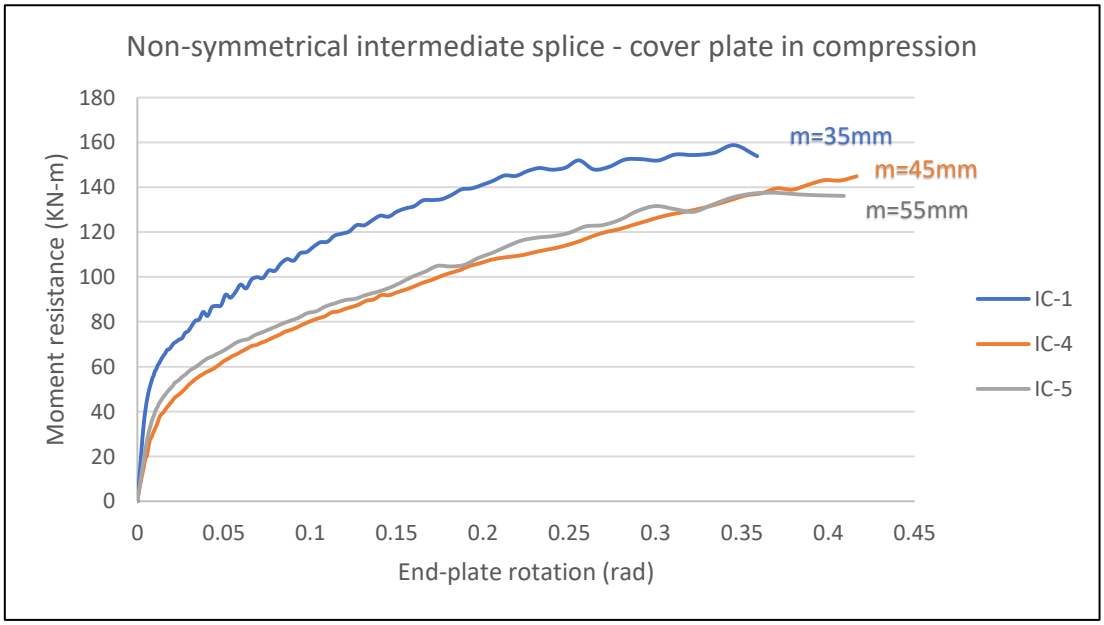

Figure 6-10: Effect of "m" on non-symmetrical intermediate splice (case 1)

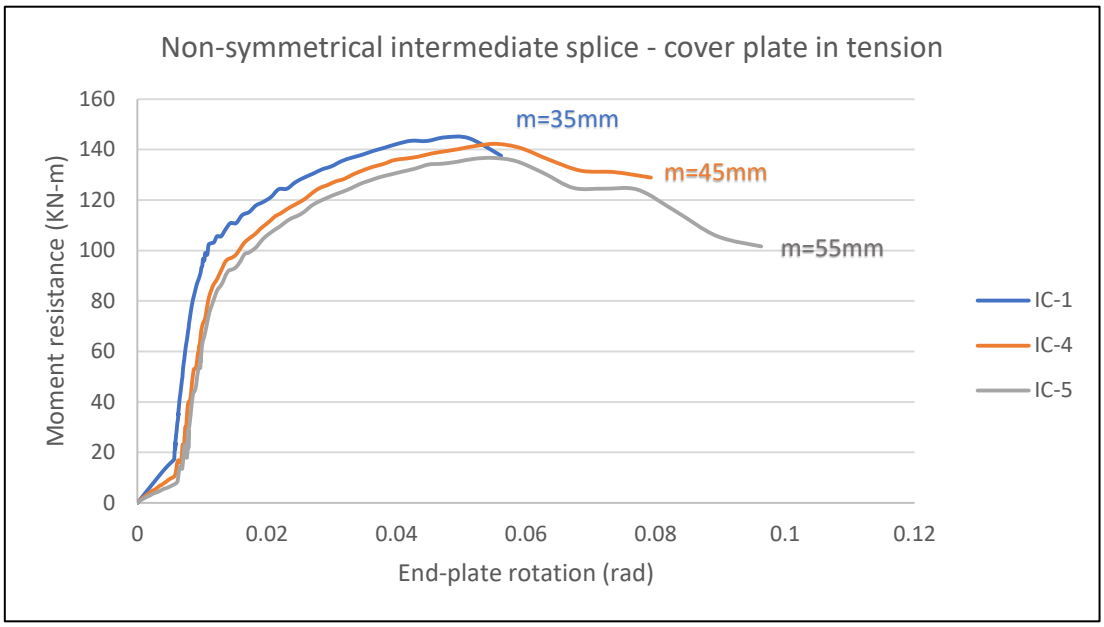

Figure 6-11: Effect of "m" on non-symmetrical intermediate splice (case 2)

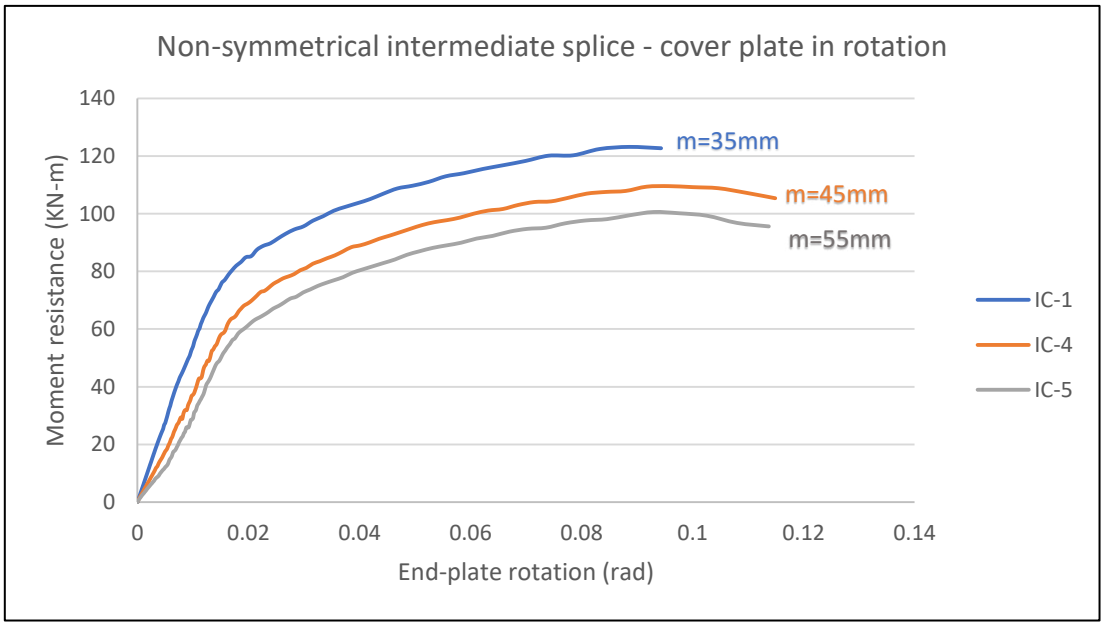

Figure 6-12: Effect of "m" on non-symmetrical intermediate splice (case 3)

6.2.2 Effect of parameter "c":

Parameter "c" had a negligible effect on the overall load-displacement curves of the specimens. However, lowering parameter "c" had a negative effect on the overall moment rotation curves. Lower value of "c" meant smaller lever arm distance of bolts to the compression point. Decreased stiffness and yield resistance were noticed as distance between two bolts in a row was decreased.

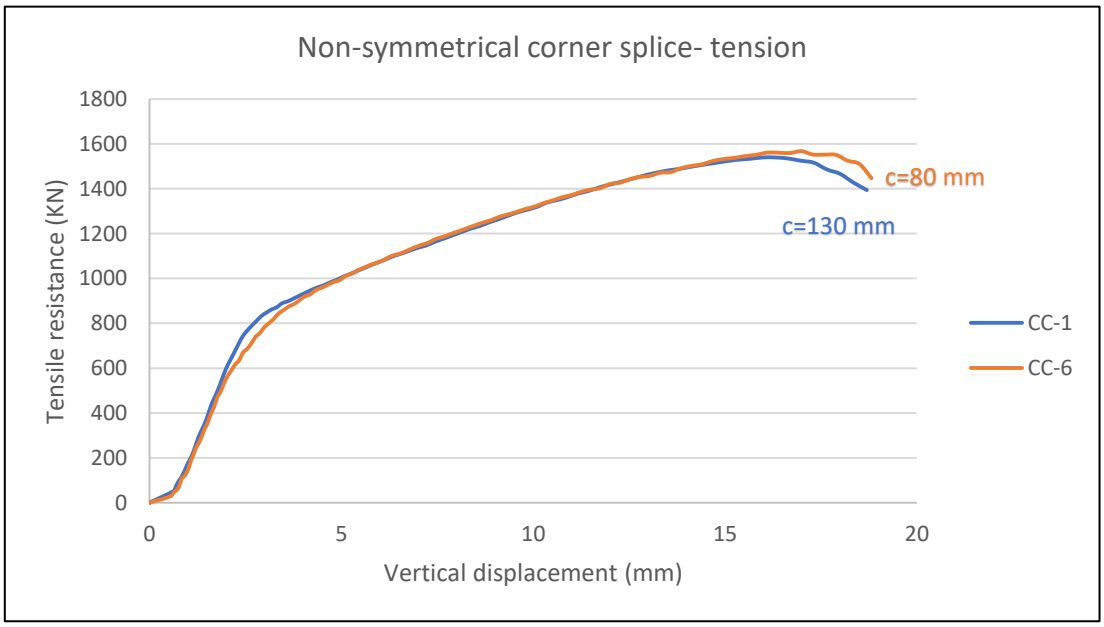

Figure 6-13: Effect of "c" on tensile resistance of non-symmetrical corner splice

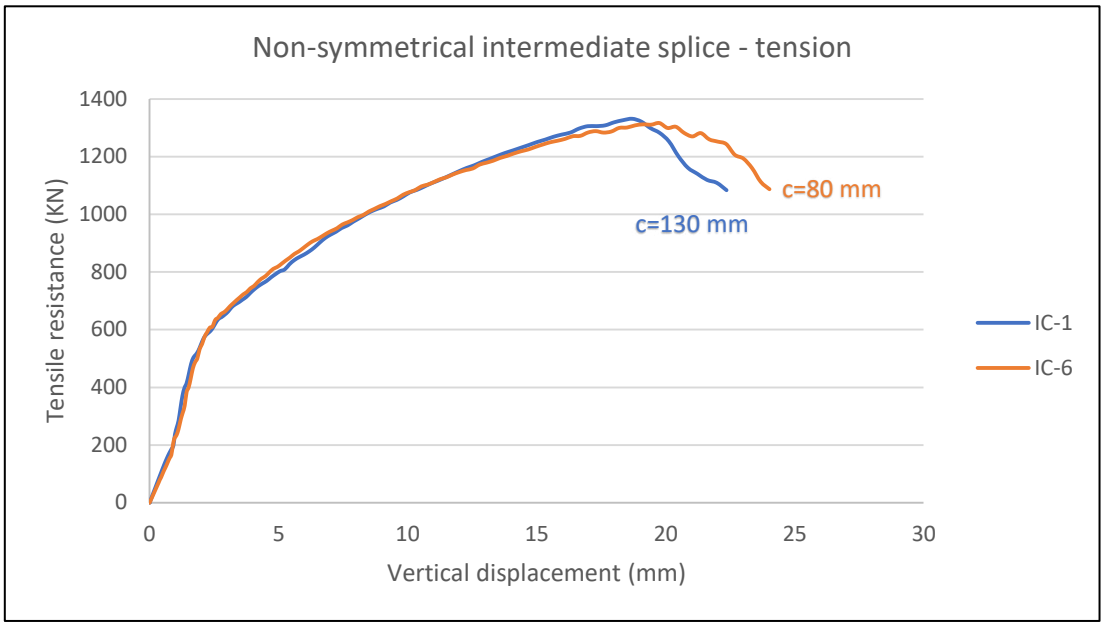

Figure 6-14: Effect of "c" on tensile resistance of non-symmetrical intermediate splice

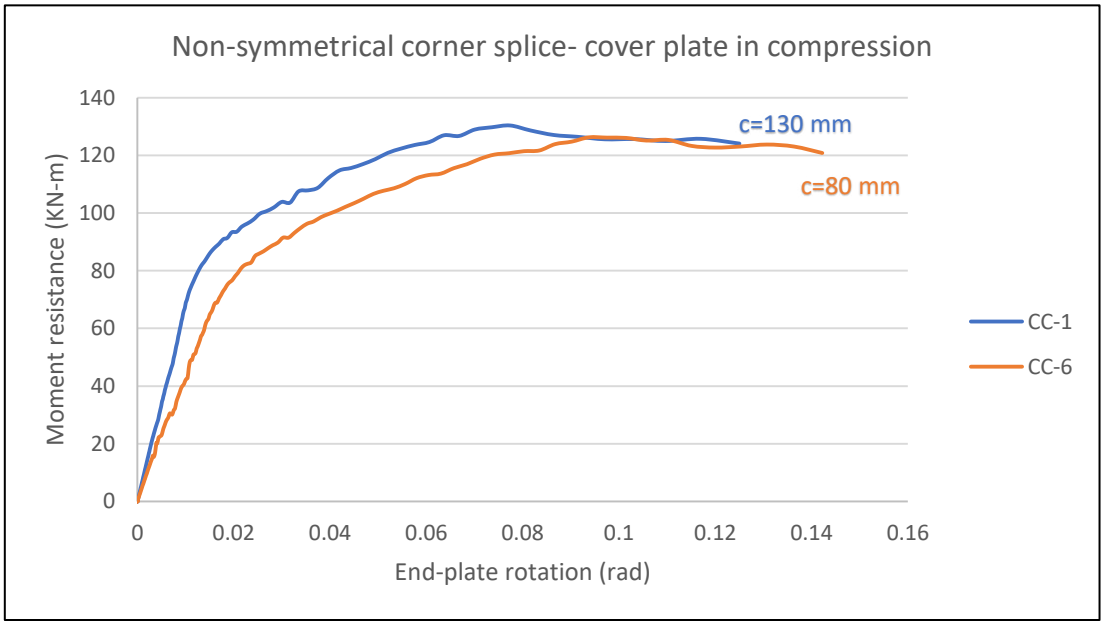

Figure 6-15: Effect of "c" on non-symmetrical corner splice (case 1)

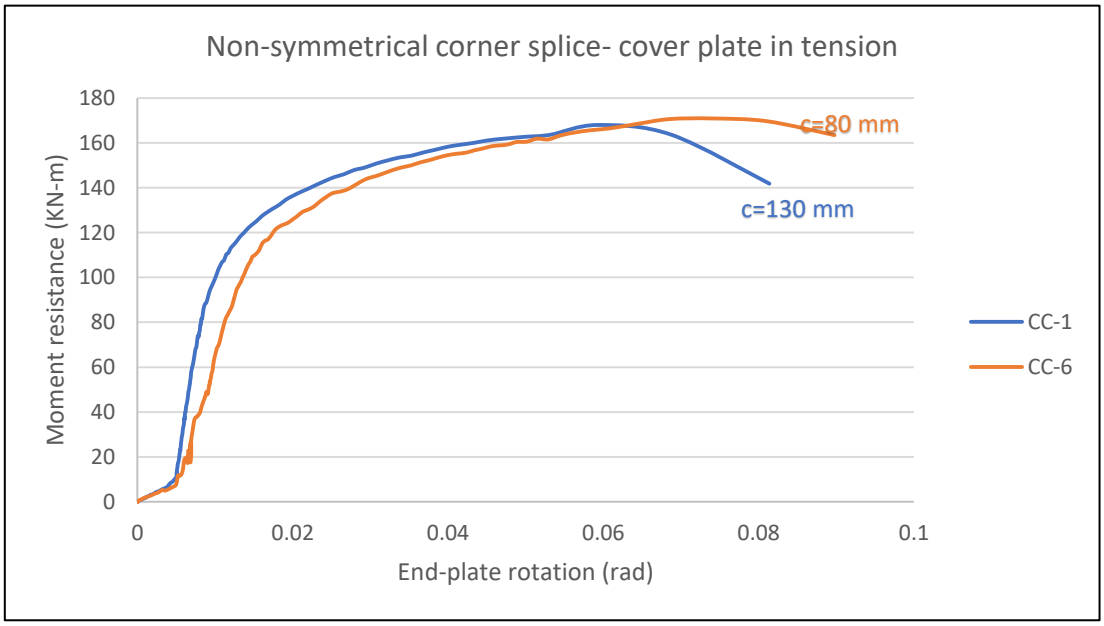

Figure 6-16: Effect of "c" on non-symmetrical corner splice (case 2)

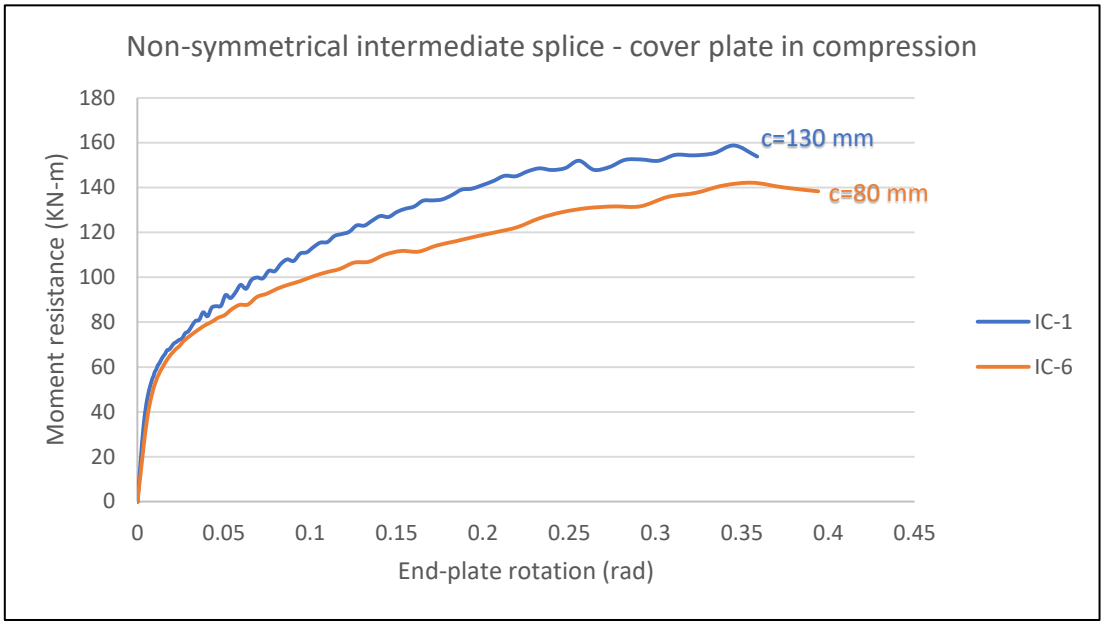

Figure 6-17: Effect of "c" on non-symmetrical intermediate splice (case 1)

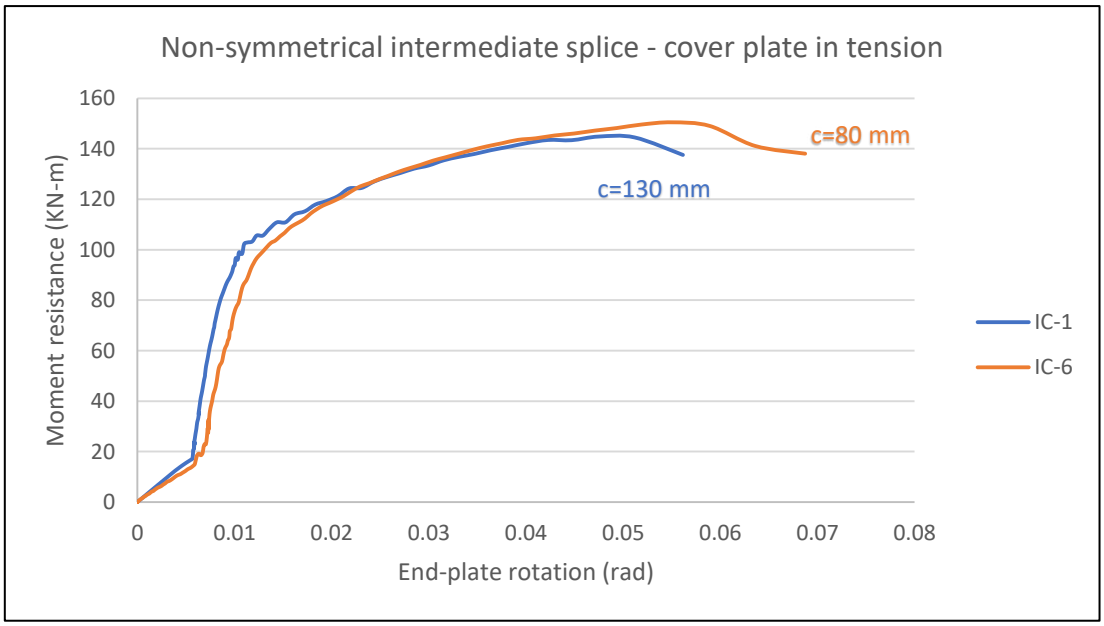

Figure 6-18: Effect of "c" on non-symmetrical intermediate splice (case 2)

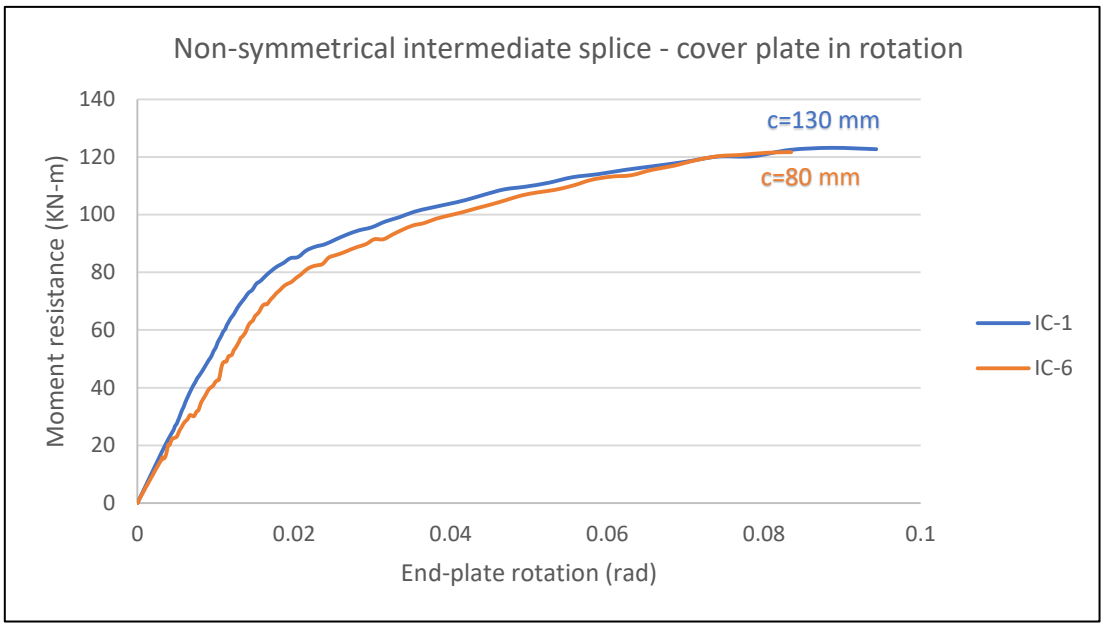

Figure 6-19: Effect of "c" on non-symmetrical intermediate splice (case 3)

6.3 Effect of thickness of end-plate and cover plate

In this section effect of end-plate and cover plate thickness on overall-moment rotation behavior is shown. Specimens with end-plate and cover plate thicknesses of 6mm, 8mm and 10mm were studied. As expected, increasing the thickness of connection components had a positive impact on the overall-moment rotation and load-displacement curves. Failure in specimen CC-1, CC-2, IC-1 and IC-2 was mostly noticed in connection components for all load cases. However, specimen CC-3 and IC-3 exhibited failure associated with column section for cover plate in compression and rotation case. In other load cases for specimen CC-3 and IC-3, significant yielding of column cross-section was noticed at failure.

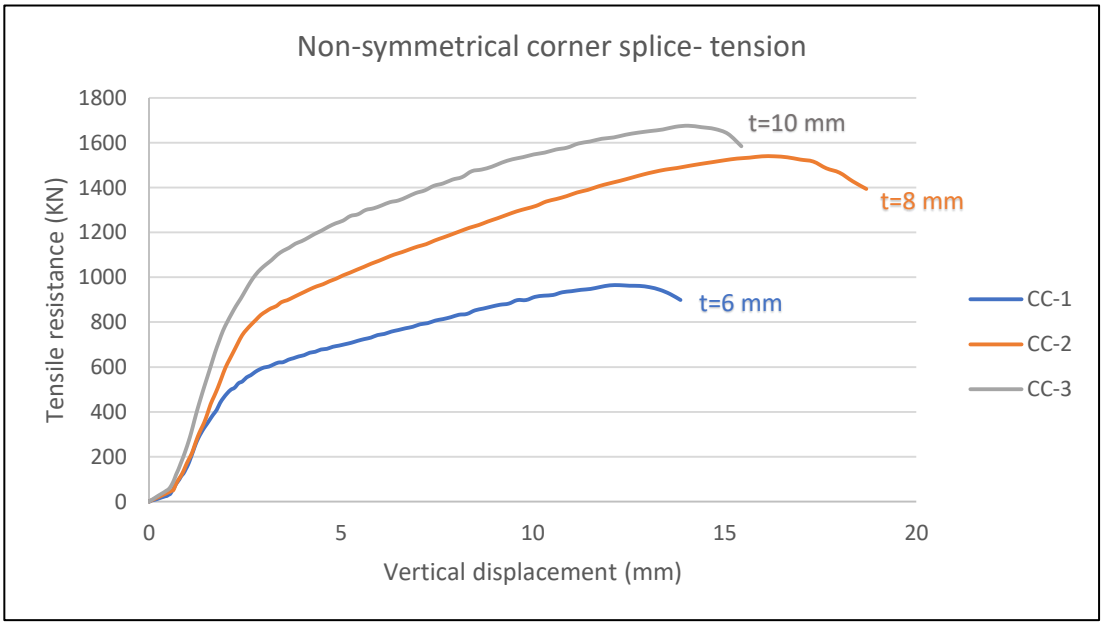

Figure 6-20: Effect of "t" on tensile resistance non-symmetrical corner splice

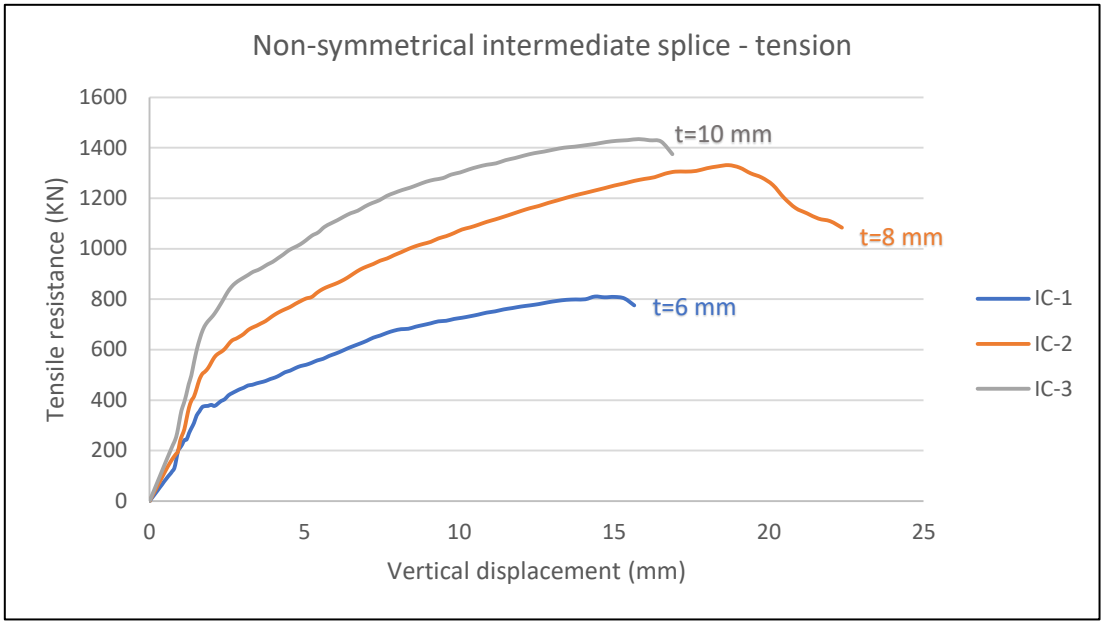

Figure 6-21: Effect of "t" on tensile resistance of non-symmetrical intermediate splice

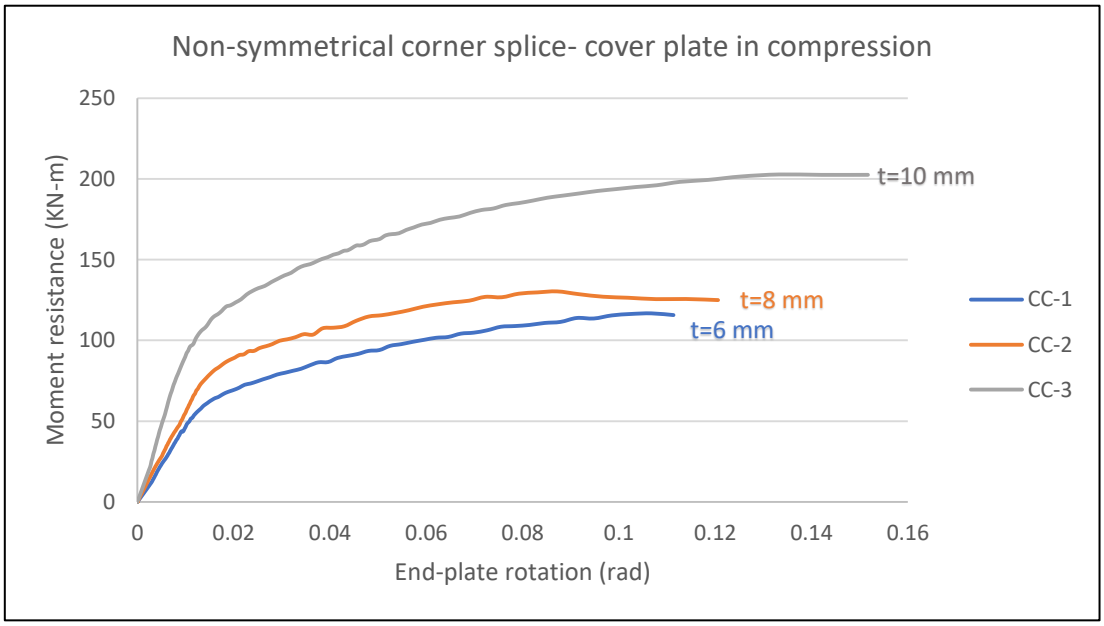

Figure 6-22: Effect of "t" non-symmetrical corner splice (case 1)

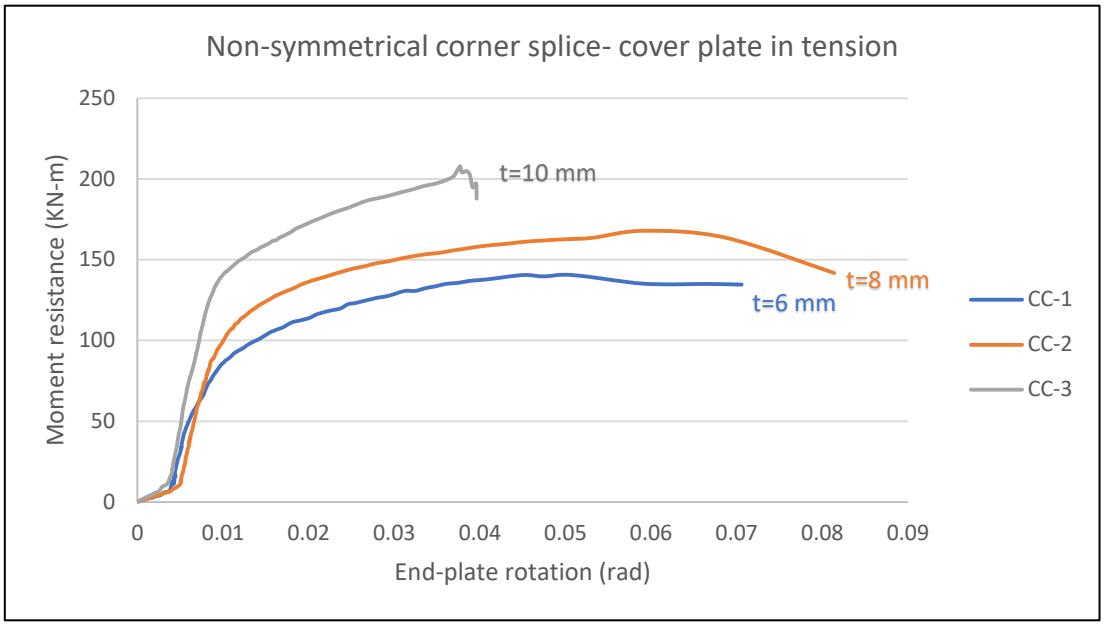

Figure 6-23: Effect of "t" on non-symmetrical corner splice (case 2)

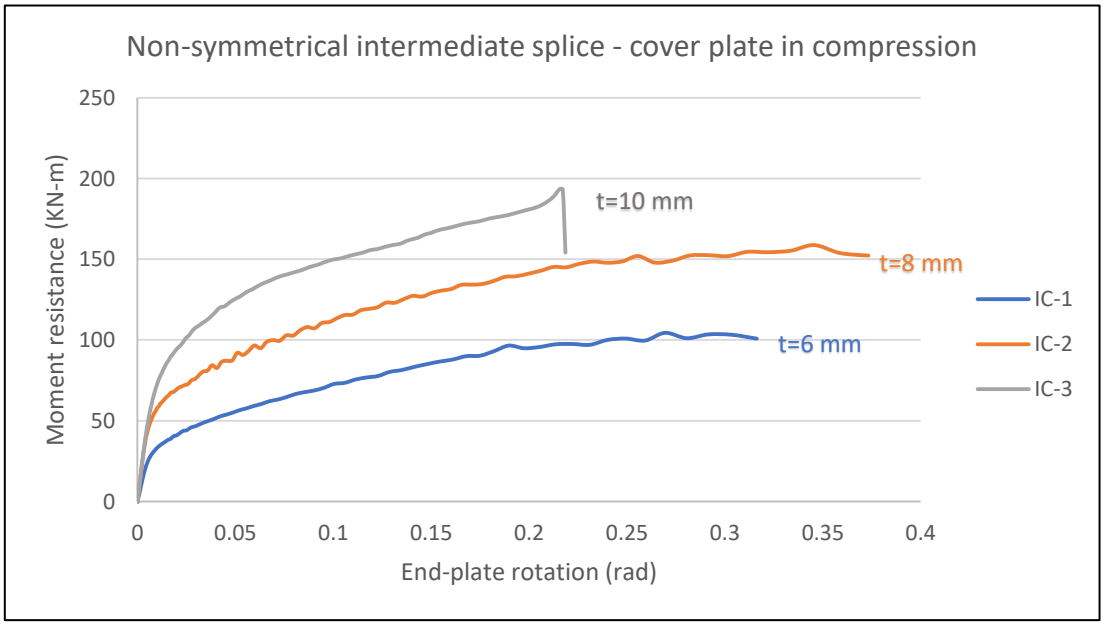

Figure 6-24: Effect of "t" on non-symmetrical intermediate splice (case 1)

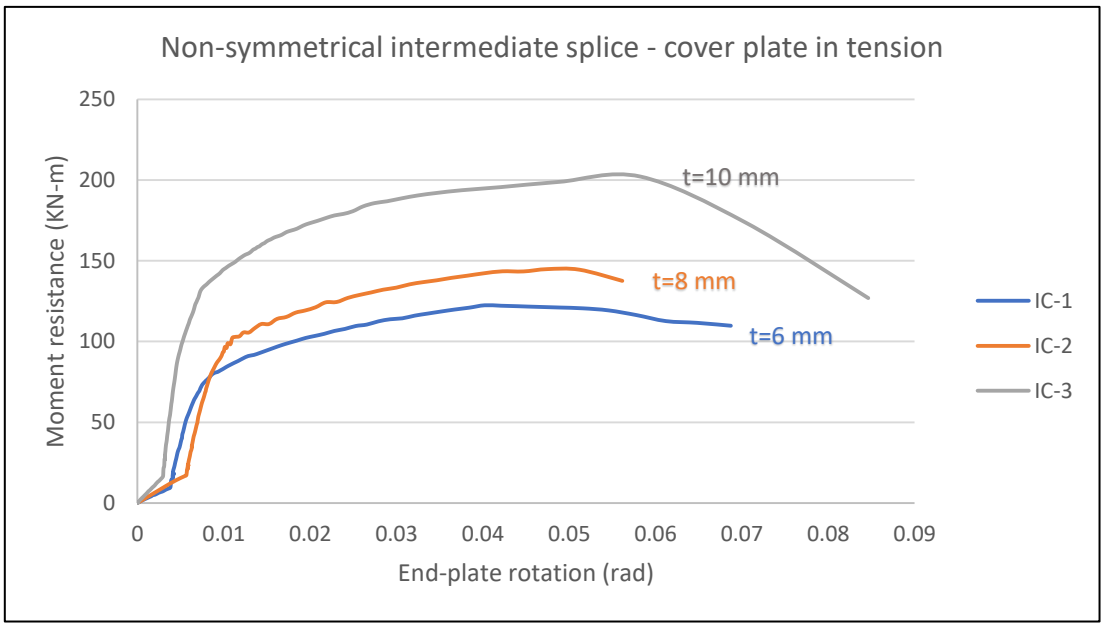

Figure 6-25: Effect of "t" on non-symmetrical intermediate splice (case 2)

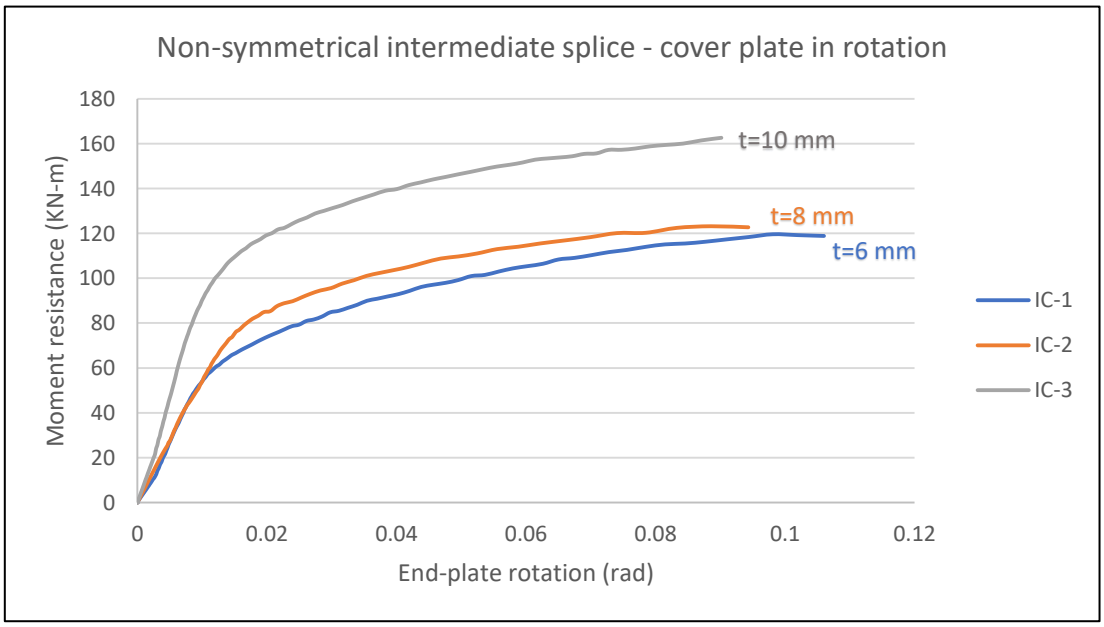

Figure 6-26: Effect of "t" on non-symmetrical intermediate splice (case 3)

Chapter 7- Application of component method to non-symmetrical column splice connection

7.1 Introduction

As described in earlier in chapter 2, application of component method involves three steps. Initially all the active components that contribute towards initial rotational stiffness $S_{j,ini}$ are identified for all cases. Second step involves computation of stiffness coefficients of relevant components. Two approaches are followed to calculate initial rotational stiffness by component method. Namely, Eurocode approach and modified Eurocode approach. Eurocode approach involves employing all the stiffness coefficients from Eurocode 1993-1-8. In modified Eurocode approach stiffness coefficients for end-plate in bending and bolts in tension were replaced with stiffness coefficients proposed by Karlsen and Aalberg. A comparison between results obtained from both approaches and finite element results is given to learn the accuracy of proposed approaches.

7.2 Non-symmetrical corner splice connection – cover plate in compression

Active components in the joint that contribute towards initial stiffness need to be identified to apply component method. In case of corner column connection, active components depend on the direction of bending. For the present case, end plate in tension and bolt in tension are the active components that contribute towards initial rotational stiffness. Yield resistance of this connection is reached at 36 KN-m as discussed in section 4.2. Contribution of side and main cover plate towards resistance in the initial stages of loading was found to be very low. Hence, in the present case contribution of cover plates is omitted in the calculations given in annex. Also, contribution of bolt 4 in end-plate is omitted due to small lever arm.

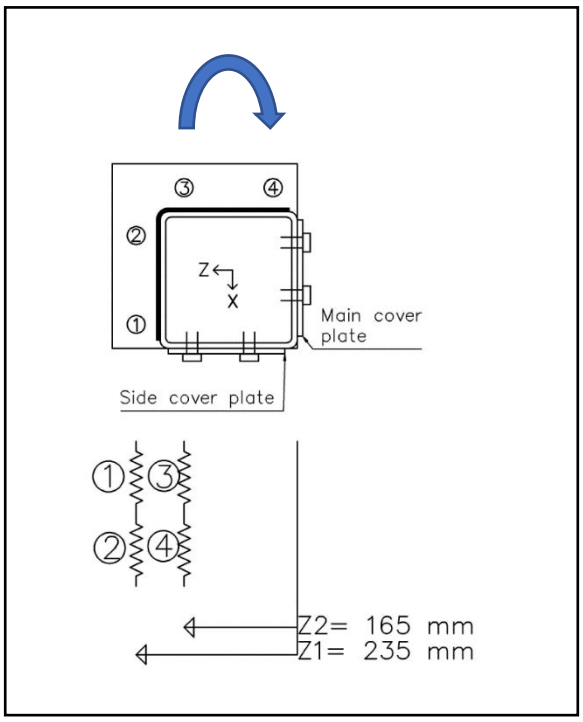

Figure 7-1: Identification and assembly of active components (CC-1/case 1)

List of joint components contributing towards initial rotational stiffness in figure 7-1.

$K_1 = End - plate\ in\ bending$
$K_2 = Bolts\ in\ tension$
$K_5 = Equivalent\ end - plate\ in\ bending$
$K_6 = Equivalent\ bolts\ in\ tension$

7.3 Non-symmetrical corner splice connection – cover plate in tension

Active components of corner column connection for present bending case vary from the previous case. End-plate and both cover plates contribute towards initial rotational stiffness in this case. Contribution of cover plates towards resistance was found to be negligible until a moment of 17 KN-m was reached. Yield resistance of this connection is reached at 55 KN-m due to yielding of end-plate. Contribution of cover plates towards resistance was significant at yield resistance. Half of the width of side cover plate is considered to be effective for initial rotational stiffness. Also, contribution of bolt 3 in end-plate is omitted due to small lever arm.

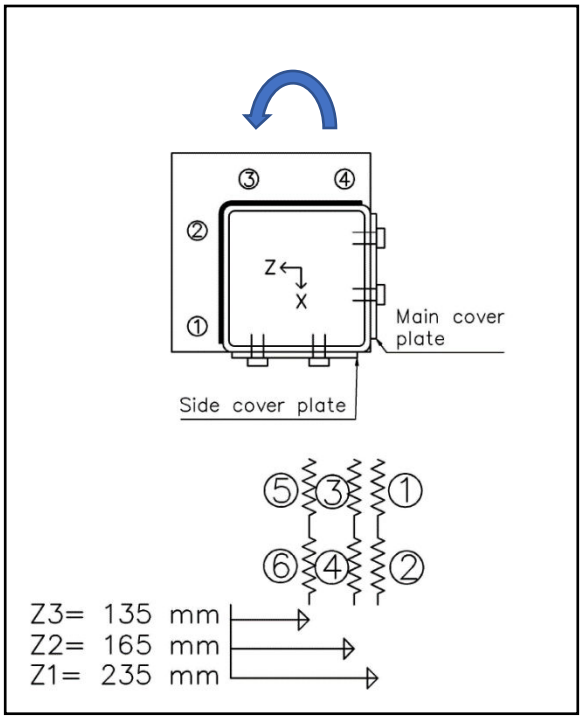

Figure 7-2: Identification and assembly of active components (CC-1/case 2)

List of joint components contributing towards initial rotational stiffness in figure 7-2.

$K_1 = Cover\ plate\ in\ tension$
$K_2 = Bolts\ in\ shear$
$K_3 = Equivalent\ end - plate\ in\ bending$
$K_4 = Equivalent\ bolts\ in\ tension$
$K_5 = Equivalent\ cover\ plate\ in\ tension$
$K_6 = Bolts\ in\ shear$

7.4 Non-symmetrical intermediate splice – cover plate in compression

Yield resistance of intermediate column for the present bending case is reached at 45 KN-m due to yielding of end-plate. End-plate in bending and bolt in tension are the two components active in this case. Main cover plate doesn't contribute towards resistance until singificant yielding of end-plate has taken place. Hence, contribution of main cover plate towards intital rotational stiffness is neglected. Bolts 2,3,4 and 5 in end-plate are active in tension. While, bolts 1 and 6 are omitted due to small lever arm.

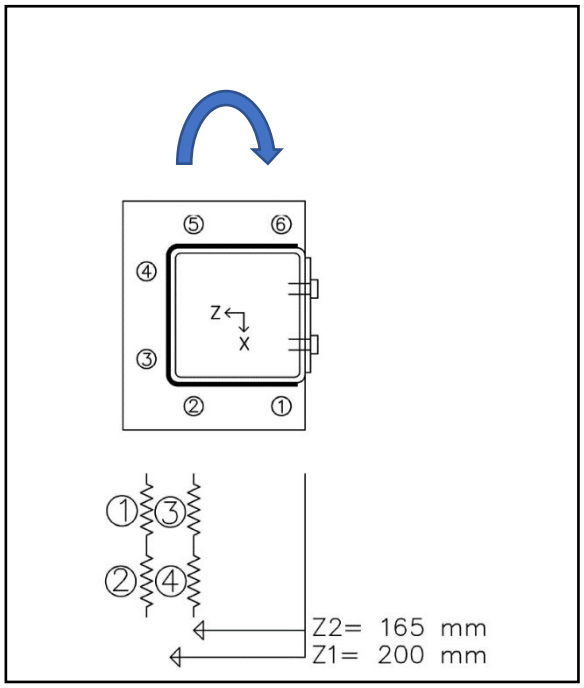

Figure 7-3: Identification and assembly of active components (IC-1/case 1)

List of joint components contributing towards initial rotational stiffness in figure 7-3.

$K_1 = End - plate\ in\ bending$
$K_2 = Bolts\ in\ tension$
$K_1 = End - plate\ in\ bending$
$K_2 = Bolts\ in\ tension$

7.5 Non-symmetrical intermediate splice – cover plate in tension

Based on FE results, contribution of cover plate towards resistance was found to be negligible until a moment of 17 KN-m. Yield resistance of the present connection is reached at 65 KN-m due to yielding of end-plate. Contribution of cover plate towards resistance was significant at this stage. Initial rotational stiffness can be predicted from 17 KN-m to 65 KN-m by considering the joint components shown in figure 7-4. End-plate and cover plate contribute towards initial rotational stiffness in the present case of intermediate column. Bolts 1 and 6 in end-plate are active, while contribution of bolts 2 and 5 is neglected due to small lever arm.

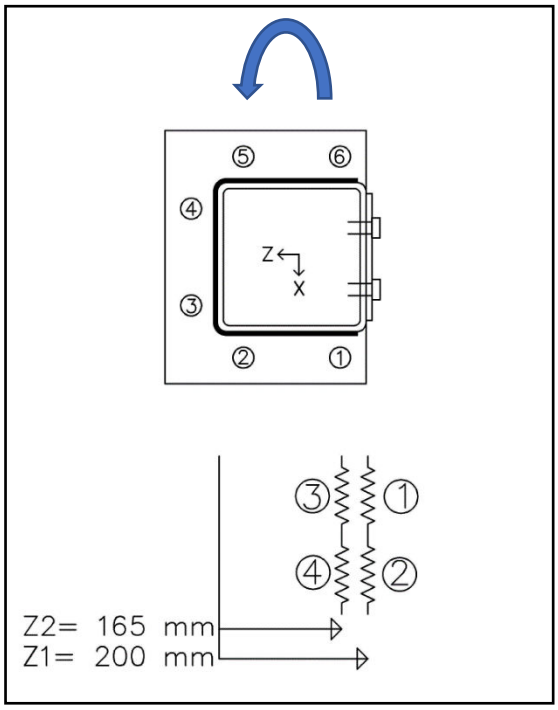

Figure 7-4: Identification and assembly of active components (IC-1/case 1)

List of joint components contributing towards initial rotational stiffness in figure 7-4.

$K_1 = Cover\ plate\ in\ tension$
$K_2 = Bolts\ in\ shear$
$K_3 = End - plate\ in\ bending$
$K_4 = Bolts\ in\ tension$

7.6 Non-symmetrical intermediate splice – cover plate in rotation

Active components for the present case are similar to corner column with load case- cover plate in compression. Both the specimens exhibit similar behavior until yield resistance is reached. Yield resistance of the connection is reached at 36 KN-m due to yielding of end-plate. Based on FE results, contribution of cover plate towards resistance was negligible until a moment close to yield resistance was reached. Hence, cover plate is omitted for calculating intial rotational stiffness. Bolts 5,4 and 6 in end-plate are considered to be active.

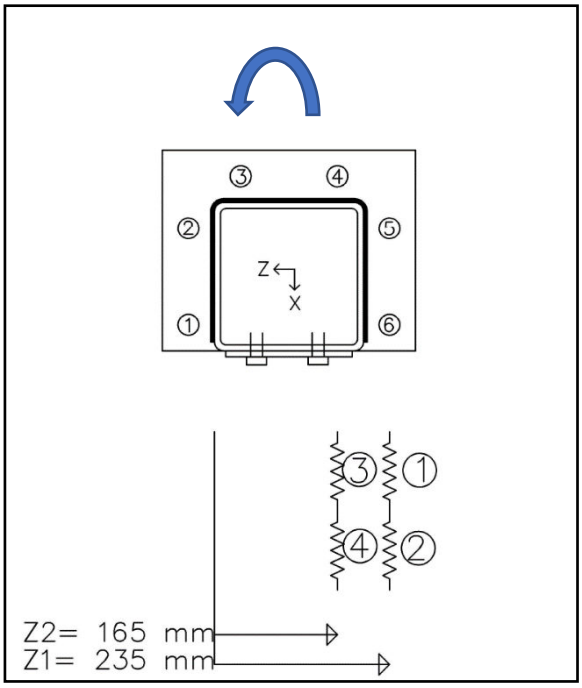

Figure 7-5: Identification and assembly of active components (IC-1/case 1)

List of joint components contributing towards initial rotational stiffness in figure 7-5.

$K_1 = End - plate\ in\ bending$
$K_2 = Bolts\ in\ tension$
$K_3 = Equivalent\ end - plate\ in\ bending$
$K_4 = Equivalent\ bolt\ in\ tension$

7.7 Stiffness coefficients

7.7.1 End-plate in bending and bolts in tension

Stiffness coefficients of components end-plate in bending (k_1) and bolts in tension (k_2) are provided in table 6.6 of EC 1993-1-8. These coefficients were developed based on T-stub theory. l_{eff} is the effective length of T-stub strength calculation, t_p is the thickness of plate, m is the distance between bolt and column face, A_s and L_b are the shear area and length of bolt. Factor 0.85 in equation represents the relationship between initial effective length $(l_{eff,ini})$ and l_{eff}.

$$k_1 = \frac{0.85\, l_{eff}\, t_p^3}{m^3} \tag{7.1}$$

$$k_2 = \frac{1.6\, A_s}{L_b} \tag{7.2}$$

However, these stiffness coefficients are developed based on joints between I and H-sections, where t-stub theory is predominant. In this thesis square hollow sections are used for columns in the connection. Stiffness coefficients of end-plate in bending and bolts in tension provied by eurocode were found to overestimate the stiffness of a bolted hollow section end-plate joint by atleast 50% [9]. Based on beam theory, a stiffness model for bolted hollow section end-plate joint was developed by Karsen and Aalberg. Both the eurocode stiffness model and Karlsen-Aalberg stiffness model is applied in the current situation to make a comparision.

$$k_1 = \frac{4n\,(3a+3m\alpha+n\alpha)\,A_s}{(6am+6an+3m^2\alpha+2n^2\alpha+6nm\alpha)\,L_b} \tag{7.3}$$

$$k_2 = \frac{2\,(3a+3m\alpha+n\alpha)\,l_{eff,ini}\,t_p^3}{m^2(3m^2\alpha+4nm\alpha+12am+12an)} \tag{7.4}$$

Parameters m and n are bolt distance from column face and plate edge. Parameter “a” is taken half of width of tubular section. α the is rigidty factor introduced to account for additional bending stiffness of the plate inside the hollow section. In the present case, α is set to zero, meaning end plate has similar stiffness throughout the plate. Similar yield patterns given in eurocode were noticed in hollow section end-plate joints bolted on two sides [9]. While, global yield line patterns may need to be applied for joints bolted on four sides. Hence, intial effective length $l_{eff,ini}$ is taken as 0.85 times effective lengths l_{eff} obtained from table 6.6 (effective lengths for end-plate) of EC 1993-1-8. A_s and L_b are the shear area and lengths of bolts in end plate.

Bolt row location	Bolt row considered individualley	
	Circular patterns $l_{eff,cp}$	Non-circular patterns $l_{eff,nc}$
Bolt row outside tension flange of beam	Smallest of: $2\pi m_x$ $\pi m_x + w$ $\pi m_x + 2e$	Smallest of: $4m_x + 1,25e_x$ $e + 2m_x + 0,625e_x$ $0,5b_p$ $0,5w + 2m_x + 0,625e_x$

Table 7-1: Effective length for bolt row outside tension flange [9]

7.7.2 – Cover plate in tension and bolts in shear

Stiffness coefficient of cover plate in tension (k_3) is similar as the eurocode stiffness provided for column web in tension in table 6.11 of EC 1993-1-8. Factor 0.7 refers to the ratio between the design resistance and maximum elastic resistance which is taken as 2/3 [4]

$$k_3 = 0.7 b_{eff} \frac{t_c}{d_c} \tag{7.5}$$

b_{eff} is the effective width of cover plate, t_c is the thickness of cover plate and d_c is the length of cover plate as shown in figure. While, stiffness coefficient of equivalent cover plate in tension is calculated by considering half of the effective width of plate

Cover plate is welded to the top column and bolted to the bottom column. Cover plates transfers load from top column through weld and though six bolts to the bottom column. Length of cover plate that is welded to top column is considered to infinitely rigid and doesn't affect the end-plate rotation. Extension of plate under tensile load is only dominant along the length d_c shown in figure 7-6. Hence, effective length of cover plate that affects the connection rotation is taken as d_c.

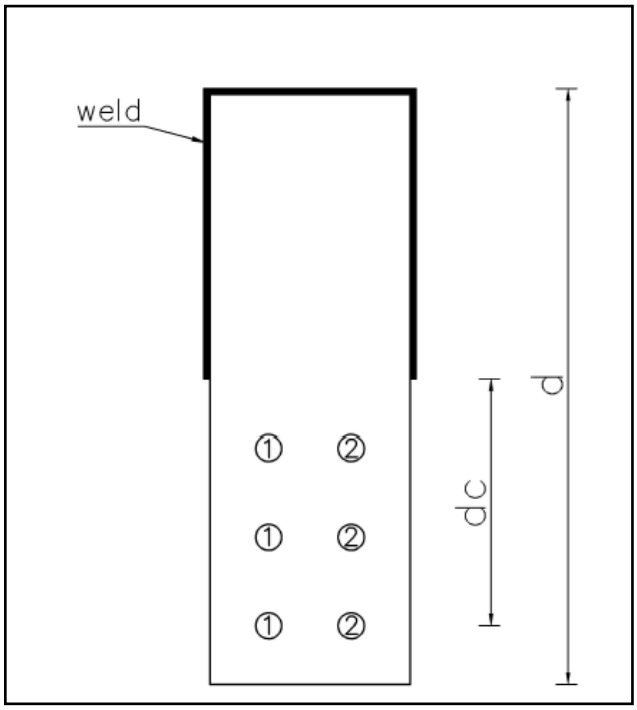

Figure 7-6: Effective length of cover plate

Stiffness coefficent of bolts in shear is calculated using the eurocode formula provided in table 6.11 of EC 1993-1-8.

$$k_4 = \frac{16\, n_b\, d^2\, f_{ub}}{E\, d_{M16}} \tag{7.6}$$

n_b is the number of bolt rows, d is the diameter of bolt, f_{ub} is the ultimate strength of bolt, E is the Young's modulus of bolt material and d_{M16} is the diameter of M16 bolt.

7.8 Comparision of stiffness obtained through Abaqus and component method

In this section, comparision of initial rotational stiffness obtained from finite element results and modified eurocode model is given for specimens CC-1 and IC-1 are given in graphical form. Comparision of results from Eurocode approach, modified Eurocode approach and finite element results of all the specimens in given in tabular form.

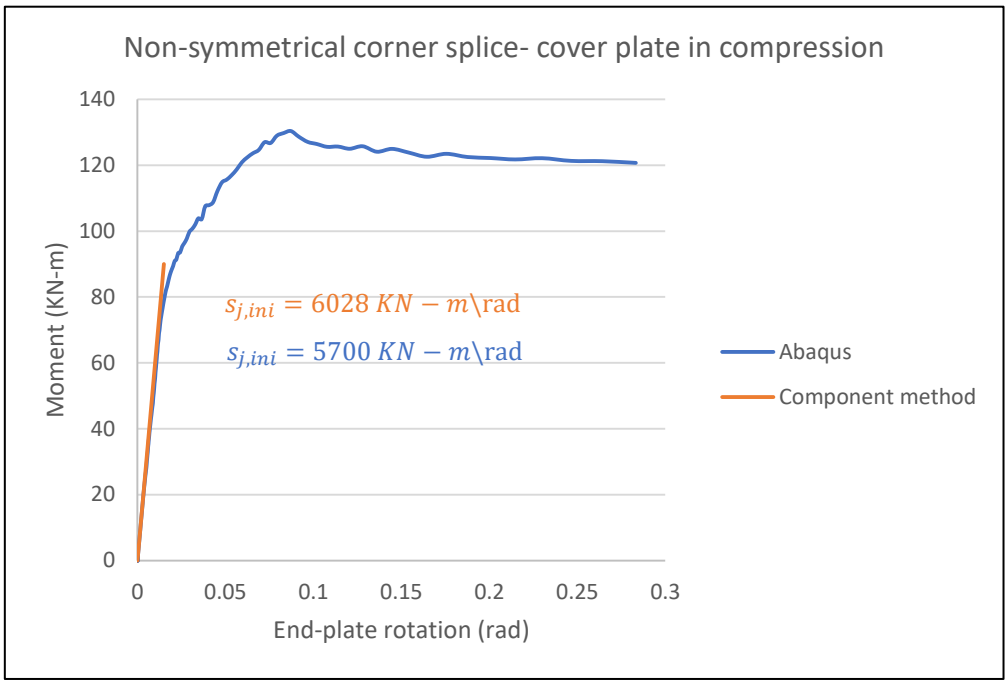

Figure 7-7: Comparision of initial rotation stiffness for specimen CC-1 (case 1)

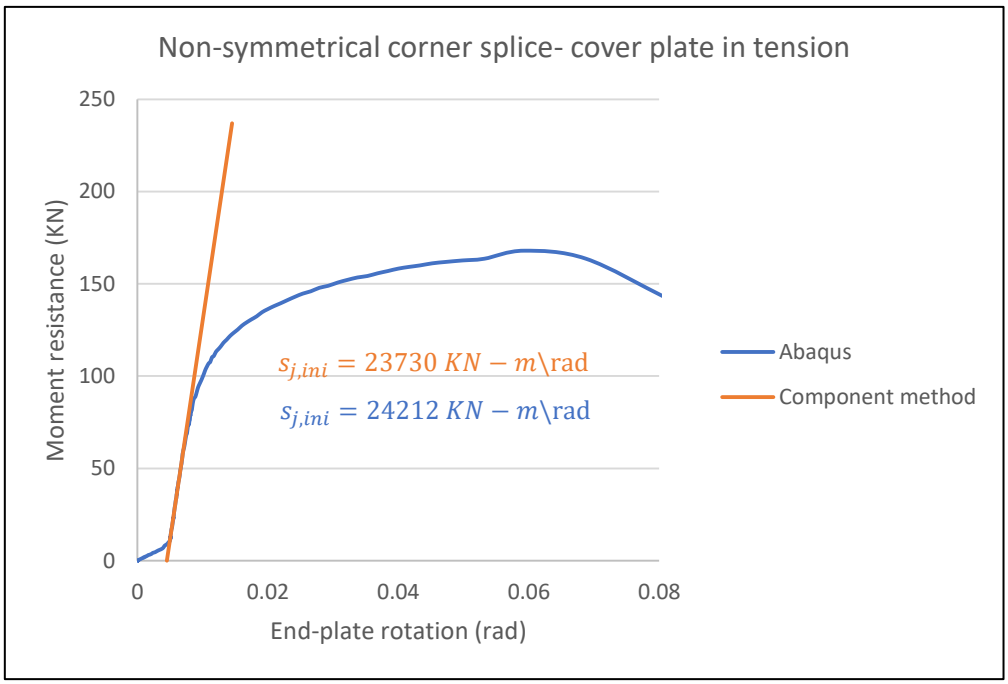

Figure 7-8: Comparision of initial rotation stiffness for specimen CC-1 (case 2)

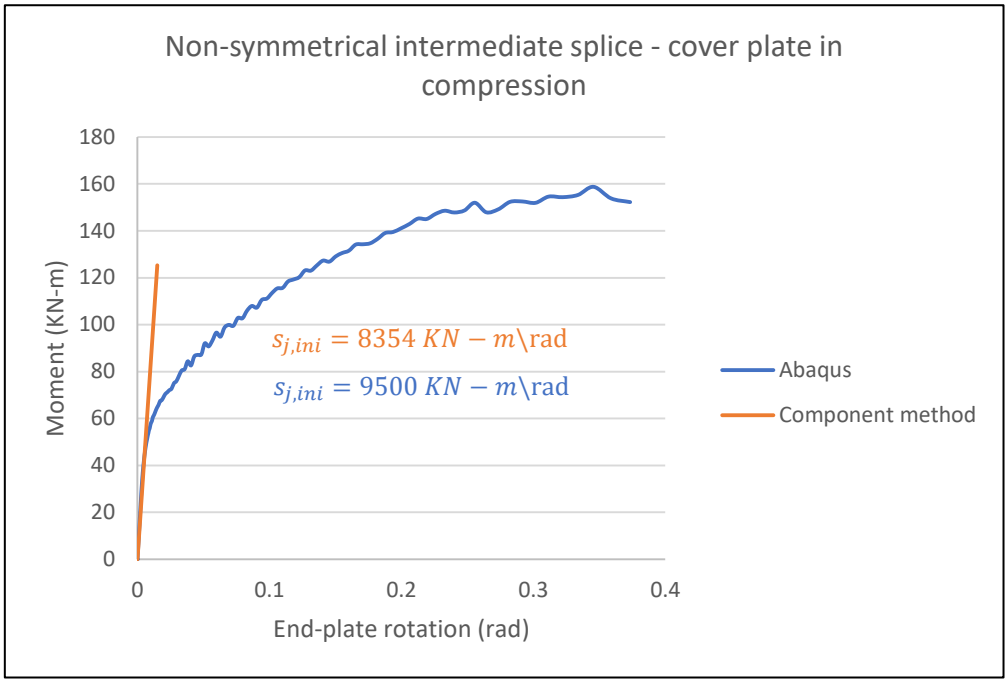

Figure 7-9: Comparision of initial rotation stiffness for specimen IC-1 (case 1)

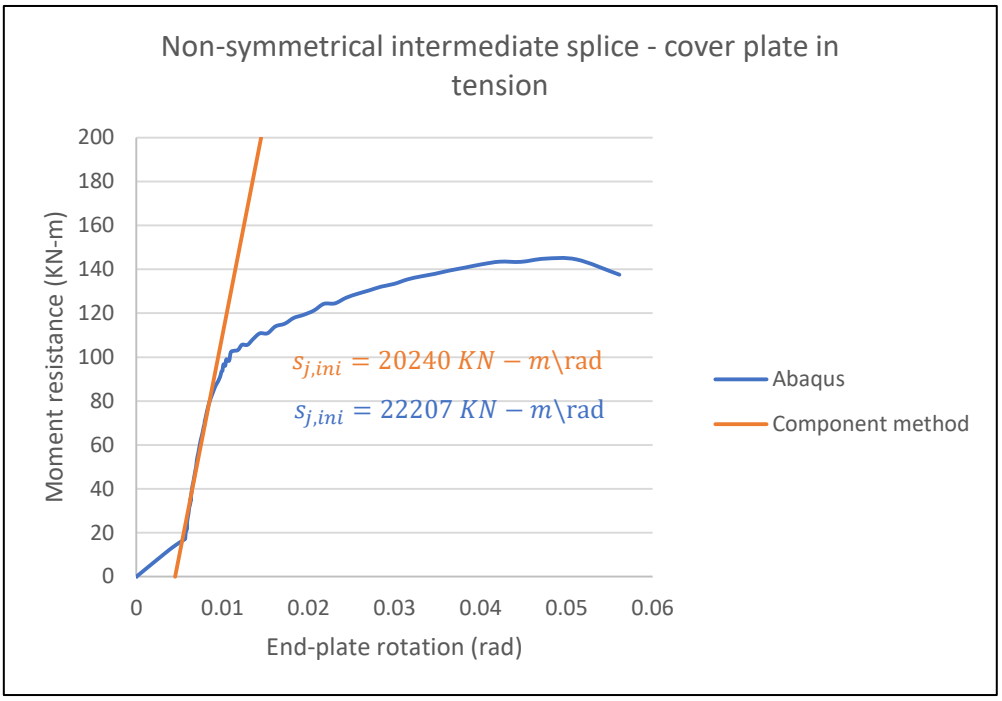

Figure 7-10: Comparision of initial rotation stiffness for specimen IC-1 (case 2)

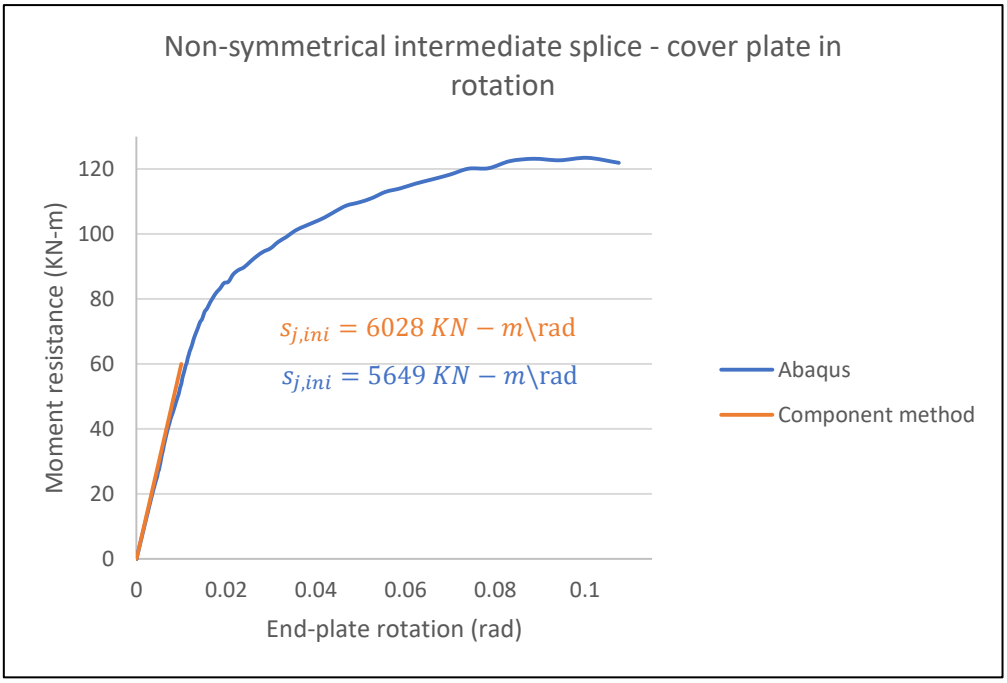

Figure 7-11: Comparision of initial rotation stiffness for specimen IC-1 (case 3)

Initial rotational stiffness (KN-m/rad)			
Specimen	**Abaqus**	**Eurocode (modified)**	**Ratio**
CC-1	5700	6028	1.1
CC-2	4160	2674	0.6
CC-3	9300	11260	1.2
CC-4	3940	3673	0.9
CC-5	2715	2372	0.9
CC-6	5000	5839	1.2
IC-1	9500	8354	0.9
IC-2	5315	3627	0.7
IC-3	12500	15500	1.2
IC-4	5000	5452	1.1
IC-5	4226	3825	0.9
IC-6	7462	6719	0.9

Table 7-2: Comparison of $S_{j,ini}$ for specimen with load case-cover plate in compression

Specimen	**Abaqus**	**Eurocode (modified)**	**Ratio**
CC-1	24212	23730	1
CC-2	22154	19310	0.9
CC-3	32139	28700	0.9
CC-4	25128	23610	0.9
CC-5	22238	23360	1.1
CC-6	24087	23770	1
IC-1	22207	20240	0.9
IC-2	20182	15810	0.8
IC-3	28000	24850	0.9
IC-4	18000	19330	1.1
IC-5	15858	18820	1.2
IC-6	19864	19640	1

Table 7-3: Comparison of $S_{j,ini}$ for specimen with load case-cover plate in tension

Specimen	**Abaqus**	**Eurocode (modified)**	**Ratio**
IC-1	5649	6028	1.1
IC-2	4200	2674	0.6
IC-3	9360	11260	1.2
IC-4	3485	3673	1.1
IC-5	2443	2372	1
IC-6	5710	5839	1

Table 7-4: Comparison of $S_{j,ini}$ for specimen with load case-cover plate in rotation

Initial rotational stiffness (KN-m/rad)			
Specimen	**Abaqus**	**Eurocode**	**Ratio**
CC-1	5700	21510	3.8
CC-2	4160	9726	2.3
CC-3	9300	37440	4
CC-4	3940	13030	3.3
CC-5	2715	7554	2.8
CC-6	5000	19980	4
IC-1	9500	25120	2.7
IC-2	5315	11260	2.1
IC-3	12500	44200	3.5
IC-4	5000	14480	2.9
IC-5	4226	9187	2.2
IC-6	7462	23070	3.1

Table 7-5: Comparison of $S_{j,ini}$ for specimen with load case-cover plate in compression

Specimen	**Abaqus**	**Eurocode**	**Ratio**
CC-1	24212	27790	1.1
CC-2	22154	20160	0.9
CC-3	32139	36470	1.2
CC-4	25128	24500	1
CC-5	22238	22860	1.1
CC-6	24087	25970	1.1
IC-1	22207	25040	1.1
IC-2	20182	18100	0.9
IC-3	28000	32230	1.2
IC-4	18000	21770	1.2
IC-5	15858	21120	1.3
IC-6	19864	23270	1.2

Table 7-6: Comparison of $S_{j,ini}$ for specimen with load case-cover plate in tension

Specimen	**Abaqus**	**Eurocode**	**Ratio**
IC-1	5649	21510	3.7
IC-2	4200	9726	2.3
IC-3	9360	37440	4
IC-4	3485	13030	3.8
IC-5	2443	7554	3.1
IC-6	5710	19980	3.5

Table 7-7: Comparison of $S_{j,ini}$ for specimen with load case-cover plate in rotation

From tables 7-2, 7-3 and 7-4 it can be noticed that modified Eurocode approach which employed Karlsen-Aalberg stiffness model gives a fair approximation of initial rotational stiffness of the joint. Predicted stiffness was mostly on the conservative side. However, in some cases modified Eurocode model overestimated initial rotational stiffness by 1.2 times. From tables 7-5 and 7-7 it can be noticed that, Eurocode approach employing end-plate and bolt in tension stiffness coefficients from EC 1993-1-8, overestimated the initial rotational stiffness by at least 2 times. However, difference in stiffness for specimens with cover plate in tension case was lower than in other two bending cases. This is due to cover plate carrying most of the applied load. Results obtained through modified Eurocode approach are in acceptance with the results of finite element models.

Chapter 8 – Conclusions and future work

8.1 Conclusions

Based on finite element results obtained for non-symmetrical column splice connection, the following conclusions have been made about the overall behavior:

- Due to non-symmetrical layout of the connection, failure modes vary based on loading situation.
- Layout of the connection in itself causes uneven force distribution in the connection. This leads to torsion in the columns. Hence, the rotation of end-plate varied based on section under consideration.
- In case of non-symmetrical column splice under a tensile load, bolts in end-plate that are away from cover plate were relatively highly stressed. This leads to uneven vertical displacement along the four sides of column. Cover plates act in combined tension and shear in case of non-symmetrical corner splice. In case of non-symmetrical intermediate splice cover plate acts in combined tension and bending.
- Bolt hole clearance provided for connecting cover plate to column face has a significant effect on the overall moment-rotation curve. This led to considerable rotation without resistance increase in the initial part of the moment-rotation curve. This causes the elastic part of the curve to have two slopes.
- Not all of the components in the connection contribute to initial rotational stiffness. This was mainly due to bolt hole clearance in the cover plates. Cover plate requires a certain vertical displacement before utilizing its maximum capacity. This causes end-plate to be highly stressed in the initial stages of loading, leading to yielding of end-plate before cover plate is completely active in carrying load. However, this wasn't observed in case of cover plate in tension, since cover plate was the dominant component in carrying load.
- Overall moment-rotation and load-displacement curves do not exhibit typical flattening of the curve in case end-plate is the first component to yield. This is caused due to the presence of cover plate which limits the rotation of end-plate after yield point.
- Non-symmetrical column splice connection exhibits higher resistance than end-plate splice for all the load cases. For non-symmetrical corner splice, ultimate bending resistance and tensile resistance is increased by at least 27% and 41%. In case of non-symmetrical intermediate splice, ultimate bending resistance and tensile resistance is increased by at least 13% and 12.5%.
- Overall resistance and initial rotational stiffness were decreased when the bolts in end-plate were moved away from the column face. Similar characteristics were noticed when bolts in end-plate were moved closer to each other. In addition, overall resistance and initial stiffness improved when thickness of end-plate and cover plate were increased. However, column cross-section yield and failure were noticed when

connection component thickness was set to 10mm i.e. larger than the thickness of column cross-section.

Based on the initial rotational stiffness obtained for non-symmetrical column splice connection by applying component method, the following conclusions have been made:

- Finite element models of non-symmetrical column splice connection provide acceptable results based on the initial stiffness prediction by component method using modified Eurocode approach.
- Stiffness coefficients for bolts in shear and cover plate in tension provided in Eurocode 1993-1-8 can be directly employed in component method to predict stiffness. However, effective depth of the cover plate is taken from the center of bottom bolt hole to edge of weld.
- Employing stiffness coefficients for end-plate in bending and bolts in tension provided in Eurocode 1993-1-8 overestimated the initial rotational stiffness by at least 2 times.
- Stiffness coefficients for end-plate in bending and bolts in tension proposed by Karlsen- Aalberg are the most appropriate coefficients for end-plate connection between tubular sections. Initial stiffness predicted using the above coefficients provides acceptable results with finite element models. This approach provided results that are mostly on the conservative side with respect to finite element results. However, in a few cases stiffness was overestimated by a maximum of 1.2 times which is acceptable.

8.2 Future work

- Experimental studies will be conducted in future with specimen CC-1 and IC-1. This will aid to validate and calibrate the finite element models.
- Current parametric studies can be extended further to study the effect of bolt size and bolt position in cover plate on the overall behavior of non-symmetrical column splice connection.
- Presented research in non-symmetrical column splice connections can also be extended to the use of rectangular hollow sections.

.

References

1. Eurocode 1993- design of steel structures, part 1-8: Design of joints
2. Bayo.E, Cabrero.JM, Gil.B (2005), An effective component-based method to model semi-rigid connections for the global analysis of steel and composite structure, Engineering structures 28 (97-108)
3. Simoes da Silva.L (2008), Towards a consistent design approach for steel joints under generalized loading, Journal of construction research 64 (1059-1075)
4. Weynand.K, Jaspart.JP, Steenhuis.M (1997), The stiffness model of revised Annex J of Eurocode 3, Proceedings of the 3rd international workshop on connections (441-452)
5. Jaspart.JP, Weynand.K (2016), Design of joints in steel and composite strucutres, ECCS -Eurocode Design Manuals
6. Piluso.V, Rizzano.G (2008), Experimental analysis and modeling of bolted T-stubs under cyclic loads, Journal of construction research 64 (6) (665-669)
7. The steel construction institute, www.steelconstruction.info
8. H. Thai, B. Uy (2015), Finite element modelling of blind bolted composite joints, Journal of constructional steel research edition 112(339-353)
9. Karlsen.F.T, Aalberg.A (2012), Bolted RHS end-plate joints in axial tension, Nordic steel construction conference 2012
10. Wheeler.A.T, Clarke.M.J , Hancock.G.J (2000), FE modeling of four-bolt, tubular moment end-plate connections, ASCE- Journal of structural engineering vol. 126 (816-822)
11. Kim.J, Yoon.JC, Kang.BS (2007), Finite element analysis and modeling of structure with bolted joints, Applied Mathematical Modeling 31 (895-911)
12. Abaqus user guide, Version 6.14, Simulia corp.
13. Pavlovic.M (2013), Reistance of bolted shear connectors in prefabricated steel-comcrete composite decks, Doctoral dissertation, University of Belgrade
14. CalculiX user manual, Version 2.7
15. Wheeler.A.T, Clarke.M.J, Hancock.G.J, Murray.T.M (1998), Design model for bolted moment end plate connections joining rectangular hollow sections, Journal of structural engineering, 124 (164-178)

16. Kato.B, Hirose. R (1985), Bolted tension flanges joining circular hollow section members, Journal of steel research, 5 (79-101)
17. Packer.J, Bruno.L, Birkemoe.P (1989), Limit analysis of bolted RHS flange plate joints, ASCE- Journal of structural engineering, vol.115 (2226-2242)
18. Wheeler.A.T, Clarke.M.J , Hancock.G.J (2000), FE modeling of four-bolt, tubular moment end-plate connections, ASCE- Journal of structural engineering vol. 126 (816-822)
19. Willibald.S, Packer.JA, Puthli.R.S (2002), Experimental study of bolted HSS flange - plate connections in axial tension, ASCE- Journal of structural engineering, vol.128 (328-336)
20. Wang.Y.Q, Zong.L, Shi.Y.J (2013), Bending behavior and design model of bolted flange-plate connections, Journal of constructional steel research 84 (1-16)
21. J. Wang, N.Zhang , S.Guo (2016), Experimental and numerical analysis of blind bolted moment joints to CFTST columns, Thin-walled structures 109 (185-201)
22. J. Lee, H.M. Goldsworthy, E.F. Gad (2010), Blind bolted T-stub connections to unfilled hollow section columns in low rise structures, Journal of constructional steel research 66 (981-992)
23. S. Fernando, Joint design using oneside structural fastener, Technical note AFI/03/012, Ajax fasteners innovations
24. O. Bursi, J.P. Jaspart (1997), Benchmarks for finite element modelling of bolted steel connections, Journal of constructional steel research, Vol. 43 (17-42)
25. O. Bursi, J.P. Jaspart (1998), Basic issues in the finite element simulation of extended end plate connections, Computers and structures, Vol 69 (361-382)

Annex-A: Procedure to apply component method

Component	Stiffness coefficient k_i	
Column web panel in shear	Unstiffened, single-sided joint, or a double-sided joint in which the beam depths are similar	stiffened
	$k_1 = \frac{0{,}38A_{VC}}{\beta z}$	$k_1 = \infty$
	z is the lever arm from Figure 6.15; β is the transformation parameter from 5.3(7).	
Column web in compression	unstiffened	stiffened
	$k_2 = \frac{0{,}7\, b_{eff,c,wc}\, t_{wc}}{d_c}$	$k_2 = \infty$
	$b_{eff,c,wc}$ is the effective width from 6.2.6.2	
Column web in tension	stiffened or unstiffened bolted connection with a single bolt-row in tension or unstiffened welded connection	stiffened welded connection
	$k_3 = \frac{0{,}7 b_{eff,t,wc}\, t_{wc}}{d_c}$	$k_3 = \infty$
	$b_{eff,t,wc}$ is the effective width of the column web in tension from 6.2.6.3. For a joint with a single bolt-row in tension, $b_{eff,t,wc}$ should be taken as equal to the smallest of the effective lengths ℓ_{eff} (individually or as part of a group of bolt-rows) given for this bolt-row in Table 6.4 (for an unstiffened column flange) or Table 6.5 (for a stiffened column flange).	
Column flange in bending (for a single bolt-row in tension)	$k_4 = \frac{0{,}9\ell_{eff}\, t_{fc}^{\,3}}{m^3}$ ℓ_{eff} is the smallest of the effective lengths (individually or as part of a bolt group) for this bolt-row given in Table 6.4 for an unstiffened column flange or Table 6.5 for a stiffened column flange; m is as defined in Figure 6.8.	
End-plate in bending (for a single bolt-row in tension)	$k_5 = \frac{0{,}9\ell_{eff}\, t_p^{\,3}}{m^3}$ ℓ_{eff} is the smallest of the effective lengths (individually or as part of a group of bolt-rows) given for this bolt-row in Table 6.6; m is generally as defined in Figure 6.11, but for a bolt-row located in the extended part of an extended end-plate $m = m_x$, where m_x is as defined in Figure 6.10.	
Flange cleat in bending	$k_6 = \frac{0{,}9\ell_{eff}\, t_a^{\,3}}{m^3}$ ℓ_{eff} is the effective length of the flange cleat from Figure 6.12; m is as defined in Figure 6.13.	

Figure A-1: List of stiffness coefficients of connection components as given in Eurocode 1993-1-8 [1]

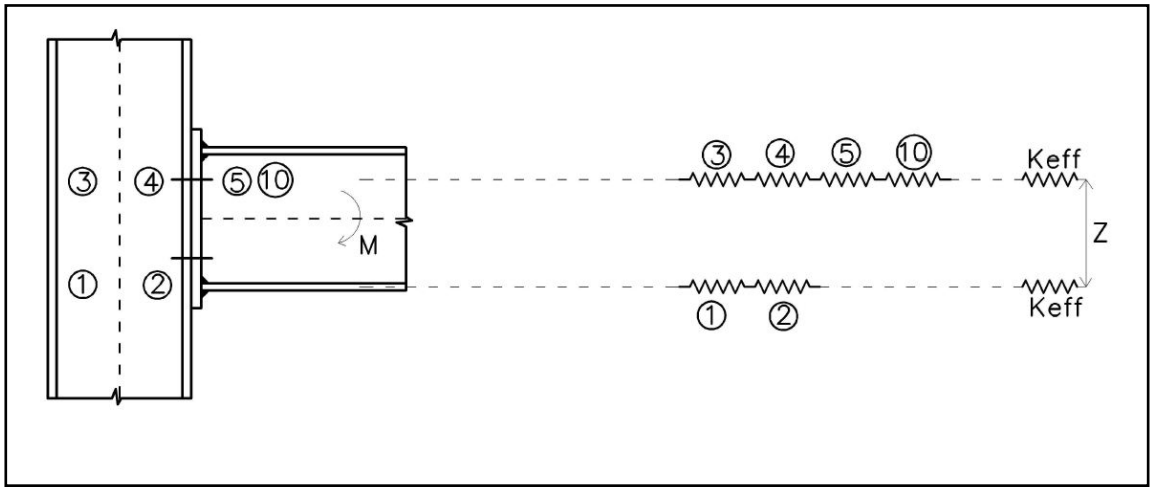

Figure A-2: Assembly of connection components

$$k_{eff} = \frac{1}{\sum_i \frac{1}{k_i}} \qquad k_{eq} = \frac{\sum_j k_{eff,j} \; z_j}{z_{eq}} \qquad z_{eq} = \frac{\sum_j k_{eff,j} z_j^{\,2}}{\sum_j k_{eff,j} z_j}$$

$k_i = Stiffness\ coefficient\ representing\ component\ i$
$z_j = distance\ between\ effective\ spring\ and\ centre\ of\ compression$
$z_{eq} = equivalent\ arm\ length$
$k_{eq} = Equivalent\ stiffness\ coefficent\ taking\ into\ account\ the\ stiffness\ coefficients\ k_i\ of\ basic\ components$

$$S_j = \frac{Ez^2}{\mu \sum_i \frac{1}{k_i}}$$

$S_j = Rotational\ stiffness\ of\ the\ connection$
$E = Young's\ modulus\ of\ steel$
$\mu = stiffness\ ratio = 1;\ if\ M_{j,Ed} \leq \frac{2}{3} M_{j,Rd}$
$\mu = \left(1.5 \frac{M_{j,Ed}}{M_{j,Rd}}\right)^{\psi};\ if\ \frac{2}{3} M_{j,Ed} \leq M_{j,Ed} \leq M_{j,Rd}$
$M_{j,Rd} = Design\ moment\ resistance\ of\ the\ joint$

Coefficient ψ can be obtained from table below

Type of connection	ψ
Welded	2,7
Bolted end-plate	2,7
Bolted angle flange cleats	3,1
Base plate connections	2,7

Table A-1: Value of coefficients for calculating stiffness ratio [1]

Annex-B: T-stub failure modes

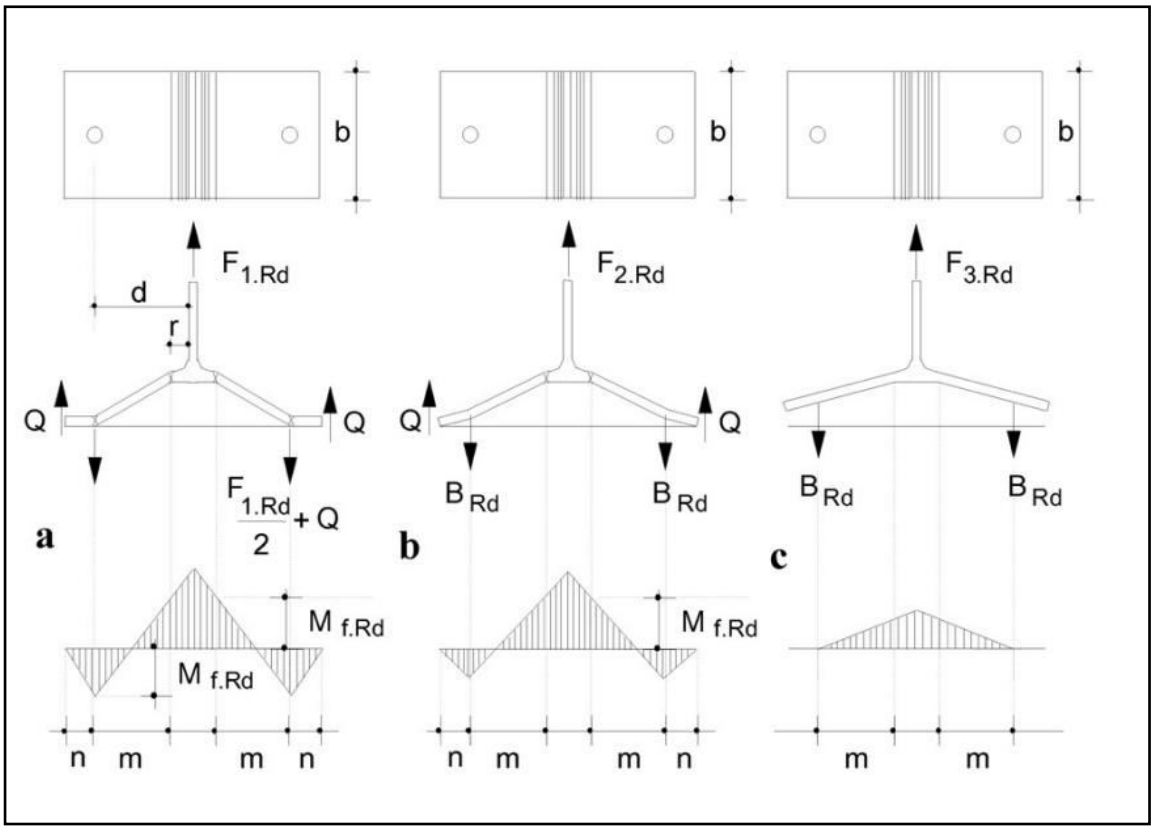

Figure B-1: T-stub failure modes [6]

Annex-C: Manual calculation for non-symmetrical corner splice connection

C.1 Non-symmetrical corner splice – cover plate in compression (specimen CC-1)

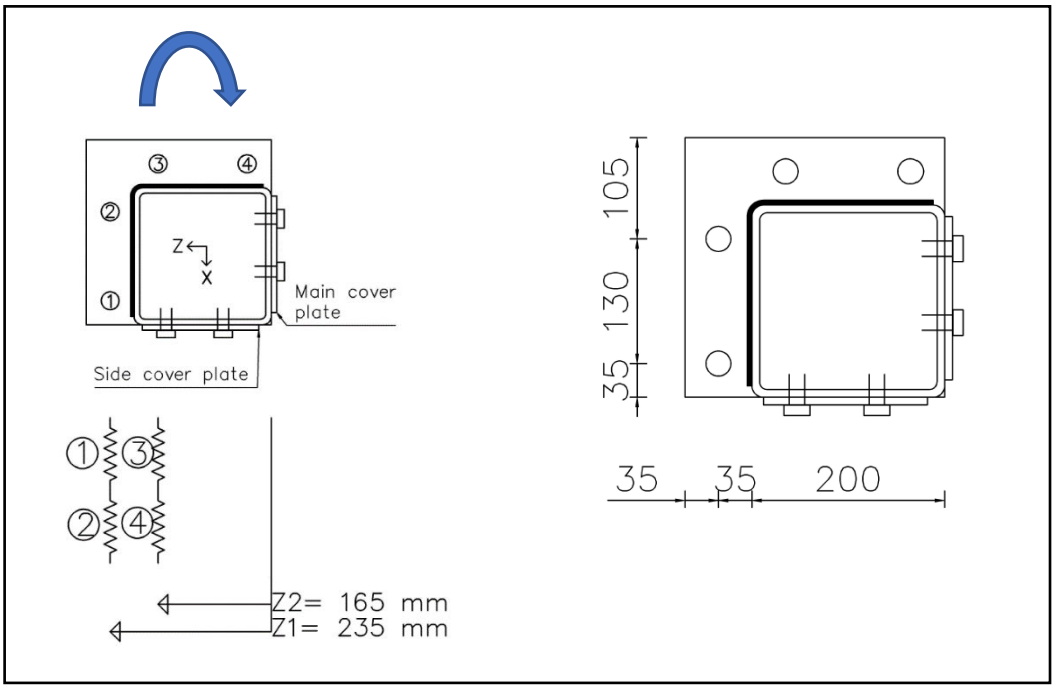

Figure C-1: Plan and elevation of specimen CC-1 (case 1)

Evaluation of individual stiffness co-efficients:

Individual effective lengths for end-plate in bending

Bolt row location	Bolt row considered individualley	
	Circular patterns $l_{eff,cp}$	Non-circular patterns $l_{eff,nc}$
Bolt row outside tension flange of beam	Smallest of: $2\pi m_x$ $\pi m_x + w$ $\pi m_x + 2e$	Smallest of: $4m_x + 1,25e_x$ $e + 2m_x + 0,625e_x$ $0,5b_p$ $0,5w + 2m_x + 0,625e_x$

Table C-1: Individual effective length for bolt row outside tension flange

Individual effective length for bolt row comprising bolt 1 and 2
$m = 35mm; e_x = 35mm; e = 35mm; w = 130, b_p = 270mm$

From table C-1:
Non-circular patterns: $l_{eff,nc}$
$4m_x + 1.25e_x = 183.75mm$
$e + 2m_x + 0.625\ e_x = 126.875\ mm$
$0.5\ b_p = 135mm$
$0.5w + 2m_x + 0.625e_x = 156.875\ mm$

Circular patterns: $l_{eff,cp}$
$2\pi m_x = 219.8mm$
$\pi m_x + w = 239.9mm$
$\pi m + 2e = 179.9mm$

$l_{eff,1} = l_{eff,nc} = 126\ mm < l_{eff,cp} = 179.9\ mm$
$l_{eff,2} = l_{eff,nc} = 126\ mm$
Therefore, effective length for bolt row consisting of bolt 1 and 2 is 126.875 mm

Individual effective length for bolt 3
$m = 35mm; e_x = 35mm; e = 105mm; w = 130$

Non-circular patterns: $l_{eff,nc}$
$4m_x + 1.25e_x = 183.75\ mm$
$e + 2m_x + 0.625\ e_x = 196.875\ mm$
$0.5\ b_p = 135mm$
$0.5w + 2m_x + 0.625e_x = 156.875\ mm$

Circular patterns: $l_{eff,cp}$
$2\pi m_x = 219.8\ mm$
$\pi m_x + w = 239.9\ mm$
$\pi m + 2e = 319.9\ mm$

$l_{eff,1} = l_{eff,nc} = 135mm < l_{eff,cp} = 219.9\ mm$
$l_{eff,2} = l_{eff,nc} = 135\ mm$
Thereforce effective length for bolt row consisting of bolt 3 is 135mm

1. K_1 - End plate in bending

   $a = 100\ mm; m = 35\ mm; n = 35\ mm; \alpha = 1; t = 8\ mm; l_{eff} = 126.875\ mm$

$$K_1 = \frac{2\ (3a + 3m\alpha + n\alpha)0.85\ l_{eff}\ t^3}{m^2\ (3m^2\alpha + 4nm\alpha + 12am + 12an)} = 0.428$$

2. K_2 - Bolts in tension

$$a = 100mm; m = 35mm; n = 35mm; \alpha = 1$$
$$A_s = 353\ mm^2;\ \ L_b = 36.6mm$$

$$K_2 = 4n\frac{3a + 3m\alpha + n\alpha}{6am + 6an + 3m^2\alpha + 6nm\alpha} * (A_s/L_b) = \ 10.71$$

3. K_3 - Equivalent end plate in bending

$$a = 100mm; m = 35mm; n = 35mm; \alpha = 1; t = 8mm; l_{eff} = 135\ mm$$

$$K_3 = \frac{(3a + 3m\alpha + n\alpha)0.85\ l_{eff}\ t^3}{m^2\ (3m^2\alpha + 4nm\alpha + 12am + 12an)} = 0.228$$

4. K_4 - Equivalent bolt in tension

$$a = 100mm; m = 35mm; n = 35mm; \alpha = 1$$
$$A_s = 353\ mm^2;\ \ L_b = 36.6mm$$

$$K_4 = 4n\frac{3a + 3m\alpha + n\alpha}{6am + 6an + 3m^2\alpha + 6nm\alpha} * (A_s/L_b) = \ 5.355$$

Effective stiffness co-efficients of equivalent bolt rows:

$$K_{eff1} = \frac{K_1 * K_2}{K_1 + K_2} = \ 0.412$$

$$K_{eff2} = \frac{K_3 * K_4}{K_3 + K_4} = 0.219$$

Equivalent lever arm:

$$Z_{eq} = \frac{\left(K_{eff1} * Z_1^2\right) + \left(K_{eff2} * Z_2^2\right)}{(K_{eff1} * Z_1) + (K_{eff2} * Z_2)} = 216\ mm$$

Equivalent stiffness:

$$K_{eq} = \frac{(K_{eff1} * Z_1) + (K_{eff2} * Z_2)}{Z_{eq}} = 0.615$$

Initial joint stiffness:

$$S_{j,ini} = \frac{E * Z_{eq}^2}{(\frac{1}{K_{eq}})} = 6028\ KN - m/rad$$

C.2 Non-symmetrical corner splice – cover plate in tension (specimen CC-1)

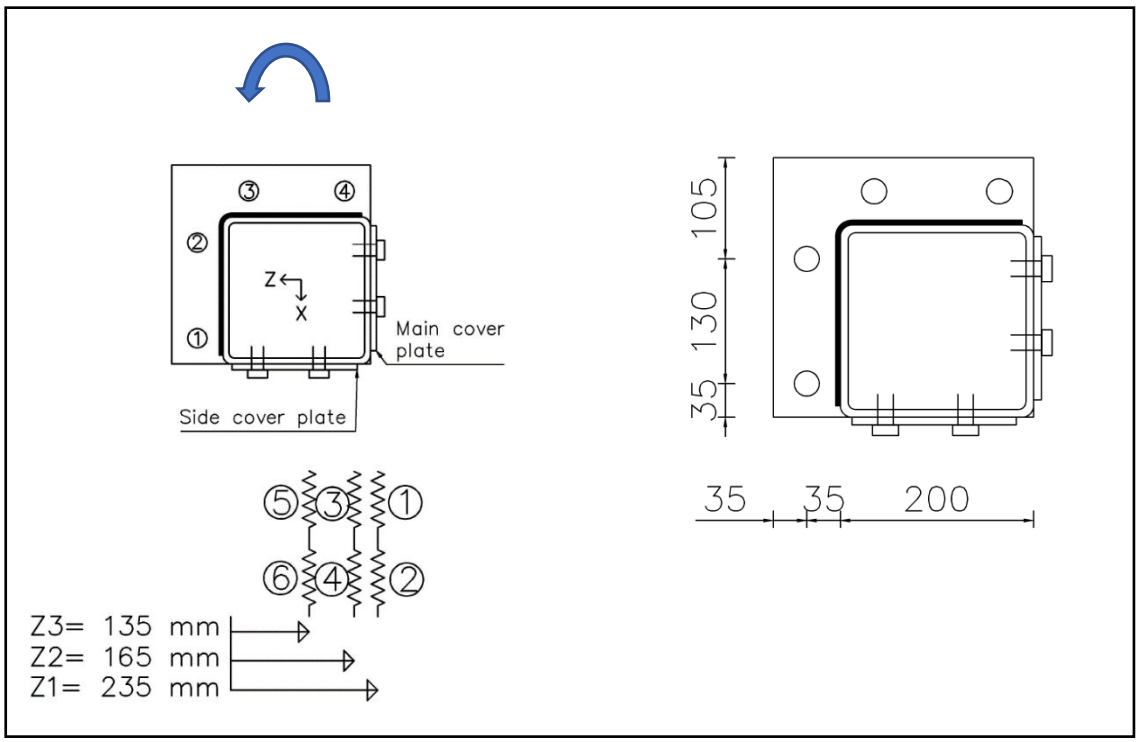

Figure C-2: Plan and elevation of specimen CC-1 (case 2)

Individual stiffness coefficients:

Individual effective length for bolt 4
$m = 35mm; e_x = 35mm; e = 35\ mm; w = 130mm; b_p = 270\ mm$

From table C-1
Non-circular patterns: $l_{eff,nc}$
$4m_x + 1.25e_x = 183.75\ mm$
$e + 2m_x + 0.625\ e_x = 126.875\ mm$
$0.5\ b_p = 135mm$
$0.5w + 2m_x + 0.625e_x = 156.875\ mm$

Circular patterns: $l_{eff,cp}$
$2\pi m_x = 219.8\ mm$
$\pi m_x + w = 239.9\ mm$
$\pi m + 2e = 179.9\ mm$

$l_{eff,1} = l_{eff,nc} = 126.875\ mm < l_{eff,cp} = 179.9\ mm$
$l_{eff,2} = l_{eff,nc} = 126.875\ mm$
Thereforce effective length for bolt row consisting of bolt 4 is 126.875 mm

1. K_1 – Cover plate in tension

$b_{eff} = 170 - (2 * 22) = 126\ mm;\ t_c = 8mm;\ \ d_C = 208\ mm$

$$K_1 = \frac{0.7\ b_{eff}\ t_c}{d_c} = 3.392$$

2. K_2- Bolts in shear

$n_b = 3;\ \ d = 20mm;\ \ f_{ub} = 1000Mpa;\ \ E = 210{,}000\ Mpa;\ \ d_{M16} = 16mm$

$$K_2 = \frac{16 n_b d^2 f_{ub}}{E d_{M16}} = 5.714$$

3. K_3 - Equivalent end plate in bending

$a = 100mm; m = 35mm; n = 35mm; \alpha = 1; t = 8mm; l_{eff} = 126.875\ mm$

$$K_3 = \frac{(3a + 3m\alpha + n\alpha)0.85\ l_{eff}\ t^3}{m^2\ (3m^2\alpha + 4nm\alpha + 12am + 12an)} = 0.214$$

4. K_4 - Equivalent bolt in tension

$$a = 100mm; m = 35mm; n = 35mm; \alpha = 1$$
$$A_s = 353\ mm^2;\ \ L_b = 36.6mm$$

$$K_4 = 4n\frac{3a + 3m\alpha + n\alpha}{6am + 6an + 3m^2\alpha + 6nm\alpha} * (A_s/L_b) = \ 5.355$$

5. K_5 – Equivalent cover plate in tension

$$b_{eff} = \big(170 - (2 * 22)\big)/2 = 63\ mm$$
$$d_c = 208\ mm: t_c = 8mm$$

$$k_5 = 0.7\ b_{eff}\frac{t_c}{d_c} = 1.696$$

6. K_6 - Bolts in shear

$n_b = 3;\ \ d = 20mm;\ \ f_{ub} = 1000Mpa;\ \ E = 210{,}000\ Mpa;\ \ d_{M16} = 16mm$

$$K_6 = \frac{16 n_b d^2 f_{ub}}{E d_{M16}} = 5.714$$

Effective stiffness co-efficients of equivalent bolt row:

$$K_{eff1} = \frac{K_1 * K_2}{K_1 + K_2} = 2.129$$

$$K_{eff2} = \frac{K_3 * K_4}{K_3 + K_4} = 0.206$$

$$K_{eff3} = \frac{K_5 * K_6}{K_5 + K_6} = 1.308$$

Equivalent lever arm:

$$Z_{eq} = \frac{\left(K_{eff1} * Z_1^2\right) + \left(K_{eff2} * Z_2^2\right) + \left(K_{eff3} * Z_3^2\right)}{\left(K_{eff1} * Z_1\right) + \left(K_{eff2} * Z_2\right) + \left(K_{eff3} * Z_3\right)} = 179\ mm$$

Equivalent stiffness:

$$K_{eq} = \frac{\left(K_{eff1} * Z_1\right) + \left(K_{eff2} * Z_2\right) + \left(K_{eff3} * Z_3\right)}{Z_{eq}} = 3.524$$

Initial joint stiffness:

$$S_{j,ini} = \frac{E * Z_{eq}^2}{\left(\frac{1}{K_{eq}}\right)} = 23{,}730\ KN - m/rad$$

Annex–D: Manual calculation for non-symmetrical intermediate splice connection

D.1 Non-symmetrical intermediate splice – cover plate in compression (specimen IC-1)

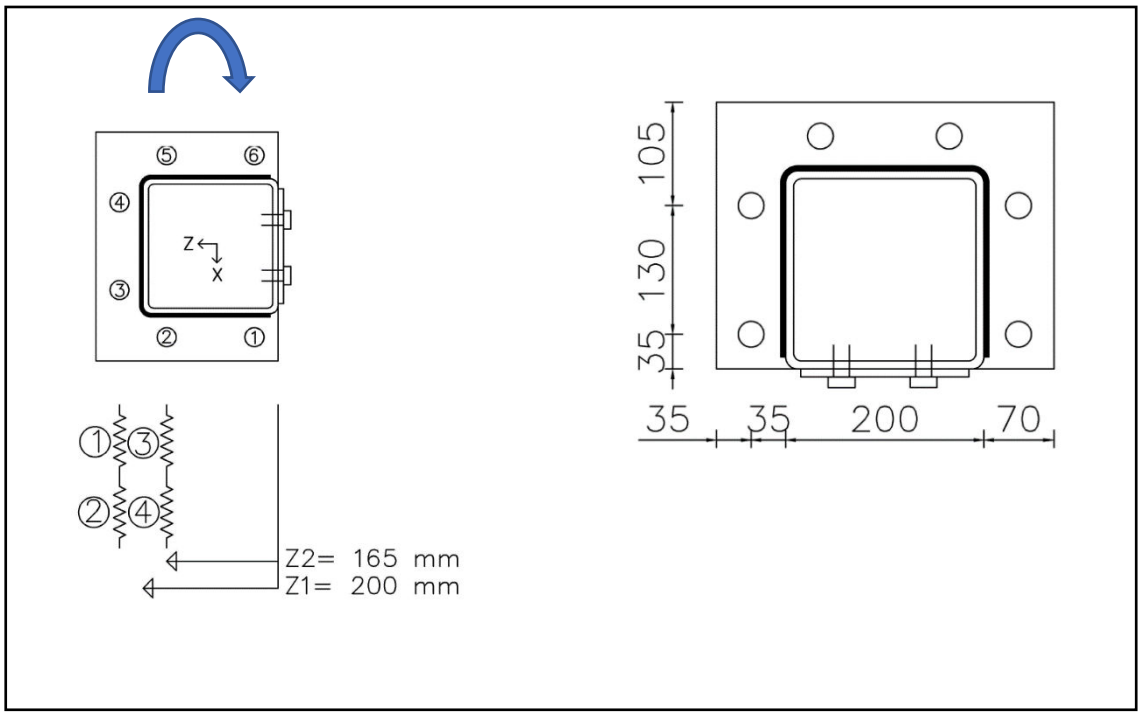

Figure D-1 : Plan and elevation of specimen IC-1 (case 1)

Individual stiffness coefficients:

Individual effective length for bolt row consisting of bolt 3 and 4
$m = 35mm; e_x = 35mm; e = 105mm; w = 130\ mm; b_p = 340\ mm$

From table C-1:
Non-circular patterns: $l_{eff,nc}$
$4m_x + 1.25e_x = 183.75\ mm$
$e + 2m_x + 0.625\ e_x = 196.875\ mm$
$0.5\ b_p = 170mm$
$0.5w + 2m_x + 0.625e_x = 156.875\ mm$

Circular patterns: $l_{eff,cp}$
$2\pi m_x = 219.8\ mm$
$\pi m_x + w = 239.9\ mm$
$\pi m + 2e = 319.9\ mm$

$l_{eff,1} = l_{eff,nc} = 156.875mm < l_{eff,cp} = 219.9\ mm$
$l_{eff,2} = l_{eff,nc} = 156.875\ mm$
Thereforce effective length for bolt row consisting of bolt 3 and 4 is 156.875 mm

Individual effective length for bolt row consisting of bolt 2 and 5
$m = 35mm; e_x = 35mm; e = 105mm; w = 130\ mm; b_p = 270\ mm$

Non-circular patterns: $l_{eff,nc}$
$4m_x + 1.25e_x = 183.75\ mm$
$e + 2m_x + 0.625\ e_x = 196.875\ mm$
$0.5\ b_p = 135mm$
$0.5w + 2m_x + 0.625e_x = 156.875\ mm$

Circular patterns: $l_{eff,cp}$
$2\pi m_x = 219.8\ mm$
$\pi m_x + w = 239.9\ mm$
$\pi m + 2e = 319.9\ mm$

$l_{eff,1} = l_{eff,nc} = 135\ mm < l_{eff,cp} = 219.9\ mm$
$l_{eff,2} = l_{eff,nc} = 135\ mm$
Thereforce effective length for bolt row consisting of bolt 2 and 5 is 135 mm

1. K_1 - End plate in bending

$$a = 100mm; m = 35mm; n = 35mm; \alpha = 1; t = 8mm; l_{eff} = 156.875\ mm$$

$$K_1 = \frac{2\ (3a + 3m\alpha + n\alpha)0.85\ l_{eff}\ t^3}{m^2\ (3m^2\alpha + 4nm\alpha + 12am + 12an)} = 0.53$$

2. K_2 - Bolts in tension

$$a = 100mm; m = 35mm; n = 35mm; \alpha = 1$$
$$A_s = 353\ mm^2;\ \ L_b = 36.6mm$$

$$K_2 = 4n\frac{3a + 3m\alpha + n\alpha}{6am + 6an + 3m^2\alpha + 6nm\alpha} * (A_s/L_b) = \ 10.71$$

3. K_3 - End plate in bending

$$a = 100mm; m = 35mm; n = 35mm; \alpha = 1; t = 8mm; l_{eff} = 135\ mm$$

$$K_3 = \frac{2\ (3a + 3m\alpha + n\alpha)0.85\ l_{eff}\ t^3}{m^2\ (3m^2\alpha + 4nm\alpha + 12am + 12an)} = 0.456$$

4. K_4 - Bolts in tension

$$a = 100mm; m = 35mm; n = 35mm; \alpha = 1$$
$$A_s = 353\ mm^2;\ \ L_b = 36.6mm$$

$$K_4 = 4n\frac{3a + 3m\alpha + n\alpha}{6am + 6an + 3m^2\alpha + 6nm\alpha} * (A_s/L_b) = \ 10.71$$

Effective stiffness co-efficients of equivalent bolt row:

$$K_{eff1} = \frac{K_1 * K_2}{K_1 + K_2} = \ 0.505$$

$$K_{eff2} = \frac{K_3 * K_4}{K_3 + K_4} = 0.437$$

Equivalent lever arm:

$$Z_{eq} = \frac{\left(K_{eff1} * Z_1^2\right) + \left(K_{eff2} * Z_2^2\right)}{\left(K_{eff1} * Z_1\right) + \left(K_{eff2} * Z_2\right)} = 208.526\ mm$$

Equivalent stiffness:

$$K_{eq} = \frac{\left(K_{eff1} * Z_1\right) + \left(K_{eff2} * Z_2\right)}{Z_{eq}} = 0.915$$

Initial joint stiffness:

$$S_{j,ini} = \frac{E * Z_{eq}^2}{(\frac{1}{K_{eq}})} = 8354\ KN - m/rad$$

D.2 Non-symmetrical intermediate splice – cover plate in tension (specimen IC-1)

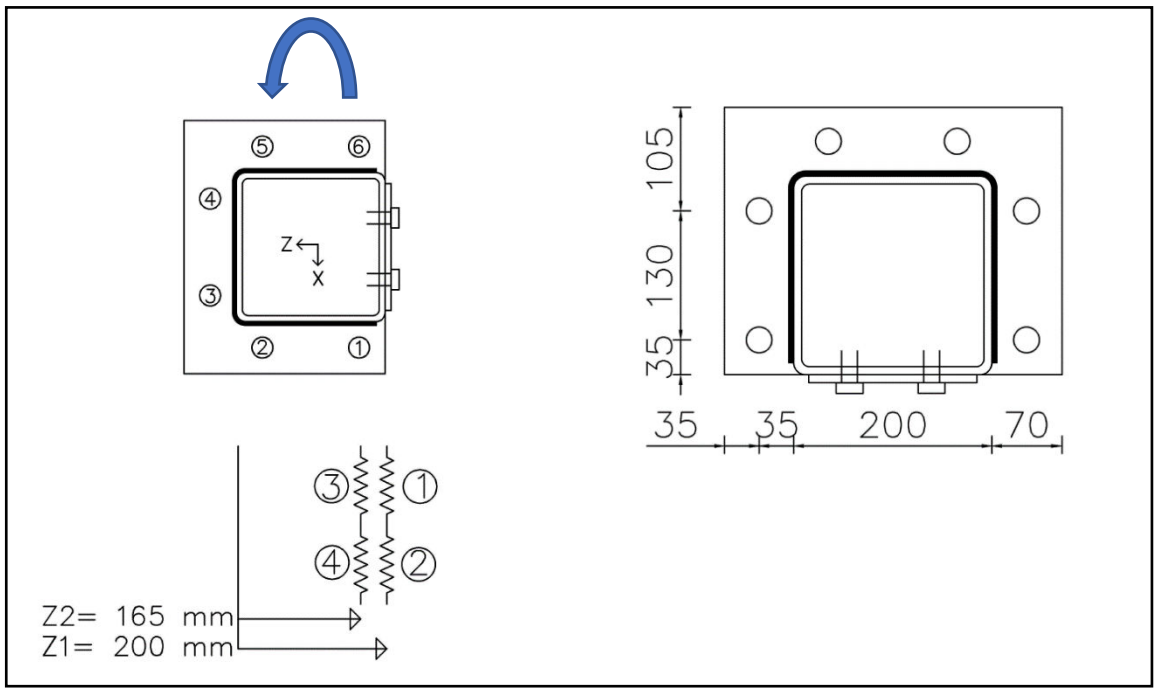

Figure D-2: Plan and elevation of specimen IC-1 (case 2)

Individual stiffness coefficients:

Individual effective lengths for bolt row consisting of bolt 1 and 6
$m = 35mm; e_x = 35mm; e = 35\ mm; w = 130mm; b_p = 270\ mm$

From table A-1
Non-circular patterns: $l_{eff,nc}$
$4m_x + 1.25e_x = 183.75\ mm$
$e + 2m_x + 0.625\ e_x = 126.875\ mm$
$0.5\ b_p = 135mm$
$0.5w + 2m_x + 0.625e_x = 156.875\ mm$

Circular patterns: $l_{eff,cp}$
$2\pi m_x = 219.8\ mm$
$\pi m_x + w = 239.9\ mm$
$\pi m + 2e = 179.9\ mm$

$l_{eff,1} = l_{eff,nc} = 126.875\ mm < l_{eff,cp} = 179.9\ mm$
$l_{eff,2} = l_{eff,nc} = 126.875\ mm$

Thereforce effective length for bolt row consisting of bolt 1 and 6 is 126.875 mm

1. K_1 – Cover plate in tension

$$b_{eff} = 170 - (2 * 22) = 126\ mm$$
$$t_c = 8mm:\ d_C = 208\ mm$$
$$K_1 = \frac{0.7 * b_{eff} * t_c}{d_c} = 3.392$$

2. K_2- Bolts in shear

$$n_b = 3;\ \ d = 20mm;\ \ f_{ub} = 1000Mpa;\ \ E = 210{,}000\ Mpa;\ \ d_{M16} = 16mm$$

$$K_2 = \frac{16 n_b d^2 f_{ub}}{E d_{M16}} = 5.714$$

3. K_3 -End plate in bending

$$a = 100mm; m = 35mm; n = 35mm; \alpha = 1; t = 8mm; l_{eff} = 126.875\ mm$$

$$K_3 = \frac{2\ (3a + 3m\alpha + n\alpha)0.85\ l_{eff}\ t^3}{m^2\ (3m^2\alpha + 4nm\alpha + 12am + 12an)} = 0.428$$

4. K_4 - Bolt in tension

$$a = 100mm; m = 35mm; n = 35mm; \alpha = 1$$
$$A_s = 353\ mm^2;\ \ L_b = 36.6mm$$

$$K_4 = 4n \frac{3a + 3m\alpha + n\alpha}{6am + 6an + 3m^2\alpha + 6nm\alpha} * (A_s/L_b) =\ 10.71$$

Effective stiffness co-efficients of equivalent bolt row:

$$K_{eff1} = \frac{K_1 * K_2}{K_1 + K_2} =\ 2.129$$

$$K_{eff2} = \frac{K_3 * K_4}{K_3 + K_4} = 0.412$$

Equivalent lever arm:

$$Z_{eq} = \frac{\left(K_{eff1} * Z_1^2\right) + \left(K_{eff2} * Z_2^2\right)}{\left(K_{eff1} * Z_1\right) + \left(K_{eff2} * Z_2\right)} = 195.181\ mm$$

Equivalent stiffness:

$$K_{eq} = \frac{\left(K_{eff1} * Z_1\right) + \left(K_{eff2} * Z_2\right)}{Z_{eq}} = 2.529$$

Initial joint stiffness:

$$S_{j,ini} = \frac{E * Z_{eq}^2}{\left(\frac{1}{K_{eq}}\right)} = 20{,}240\ KN - m/rad$$

D.3 Non-symmetrical intermediate splice – cover plate in rotation (specimen IC-1)

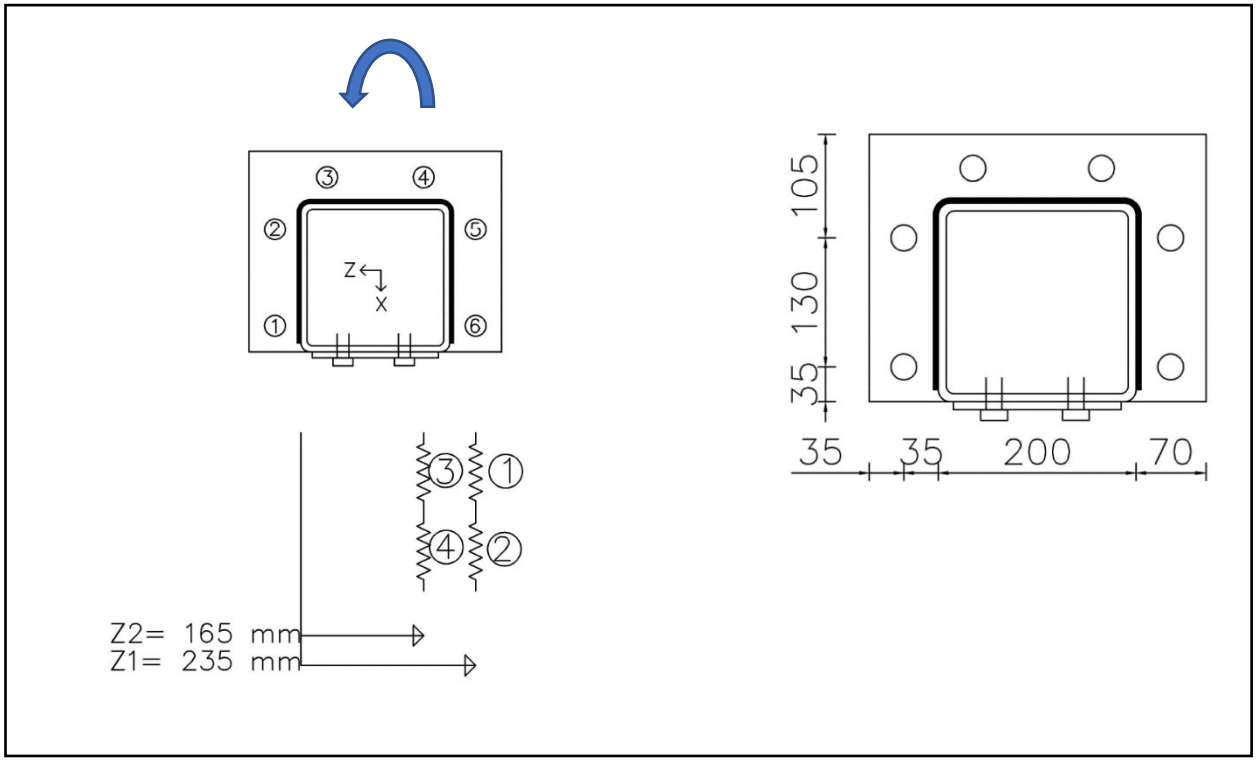

Figure D-3: Plan and elevation of specimen IC-1 (case 3)

Individual stiffness coefficients

Individual effective length for bolt row comprising bolt 6 and 5
$m = 35mm; e_x = 35mm; e = 35mm; w = 130, b_p = 270mm$

From table C-1,
Non-circular patterns: $l_{eff,nc}$
$4m_x + 1.25e_x = 183.75mm$
$e + 2m_x + 0.625\ e_x = 126.875\ mm$
$0.5\ b_p = 135mm$
$0.5w + 2m_x + 0.625e_x = 156.875\ mm$

Circular patterns: $l_{eff,cp}$
$2\pi m_x = 219.8mm$
$\pi m_x + w = 239.9mm$
$\pi m + 2e = 179.9mm$

$l_{eff,1} = l_{eff,nc} = 126.875\ mm < l_{eff,cp} = 179.9\ mm$

$l_{eff,2} = l_{eff,nc} = 126.875\ mm$
Therefore, effective length for bolt row consisting of bolt 6 and 5 is 126.875 mm

Individual effective length for bolt row consisting of bolt 4
$m = 35mm; e_x = 35mm; e = 105mm; w = 130\ mm; b_p = 270\ mm$

Non-circular patterns: $l_{eff,nc}$
$4m_x + 1.25e_x = 183.75\ mm$
$e + 2m_x + 0.625\ e_x = 196.875\ mm$
$0.5\ b_p = 135mm$
$0.5w + 2m_x + 0.625e_x = 156.875\ mm$

Circular patterns: $l_{eff,cp}$
$2\pi m_x = 219.8\ mm$
$\pi m_x + w = 239.9\ mm$
$\pi m + 2e = 319.9\ mm$

$l_{eff,1} = l_{eff,nc} = 135mm < l_{eff,cp} = 219.9\ mm$
$l_{eff,2} = l_{eff,nc} = 135\ mm$
Thereforce effective length for bolt row consisting of bolt 3 is 135mm

<u>Evaluation of individual stiffness co-efficients:</u>

1. K_1 - End plate in bending

$$a = 100mm; m = 35mm; n = 35mm; \alpha = 1; t = 8mm; l_{eff} = 126.875\ mm$$

$$K_1 = \frac{2\ (3a + 3m\alpha + n\alpha)0.85\ l_{eff}\ t^3}{m^2\ (3m^2\alpha + 4nm\alpha + 12am + 12an)} = 0.428$$

2. K_2 - Bolts in tension

$$a = 100mm; m = 35mm; n = 35mm; \alpha = 1$$
$$A_s = 353\ mm^2;\ \ L_b = 36.6mm$$

$$K_2 = 4n\frac{3a + 3m\alpha + n\alpha}{6am + 6an + 3m^2\alpha + 6nm\alpha} * (A_s/L_b) = \ 10.71$$

3. K_3 - Equivalent end plate in bending

$$K_3 = \frac{(3a + 3m\alpha + n\alpha)0.85\, l_{eff}\, t^3}{m^2\,(3m^2\alpha + 4nm\alpha + 12am + 12an)} = 0.228$$

4. K_4 - Equivalent bolt in tension

$$a = 100mm; m = 35mm; n = 35mm; \alpha = 1; t = 8mm; l_{eff} = 135\ mm$$

$$K_4 = 4n\frac{3a + 3m\alpha + n\alpha}{6am + 6an + 3m^2\alpha + 6nm\alpha} * (A_s/L_b) = \ 5.355$$

Effective stiffness co-efficients of equivalent bolt row:

$$K_{eff1} = \frac{K_1 * K_2}{K_1 + K_2} = \ 0.412$$

$$K_{eff2} = \frac{K_3 * K_4}{K_3 + K_4} = 0.219$$

Equivalent lever arm:

$$Z_{eq} = \frac{\left(K_{eff1} * Z_1^2\right) + \left(K_{eff2} * Z_2^2\right)}{(K_{eff1} * Z_1) + (K_{eff2} * Z_2)} = 215.997\ mm$$

Equivalent stiffness:

$$K_{eq} = \frac{\left(K_{eff1} * Z_1\right) + \left(K_{eff2} * Z_2\right)}{Z_{eq}} = 0.615$$

Initial joint stiffness:

$$S_{j,ini} = \frac{E * Z_{eq}^2}{(\frac{1}{K_{eq}})} = 6028\ KN - m/rad$$